

# **Semi-synthesis and Biological Evaluation of Prenylated Rab Proteins**

## **Dissertation**

zur Erlangung des akademischen Grades  
eines Doktors der Naturwissenschaften (Dr. rer. nat.)  
des Fachbereichs Chemie der Universität Dortmund

Angefertigt am Max-Planck-Institut für molekulare Physiologie  
in Dortmund

Eingereicht von Dipl.-Biochemiker Thomas Durek  
aus Berlin

Dortmund, Juni 2004

1. Gutachter : Prof. Dr. R.S. Goody
2. Gutachter : Prof. Dr. H. Waldmann

Die vorliegende Arbeit wurde in der Zeit von November 2000 bis Juni 2004 am Max-Planck-Institut für molekulare Physiologie in Dortmund unter der Anleitung von Prof. Dr. Roger S. Goody, Dr. Kirill Alexandrov und Prof. Dr. Herbert Waldmann durchgeführt.

Hiermit versichere ich an Eides statt, dass ich die vorliegende Arbeit selbständig und nur mit den angegebenen Hilfsmitteln angefertigt habe.

Dortmund, Juni 2004

Thomas Durek

## Contents

Contents .....	i
Abbreviations .....	iii

### **1. Introduction** **2**

1.1. Vesicular Transport .....	2
1.1.1. Rab proteins .....	4
1.1.2. The structural basis of Rab function .....	7
1.1.3. Rab geranylgeranylation.....	9
1.2. Chemical protein synthesis.....	12

### **2. Aims of the project** **21**

### **3. Results and Discussion** **25**

3.1. Development of a semi-synthetic strategy facilitating access to prenylated Rab/Ypt proteins .....	25
3.1.1. General considerations – Case studies .....	25
3.1.2. Expression and purification of Rab/Ypt C-terminal $\alpha$ -thioesters .....	30
3.1.3. An unexpected behaviour of Rab5 thioesters terminating in glutamine or asparagine.....	33
3.1.4. Expressed protein ligation with prenylated peptides.....	37
3.1.5. Development of a purification strategy. ....	42
3.1.6. Overview of semi-synthetic protein complexes.....	48
3.2. Characterization of the interaction of GGTase-II with single-prenylated reaction intermediates and the doubly prenylated product .....	51
3.3. A sensitive, real-time fluorescence based prenylation assay .....	63
3.4. The molecular basis of Rab:RabGDI interaction.....	67
3.4.1. The structure of monoprenylated Ypt1 in complex with RabGDI .....	70
3.5. Other semi-synthetic complexes intended for crystallographic analysis ...	79

### **4. Summary and Conclusions** **83**

### **4. Summary and Conclusions (german)** **86**

### **5. Materials and Methods** **90**

5.1. Materials .....	90
5.1.1. Chemicals.....	90
5.1.2. Peptides .....	90
5.1.3. General instrumentation .....	92
5.1.4. Frequently used buffers and growth media .....	92
5.2. Analytical methods .....	93
5.2.1. MALDI-TOF-mass spectrometry.....	93

---

5.2.2.	LC-MS measurements.....	93
5.2.3.	Analytical reversed-phase (RP) and gel filtration (GF) HPLC.....	94
5.2.4.	Denaturing SDS-PAGE .....	94
5.2.5.	Western-Blot.....	95
5.3.	Biochemical methods .....	96
5.3.1.	Expression and purification of GGTase-II, REP-1, RabGDI, MRS6p and Rab7wt .....	96
5.3.2.	Expression and purification of Rab/Ypt-thioester proteins .....	96
5.3.3.	Ligation of geranylgeranylated peptides to Rab/Ypt-thioester .....	98
5.3.4.	<i>In vitro</i> protein prenylation .....	99
5.4.	Biophysical methods.....	100
5.4.1.	Fluorescence titrations – determination of $K_d$ .....	100
5.4.2.	Transient kinetics – determination of $k_{off}$ .....	101
5.4.3.	Monitoring the prenylation reaction.....	102
5.5.	Molecular biology.....	103
5.5.1.	Plasmids and bacterial strains.....	103
5.5.2.	Preparation and transformation of competent cells .....	104
5.5.3.	Purification of DNA .....	105
5.5.4.	PCR.....	106
5.5.5.	Restriction enzyme digestion.....	107
5.5.6.	Ligation.....	108

---

## **6. References** **110**

---

## **7. Appendices** **131**

7.1.	Derivation of equations.....	131
7.1.1.	Reversible second-order reactions - equilibrium titrations .....	131
7.1.2.	Kinetics of ligand dissociation.....	133
	Acknowledgements .....	134

## Abbreviations

Å	Angstrom (1 Å = 0.1 nm = 10 <sup>-10</sup> m)
AA	Amino acid
CBD	Chitin-binding domain
CBR	C-terminus binding region
CHAPS	3-[(3-Cholamidopropyl)-dimethylammonio]-propansulfonat
CHM	Choroideremia
Cmc	Critical micelle concentration
CTAB	Cetyltrimethylammoniumbromide
Da	Dalton
Dans / Dansyl	5-Dimethylaminonaphtalin-1-sulfonyl
DDMAB	<i>N</i> -Dodecyl- <i>N,N</i> -(dimethylammonio)butyrate
DTE	1,4-Dithioerythritol
EPL	Expressed protein ligation
FTase	Farnesyltransferase
FRET	Fluorescence resonance energy transfer
GAP	GTPase activating protein
GDF	GDI displacement factor
GDI	GDP dissociation inhibitor
GdmHCl	Guanidinium hydrochloride
GEF	Guaninenucleotide exchange factor
GF	Gel filtration
GG	Geranylgeranyl
GGPP	Geranylgeranylpyrophosphate
GGTase	Geranylgeranyltransferase
GST	Glutathione S-transferase
GTPase	Guaninetriphosphate phosphatase
HPLC	High performance liquid chromatography
HOPS	Homotypic fusion and vacuole protein sorting
Hsp	Heat shock protein
IPTG	Isopropyl-β-D-thiogalactoside
LC-MS	Liquid chromatography-mass spectrometry
LDAO	Lauryldimethylamine- <i>N</i> -Oxid
MALDI-TOF-MS	Matrix assisted laser desorption/ionization-time of flight mass spectrometry
MEL	Mobile effector loop
MetAP	Methionylaminopeptidase
MWCO	Molecular weight cut off
NBD	7-Nitrobenz-2-oxa-1,3-diazol-4-yl
NCL	Native chemical ligation
NSF	<i>N</i> -ethyl-maleimide sensitive fusion protein
OD <sub>600</sub>	Optical density at 600 nm
Rab	Ras-like (protein) from Rat brain
Ras	Rat adeno sarcoma
REP	Rab escort protein
RP-HPLC	Reversed-phase high performance liquid chromatography
RRF	Rab recycling factor
RT	Room temperature
SDS	Sodium dodecyl sulfate
Sec	Secretory protein

---

SNAP	Soluble NSF attachment protein
SNARE	Soluble NSF attachment protein receptor
SPPS	Solid phase peptide synthesis
StBu	<i>S-tert</i> -butyl
TEV	Tobacco Etch Virus
TFA	Trifluoroacetic acid
T <sub>K</sub>	Krafft point
TX-100/TX-114	Triton X-100/Triton X-114
VAMP	Vesicle associated membrane protein
Xaa/Yaa	designates any amino acid residue
Yip	Ypt-interacting protein
Ypt	Yeast protein transport

One- and three-letter abbreviations for amino acids were used according to the recommendations of the International Union of Pure and Applied Chemistry (IUPAC) and the International Union of Biochemistry (IUB).<sup>[1]</sup>

# 1. Introduction

*“Things should be made as simple as possible,  
but not any simpler.”*

Albert Einstein

# 1. Introduction

## 1.1. Vesicular Transport

Controlled fusion and fission of biological membranes is essential for all forms of life. Eukaryotes in particular, due to a high degree of compartmentation, subcellular specialization and differentiation, require sophisticated mechanisms that ensure regulated and specific membrane turnover. Within cells, exo- and endocytosis as well as transfer between subcellular compartments are mediated by vesicular transport. Vesicle formation (budding), targeting to the destination membrane and fusion are controlled by a large number of proteins conserved throughout evolution.

Central to vesicle fusion is the mutual recognition of vesicular v-SNAREs and target t-SNAREs, forming very stable four-helical coiled-coil bundles (see Figure 1-1 inset)\*. The initial priming stage involves the disruption of *cis*-SNARE complexes (i.e. complexes formed between SNAREs located on the same membrane) by the ATPase NSF (*N*-ethyl-maleimide sensitive fusion protein) and its cochaperone  $\alpha$ -SNAP.<sup>[4]</sup> The activated SNAREs are then competent to form *trans*-SNARE complexes, resulting in a positioning of the vesicle in close proximity to the target membrane (docking). The progressive zipping of *trans*-SNARE complexes is finally believed to exert a mechanical force on the membranes via their transmembrane regions, resulting in pore formation and mixing of luminal contents.<sup>[5]</sup> Although purified SNAREs reconstituted into separate liposomes can alone mediate a fusion reaction on the order of minutes,<sup>[6]</sup> physiological fusion reactions, which often happen in the microsecond range, require additional accelerating factors. These probably include  $\text{Ca}^{2+}$  sensing proteins and associated factors (calmodulin, synaptotagmins, protein phosphatase 1) that trigger membrane fusion upon localized transient  $\text{Ca}^{2+}$  fluxes preceding every fusion reaction.<sup>[7,8]</sup> Studies of yeast homotypic vacuolar fusion recently identified the V0 part of the vacuolar ATPase to be activated by  $\text{Ca}^{2+}$ /Calmodulin and demonstrate formation of *trans*-V0 channels between the docked membranes.<sup>[9]</sup> Speculations that these protein channels radially expand and become the initial fusion pore are highly controversial, but could explain many observations from different fusion systems (discussed in <sup>[10,11]</sup>).

---

\* A new nomenclature classifies SNAREs according to invariant arginine (R) or glutamine residues (Q) present in the SNARE binding domains, which form the four helix bundle.<sup>[2,3]</sup>

The mostly unique intracellular localizations of SNARE family members and their specific interactions led to the formulation of the SNARE hypothesis,<sup>[12,13]</sup> that the formation of specific SNARE complexes between SNARE partners associated with the same transport step mediates vesicle docking at the correct target membrane. It now appears however, that SNARE pairing is rather promiscuous and that additional components have to ensure specificity by adding an extra layer of control.<sup>[14-17]</sup>

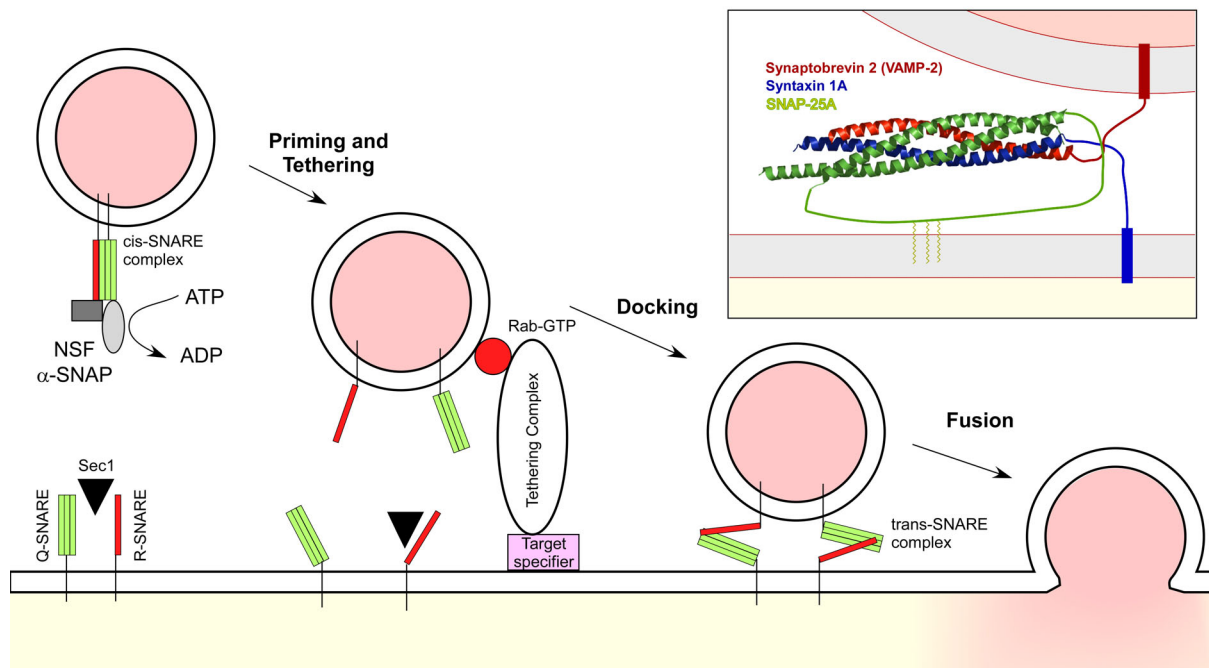


Figure 1-1: Vesicle fusion with target membranes can be biochemically dissected into 4 steps. Priming: The ATP-driven disruption of *cis*-SNARE complexes by NSF and α-SNAP. Tethering: Weak association between large tethering complexes mediated by Rab proteins. Docking: Strong association between v- and t-SNAREs leading to *trans*-SNARE pairing, initiated by Rab proteins. Fusion: membrane fusion triggered by zipper of SNAREs and associated regulatory proteins. Inset: A structural view on *trans*-SNARE pairing. Synaptobrevin 2 (VAMP-2, red, v/R-SNARE), Syntaxin 1A (blue, t/Q-SNARE) and SNAP-25A (green, t/Q-SNARE) form a four helical coiled-coil bundle (SNARE complex). Transmembrane and linker regions are drawn schematically.

### 1.1.1. Rab proteins

Rab proteins are small Ras-related GTP-binding proteins that are believed to be key regulators of vesicular transport. With more than 60 members identified in mammalian cells and 11 members in yeast (termed Ypt proteins and Sec4p) they form the largest group of the Ras superfamily.<sup>[18]</sup> Apparently, the increased complexity of vesicular transport routes inside mammalian cell types compared to lower eukaryotes resulted in a significant expansion of the Rab family.<sup>[19]</sup> Indeed, certain Rab proteins could be assigned to distinct compartments and transport steps present in all eukaryotes, whereas other Rab isoforms were found to participate in specialized fusion processes in differentiated cells. The number of rab proteins in the eukaryotic cell is dwarfed by the number of rab interacting proteins, reflecting the complexity of Rab controlled networks (for review see <sup>[20]</sup>). For example, more than 20 proteins were shown to be bound to Rab5 in its GTP bound form.<sup>[21]</sup>

As for other GTPases, central to Rab functioning is their ability to cycle between active GTP- and inactive GDP-bound conformations, thereby acting as molecular 'on/off' switches. In the active conformation Rab proteins recruit Rab effectors, a heterogeneous group of proteins, which exert various functions during vesicular transport. Rabs are converted into the inactive conformation by GTP hydrolysis, that leads to effector dissociation and Rab extraction from the membrane. The Rab protein is then recycled back to the donor compartment and reactivated by exchange of GDP for GTP. The combined cycles, i.e. GTP/GDP cycling and membrane association/cytosolic localization, are known as the Rab cycle, which is shown in Figure 1-2.

Several recent studies suggest a role of rab proteins and their effectors in vesicle formation.<sup>[22]</sup> For example, the mannose-6-phosphate receptor (MPR), which sequesters cargo proteins into budding clathrin-coated vesicles, was shown to bind indirectly to Rab9-GTP via its effector TIP47 (tail interacting protein of 47 kDa). It seems reasonable that the endosome specific Rab protein triggers the recruitment of TIP47 to MPRs in a organelle specific manner resulting in specific and efficient MPR recycling.<sup>[23]</sup> Besides assisting cargo incorporation into budding vesicles (see also <sup>[24]</sup>), Rabs might additionally define the destination of the budding vesicle by recruiting proteins necessary for subsequent docking and fusion steps.<sup>[25]</sup>

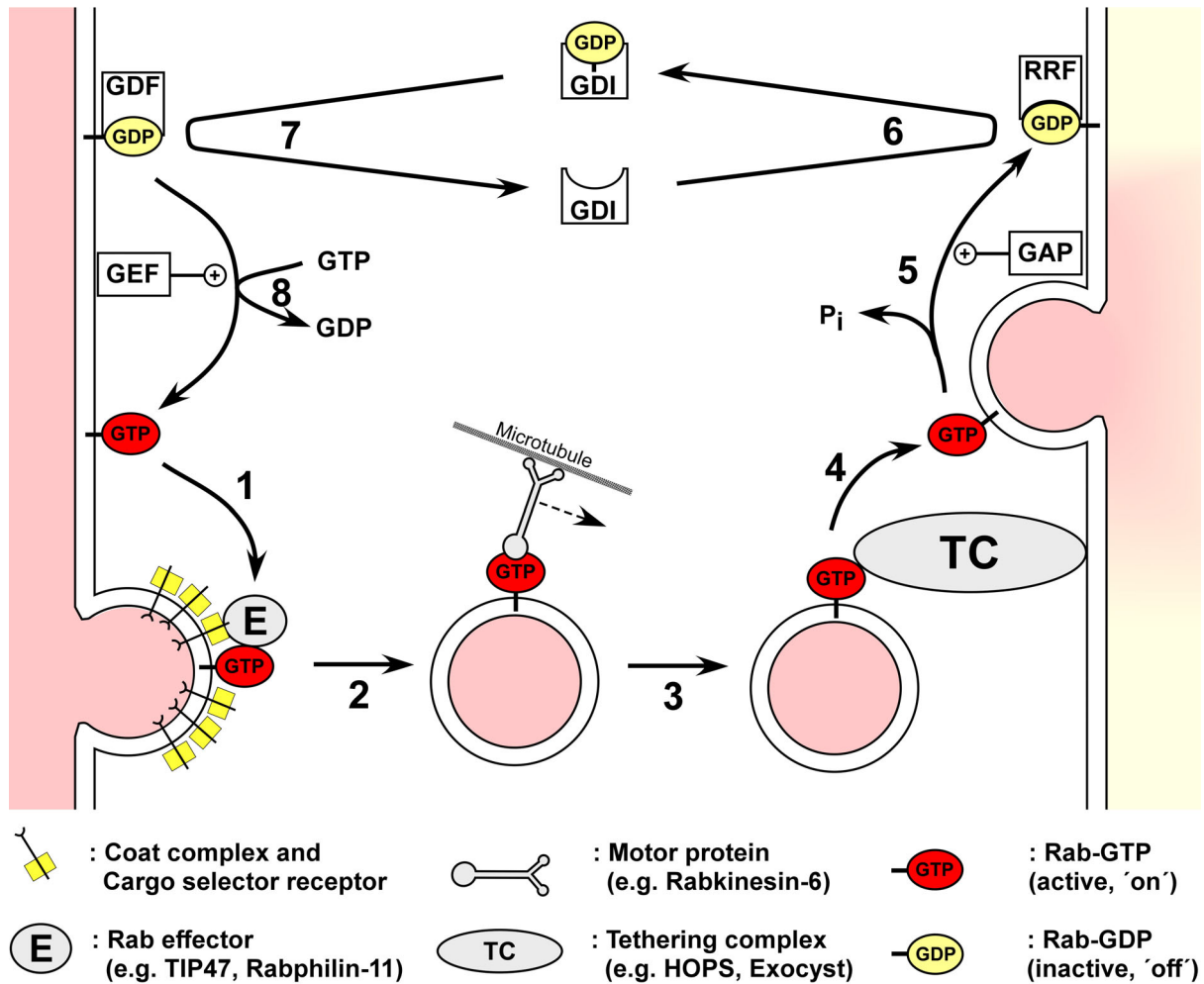


Figure 1-2: The Rab cycle. See text for a detailed description. E = effector, TC = tethering complex, GAP = GTPase activating protein, RRF = Rab recycling factor, GDI = GDP dissociation inhibitor, GDF = GDI displacement factor, GEF = guanine nucleotide exchange factor.

Following vesicle formation, at least some Rabs link transport vesicles to the cytoskeleton via kinesin/dynein-like motor-proteins, which confer actively directed vesicle movement along these structures.<sup>[26,27]</sup> Rab6 has been shown to interact directly with a kinesin-like effector protein, termed Rabkinesin-6, which probably acts as a microtubule plus-end directed motor and has been implicated in cytokinesis during mitosis.<sup>[28,29]</sup> Another well studied example involves the interaction of Rab27a with Myosin Va via melanophilin, the potential Rab27a effector.<sup>[30]</sup> Myosin Va is believed to tether melanosomes to the actin cytoskeleton, which actively retains these organelles near the cell periphery of melanocytes, where they are eventually transferred to keratinocytes for proper skin and hair pigmentation.<sup>[31,32]</sup> This model is supported by several mutations in Rab27a<sup>[33]</sup> and Myosin Va<sup>[34]</sup> that lead to Griscelli Syndrome, a rare inherited disorder of pigmentation arising from the arrest and the

accumulation of melanosomes in the perinuclear region of melanocytes, that is accompanied by severe immunological or neurological defects (see <sup>[35]</sup> for review).

When the transport vesicle approaches its target membrane (Figure 1-2, step 3), Rab proteins initiate the assembly of tethering complexes by interacting with soluble effector proteins.<sup>[36,37]</sup> Tethering effectors fall into two main classes: A group of proteins forming extended homodimeric coiled-coil structures (e.g. EEA1, Uso1p, p115) and oligomeric complexes (e.g. HOPS, Exocyst, TRAPP and COG-complexes).<sup>[38,39]</sup> Although the details of their functioning remains elusive, most of them could be assigned to a distinct transport step and were shown to bind to Rabs and membranes.<sup>[40,41]</sup> Apparently, tethering complexes and Rabs precede *trans*-SNARE pairing representing the first specificity determinant during vesicle fusion. Moreover, Rabs and the tethering complexes might either directly or indirectly trigger SNARE pairing and subsequent fusion, as can be inferred from their numerous interactions with components of the SNARE fusion machinery (e.g. with NSF,<sup>[42]</sup> Sec1-like proteins,<sup>[43]</sup> or SNAREs directly,<sup>[44-46]</sup> discussed in <sup>[47]</sup>).

Rab GTP hydrolysis is not obligatory for fusion,<sup>[48,49]</sup> rather the rate of nucleotide hydrolysis seems to define the timeframe for rab effector recruitment and therefore influences the progression of tethering, docking and fusion steps (but see also <sup>[50]</sup> for an alternative model). Hence, the steady-state level of activated Rab-GTP regulates the extent of fusion reactions and is, not surprisingly, highly regulated by additional factors. For example some of the above mentioned tethering complexes were shown to preserve the GTP bound state, thereby locking Rabs in the activated state by either promoting GDP to GTP exchange<sup>[51]</sup> or inhibiting GTPase activating protein (GAP) induced GTPase activity.<sup>[52]</sup> Following fusion, Rab proteins are inactivated by GTP hydrolysis stimulated by GAPs, which converts them back to their GDP bound form (see <sup>[53]</sup> for a review of this class of proteins).<sup>[54,55]</sup> Rab-GDP is targeted by Rab GDP-dissociation inhibitor (RabGDI), which upon binding inhibits Rab reactivation<sup>[56]</sup> and extracts them from the membrane into the cytosol.<sup>[57]</sup> It is likely that this step is mediated by additional factors, termed Rab recycling factors (RRFs).<sup>[58]</sup> One potential RRF candidate essential for Rab3A membrane extraction at the synapse was recently identified as a heat shock protein (Hsp) complex, consisting of Hsp90, Hsc70 and cysteine string protein (CSP).<sup>[59]</sup> RabGDI delivers Rab proteins back to the donor membrane, consequently ensuring efficient Rab recycling.<sup>[60,61]</sup> The delivery process (Figure 1-2, step 7) probably involves proteins termed GDI displacement factors

(GDFs), that serve as the membrane receptor for Rabs and are believed to be key for the Rab compartment specific localisation.<sup>[62]</sup> Although the above mentioned Hsp complex might potentially also serve as a GDF,<sup>[59]</sup> the precise identity of GDFs has remained elusive, hindering a deeper understanding of the process. Recently, human Yip3p (PRA-1) was shown to catalytically displace RabGDI and to specifically recruit endosomal Rabs to reconstituted liposomes.<sup>[63]</sup> Yeast Yip (Ypt-interacting protein) family members (analogs exist in mammals, termed prenylated Rab acceptor (PRA)) were initially identified as proteins that can interact with Rabs in either their GDP or GTP bound state<sup>[64]</sup> and with each other,<sup>[65,66]</sup> and some members were found to be essential for yeast viability and vesicular transport.<sup>[67]</sup> Although the assigned GDF activity offers an interesting model for Yip mediated Rab recruitment, additional interactions with other components of the fusion machinery (e.g. with SNAREs<sup>[64]</sup> and vesicle coat proteins<sup>[68]</sup>) suggest a broader role for Yips in vesicular transport, which needs to be addressed.<sup>[69]</sup> Upon membrane binding, Rabs are converted to the active form by GDP to GTP exchange mediated by guanine nucleotide exchange factors (GEF) and the cycle starts again.<sup>[60,61]</sup> Interestingly, Rab activation seems often to be spatially and temporally restricted to the site of function, which is supported by the finding that numerous GEFs are in fact members of large protein complexes, that act also as rab effectors.<sup>[70,71]</sup>

### 1.1.2. The structural basis of Rab function

Rab GTPases contain conserved sequence elements that mediate GDP/GTP binding, effector recognition and subcellular localization. Although distantly related to Ras and other small GTPases (< 30 % amino acid overall identity), they share short highly conserved motifs, termed PM and G motifs, which participate in phosphate/magnesium and guanine base binding, respectively (see Figure 1-3B,C).<sup>[72]</sup> The Rab structural fold is similar to all small GTPases of the Ras superfamily (also referred to as the GTPase-fold) consisting of a six stranded beta sheet surrounded by five alpha helices.<sup>[73,74]</sup> Conformational changes accompanying GTP to GDP hydrolysis and  $\gamma$ -phosphate release, as originally observed in Ras,<sup>[75,76]</sup> were also recently confirmed for Rab proteins,<sup>[77-79]</sup> although significant variations exist, which might explain differences in the rates of GTP hydrolysis and GDP exchange. These regions of major conformational changes, were termed switch I and switch II and form the  $\beta$ ,  $\gamma$ -phosphate-magnesium ion binding pocket together with

the so called P-loop (Figure 1-3A). As mentioned above, key to Rab functioning is their participation in numerous interactions with upstream regulators and downstream effector molecules. The interacting proteins were proposed to recognize the correct nucleotide bound state by binding to switch I (also known as effector domain) and switch II regions based on genetic and functional studies employing mutant chimeric Rab proteins.<sup>[80,81]</sup> Further extensive sequence analysis studies revealed the presence of five Rab family motifs (RabF1-5) and four Rab subfamily motifs (RabSF1-4), that localize mainly around switch I and II and are conserved among different species (Figure 1-3B-D).<sup>[18,82]</sup> RabF motifs can be used for unambiguous identification of Rab proteins, whereas RabSF motifs determine the relatedness to one of the ten Rab subfamilies.

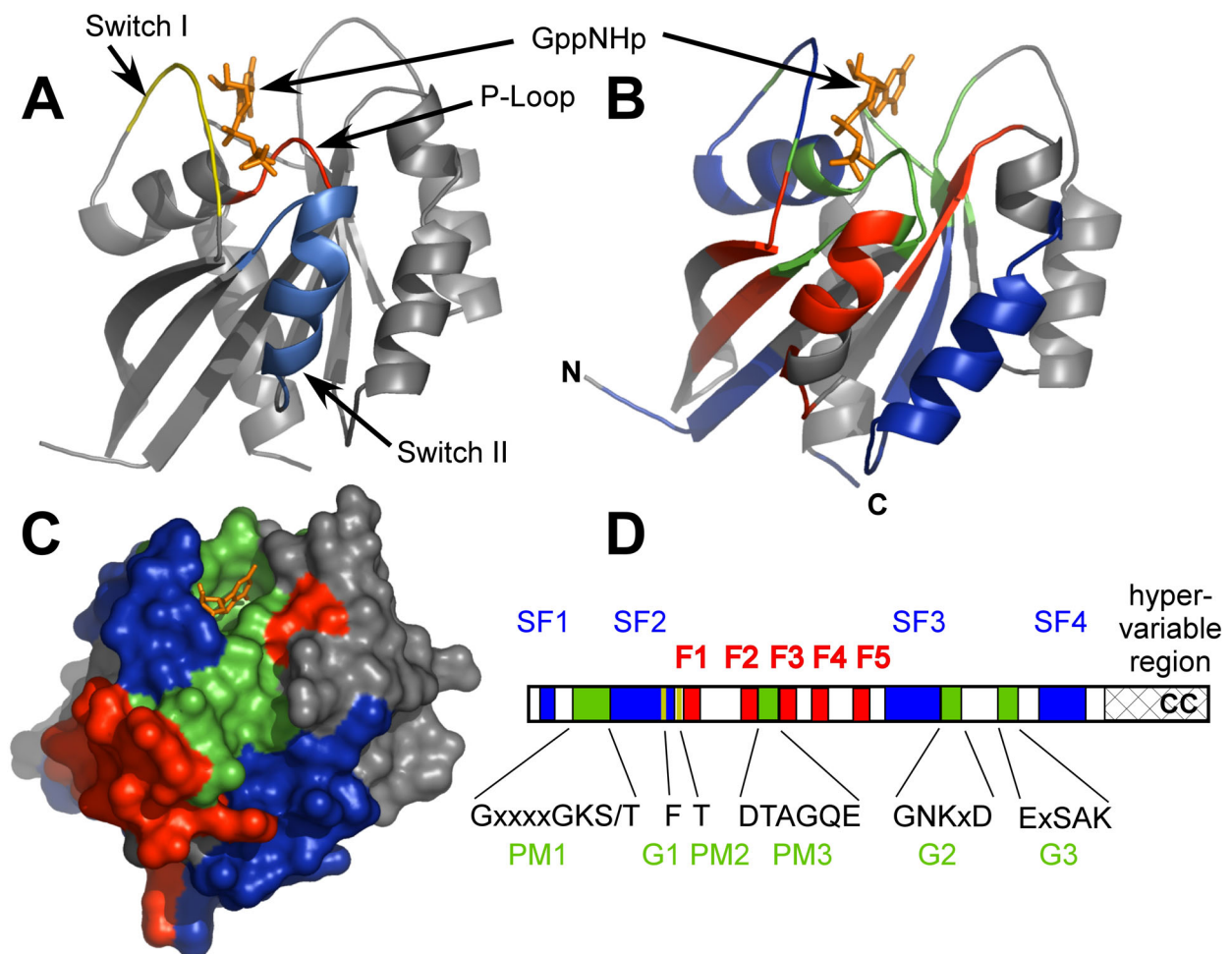


Figure 1-3: Structural features of Rab proteins. **A)** Ribbon representation of Rab3 (PDB entry code 3RAB) complexed with GppNHp (colored orange).<sup>[73]</sup> Switch I (yellow), Switch II (blue) and the P-Loop are indicated. **B)** Location of PM and G motifs (green), Rab family motifs (F, red) and Rab subfamily motifs (SF, blue). **C)** Surface representation of B. **D)** Organization of the identified motifs along the primary sequence. CC represents the prenylation motif.

Concerning the binding of interacting proteins, RabF motifs were proposed to be mainly recognized by general Rab regulators (such as GDI and REP, see below), whereas specific interactions with a certain subset of Rabs additionally require RabSF regions (e.g. most Rab-effector interactions and to some extent GEFs and GAPs). Confirmation of this model comes from several mutagenesis studies (e.g. [83]) and the structure of Rab3a complexed to the effector domain of Rabphilin-3A.[84] Although several Rabs are now structurally characterized,[85-88] this remains the only known Rab:effector structure. Given the numerous interactions Rabs participate in, the lack of structural information is striking. Another important structural feature of Rab proteins was identified by Chavrier et al.[89,90] and termed hypervariable region which comprises ca. 30 amino acid residues in the C-terminal region (Figure 1-3D). This region is presumed to serve as a targeting signal for the subcellular localization of Rab proteins and is at least in some cases subject to additional regulation. For example, phosphorylation within the hypervariable region of Rab4 during mitosis was shown to prevent membrane recruitment leading to accumulation of Rab4 in the cytosol.[91,92]

Adjacent to the hypervariable region, directly at or near the C-terminus, hydrophobic geranylgeranyl isoprenoids are post-translationally attached to conserved cysteine residues.[93] This modification mediates the reversible attachment of Rab proteins to membranes and is essential for proper Rab functioning.[94]

### 1.1.3. Rab geranylgeranylation

Geranylgeranylation of Rab proteins is a posttranslational process catalyzed by Geranylgeranyltransferase type II (GGTase-II or RabGGTase), which transfers geranylgeranyl moieties from geranylgeranylpyrophosphate (GGPP) to C-terminal cysteine residues linking them via stable thioether bonds (Figure 1-4A).[95] GGTase-II belongs to the family of protein prenyltransferases together with Farnesyltransferase (FTase) and GGTase-I, which act on Ras and Rac/Rho GTPases, respectively.[96] FTase and GGTase-I are also known as CaaX prenyltransferases. The term refers to the short C-terminal substrate sequences recognized by both enzymes, where 'C' stands for the cysteine which is to be modified, 'a' designates an aliphatic residue and the identity of 'X' determines whether 'C' will be farnesylated by FTase (X = Ala, Gln, Met, Ser) or geranylgeranylated by GGTase-I (X = Leu).[95,97,98] In contrast, Rab prenylation motifs are more heterogenic including terminal CXC, CC,

CCX, CCXX and CCXXX sequences,<sup>[99,100]</sup> where both cysteines are modified by GGTase-II.<sup>[101]</sup> Rab proteins terminating with CXC sequences are additionally methyl esterified by an *S*-adenosyl-L-methionine (SAM) dependent enzyme activity following the prenylation reaction.<sup>[102-104]</sup>

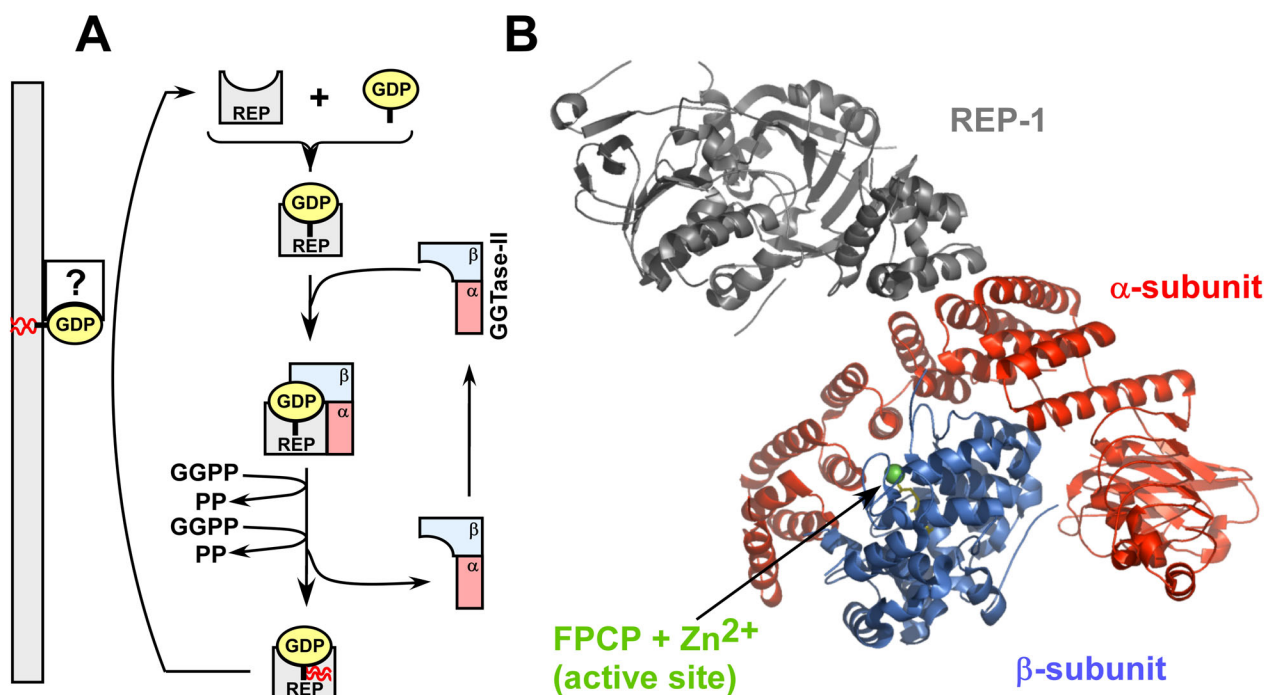


Figure 1-4: GGTase-II catalyzed geranylgeranylation of Rab proteins. **A**) Simplified reaction scheme (classical pathway). Rab-GDP, REP-1 and GGTase-II form a ternary complex. Prenyl groups are transferred in two consecutive reactions from GGPP to Rab. Another molecule of GGPP dissociates the double prenylated ternary complex (not shown) and Rab is delivered to membranes by the action of REP. **B**) Structure of the complex between GGTase-II ( $\alpha$  and  $\beta$  subunit are colored red and blue, respectively. PDB entry code 1LTX), REP-1 (grey) and farnesylphosphonylmethylphosphonate (FPCP, analog of farnesylpyrophosphate, green).<sup>[105]</sup> REP can associate with GGTase-II in an isoprenoid pyrophosphate dependant manner without prior binding to Rab (alternative pathway).<sup>[106]</sup>

GGTase-II consists of two subunits ( $\alpha$  and  $\beta$ ) forming a heterodimer of ca. 100 kDa that requires  $Zn^{2+}$  and  $Mg^{2+}$  for activity (Figure 1-4B).<sup>[107,108]</sup> In contrast to the other prenyltransferases, GGTase-II additionally requires a protein cofactor, originally termed component A, that was later identified as the product of the choroideremia (CHM) gene and eventually renamed as rab escort protein (REP).<sup>[107,109,110]</sup> REP associates with the unprenylated Rab protein preferentially in its GDP bound form<sup>[111-113]</sup> and facilitates its recognition by the catalytic GGTase  $\alpha/\beta$ -heterodimer (Figure 1-4A).<sup>[110,114,115]</sup> Upon ternary complex formation, GGTase-II transfers both isoprenoids in two independent, consecutive reactions, with the monoprenylated intermediate being strongly bound to the enzyme.<sup>[116,117]</sup> Following double prenylation, binding of another GGPP molecule triggers release of the prenylated

Rab:REP complex<sup>[118]</sup> and Rab is delivered to the membrane with assistance of REP.<sup>[119]</sup> Two ubiquitously expressed isoforms of REP have been identified in mammalian cells (REP-1 and REP-2),<sup>[120]</sup> whereas only a single protein mediates Rab prenylation in yeast (named Mrs6p or Msi4p).<sup>[121]</sup> Loss of REP-1 function has been linked to choroideremia (CHM), an X-linked inherited disease characterized by progressive retinal degeneration leading to complete blindness in adults.<sup>[109,122]</sup> The molecular mechanism underlying CHM was proposed to involve inefficient prenylation of certain Rabs due to malfunctioning of REP-1, which cannot be compensated by the REP-2 isoform. Although, Rab27a was found to accumulate unprenylated in CHM cells,<sup>[123]</sup> its role in CHM is under intensive debate.<sup>[124]</sup> For example Rab27a is widely expressed in several tissues unaffected in CHM patients, and its malfunction has been convincingly linked to Griscelli syndrome (see above) giving rise to symptoms not observed in CHM patients.

Interestingly, REP and RabGDI (see above) share approximately 30 % sequence identity and are structurally and functionally related.<sup>[105,109]</sup> Both proteins form the RabGDI/CHM family,<sup>[125]</sup> can bind prenylated Rabs preferentially in their GDP bound state, inhibit GDP release from the GTPase domain and can deliver the Rab proteins to their proper membrane site. However, RabGDI cannot replace REP in the prenylation reaction due to its low affinity for unprenylated Rabs,<sup>[126]</sup> whereas REP cannot functionally replace RabGDI's ability to extract Rab proteins from membranes. Consequently both proteins are not functionally interchangeable as was demonstrated by complementation experiments performed in yeast.<sup>[121,127]</sup>

In summary, geranylgeranylation is believed to be crucial for the proper functioning of all Rab proteins. On a molecular level the role of the lipids seems to be at least two-fold: First, the geranylgeranyl groups are integral components of Rab interactions with other regulatory proteins. Currently several factors are known, that require prenylation for productive binding to Rab proteins: RabGDI,<sup>[126]</sup> several members of the Yip family<sup>[65,128]</sup> (including PRA-1<sup>[64,129]</sup>), Rab3-GAP<sup>[130]</sup> and Rab3-GEF.<sup>[131]</sup>

Secondly, the hydrophobic isoprenoids mediate the essential membrane attachment of Rab proteins, probably by inserting into the lipid bilayer. Unprenylated Rabs cannot associate with membranes and are intracellularly restricted to the cytosol where they cannot fulfill their biological role. It is noteworthy, that the precise role of the lipid and the prenylation motif in Rab membrane targeting (beside the hypervariable region) is controversial: Recent studies suggest that double prenylation is required for correct

localization of Rab proteins to their characteristic subcellular target membrane, whereas single prenylated Rabs are mistargeted and appeared to be nonfunctional.<sup>[132,133]</sup> In contrast, Overmeyer et al. reported correct targeting of single prenylated Rab1.<sup>[134]</sup> Moreover, complete replacement of the prenylation motif by a transmembrane helix was found not to impair vesicular transport.<sup>[135]</sup> A consistent explanation of these findings is hindered by the complicated *in vivo* situation associated with GGTase-I and -II mediated prenylation reactions and the potentially pleiotropic effects of the significant structural modifications of the GTPase that were used to study these processes.

On the other hand, many *in vitro* studies of Rab proteins are dependent on the availability of the posttranslationally modified form. In order to obtain prenylated Rabs, these are traditionally expressed and purified from animal tissues or from insect cell cultures infected with recombinant baculovirus. These methods generally suffer from low yields and inflexibility regarding the lipid modification. Both disadvantages could be bypassed by an alternative approach, which makes use of chemical protein synthesis instead of utilizing the often rigid and limiting cellular machinery.

## 1.2. Chemical protein synthesis

The idea of producing and engineering proteins via total synthesis continues to attract considerable attention since the development of solid-phase peptide synthesis (SPPS) by Merrifield.<sup>[136]</sup> The advantage of varying the covalent (primary) structure of proteins without limitations is generally believed to facilitate a better understanding of structure-function relationships.

Indeed, Merrifield's stepwise SPPS was used to assemble ribonuclease A,<sup>[137]</sup> growth factors (e.g. <sup>[138]</sup>) and HIV-1 protease.<sup>[139]</sup> In the case of HIV-1 protease, further studies enabled important insights into the structure of the molecule, both unliganded<sup>[140]</sup> and as complexes with substrate-derived inhibitors.<sup>[141]</sup> Additionally, backbone engineering and site specific labeling with NMR probe nuclei shed light on the aspartyl protease catalytic mechanism.<sup>[142,143]</sup>

Despite of its utility for studying small proteins (< 100 AA), stepwise SPPS has serious drawbacks: Poor solvation and formation of secondary structures of the growing, fully protected peptide chain may significantly reduce the efficiency at each synthetic step resulting in the accumulation of byproducts. In contrast to stepwise

SPPS, convergent synthesis uses the assembly of protected peptide fragments to prepare proteins. Although some larger proteins have been prepared using this strategy (GFP, 238 AA),<sup>[144]</sup> convergent synthesis suffers from poor solubility of protected peptides, low reaction rates and potential epimerization (racemization). Alternatively, chemoselective ligations have been developed, which allow linking of *unprotected* peptide fragments.

### 1.2.1. Chemoselective ligation approaches

Figure 1-5 presents some of the most popular and elegant reactions employed by synthetic organic chemistry known to date. With the exception of reaction A, they all rely on an initial capture step (either thioester- or imine-capture), which provides the entropic activation for the following intramolecular amine acylation step.<sup>[145,146]</sup> Chemoselective ligation was made more attractive by native chemical ligation (NCL) and, more recently, by a variation of the Staudinger reaction, both generating a native peptide bond at around neutral pH (Figure 1-5D,E).

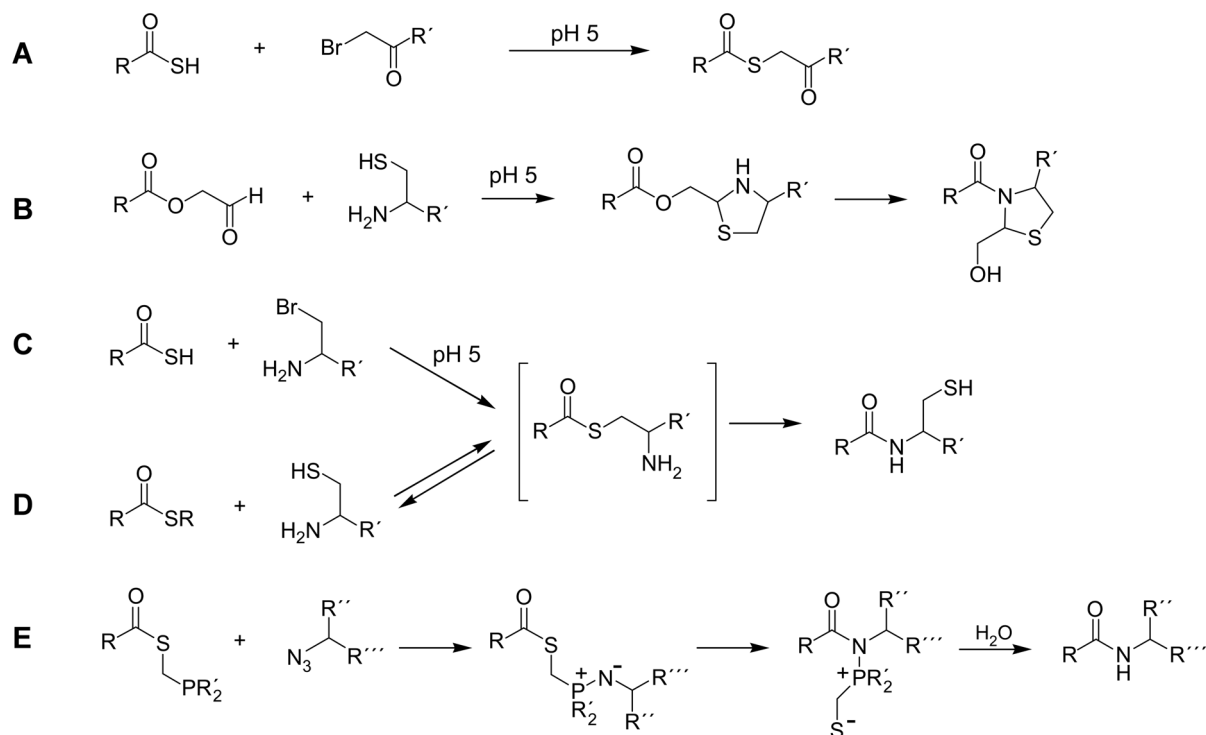


Figure 1-5: Selection of chemoselective coupling reactions for coupling of unprotected polypeptides in aqueous solution. **A**) Thioester forming ligation.<sup>[142]</sup> **B**) Imine-capture followed by tautomerization and pseudoproline formation.<sup>[147]</sup> **C**) Cystein ligation via thioalkylation capture of bromoalanine.<sup>[148]</sup> **D**) Cystein ligation through thioester capture by thiol-thioester exchange (native chemical ligation).<sup>[149]</sup> **E**) Staudinger ligation.<sup>[150,151]</sup>

The initial thiol-thioester exchange step in NCL is fully reversible, whereas the second acylation step is irreversible under the conditions used. Therefore, only the desired amide is formed, even in the presence of unprotected internal cysteine residues. In contrast, reactions A to C require acidic conditions or protection of internal cysteine residues (lysine in the case of B) to minimize side reactions. First described by Wieland,<sup>[152]</sup> NCL is restricted to peptide ligation sites at an Xaa-Cys bond, formed by reacting peptide fragments carrying either a C-terminal (Xaa-)  $\alpha$ -thioester or an N-terminal cysteine residue (Figure 1-5D).

Due to the naturally low abundance and often irregular distribution of cysteine residues in proteins, numerous approaches were tried to overcome this limitation. For example, the development of N-linked thiol auxiliary groups, which can be removed after peptide ligation, in principle<sup>†</sup> extended the applicability of NCL to any Xaa-Yaa peptide bond.<sup>[155,156]</sup>

NCL has been widely used in the total synthesis of small proteins and protein domains (reviewed by <sup>[157]</sup>), but its utility was significantly broadened by the demonstration that both essential components (C-terminal  $\alpha$ -thioester and N-terminal cysteine residue containing fragments) can be produced recombinantly. Whereas cysteine belongs to the 20 genetically encoded amino acids, activated thioesters are naturally rare, but have recently been shown to be key intermediates in the intein mediated splicing reaction of proteins.

### 1.3. Inteins

Inteins were first identified by two groups in 1990 as protein insertion sequences that are flanked by host protein sequences (N- and C-exteins) and must be removed by a posttranslational process termed protein-splicing.<sup>[158,159]</sup> In analogy to RNA splicing, the intervening intein sequence is precisely excised, and the flanking N- and C-exteins are joined by a normal peptide bond. So far more than 130 inteins were identified in eubacteria, archaea and lower eukaryotes including fungi and algae (InBase,<sup>[160]</sup> <http://www.neb.com/neb/inteins.html>). According to Evans and Xu<sup>[161]</sup> inteins can be divided into four basic classes:

---

<sup>†</sup> For unknown reasons, C $_{\alpha}$ -sterically hindered amino acids gave very poor ligation yields with any of the reported auxiliaries linked to the amino group. Therefore this approach, so far, is restricted to Xaa-Gly/Ala ligation sites.<sup>[153,154]</sup>

A. Maxi-inteins (or bifunctional inteins, Figure 1-6) have the typical N- and C-terminal splicing domains interrupted by a homing endonuclease, which permits intein spread to inteinless genes via a homing mechanism.<sup>[162]</sup>

B. Mini-inteins were first generated by removing the endonuclease domain at the gene level, demonstrating that protein splicing domains alone were sufficient for protein splicing. A naturally occurring mini-intein was discovered later in the *Mycobacterium xenopi gyrA* gene.<sup>[163]</sup>

C. Split-inteins (or *trans*-splicing inteins) lack a covalent linkage between their N- and C-terminal splicing domains. The two intein sequences reconstitute a functional intein which can undergo protein *trans*-splicing *in vitro*<sup>[164-166]</sup> and *in vivo*.<sup>[167]</sup>

D. Alanine-inteins possess an alanine residue instead of the catalytic important cysteine/serine residue at the N-terminal splice junction and bypass the first step in the protein splicing mechanism.<sup>[168]</sup>

Although the biological role of inteins and protein splicing remains unclear, the mechanism underlying this process has been studied and exploited extensively.

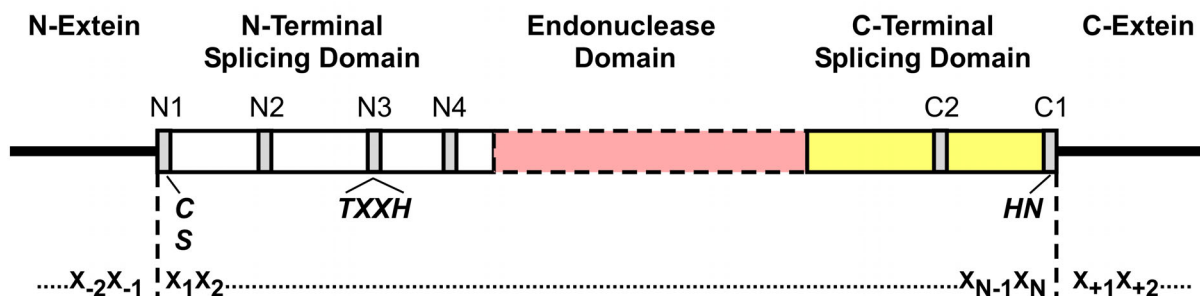


Figure 1-6: Schematic illustration of the intein structure: Amino acid numbering system, primary sequence motifs, conserved residues and domain organization are indicated. An X stands for a nonconserved residue.

### 1.3.1. Protein splicing mechanism

With the exception of the alanine-inteins,<sup>[168]</sup> protein splicing consists of four concerted reactions of which the first three are selfcatalyzed<sup>‡</sup> by the intein (Figure 1-7).

The first step is activation of the N-terminal splice junction. An N→S (O) acyl rearrangement at cysteine 1 (serine 1) moves the N-extein to the side-chain forming a linear (thio-)ester intermediate (for amino acid numbering see Figure 1-6).<sup>[170]</sup>

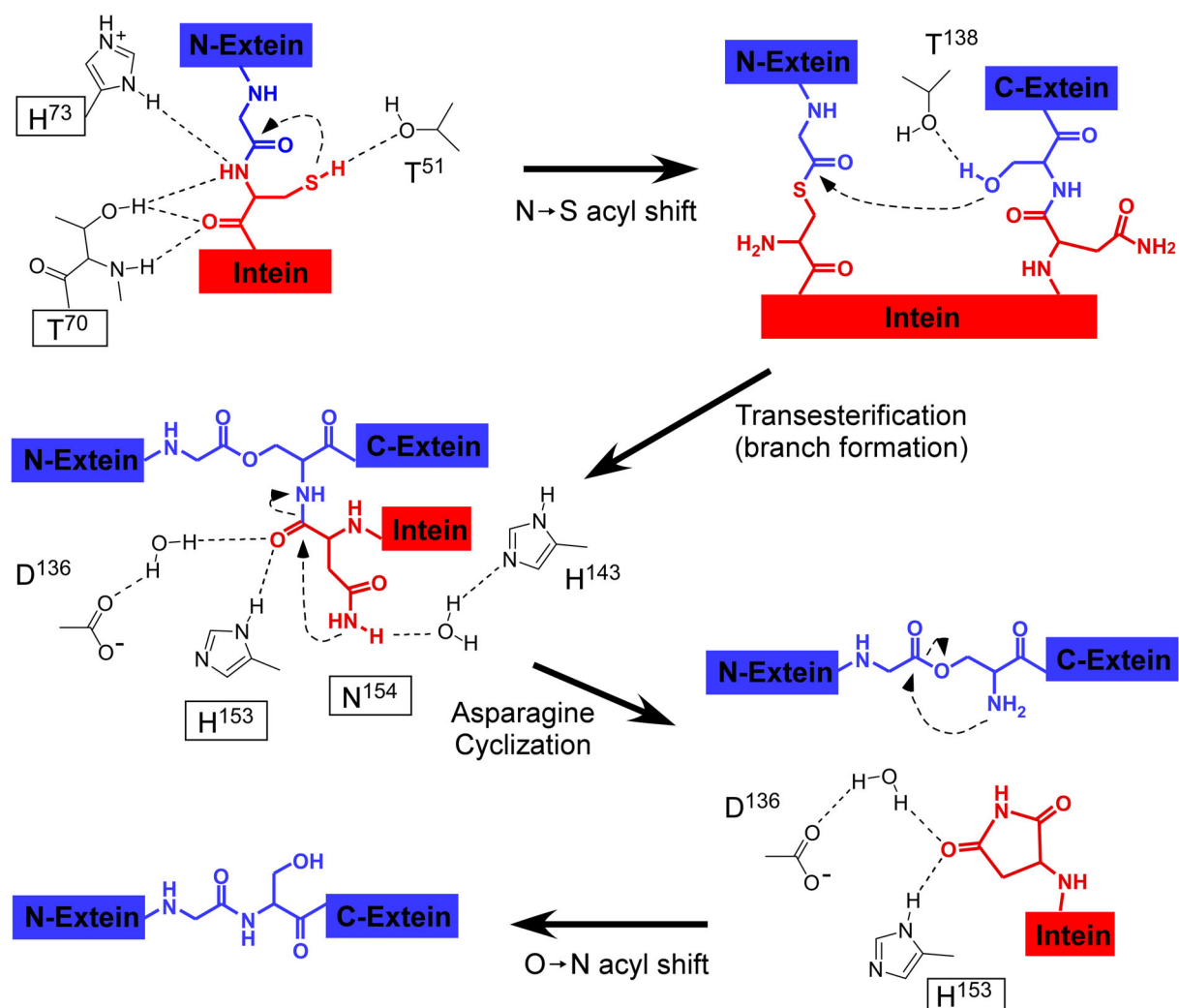


Figure 1-7: Protein splicing mechanism for the *Synechocystis* sp. DnaB intein. Blue and red represent extein and intein residues respectively. Active site residues are colored black. Highly conserved residues are Thr<sup>70</sup>, His<sup>73</sup>, His<sup>153</sup> and Asn<sup>154</sup>. See text for description. Modified from Ding et al.<sup>[175]</sup>

<sup>‡</sup> The term self-catalyzed might be contradictory since the catalyst (the intein) is not regenerated in a form capable of performing additional reaction cycles. However, inteins display several features (e.g. substrate specificity, stabilization of reactive intermediates) characteristic of classical enzymes and may be viewed as primitive enzymes.<sup>[169]</sup>

Next, trans(thio-)esterification occurs when the activated thioester is attacked by the sulfhydryl (hydroxyl) group of cysteine+1 (serine+1) resulting in cleavage at the N-terminal splice junction and formation of a branched intermediate.<sup>[171]</sup> The branch is resolved by cyclization of the conserved intein C-terminal asparagine forming a succinimide.<sup>[172,173]</sup> The release of the intein leaves the N-extein attached to the side chain of cysteine+1 (serine+1) via a thioester (ester) bond, which is resolved by a spontaneous S(O)→N acyl transfer linking the N- and C-exteins via a native peptide bond.<sup>[174]</sup> The outlined mechanism is supported by extensive mutagenesis and structural studies, which enabled the precise manipulation of certain reaction steps and demonstrated that these can occur independently of each other.<sup>[176,177]</sup> Although protein splicing mediated by inteins inserted between foreign exteins is generally less efficient than splicing in the native context,<sup>[171]</sup> splicing has no strict sequence requirements in either of the exteins, except for the extein residues directly adjacent to the cleavage sites (Xaa-1/+1). This promoted the application of inteins as protein engineering tools, including the use of split inteins for protein head-to-tail cyclization,<sup>[178,179]</sup> segmental isotopic labeling to extend NMR analysis to larger proteins,<sup>[180,181]</sup> protein *in-vivo* labeling<sup>[182]</sup> and for detecting protein-protein interactions.<sup>[183,184]</sup> One of the earliest application of modified inteins, however, was based on their ability to generate thioester-tagged proteins for NCL.

#### 1.4. Expressed protein ligation and protein semi-synthesis

Expressed protein ligation (EPL) is a variation of NCL in which one or more of the peptide segments used to assemble a protein is produced recombinantly, permitting synthetic peptides to be chemo- and regioselectively coupled to recombinant proteins.<sup>[185-187]</sup> EPL combines the structural flexibility of chemical (peptide) synthesis with the ability of recombinant DNA methodologies to generate large polypeptides (proteins), thereby enabling the semi-synthesis of much larger proteins.

As shown in Figure 1-8,  $\alpha$ -thioester derivatives of recombinant proteins can be prepared by thiolysis of mutated intein fusions. In this case the target protein is fused to the N-terminus of a modified intein, which cannot undergo C-terminal cleavage.<sup>[172]</sup> The intein catalyzes an N→S acyl shift leading to a linear thioester linked intermediate, which can be cleaved by transthioesterification with thiol containing compounds, liberating the  $\alpha$ -thioester tagged protein. Commercially available

systems additionally use affinity tags (mainly chitin-binding domain (CBD)), which allow facile affinity purification and inducible self-cleavage of expressed proteins.<sup>[188]</sup>

If the  $\alpha$ -thioester fragment is accessible by total synthetic means (< 50 AA), several protocols employing Boc- or Fmoc-based SPPS are now established and were recently discussed in detail by Hofmann and Muir.<sup>[189]</sup>

In contrast, preparation of recombinant proteins bearing an N-terminal cysteine is often more complicated and always involves specific removal of an N-terminal leader sequence from a precursor protein. Proteolytic cleavage of an expressed protein precursor with the cysteine residue adjacent to a protease cleavage site was demonstrated by *in vitro* processing with tobacco etch virus (TEV) protease<sup>[190]</sup> and Factor Xa protease,<sup>[191,192]</sup> as well as *in vivo*, utilizing endogenous methionylaminopeptidase (MetAp).<sup>[193]</sup> Unfortunately, unspecific and often inefficient proteolysis and the requirement for a further purification step restrict the general applicability of these methods.

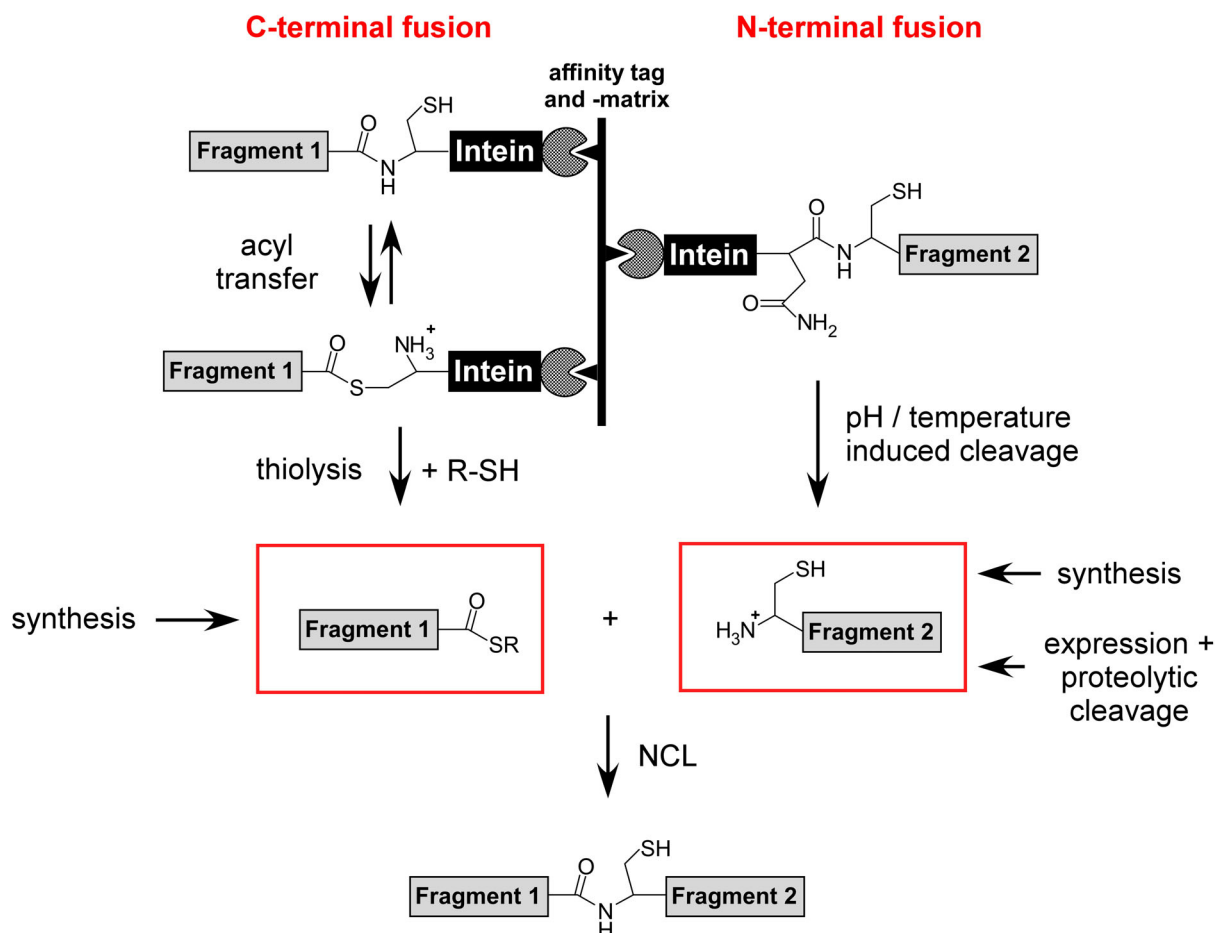


Figure 1-8: Basic concept of EPL. Recombinantly expressed proteins bearing a C-terminal thioester or an N-terminal cysteine can be prepared by fusion to and subsequent cleavage of engineered inteins. The isolated fragments are ligated in a manner similar to NCL.

As an alternative, C-terminal cleavage of Cys1Ala mutant inteins (which cannot undergo N-terminal cleavage) can be induced by a change in pH or temperature (see Figure 1-8.).<sup>[194]</sup> The target protein starting with a cysteine residue is fused to the C-terminus of a CBD-intein construct. Upon affinity purification and induction of splicing, the target protein carrying the N-terminal cysteine is released from the chitin column. Although no exogenous protease is required, spontaneous (even *in vivo*) cleavage may result in premature loss of the intein and the associated affinity tag. In summary, protein splicing and its modulation provide the means for site-specific and genetically codeable labeling of recombinant proteins, which can be further exploited by EPL or other techniques.

Since its introduction, EPL has been applied to many different proteins (reviewed by <sup>[195]</sup>). In many cases, site-specific introduction of probes such as fluorophores, isotopes, affinity tags, posttranslational modifications or unnatural amino acids permitted the exploration of important functional questions. Most applications aim at modifications located within ~ 50 residues of the N- or C-terminus, which allows target molecule assembly from two fragments, one synthetic and one recombinant. Furthermore, sequential EPL strategies (i.e. the ligation of three or more fragments) offer the possibility to modify any residue within the entire primary protein sequence.<sup>[196,197]</sup>

## **2. Aims of the project**

“Nature is wont to hide herself.”

Heraclitus

## 2. Aims of the project

The recent advances in the field of intein chemistry paved the way for the application of methods of synthetic organic chemistry to the modification of large proteins. Such a symbiosis of chemistry and biology can be considered to be extremely useful, for the generation of proteins, difficult or impossible to obtain by purely recombinant methods. For several reasons, prenylated Rab proteins represent ideal targets for a semi-synthetic strategy, as for example depicted in Figure 2-1. Such an approach, based on expressed protein ligation (EPL), would allow the production of geranylgeranylated proteins from two polypeptide fragments: a large, C-terminally truncated and unprenylated precursor fragment generated by recombinant techniques, and a short prenylated peptide derived from total synthesis, which completes the Rab C-terminus upon ligation.

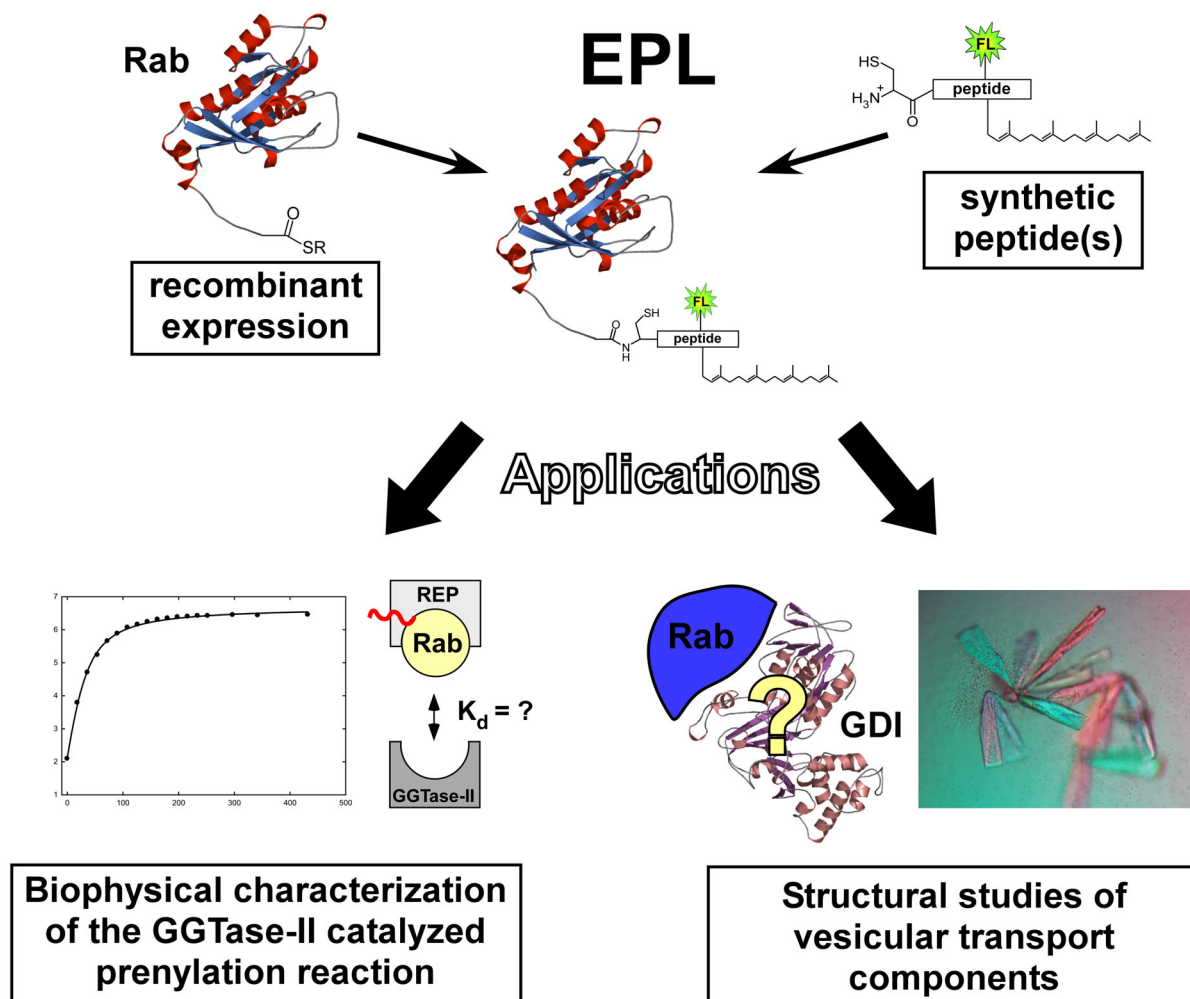


Figure 2-1: Expressed protein ligation (EPL) for the production of prenylated Rab GTPases. The approach permits the coupling of recombinantly derived thioester-tagged proteins to synthetic peptides. The lower part of the figure shows some applications of such proteins, which were explored in this study.

If applicable on a routine basis, the approach would circumvent many problems inherent to conventional expression and purification systems (see Chapter 1.1.3.). Furthermore, the power of organic chemistry to incorporate virtually any structure into the synthetic peptide component could permit the generation of a broad array of functionalized Rab proteins of defined structure. These functionalities, such as spectroscopic probes, affinity-tags or crosslinkers, are expected to drive the development of new experimental designs to further explore Rab protein function. Prenylated Rabs modified in this way cannot easily be obtained by traditional methods of protein chemistry.

In the context of Rab proteins, the mechanism of geranylgeranylation catalyzed by GGTase-II/REP has been a subject of intensive research (see below). Although the molecular details leading to the formation of the catalytically competent enzyme-substrate complex (the quaternary Rab:REP:GGTase-II:GGPP complex) are now credibly clarified, the steps following its assembly remain controversial. At least partially this is due to the poorly characterized single prenylated reaction intermediate complex, which transiently accumulates during the prenylation reaction, as well as due to a lack of time resolved methods to monitor the enzymatic conversion. In fact, chemically defined and homogeneously single prenylated Rab proteins capable of accepting the second prenyl group cannot be generated by any established method. However, the semi-synthetic approach appears to be suitable to enable access to these proteins.

Another field of active research is the structure elucidation of proteins involved in vesicular transport. In particular, general regulators that act on all Rab proteins, such as REP, GGTase-II or RabGDI, have received considerable attention. Structural studies typically require large amounts (i.e. several milligramms) of purified and prenylated Rab proteins, which are not easily obtainable. On condition that the prenylated peptide and the truncated Rab-thioester are readily accessible, the EPL reaction can also be expected to furnish prenylated Rabs in preparative amounts.

This study aimed at the development of protocols permitting the semi-synthesis of prenylated Rab proteins by means of EPL. Ideally, such an approach is expected to be generally applicable to different Rabs and different peptides and capable of producing large amounts of pure and homogenous protein material in a short period of time. In order to demonstrate the usefulness of the approach as well as to gain further insights into the prenylation reaction, Rab proteins carrying a single prenyl

---

group attached to either biologically relevant cysteine residue as well as the doubly modified form were envisaged. These structures can be expected to shed new light on the interaction of GGTase-II with its single prenylated reaction intermediate(s) and double prenylated product.

A further aim of this work was to provide sufficient amounts of prenylated Rab proteins complexed to various interacting proteins for further crystallographic studies. The work was carried out in close collaboration with members of Prof. Dr. Waldmann's lab at the MPI-Dortmund. The prenylated peptides used throughout this study (unless otherwise indicated) were synthesized and provided by Dr. Ines Heinemann, Dr. Lucas Brunsveld and Anja Watzke.

# 3. Results and Discussion

*“The most exciting phrase to hear in science,  
the one that heralds the most discoveries,  
is not ‘Eureka!’, but ‘That’s funny’.”*

*Isaac Asimov*

## 3. Results and Discussion

### 3.1. Development of a semi-synthetic strategy facilitating access to prenylated Rab/Ypt proteins

Key to the outlined objectives was the elaboration of detailed and generally applicable protocols, which should enable production of semi-synthetic Rab/Ypt proteins by means of EPL. EPL was extensively applied to a variety of different proteins and peptides.<sup>[195,198]</sup> In the context of small GTPases, EPL was recently used to generate fluorescently labeled unprenylated Rab7 protein,<sup>[199]</sup> which has proven to be a valuable tool for spectroscopic interaction studies.<sup>[106,116,118]</sup> Moreover, a different semi-synthetic strategy based on maleimidocaproyl (MIC) coupling to a single surface exposed cysteine residue was exploited to produce farnesylated (C<sub>15</sub> isoprenoid) and otherwise modified Ras proteins.<sup>[200]</sup> One could conjecture that these developed procedures could also be directly applied to the EPL mediated semi-synthesis of geranylgeranylated Rab proteins. However, for reasons discussed below, this turned not out to be the case.

The first part of this chapter (3.1.) will demonstrate and discuss the development of a suitable strategy for EPL semi-synthesis of prenylated Rab proteins, whereas the following chapters (3.2.-3.5.) will deal with potential applications of proteins generated in such a manner.

#### 3.1.1. General considerations – Case studies

The utility of EPL stems from its undemanding structural requirements, i.e. any  $\alpha$ -thioester can theoretically be coupled to any N-terminal cysteine containing peptide in the presence of fully unprotected functional groups usually found in proteins. However, depending on the application of the resulting semi-synthetic proteins, certain criteria regarding the design of the peptide fragment should be considered in order to meet different experimental needs:

1. The synthetic peptide fragment should be small (2-10 AA) in order to minimize the synthetic effort and should resemble (or ideally match) the wild type sequence as close as possible. The significance of this prerequisite is underlined by the importance of the C-terminal region for Rab membrane targeting and anchorage. Figure 3-1 reveals that in some cases certain deviations from the wild type structure

are inevitable due to the planned experimental intentions and synthetic requirements. For example, semi-synthetic Rab7 proteins with a different geranylgeranyl pattern were designed for studying their interactions with GGTase-II by means of fluorescence spectroscopy (see Chapter 3.2.). The synthetic peptide fragment was thought to contain both prenylatable cysteine residues and an additional N-terminal cysteine for coupling to truncated Rab7 proteins (synthetic necessity). However, the next possible native cysteine upstream of the prenylation cysteines is Cys<sup>143</sup>, which is buried in the GTPase domain. Such a large truncation (Rab7 $\Delta$ 64) is likely to affect the GTPase fold and accessibility of the Rab-thioester group, besides requiring a huge synthetic effort for obtaining the complementing prenylated 64-mer peptides. Thus, as a compromise the ligation site was placed between Ser<sup>201</sup> and Ala<sup>202</sup>, which formally resulted in a Ala<sup>202</sup>Cys mutation, an exchange that can be expected to be neglectable (Figure 3-1).<sup>[199]</sup>

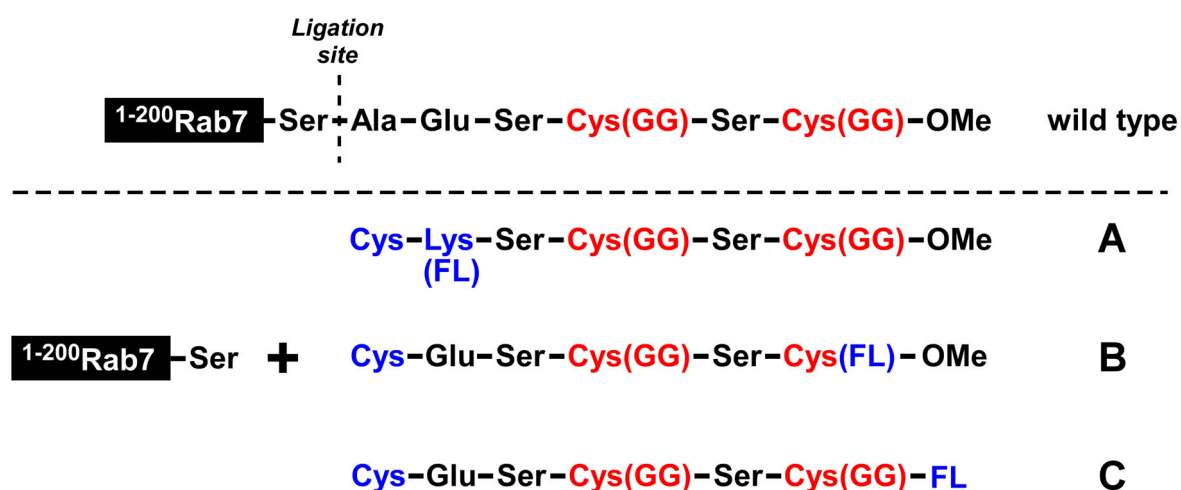


Figure 3-1: Development of a semi-synthesis strategy for Rab7. The ligation site was placed between Ser<sup>201</sup> and Ala<sup>202</sup>. Three types of peptides (series A-C) with different fluorophore attachment sites were considered (FL = fluorescence label, GG = geranylgeranyl, OMe = methylesterification of the Rab C-terminus).

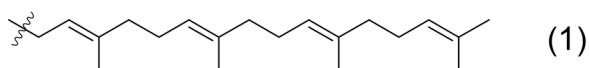
In the context of choosing the site of ligation,<sup>[201]</sup> it is also important to consider the identity of the C-terminal amino acid residue in the thioester-containing peptide segment. Although all 20 naturally occurring amino acids are suitable for NCL when placed at the C-terminus of an  $\alpha$ -thioester model peptide, some of them are associated with extremely slow reaction rates (e.g. Ile, Val and Pro).<sup>[202]</sup> Moreover, when the thioester-containing peptide segment is intended to be produced by

bacterial expression systems, the nature of this amino acid also appears to influence the cleavage of the intein-fusion protein (see chapter 3.1.2.).<sup>[203]</sup>

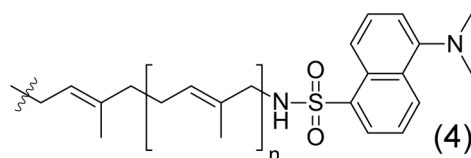
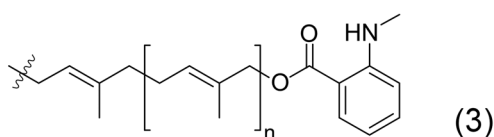
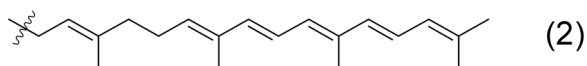
In the case of the above mentioned Rab7 project, an additional modification was necessary in order to incorporate a sensitive fluorescent probe, which in principle could be attached to various sites of the peptide.

2. The positioning of a non-native reporter group is often a compromise between seeking a site that gives highly sensitive and specific signals and, on the other hand, reducing the potential adverse influence of the introduced modification on the effect under study to a minimum. At the beginning of this study no structural data concerning the interaction of Rab/Ypt proteins with REP-1 and GGTase-II or RabGDI were available, hindering an optimal structure-based positioning of the fluorophore. Figure 3-1 demonstrates three positions, to which a fluorophore or any other modification can be introduced into the peptide. First, the fluorophore could be attached to the side chain of amino acids flanking the prenylatable cysteines. In this study Glu<sup>203</sup> directly adjacent to the ligation cysteine was replaced by lysine, which allows the  $\epsilon$ -amino group to be further functionalized by alkylation or acylation. Introduction of the small dansyl fluorophore via a sulphonamide linkage at this site was shown to have no impact on the interaction of Rab7 with REP-1 and GGTase-II and not to affect prenylation or the rate of Rab GTP hydrolysis.<sup>[199]</sup> Still, bulkier fluorophores appear to interfere with the prenylation reaction (Dr. Alexandrov, MPI-Dortmund, unpublished observations) suggesting the exploration of alternative sites. Secondly, fluorophores could be incorporated into the isoprenoid group(s). These functionalized prenyl analogs (Figure 3-2), which resemble the native geranylgeranyl lipids in length, have been used in many cases for studying certain aspects of protein isoprenylation<sup>[204-206]</sup> and isoprenoid-protein interaction.<sup>[207,208]</sup> Two types of analogs are frequently employed: photoactivatable derivatives,<sup>[208]</sup> which enable photoaffinity labeling (PAL) to interaction partners upon photoirradiation, and fluorescent analogs. In some of the reported cases the biological *in vivo* activity of such engineered proteins is retained despite the modification.<sup>[209,210]</sup> However, depending on the hydrophobicity and bulkiness of the analogs used, this outcome cannot always be expected.

## Geranylgeranyl



## Fluorescent derivatives



## Photoactivatable analogs

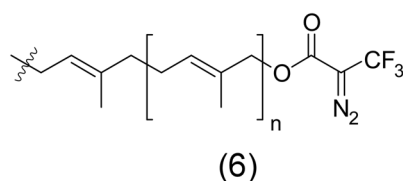
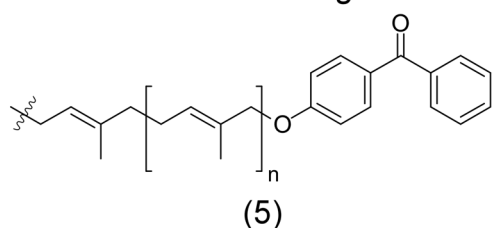


Figure 3-2: Isoprenoid modifications. Geranylgeranyl (1) and fluorescent and photoactivatable analogs. Didehydrogeranylgeranyl ( $\Delta\Delta$ GG, 2),<sup>[207]</sup> mant (3) or dansyl (4) labeled geranyl ( $n = 1$ ) or farnesyl ( $n = 2$ ) derivatives as examples for fluorescent analogs.<sup>[204,206]</sup> Benzophenone (5) and 2-diazo-3,3,3-trifluoropropionyloxy (DATFP, 6) derivatives as photoactivatable analogs.<sup>[208-212]</sup>

Thirdly, fluorophores could be attached to the C-terminal  $\alpha$ -carboxyl group. In the case of Rab7 this would lead to replacement of the methylester, which arises from a posttranslational modification affecting all Rabs terminating in CXC.<sup>[103]</sup> The precise molecular role of this methylesterification is not understood and therefore the consequences of its modification cannot easily be predicted. Although apparently not required by the majority of Rab proteins and despite its small size, methylesterification was found to contribute significantly to the hydrophobicity<sup>[213]</sup> and membrane binding potential<sup>[214-216]</sup> of prenylated model peptides. Furthermore, carboxymethylation seems to be required for efficient *in vitro* membrane binding of prenylated Ypt5 protein,<sup>[217]</sup> and controlled methylation/demethylation was also postulated to developmentally regulate the function of Rab3D.<sup>[218]</sup> In this study substitution of the Rab7 methylester with a dansyl derivative was employed for studying its consequences on the ability of Rab7 to interact with REP-1 and RabGDI (Figure 3-1).

In conclusion, the lack of information concerning the precise molecular role of a) the C-terminal peptide tail, b) the geranylgeranyl isoprenoids, and c) the carboxy-

methylation largely precluded a rational positioning of a reporter group. Thus different sites had to be tested, in order to assess the consequences of the fluorophore incorporation at each position. On the other hand, many other potential applications of prenylated Rab proteins do not strictly require additional reporter groups (e.g. crystallographic analysis). Especially in cases where the Rab protein contains a CC prenylation motif, the synthetic effort could be reduced to Cys-Cys(GG) dipeptides or Cys-Cys(GG)-Cys(GG) tripeptides, depending on whether single or doubly prenylated proteins are desired (Figure 3-3).

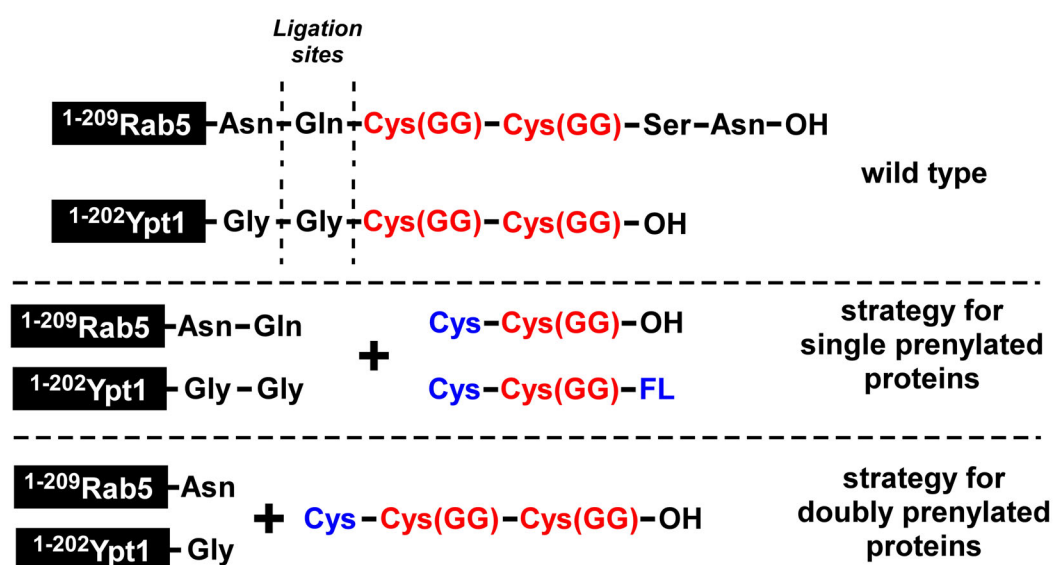


Figure 3-3: Development of a semi-synthesis strategy for Rab5 and Ypt1.

3. From the perspective of chemical synthesis, geranylgeranylated peptides can be prepared employing solid- or solution phase methods (see <sup>[219-222]</sup>). Although not subject of this study, for the semi-synthetic strategy it is important to note the pronounced acid-lability of isoprenoids, giving rise to addition and rearrangement reactions.<sup>[223]</sup> Together with the well known base-lability of thioesters, this largely restricts the EPL reaction conditions to neutral pH.

### 3.1.2. Expression and purification of Rab/Ypt C-terminal $\alpha$ -thioesters

The bacterial expression strategy for generation of truncated Rab protein  $\alpha$ -thioesters is shown in Figure 1-8. This requires the truncated target Rab gene to be inserted upstream of an intein-chitin-binding-domain (CBD) construct. Following expression and affinity purification of the three-part fusion protein, the Rab protein of interest is precisely cleaved from the intein-CBD as a C-terminal  $\alpha$ -thioester. Several *E. coli* expression vectors are now commercially available that allow the target DNA to be easily subcloned in frame of various engineered inteins (for review of commercially available intein vectors see <sup>[203,224]</sup>). All vectors utilize the T7/*lac* promoter to provide stringent control of fusion protein expression<sup>[225]</sup> and a chitin-binding domain (5 kDa) from *Bacillus circulans*.<sup>[226]</sup> Two vectors that were frequently used in this study are depicted in Figure 3-4.

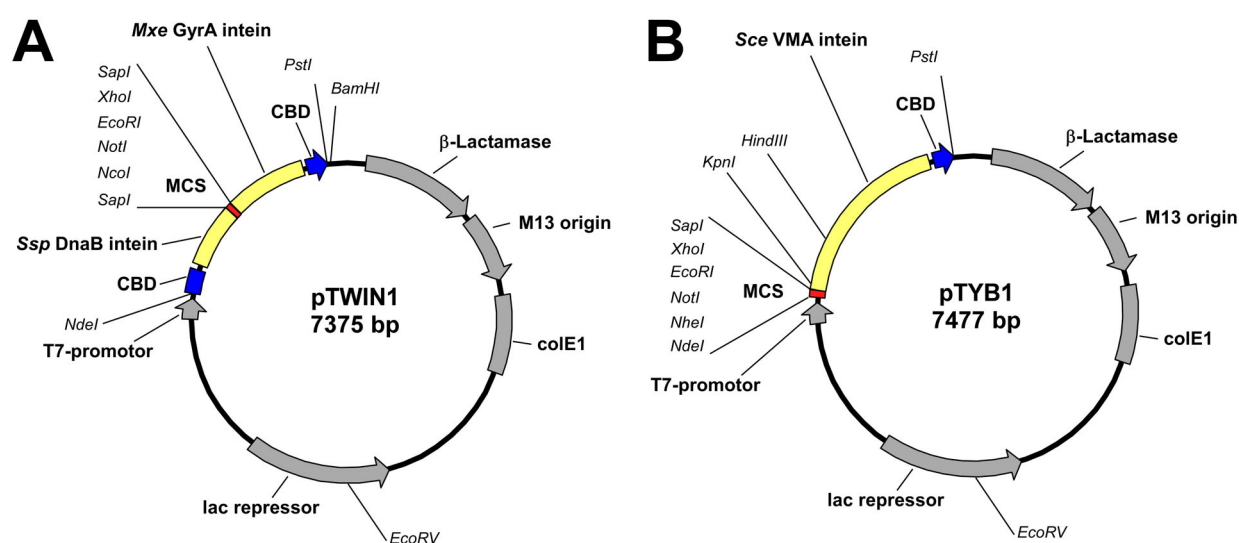


Figure 3-4: Commercially available intein vectors **A)** The pTWIN1 vector utilizes two mini-inteins. Depending on the cloning strategy, target proteins can be fused C- and/or N-terminally to the inteins. **B)** The pTYB1 vector employs the *Saccharomyces cerevisiae* vacuolar membrane ATPase (*Sce VMA*) maxi-intein as a C-terminal fusion. MCS = multiple cloning site, CBD = chitin-binding domain.

Although in practical terms it is difficult to know which intein expression system will work best for a given target protein, it is advisable to consider the following points for choosing a suitable intein vector. First, intein cleavage is mainly affected by the nature of the extein amino acid adjacent to the scissile peptide bond.<sup>[203,224]</sup> Certain amino acids are associated with intein inactivity, premature *in vivo* cleavage and low reaction rates, when used in combination with particular inteins. Because inteins

have different amino acid preferences for this position, the choice of the split site (often identical with the later ligation site) and of the intein should be considered together. Secondly, the size of the intein used might affect the soluble expression levels of the corresponding fusion protein.<sup>[201,227]</sup> For example, the *S. cerevisiae* vacuolar membrane ATPase intein (Sce VMA1, 455 AA, present in pTYB type vectors) is significantly larger than the *Mycobacterium xenopi* DNA gyrase A intein (*Mxe* GyrA, 198 AA, available in pTXB type and pTWIN1 vectors), due to the presence of an additional endonuclease domain. As a result, the small size of the *Mxe* GyrA intein permitted in many cases the fusion protein to be *in vitro* refolded from inclusion bodies,<sup>[228,229]</sup> whereas the Sce VMA1 intein was shown to refold less efficiently.<sup>[230,231]</sup> This property might become handy in the case of cytotoxic proteins, which can often only be expressed under conditions that favor inclusion body formation (and hence inactivation of the protein) and have to be refolded during purification.<sup>[228]</sup>

All truncated Rab/Ypt protein thioesters were expressed as C-terminal intein fusions<sup>§</sup> using pTYB1 or pTWIN1 expression vectors (see Figure 3-4). Vectors were prepared using standard PCR subcloning procedures employing in most cases ligation sites recommended by New England Biolabs.<sup>[224]</sup> The various expression vectors were then transformed into BL21(DE3) cells and a series of preliminary studies undertaken to identify optimal expression conditions (IPTG concentration, induction time and temperature were varied). For soluble Rab/Ypt fusion protein expression the induction temperature had to be lowered to 18-22° C in all cases examined so far.<sup>[232]</sup> At more elevated temperatures, inclusion body formation was observed for the *Mxe* GyrA as well as for the Sce VMA1 intein fusion proteins.

Purification of the Rab/Ypt fusion proteins from crude cell extracts employing chitin agarose beads was straightforward. The tight binding of the CBD to the chitin matrix permits non-specifically bound material to be removed utilizing stringent wash conditions (e.g. high salt concentration or use of non-ionic detergents). However, prolonged storage (> 1 d) of the immobilized fusion protein under such conditions led to a significant reduction of the intein's cleavage efficiency and an increased premature release of the target protein. In practical terms, it is advisable to work as fast as possible at a constant temperature of 4° C. Starting with crude cell lysate the whole procedure should reach the thiol induced cleavage stage within 4-6 hours.

---

<sup>§</sup> i.e. the Rab C-terminus is fused to the N-terminus of the intein-CBD construct.

In principle thiol-induced cleavage and ligation to a N-terminal cysteine containing peptide fragment could be carried out simultaneously in a one-pot reaction by simply adding peptide and thiol additive to the immobilized intein fusion protein.<sup>[185,186,197,230]</sup> However, this approach restricts the application of additives that can be present in the reaction mixture, since the intein must remain folded and active during the ligation reaction. Taking into account the observed instability of the immobilized fusion protein (see above), it appeared more advantageous to isolate and characterize the recombinant protein  $\alpha$ -thioesters first.

Cleavage was in all cases performed in the presence of 500 mM 2-mercaptoethanesulfonic acid (MESNA) at room temperature for 12-16 h. Beside MESNA,<sup>[187]</sup> a variety of compounds were tested for the induction of thiolysis of the intein fusion proteins including 3-mercaptopropanesulfonic acid (MPSNA),<sup>[230]</sup> DTT,<sup>[188]</sup>  $\beta$ -mercaptoethanol ( $\beta$ -ME),<sup>[188]</sup> ethanethiol<sup>[181]</sup> and thiophenol.<sup>[230]</sup> In contrast to MESNA, these compounds partially have the disadvantage of low solubility in aqueous buffers at around neutral pH (e.g. thiophenol), a high tendency for spontaneous oxidation forming insoluble symmetrical disulfides (thiophenol), a high hydrolysis rate of the respective  $\alpha$ -thioesters (MPSNA, thiophenol),<sup>[230]</sup> an unpleasant odor (thiophenol,  $\beta$ -ME, ethanethiol) and a low reactivity in subsequent EPL (NCL) reactions (ethanethiol, DTT,  $\beta$ -ME). In practical terms the last point is usually of less significance, since the reactivity can be reestablished by *in situ* trans-thioesterification during the ligation reaction with more potent thiol compounds (e.g. thiophenol, see 3.1.3.).<sup>[233,234]</sup>

Incubation of the Rab/Ypt-intein fusion protein with such high concentrations of MESNA (0.5 M) resulted in almost quantitative cleavage (see Figure 3-5). It was also observed that these conditions led to denaturation of a minor fraction (< 5 %) of CBD containing polypeptides, which were released from the chitin column along with the desired Rab/Ypt  $\alpha$ -thioesters. These minor impurities were considered acceptable, since additional purification steps following EPL were performed in any case.

Using a single affinity chromatographic step, 20-40 mg of Rab/Ypt thioester protein (corresponding to 40-120 mg of fusion protein) were typically obtained per liter of bacterial culture in excellent purity (> 90 %). Expression levels, cleavage efficiency and final yields were in general slightly higher for the *Mxe* GyrA intein fusion proteins (pTWIN1 vector) as compared to the *Scd* VMA1 intein fusion proteins (pTYB1 vector).

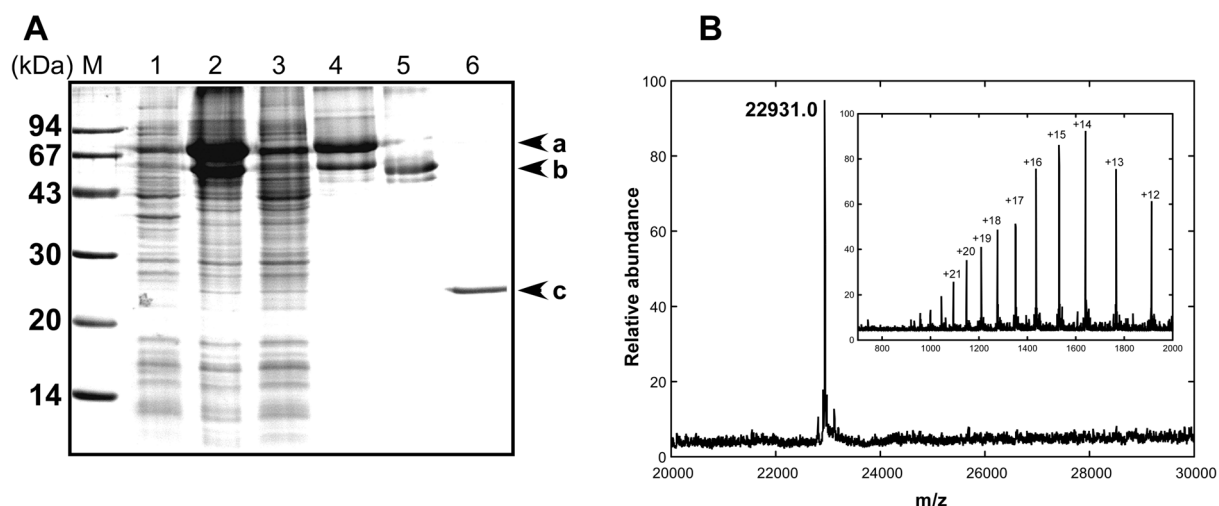


Figure 3-5: Expression and purification of Rab7 $\Delta$ 6-MESNA thioester. **A**) SDS PAGE of crude cell extract from BL21(DE3) *E. coli* cells before induction with IPTG (lane 1), after induction and expression at 20° C for 10 h (lane 2) and after incubation with chitin-binding beads (lane 3). Chitin-binding beads after washing (lane 4) and after MESNA induced cleavage (lane 5), resulting in elution of the Rab7 $\Delta$ 6-MESNA thioester (lane 6). Arrows indicate the position of Rab7 $\Delta$ 6-Sce VMA1 intein-CBD (a), Sce VMA1 intein-CBD (b) and Rab7 $\Delta$ 6-MESNA thioester (c). M = protein standards **B**) LC-MS spectrum of the purified protein. The inset shows the original data before deconvolution. The theoretical molecular mass of  $^{2-20}Rab7\Delta6$ -MESNA is 22932.1 Da.

The identities of the produced proteins were confirmed by MALDI-MS, LC-ESI-MS and SDS-PAGE (Figure 3-5). The expressed Rab-fusion proteins were in many cases fully processed *in vivo* by the endogenous methionylaminopeptidase (MetAp) resulting in the cleavage of the starting methionine residue. The processing was dependent on the nature of the following (second) amino acid residue and was found to be in agreement with previous observations.<sup>[235]</sup> Moreover, using LC-ESI-MS analysis the presence of the reactive thioester could be inferred from its susceptibility to hydrolysis under slightly basic conditions (pH 9-10, see Figure 3-6). Under neutral conditions the MESNA  $\alpha$ -thioesters could be stored at -20 or -80° C for several months, generally without any detectable decomposition or loss of ligation efficiency.

### 3.1.3. An unexpected behaviour of Rab5 thioesters terminating in glutamine or asparagine

The described procedure allows generation of various thioester tagged proteins of defined molecular structure on a routine basis. In all cases mass spectroscopic analysis gave unambiguous results concerning the identities of the expected proteins, which was later confirmed in biochemical studies. Unexpectedly, Rab5 $\Delta$ 5 and Rab5 $\Delta$ 4 MESNA thioester proteins were found to exhibit molecular masses of

about 130 Da less than expected, which could be explained by thioester hydrolysis or exo-proteolytic cleavage of a single amino acid residue.

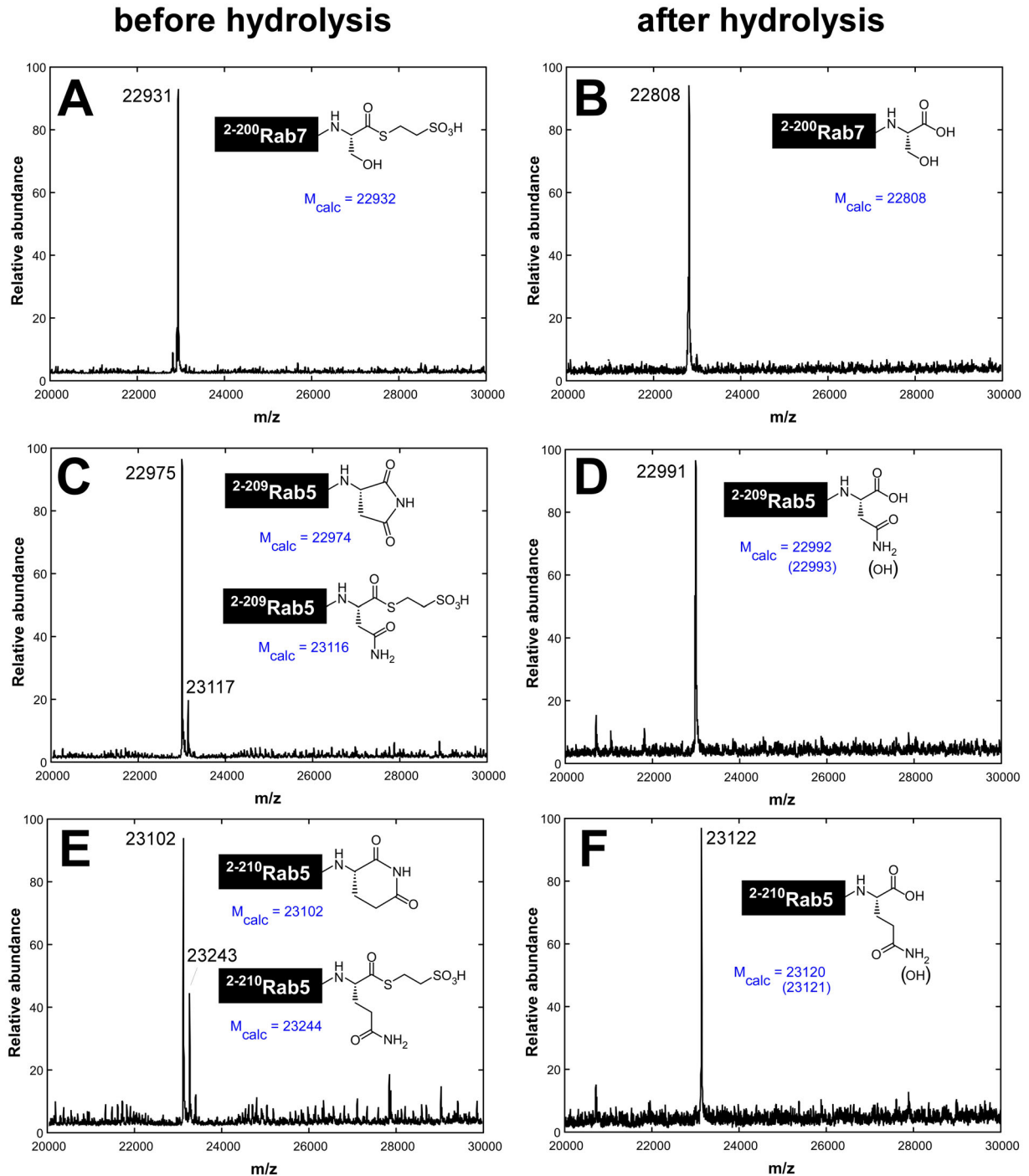


Figure 3-6: Susceptibility of protein  $\alpha$ -thioesters towards mild alkaline hydrolysis and possible succinimide and glutarimide formation in the case of terminal asparagine and glutamine  $\alpha$ -thioester residues. Rab7 $\Delta$ 6 (A, B), Rab5 $\Delta$ 5 (C, D) and Rab5 $\Delta$ 4 (E, F) were incubated at 37° C for 30 min at a pH of 9-10. Samples before (A, C, E) and after (B, D, F) hydrolysis were analyzed by LC-ESI-MS. Proposed structural modifications of the C-terminal amino acid residue together with the corresponding calculated mass (blue) are shown for all proteins (Ser<sup>201</sup> for Rab7 $\Delta$ 6, Asn<sup>210</sup> for Rab5 $\Delta$ 5 and Gln<sup>211</sup> for Rab5 $\Delta$ 4). Alkaline treatment may additionally result in deamidation at Gln and Asn residues giving rise to an additional mass shift of +1 Da. Such a small shift cannot be confidently detected, since the accuracy of the method is in the same Da range ( $\pm 1$  Da).

Initially, the latter interpretation was favored since the ligation efficiency of both proteins toward the peptide H-Cys(StBu)-Lys(Dans)-Cys(GG)-OMe was essentially indistinguishable when compared to Rab7 $\Delta$ 6-MESNA thioester (Figure 3-7C). However, when subjected to mild alkaline conditions, both proteins exhibited a mass shift of ca. +18 Da, which is in contradiction to a mass shift of -124 Da observed upon alkaline hydrolysis of the Rab7 $\Delta$ 6-MESNA thioester (Figure 3-6). Sequence analysis of the Rab5a $\Delta$ 4 and  $\Delta$ 5 mutants revealed the identities of the C-terminal amino acid residues as glutamine and asparagine, respectively (Figure 3-3). These observations could be interpreted with the formation of a five-membered succinimide ring in the case of C-terminal asparagine, and of a six-membered glutarimide ring in the case of C-terminal glutamine (Figure 3-6 and 3-7A).

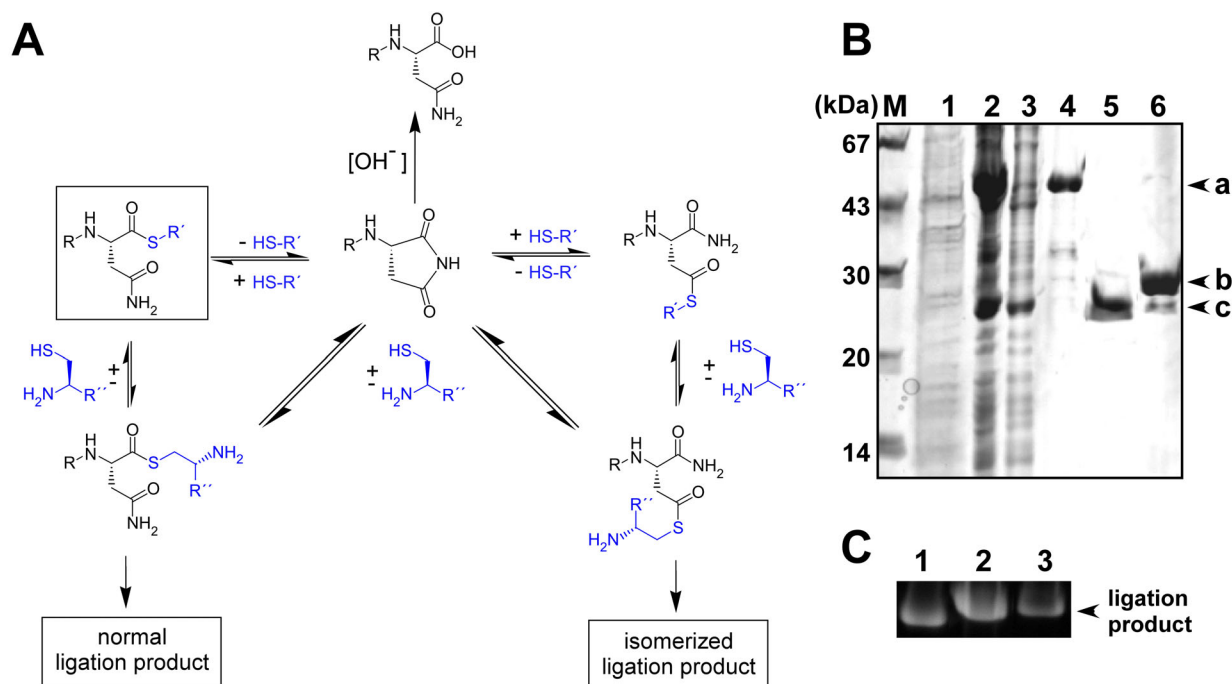


Figure 3-7: **A**) Proposed mechanism for spontaneous succinimide formation and possible side-reactions during EPL or NCL giving rise to isomerization of the terminal asparagine residue. An analogous pathway could be considered for terminal glutamine residues. **B**) Expression and purification of Rab5 $\Delta$ 5-MESNA thioester analyzed by SDS-PAGE. Crude cell lysate from uninduced (lane 1) and induced (lane 2) cells. Lysate after depletion of the CBD-fusion protein with chitin beads (lane 3). Chitin beads before (lane 4) and after (lane 6) MESNA induced cleavage. The supernatant after thiol-induced cleavage is shown in lane 5. Note that the fusion protein exhibits only a minor tendency for spontaneous (uninduced) cleavage. Arrows indicate the position of Rab5 $\Delta$ 5-Mxe GyrA intein-CBD (a), Mxe GyrA intein-CBD (b) and Rab5 $\Delta$ 5 (c). **C**) Ligation of Rab7 $\Delta$ 6 (lane 1), Rab5 $\Delta$ 5 (lane 2) and Rab5 $\Delta$ 4 thioesters/imides to the peptide H-Cys(StBu)-Lys(Dans)-Cys(GG)-OMe in the presence of 150 mM MESNA and 50 mM CTAB. The reactions were analyzed by SDS-PAGE. Product formation could be inferred from the appearance of a fluorescent band in the 20-30 kDa molecular weight range.

In such a scenario, the nitrogen of the  $\beta$ - or  $\gamma$ -carboxamide group attacks the thioester-activated carbonyl carbon of the asparaginyl/glutaminy residue, leading to intramolecular cyclization and displacement of the thiol leaving group. The proposed structures of the occurring thioester/imide species are in excellent agreement with the mass spectroscopic observations (Figure 3-6).

Interestingly, the formed imides were capable of reacting with the peptide H-Cys(StBu)-Lys(Dans)-Cys(GG)-OMe yielding a covalently linked (fluorescent) product (Figure 3-7C). Therefore, under the employed EPL reaction conditions\*\* imides seem to represent reactive compounds. Indeed, (N-alkylated) succinimides originating from asparaginyl and aspartyl cyclization have been observed in model peptides<sup>[236,237]</sup> and proteins<sup>[238,239]</sup> and typically give rise to deamidation, isomerization, racemization and polypeptide cleavage under physiological conditions.<sup>[240,241]</sup> Furthermore, studies of the alkylation reaction of thiol-containing compounds (e.g. cysteine residues in proteins) with maleimide derivatives could show that the formed succinimide thioether can undergo a number of chemical transformations at the imide functionality at around neutral pH and room temperature.<sup>[242-249]</sup> This typically involves ring opening by nucleophiles and results in the formation of succinamic acid derivatives.

Taken together these data strengthen the assumption that the observed protein succinimide and glutarimide can possibly undergo various fates during an NCL/EPL reaction. Direct aminolysis of the Rab imides could be excluded, since the prepared proteins failed to react with H-Lys(Dans)-OH (not shown). It therefore appears plausible that under the employed conditions\*\* ring opening by thiol nucleophiles, such as cysteine containing peptides or MESNA, could restore the thioester (see Figure 3-7A). In this case, the consequence would be the formation of the unnatural  $\beta$  ( $\gamma$ ) peptide bond between Asn (Gln) and Cys as a EPL side product (isomerization), since both carbonyl groups are expected to have similar reactivities. The proposed mechanism offers an explanation for the above mentioned observations and resembles the mechanism of NCL side reactions with aspartic or glutamic acid as C-terminal  $\alpha$ -thioester residues recently reported by Villain et al.<sup>[250]</sup> In these cases extensive hydrolysis and isomerization were observed, possibly due to an analogous anhydride forming cyclization of the activated dicarbonic acids. The problem can be

---

\*\* i.e. at around neutral pH in aqueous solution and in the presence of MESNA and CTAB. See chapter 3.1.4. for a discussion of the effect of CTAB on the nucleophilicity of thiol containing compounds.

minimized by employing appropriate side-chain protecting groups for the C-terminal  $\alpha$ -thioester residue, provided this fragment is accessible by total synthetic means.<sup>[250]</sup> In conclusion, despite the fact that all 20 naturally occurring amino acids were found to be compatible in a Xaa-Cys ligation,<sup>[202]</sup> one should try to avoid Asp, Asn, Glu or Gln residues, especially when side product separation and detection is critical, as is usually the case for most larger polypeptides (> 10 AA).

#### 3.1.4. Expressed protein ligation with prenylated peptides

With the Rab  $\alpha$ -thioester proteins available, we set out to undertake ligation reactions with short prenylated model peptides, which were synthesised by Dr. Ines Heinemann from the Department of Chemical Biology, MPI Dortmund. Typically, EPL is carried out in aqueous buffers (pH 7-8) at temperatures between 4 and 40° C. It is desirable to have both reactant polypeptides at high concentrations (> 1 mM) and the synthetic peptide in large molar excess (3-10 times) in the reaction mixture in order to improve the ligation yields. Additives such as chaotropes,<sup>[149]</sup> detergents or organic solvents might help to increase the solubility of the reactants and are fully compatible with EPL.<sup>[201]</sup> The rate and the yields of the ligation reaction can be further enhanced by adding catalytic thiol cofactors, such as thiophenol or MESNA,<sup>[233]</sup> which retain the cysteine side chains in the reduced state, reverse the formation of unproductive thioesters and activate less reactive thioesters by transthioesterification.

Initial studies on the ligation of geranylgeranylated peptides with Rab-MESNA thioesters were carried out using the tripeptide H-Cys-Lys(Dans)-Cys(GG)-OMe (see Table 5-2) and Rab7 $\Delta$ 6-MESNA thioester. This fluorescently labelled model peptide permits easy detection of Rab7 ligation products by means of SDS-PAGE when the unstained gel is exposed to UV light. In such a case, appearance of a fluorescent band in the 20-30 kDa molecular weight region indicates the formation of the ligation product. In contrast, the increase in apparent molecular weight cannot always be revealed by a significant change in the electrophoretic mobility of the Rab protein.

Not surprisingly, geranylgeranylated peptides, as for example shown in Table 5-2, were found to be essentially insoluble in pure aqueous solutions. Given the hydrophilic nature of the thioester fragment, conditions had to be identified under which both molecules could be maintained in solution, thus allowing their efficient ligation. The solubility problem could be partially overcome by supplementing the

reaction mixture with polar organic solvents (up to 70 % (v/v) of DMSO, ACN, EtOH, MeOH), 6 M GdmHCl or detergents. Despite the apparent solubilizing effect of the additives used, initially only high concentrations of the detergent SDS resulted in detectable EPL product formation with Rab7 $\Delta$ 6-MESNA thioester protein. Because SDS is well known for its tight binding to proteins leading to protein denaturation and is difficult to remove from protein containing solutions due to its low cmc value,<sup>[251]</sup> a usage of this detergent in further studies was not envisaged<sup>††</sup>. Nonetheless, these encouraging results prompted us to search for alternative detergents supporting solubilization of reactants and enabling EPL. To this end, more than 80 detergents were screened in the above mentioned ligation reaction assay (Figure 3-8).

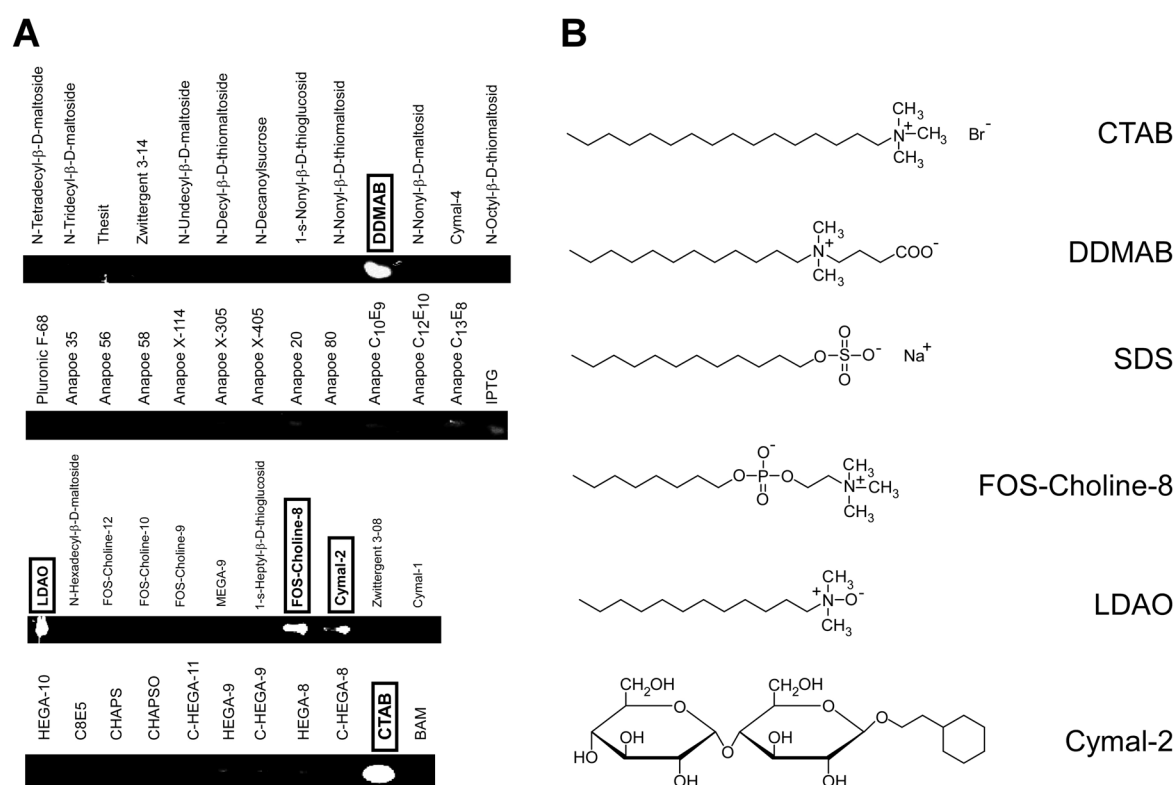


Figure 3-8: Identification of detergents that support *in vitro* ligation of prenylated peptides. **A**) Ligation of Rab7 $\Delta$ 6-MESNA thioester to H-Cys-Lys(Dans)-Cys(GG)-OME in the presence of detergents. SDS-PAGE gels exposed to UV irradiation identified successful ligation reactions by the appearance of fluorescent protein bands in the molecular weight range of 20-30kDa. **B**) Structures of detergents that are able to support *in vitro* ligation of prenylated peptides. Cetyltrimethylammonium bromide (CTAB), *N*-dodecyl-*N,N*-(dimethylammonio)butyrate (DDMAB), sodium dodecyl sulfate (SDS), *n*-octyl-phosphocholine (FOS-Choline-8), lauryldimethylamine-*N*-oxid (LDAO) and cyclohexyl-ethyl- $\beta$ -D-maltoside (Cymal-2).

<sup>††</sup> During the time this work was performed, a study employing SDS as a solubilizing additive for EPL was published. However the studied protein is exceptionally (!) stable towards SDS-denaturation.<sup>[228]</sup>

Surprisingly, only very few detergents capable of efficiently supporting the ligation reaction were eventually identified (Figure 3-8): cetyltrimethylammonium bromide (CTAB), *N*-dodecyl-*N,N*-(dimethylammonio)-butyrate (DDMAB), sodium dodecyl sulfate (SDS), *n*-octyl-phosphocholine (FOS-Choline-8), lauryldimethylamine-*N*-oxid (LDAO) and cyclohexyl-ethyl- $\beta$ -D-maltoside (Cymal-2). This low number of EPL-effective detergents (6 out of 80) was striking since most of the tested detergents were able to mediate solubilization of the lipidated peptide, suggesting that solubilization, albeit a prerequisite, is not sufficient for ligation. Moreover, ligation of the peptide H-Cys-Lys-Lys-Arg-Arg-Leu-Lys-Cys(GG)-NH-(CH<sub>2</sub>)<sub>2</sub>-NH-Dans<sup>‡‡</sup>, which is excellently soluble in detergent free aqueous solutions, onto Rab7 $\Delta$ 6-MESNA thioester can be significantly improved by addition of low concentrations of the detergent CTAB (Figure 3-9A). This compound exhibited the highest potential for EPL reactions of prenylated peptides when present at concentrations above its cmc (typically 30-50 mM) and was used in all further studies (Figure 3-8).

Comparison of the effective detergents did not reveal a common structural or physico-chemical (e.g. cmc value) feature, which could explain their remarkable impact on the EPL reaction. However, with the exception of Cymal-2 all of the effective detergents represent alkyl ionic or zwitter-ionic detergents, whereas most of the ineffective detergents belong to the non-ionic detergents. In general the latter are known to be mild detergents, which preserve the native protein structure, while the former nearly always act as denaturants and potent protein solubilizers.<sup>[254,255]</sup> One could speculate that the combined incorporation of prenylated peptide and thioester-tagged protein into the micellar aggregate results in the concentration of both reactants into a small volume (the micellar phase). As a consequence the frequency of molecular collisions can be expected to increase due to the close association of the two reacting species. Such a proximity effect (also referred to as the pseudophase model of micellar catalysis) is often the main factor responsible for the observed rate enhancement of bimolecular reactions in micellar solutions.<sup>[256]</sup> Indeed surfactant micelles have been known for the last 50 years to affect the reaction rate, mechanism and regio- and stereoselectivity of all kinds of chemical reactions.<sup>[256-258]</sup> In mechanistic terms, beside concentrating reactants within their

---

<sup>‡‡</sup> This peptide sequence was derived from the C-terminus of the Ral-A GTPase from *Drosophila melanogaster* and was synthesized by Daniel Gottlieb, Department of Chemical Biology, MPI-Dortmund. Ral GTPases constitute a family of proteins within the Ras branch of small GTPases.<sup>[252,253]</sup>

small volumes,<sup>[259-261]</sup> micelles have been proposed to stabilize substrates, intermediates or products, to orient substrates, and to change ionization potentials, dissociation constants and consequently reactivities. In the present case the contribution and significance of these effects on the EPL reaction is quite speculative. Nevertheless, specifically the cationic detergent CTAB has been reported to decrease the  $pK_a$  value of protein sulfhydryl groups by one or two pH units probably by stabilizing the ionized  $S^-$  form of the thiol.<sup>[262]</sup> Similar changes of the  $pK_a$  value in the presence of cetyltrimethylammonium cations have been observed for benzimidazole and substituted phenols.<sup>[263]</sup> Thus at a given pH, addition of CTAB might increase the fraction of the thiolate form of the C-terminal peptide fragment and, since this species represents the actual nucleophile in a EPL/NCL reaction, might account for the observed enhancement in reactivity. In this context it is important to note, that the fraction of the thiolate ions in a NCL reaction cannot be increased by simply raising the pH due to the pronounced base-lability of the activated thioester.

Micellar bound amphiphilic solutes, e.g. prenylated peptides, orient themselves so that the polar region (peptide backbone and the reactive groups) interacts with the surfactant head groups in the Stern-layer, while the hydrophobic end (geranylgeranyl moiety) contacts the hydrocarbon tails of the micelle interior (Figure 3-9B). The high charge density on the micelle surface could additionally contribute to the polarization of the carbonyl thioester, thereby enhancing its reactivity.

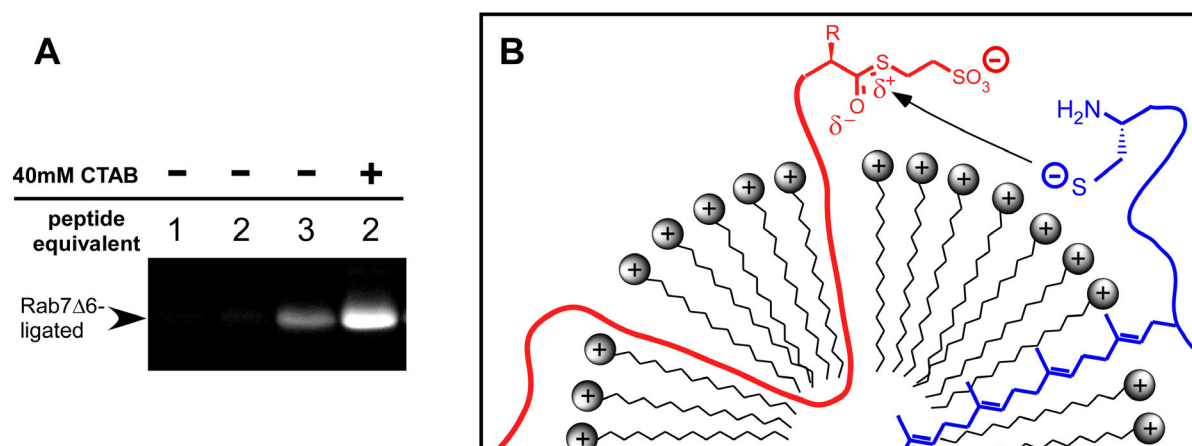
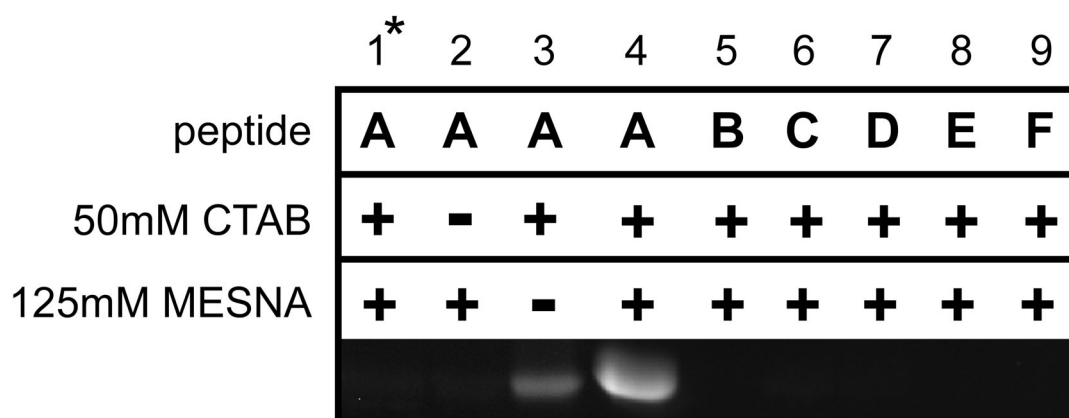


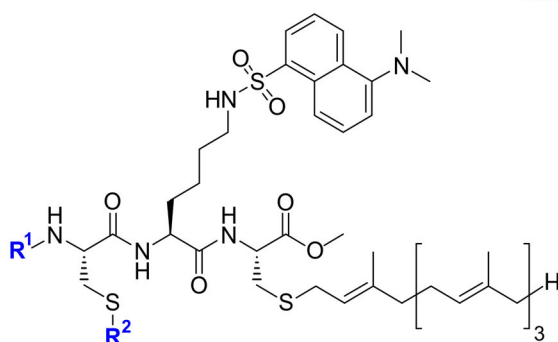
Figure 3-9: **A)** Ligation of the water-soluble Ral-A peptide to Rab7 $\Delta$ 6-MESNA thioester. Peptide equivalents used in the reaction mixture are indicated with respect to thioester-tagged protein. The reactions were analyzed by SDS-PAGE. Product formation was detected by exposing the unstained gel to UV light. **B)** Hypothetical model of the micelle catalysis effect of CTAB. Rab7 thioester is colored red and the geranylgeranylated peptide is shown in blue.

The hydrophobic character of the reactants is generally believed to mainly control their reactivities, i.e. increasing the hydrophobicity increases the influence of the micellar phase on the reaction (e.g. <sup>[261,264]</sup>). Therefore, one can expect a less significant role of the surfactant on NCL/EPL reactions with unprenylated peptides with higher hydrophilicity. On the other hand the remarkable properties of these detergents could prove especially useful for the EPL/NCL mediated (semi-) synthesis of integral membrane proteins. In such cases, the limited solubility of hydrophobic membrane polypeptides in aqueous solvents remains a substantial experimental challenge.<sup>[228,265-267]</sup> Interestingly, Hunter et al.<sup>[268]</sup> very recently described the utility of cubic lipidic phase (CLP) matrixes as NCL reaction media, which, due to their exceptional properties, seem to have certain advantages over classical micellar or liposomal systems.

In order to prove the specificity of the reaction and the reliability of the SDS-PAGE assay as well as to confirm the identity of the desired product, control ligations were carried out with various peptides under different conditions (Figure 3-10).



\* Rab7 $\Delta$ 6-OH was used instead of Rab7 $\Delta$ 6-MESNA thioester



peptide	R <sup>1</sup>	R <sup>2</sup>
<b>A</b>	H	StBu
<b>B</b>	Fmoc	StBu
<b>C</b>	Aloc	StBu
<b>D</b>	Fmoc	Mmt
<b>E</b>	Trt	Mmt
<b>F</b>	Trt	Trt

Figure 3-10: Control reactions. Ligation of Rab7 $\Delta$ 6-MESNA thioester (lanes 2 to 9) or Rab7 $\Delta$ 6-OH (lane 1) to different peptides in the presence or absence of MESNA and CTAB. The reactions were analyzed by SDS-PAGE. The gel was subsequently illuminated with UV-light indicating product formation by the appearance of a fluorescent band in the molecular weight region of 20-30 kDa.

Product formation required a C-terminal  $\alpha$ -thioester on the N-terminal fragment and the presence of an unprotected  $\alpha$ -amino and  $\beta$ -mercapto group on the C-terminal fragment. Reductively cleavable  $\beta$ -mercapto protecting groups (e.g. StBu) can be cleaved off *in situ* by addition of an excess of thiol agent (MESNA, DTE,  $\beta$ -ME), as was previously reported.<sup>[198]</sup> The minor product formation observed in the absence of MESNA (lane 3) could be attributed to a residual amount of MESNA in the Rab-thioester preparation or to a spontaneous reduction of the peptide during peptide purification or ligation. As pointed out above, CTAB was essential for a efficient ligation. These results suggest specific labeling of the Rab protein exclusively at the C-terminus and are in full agreement with the proposed NCL/EPL reaction mechanism.<sup>[149]</sup>

The extent of ligation after 8-12 h was found to be essentially independent of the reaction temperature in the range of 25-40° C. On account of the relatively high Krafft point<sup>§§</sup> of CTAB of ca. 22° C, reactions were typically not performed at temperatures lower than 30° C.

So far, the devised reaction conditions permitted any Rab  $\alpha$ -thioester to be ligated to any prenylated peptide bearing an N-terminal cysteine with excellent yields (50-90 %). The peptide was usually present in large molar excess (10 equivalents with respect to thioester-tagged protein). Hence, upon completion of the ligation reaction, ligated protein must be purified from contaminating peptide, unligated protein and potentially harmful detergent or additive (MESNA), which unexpectedly turned out to be highly problematic.

### 3.1.5. Development of a purification strategy.

Conjugation of Rabs with geranylgeranyl isoprenoids renders these proteins insoluble in aqueous solutions in the absence of membranes, suitable detergents or their natural chaperones REP or RabGDI. The employed ligation detergent (CTAB) was considered to be unsuitable for further purifications due to its potential denaturing effect, its ionic nature, its micellar size (20-30 kDa) and its low cmc value (ca. 1 mM), which makes it difficult to remove. Therefore, following ligation, an exchange of CTAB with a more appropriate additive was envisaged. For example, for

---

<sup>§§</sup>  $T_K$ , i.e. the temperature at which a detergent/solvent system passes from a hydrated crystalline state to an isotropic micellar solution. For most detergents this temperature is below the water freezing point.<sup>[269]</sup>

solubilization and purification of prenylated Rabs from eukaryotic membranes the detergents CHAPS,<sup>[270,271]</sup> sodium cholate<sup>[272]</sup> and Nonidet P-40<sup>[273]</sup> have proven to be useful in the past.

The employed ligation detergent (CTAB) was only poorly capable of mediating solubilization of the ligated and prenylated Rab proteins. Low-salt conditions resulted in almost quantitative precipitation of protein and peptide during the ligation, whereas under high-salt conditions (i.e. above 150 mM NaCl) protein and peptide were retained in solution. Initial purification attempts aimed at separation of the soluble mixture using classical biochemical techniques, such as ion-exchange, gel-filtration, hydroxyapatite or hydrophobic interaction chromatography. Unfortunately, none of these methods was capable of separating the excessive peptide from the ligated protein under various conditions. It appeared, that the geranylgeranylated Rab ligation product tightly associates with the prenylated peptide and the cationic detergent (CTAB, Figure 3-11A) and that neither one of the above mentioned methods nor more rigorous treatments, such as acetone precipitation or Triton X-114 partitioning could weaken this interaction. Strongly denaturing reversed-phase HPLC with acetonitrile/TFA as a cosolvent indicated several fluorescent species (Figure 3-11B), which probably represent different aggregation states of the fluorescent peptide with protein and/or detergent.

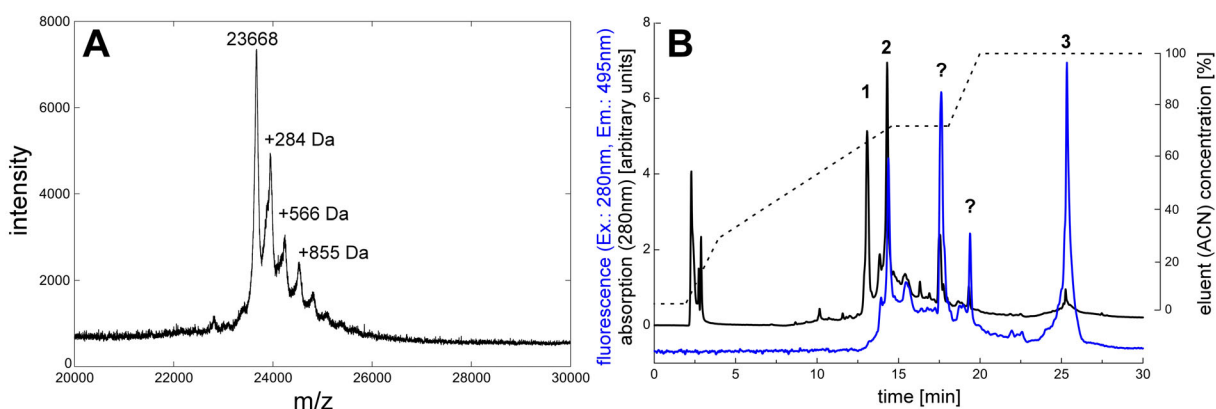


Figure 3-11: Problems associated with the purification of prenylated Rab EPL reaction products. **A)** MALDI-TOF-MS of the crude precipitate of the reaction of  $^{2-201}$ Rab7 $\Delta$ 6-MESNA thioester with CK(Dans)C(GG)-OMe in the presence of CTAB. The ligated protein ( $M_{\text{calc}} = 23679$  Da) could be identified. Additional peaks probably indicate multiple adducts with cetyltrimethylammonium cations ( $M_{\text{calc}} = 284$  Da). Usually such noncovalent interactions can only rarely be detected during MALDI-MS analysis. **B)** HPLC analysis of the crude soluble reaction mixture using reversed-phase (C4) columns. Rab7 $\Delta$ 6-MESNA thioester (1), Rab7 $\Delta$ 6-CK(Dans)C(GG)-OMe (2), and CK(Dans)C(GG)-OMe (3) were identified. Other peaks (indicated by question mark) probably represent adducts between peptide, detergent and ligated protein. All fluorescent fractions contained significant amounts of lipidated peptide.

The association between the peptide and the ligated protein was of non covalent nature and presumably the result of strong hydrophobic interactions. Eventually, we thought of an approach which makes use of the above mentioned pronounced solvent incompatibility of geranylgeranylated peptides and proteins: Whereas the lipidated peptide was found to be excellently soluble in organic solvents, such as dichloromethane or methanol, but essentially insoluble in aqueous solutions, the lipidated protein was expected to exhibit exactly the opposite behaviour. Indeed, several rounds of washing of the ligation mixture or the protein precipitate with organic solvents, such as dichloromethane or ethyl acetate, led to quantitative extraction of the peptide into the organic layer (Figure 3-12). Such a treatment typically resulted in complete protein denaturation and aggregation, if not already occurred during the ligation reaction.

The protein precipitate is insoluble in most tested solvents including methanol, ethanol, water or even 6 M urea. Therefore such solvents or chaotropes can be utilized in subsequent washing steps to remove ligation product contaminating detergents (CTAB), additives (MESNA) and possibly unligated protein.

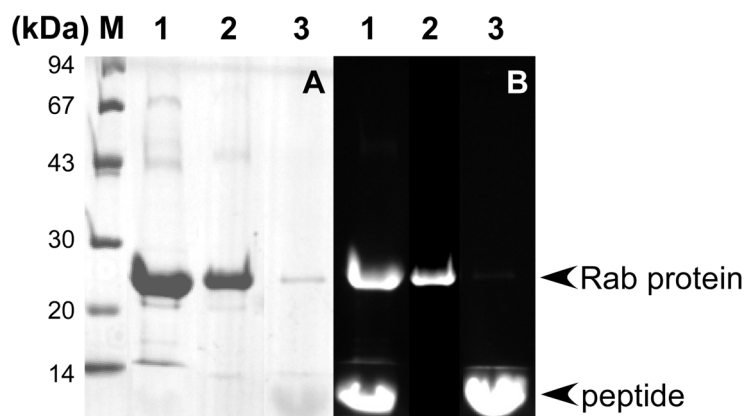


Figure 3-12: Separation of protein and contaminating peptide (CK(Dans)C(GG)-OMe) by repeated washing steps with organic solvents. Crude ligation precipitate before (lane 1) and after removal of excessive fluorescent peptide (lane 2). The extracted peptide (lane 3) can be re-used in another ligation reaction. The picture of the SDS-PAGE gel was recorded either following Coomassie-blue staining (**A**) or while illuminated with UV light (**B**).

Using this approach peptide free ligation products could be obtained (Figure 3-12, lane 2). Moreover, the extracted peptide could be recovered from the combined organic phases and reused in another round of ligation. The inevitable problem which arises from the use of denaturing conditions for protein purification, however, is the

need for an additional resolubilization and renaturation step, which is usually accomplished by *in vitro* protein refolding.

It is generally assumed that the folding of a polypeptide chain is a spontaneous process intrinsically determined by its primary structure (i.e. amino acid sequence) and depending on the appropriate environment. However finding the appropriate conditions during an *in vitro* refolding experiment can be a difficult task since no universal methods and only very few general guidelines exist.<sup>[274-276]</sup> In addition, some natural proteins may be completely resistant to any *in vitro* refolding efforts, which reflects the substantially different *in vivo* folding situation (e.g. molecular chaperone assisted cotranslational folding, protein folding catalysts, posttranslational modifications). Nevertheless, small single-domain proteins derived from total- or semi-synthesis or from bacterial inclusion bodies have been refolded with excellent yields in the past.<sup>[157,274]</sup> Small GTPases of the Ras superfamily have been successfully refolded recently,<sup>[277-279]</sup> but not a single study dealt with a posttranslationally modified protein. The presence of the C-terminal lipid(s) was expected to give rise to protein-misfolding due to the strong inter- or intramolecular interactions they could participate in (see above).

Before starting renaturation the precipitated protein material had to be solubilized by strong denaturants.<sup>[280]</sup> Up to now, only solutions of 6 M GdmHCl have been found to efficiently solubilize the precipitated ligation product. Further additives included 1,4-dithioerythritol (DTE) in order to keep all cysteines in the (naturally) reduced state and CHAPS, which was thought to promote solubilization of the geranylgeranyl lipids as well as to increase the refolding yields by suppressing aggregate formation.<sup>[281]</sup> Renaturation is usually initiated by the removal of the denaturant either by dialysis, dilution or column based techniques. Throughout this study pulse-renaturation by dilution was used, i.e. small aliquots of the denatured protein were added to the refolding solution after certain time intervals.<sup>[282,283]</sup> As a result, the transient concentration of the unfolded protein was constantly kept low, thus limiting protein aggregation side reactions. Typically a 1:25 dilution of the denatured protein into refolding solution was performed with 10 pulses over 2 h. Still, the final protein concentration was very low ranging from 10-100 µg/ml and required the handling of large volumes of refolding solutions (up to 500 ml) for preparative protein purification. Finally, the yield of the active enzyme recovered upon refolding did not only depend on the mode of renaturation and the enzyme concentration, but also critically on the

solvent composition.<sup>[282]</sup> For example, as pointed out above, a mild detergent (CHAPS) is absolutely necessary in order to mediate the solubilization of the refolded and lipid-modified Rab protein. In general the presence of cofactors or substrates (e.g. GDP or GTP) during refolding has been shown to dramatically increase the yields of renaturation for a number of proteins. When the protein contains disulfide bonds, as is the case for most secreted proteins but not for Rabs, a redox system has to be supplemented to the renaturation buffer.<sup>[275,284]</sup> In addition to these parameters, several low molecular weight compounds were empirically identified that can promote refolding and stabilization of the target protein.<sup>[285-287]</sup> The most commonly used additives are L-arginine, low concentrations of denaturants such as urea (1-2 M) and GdmHCl (up to 1 M), polyols (trehalose, sucrose, glycerol), and detergents (CHAPS, SDS, CTAB, Triton X-100). The mechanism of action of these additives on the folding process is largely unclear (but see for example <sup>[288]</sup>). They may influence both the solubility and stability of the native, denatured and intermediate states or they may act by changing the rates of proper folded product formation and the competing aggregation reaction. Due to this lack of knowledge the effect of a given additive on the folding of a particular protein cannot be predicted and must be verified for each protein. Several compounds were tested in a first screen either alone or in combination for their ability to promote refolding of the semi-synthetic proteins including urea (1 M), sorbitol (10 %), sucrose (10 %), (NH<sub>4</sub>)<sub>2</sub>SO<sub>4</sub> (0.5 M), arginine (0.4 M), trehalose (0.4 M), ethylenglykole (20 %), CTAB (2 mM), dimyristoylphosphatidylcholine vesicles (DMPC, 1 mg/ml), n-octyl- $\beta$ -D-glucosid (1 %), CHAPS (1-3 %), sodium cholate (1 %) and TX-100 (1 %).

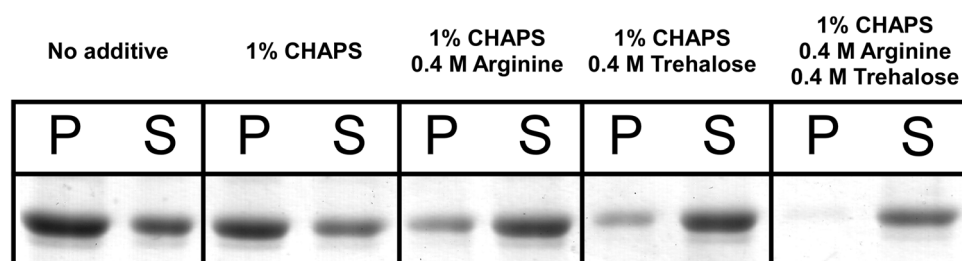


Figure 3-13: Optimization of the *in vitro* protein refolding. Different additives were screened for their ability to promote refolding of Rab7 $\Delta$ 6-CK(Dans)SCSC(GG)-OMe. All reactions contained 50 mM Hepes pH 7.5, 2.5 mM DTE, 2 mM MgCl<sub>2</sub> and 100  $\mu$ M GDP (plus residual compounds from the denaturing solution, i.e. 240 mM GdmHCl and 0.04 % CHAPS). Upon refolding according to the protocol listed in the experimental section (5.3.3.), soluble (**S**) and precipitated (**P**) proteins were separated by centrifugation. Aliquots were loaded on a 15 % SDS-PAGE gel followed by Coomassie Blue staining.

The efficiency of each additive was judged by determining the proportion of precipitated (i.e. aggregated) and soluble protein after refolding. The best condition identified so far was a combined usage of arginine, trehalose and CHAPS, which essentially completely prevented protein precipitation (Figure 3-13). Although the protein is maintained in the soluble fraction, this does not necessarily prove that it is correctly folded. Certainly, biochemical activity assays (e.g. GTP hydrolysis, or guanine-nucleotide binding/release) would provide a more sensitive measure for the functionally active state of the Rab protein. However in most cases the refolded Rab was intended for complexation with interacting proteins such as REP, RabGDI or REP:GGTase-II, which are expected to discriminate between the correctly folded and misfolded protein due to the dependence of this interaction on the integrity of the GTPase fold.<sup>[56,95,105,289]</sup> Recognition of Rab proteins by REP<sup>[111-113]</sup> or RabGDI<sup>[290]</sup> is dependent upon the GDP-bound conformation, which requires the presence of GDP during the *in vitro* protein refolding. On the other hand, supplementing the refolding buffer with other nucleotides (e.g. hydrolysis resistant or fluorescent analogues of GTP) could easily give access to differently loaded Rab proteins, which would meet the needs of various other applications.

After renaturation of the lipid-modified Rab protein further purifications turned out to be straightforward using standard biochemical procedures (Figure 3-14). The Rab protein was complexed to either REP-1 or RabGDI and the formed complex was further separated from ligation and refolding additives by dialysis and gel filtration chromatography. The only encountered problem of the described purification procedure was the handling of large volumes of very dilute protein solutions, which is a direct consequence of the necessity for low protein concentrations during refolding. Hence, prior to gel filtration the protein-containing samples had to be concentrated, which was usually carried using time-consuming size-exclusion filtrations. Preliminary data indicate that concentration could more conveniently be achieved by ion exchange chromatography employing fast-flow columns, however, this alternative needs further optimization.

The devised protocols demonstrate for the first time the applicability of the *in vitro* protein refolding approach to lipid-modified small GTPases.

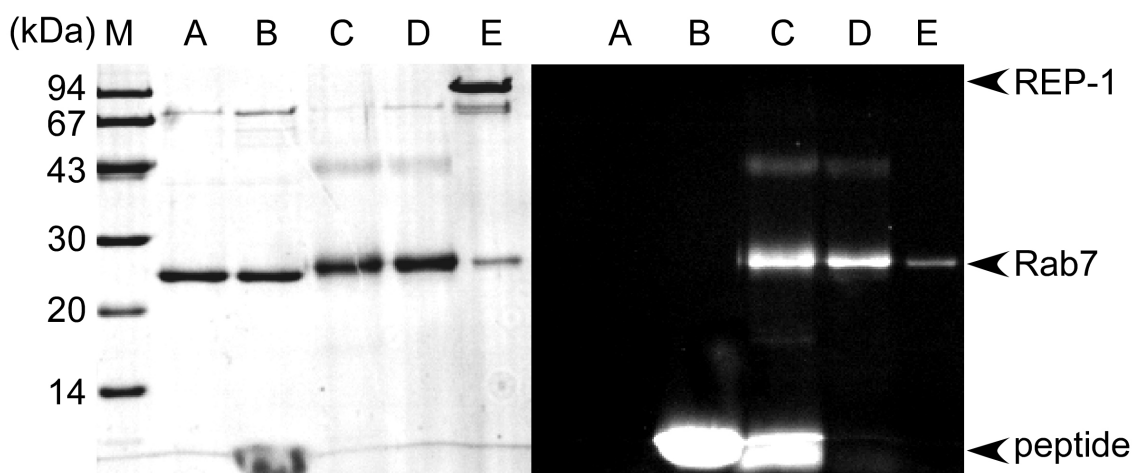


Figure 3-14: Ligation of Rab7 $\Delta$ 6-MESNA thioester with CK(Dans)SCSC(GG)-OMe and purification of the semi-synthetic Rab:REP-1 complex. Thioester tagged Rab7 (lane A), mixed with peptide (lane B) and following a 12 h incubation at room temperature (lane C). Excessive peptide was removed by washing with organic solvents (lane D). The protein was renatured, complexed to REP-1 and further purified by gel filtration (lane E). The 15 % SDS-PAGE gel was photographed while exposed to UV light (right) prior to Coomassie Blue staining (left).

### 3.1.6. Overview of semi-synthetic protein complexes

Table 3-1 summarizes the preparation results for some selected semi-synthetic prenylated Rab proteins which were complexed to RabGDI, REP-1, MRS6p and REP:GGTase-II. Various Rab proteins could be ligated to a multitude of synthetic peptides demonstrating that the devised protocols are generally applicable. In addition, the outlined purification procedure can also be adopted to the EPL semi-synthesis of farnesylated Ras proteins (data not shown, see <sup>[291]</sup>). As will be shown in the following sections, most semi-synthetic Rab proteins prepared in such a manner displayed wild-type characteristics. In four cases however, the preparation of functional and stoichiometric protein complexes was unsuccessful (Table 3-1, No. 6, 10, 11, and 15). Although the EPL and initial purifications worked as efficiently as in the other cases, the semi-synthetic Rab proteins could neither be complexed to REP-1 nor to RabGDI. Instead, following the final gel filtration chromatographic step, REP-1 was predominantly bound to the unprenylated and unligated Rab protein, whereas RabGDI largely eluted in the uncomplexed form. The ligated and prenylated Rab protein was retained on the column, probably in the denatured state. Such a behaviour was always observed when peptides bearing the dansyl fluorophore linked via ethylenediamine to the C-terminus were used in the EPL reaction, regardless of which Rab isoform was used as the thioester component.

No.	Rab thioester	Peptide	Complexed to	Purification (*)	Application and references
1	Rab7 $\Delta$ 6-MESNA	CK(Dans)SCSC(GG)-OMe	REP-1	++	Chapter 3.2. and 3.3. <sup>[292]</sup>
2			yRabGDI	++	---
3		CK(Dans)SC(GG)SC(GG)-OMe	REP-1	++	Chapter 3.2. and 3.3. <sup>[293]</sup>
4		CK(Dans)SC(GG)SC-OMe	REP-1	++	
5		CK(NBD)SCSC(GG)-OMe	REP-1	++	Chapter 3.2.
6		CESC(GG)SC(GG)-NH(CH <sub>2</sub> ) <sub>2</sub> NH-Dans	REP-1	-	Chapter 3.4. <sup>[294]</sup>
7		CESC(GG)SC(GDans)-OMe	REP-1	++	Chapter 3.1.5. <sup>[294]</sup>
8		CK(Dans)C(GG)-OMe	---	++	--- (Test-protein)
9	Rab7 $\Delta$ 2-MESNA	CC(GG)	RabGDI-1	++	Chapter 3.5.
10	Ypt7 $\Delta$ 7-MESNA	CESC(GG)SC(GG)-NH(CH <sub>2</sub> ) <sub>2</sub> NH-Dans	MRS6p	-	Chapter 3.4. <sup>[294]</sup>
11			yRabGDI	-	
12	Ypt1 $\Delta$ 2-MESNA	CC(GG)	yRabGDI	+++	Chapter 3.4. <sup>[295]</sup>
13			MRS6p	+++	Chapter 3.5.
14			MRS6p GGTase-II	+++	Chapter 3.5.
15		CC(GG)-NH(CH <sub>2</sub> ) <sub>2</sub> NH-Dans	yRabGDI	-	Chapter 3.4.
16	Ypt1 $\Delta$ 3-MESNA	CC(GG)C(GG)	yRabGDI	+++	Chapter 3.5.

Table 3-1: Selection of semi-synthetic geranylgeranylated Rab protein complexes prepared according to the devised protocols. \* The assessment is based on complex stability and purity and on the quality of the analytical data (LC-ESI-MS, MALDI-MS, GF, SDS-PAGE, etc.).

One could interpret these findings with the inability of RabGDI or REP-1 to effectively accommodate the lipidated Rab C-terminus due to sterical conflicts with the non-native reporter group. This will be discussed in view of the Ypt1:RabGDI crystal structure in chapter 3.4.

In contrast, incorporation of the dansyl fluorophore into the terminal isoprenoid moiety does not seem to impair Rab recognition by REP-1 as judged by the co-elution of both proteins upon gel filtration (Figure 3-15).

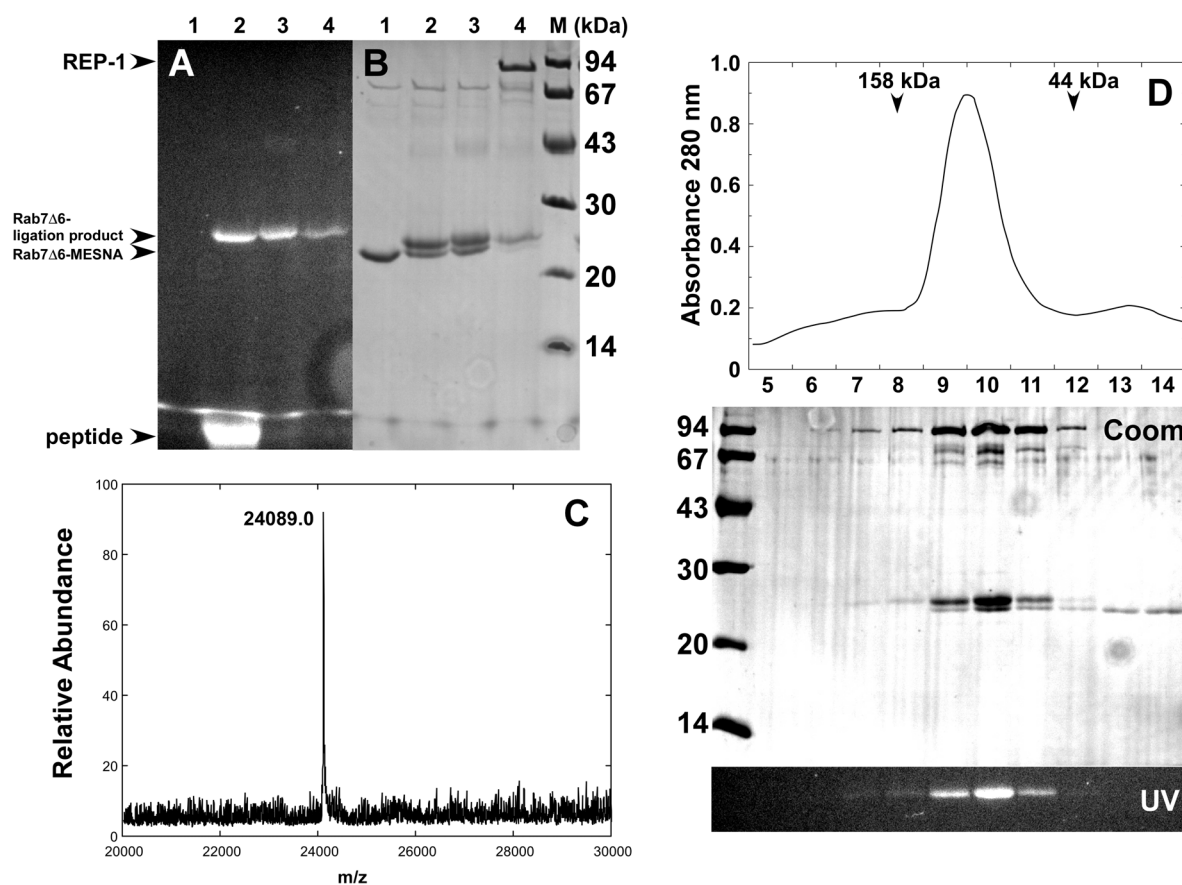


Figure 3-15: Ligation and purification of Rab7 $\Delta$ 6-CESC(GG)SC(GDans)-OMe. **A,B)** SDS-PAGE analysis of the purification procedure. Rab7 $\Delta$ 6-MESNA thioester (lane 1), after ligation to the peptide CESC(GG)SC(Gdans)-OMe (lane 2), after removal of contaminating peptide (lane 3), and after complex formation with REP-1 and gel filtration purification (lane 4). The gel was photographed either while exposed to UV light (**A**) or following Coomassie Blue staining (**B**). **C)** LC-ESI-MS spectrum of the purified Rab7:REP-1 complex. The theoretical molecular mass of  $^{2-201}$ Rab7 $\Delta$ 6-CESC(GG)SC(GDans)-OMe is 24091 Da. **D)** Preparative gel filtration chromatogram of the Rab7:REP-1 complex utilizing a Superdex 200 (16/60) column. Calibration was carried out using proteins of known molecular weight (elution position indicated by arrows). Analysis of the individual fractions by SDS-PAGE is shown below. The lower part of the gel represents the fluorescence in the molecular weight range of 20-30 kDa.

In this context, it is important to note that complexes of Rab and REP typically elute as proteins of ca. 150 kDa, which is, at first glance, inconsistent with a theoretical molecular weight of a 1:1 complex of ca. 100 kDa. Although Shen and Seabra<sup>[117]</sup> argue that prenylation could induce the formation of 2:2 or 1:2 Rab:REP complexes, it is more likely that this discrepancy is due to an anomalous Stokes radius reflecting the deviation of REP from a globular shape.<sup>[105,115]</sup> Similar deviations from the theoretical molecular weight have been observed for RabGDI using biochemical techniques such as SDS-PAGE, sucrose density gradient ultracentrifugation and gel filtration.<sup>[56]</sup> The efficiency of ligation typically ranged from 50 % to more than 95 % under the devised conditions (see for example Figure 3-14 and 3-15). The final recovery upon complex formation and purification was usually 10-50 % with respect to the utilized starting Rab-thioester. The prepared complexes were highly homogenous, and in most cases no residual unligated Rab protein could be detected (but see for example Figure 3-15A).

### **3.2. Characterization of the interaction of GGTase-II with single-prenylated reaction intermediates and the doubly prenylated product**

The catalytic process by which prenyl modification of Rab proteins occurs has been the subject of many detailed studies in the past, since it was early recognized to be essential for membrane association and formation of certain specific protein-protein interactions.<sup>[126]</sup> Elucidation of the molecular mechanism underlying Rab double prenylation by GGTase-II and REP revealed a complicated process, which is characterized by the following features (Figure 3-16):

1. According to the classical view, REP presents the newly synthesized Rab-GDP protein to GGTase-II and thereby facilitates the isoprenoid transfer.<sup>[110,114,115]</sup> Recent data suggest that REP-1 can also associate with GGTase-II alone in a phosphoisoprenoid (GGPP) dependent manner.<sup>[105,106,296]</sup> Subsequent binding of the Rab protein to the REP:GGTase-II:GGPP complex results in the formation of a prenylation competent quaternary complex (alternative pathway).
2. The association of GGTase-II with the Rab:REP-1 complex is allosterically regulated by GGPP. In the absence of GGPP the double prenylated Rab:REP product complex is bound tighter to the GGTase-II ( $K_d = 2 \text{ nM}$ )<sup>[118]</sup> than the unprenylated substrate complex ( $K_d = 120 \text{ nM}$ ).<sup>[114]</sup> To overcome this unfavourable

situation, binding of GGPP to GGTase-II increases the affinity of the enzyme for the Rab:REP substrate complex by approximately 20 fold. Conversely, the affinity for the double prenylated Rab:REP product is decreased by ca. 10 fold.<sup>[118]</sup> Thus GGPP functions as a sensor for the prenylation state of the Rab:REP complex and increases the enzyme's efficiency to perform multiple catalytic turnovers.

3. GGTase-II transfers both geranylgeranyl groups from GGPP to the C-terminus of Rab in two independent sequential reactions.<sup>[116,117,297]</sup> The order of isoprenoid addition seems to be random, i.e. in principle both cysteines can accept the geranylgeranyl group in the first round of prenylation. Still, one of the cysteines is somewhat favored but controversy remains over the exact preference.<sup>[116,117]</sup> The first prenyl transfer reaction appears to be faster than the second, which transiently results in the accumulation of single prenylated Rab reaction intermediates.<sup>[116]</sup> Interestingly, single prenylated Rab proteins have not been identified *in vivo* so far<sup>[102]</sup> and only little, if any, monoprenylated protein is eventually formed in *in vitro* prenylation reactions under conditions permitting multiple catalytic turnovers.<sup>[101,110,298]</sup> Taking into account the improper *in vivo* functioning of mutated single prenylated Rab proteins<sup>[132,133]</sup> (albeit controversial, see<sup>[134,217]</sup>), this raises the question by which mechanism(s) the enzyme ensures Rab double prenylation. A possible and very likely explanation suggests that the rate of dissociation of the monogeranylgeranylated Rab:REP complex from GGTase-II might be significantly slower than the rate of the second geranylgeranylation reaction.<sup>[116,117]</sup>

It is noteworthy, that most studies addressing these issues employed single cysteine mutant proteins (i.e. in which one of the two cysteine residues had been mutated to serine). These mutants do not allow a clear cut answer, since changing the substrate structure at or near the site of the chemical transformation can be expected to significantly affect the kinetic behaviour of the enzyme under investigation. For example in analogy to FTase,<sup>[299]</sup> it seems sensible that the essential zinc ion present in the active site of GGTase-II coordinates to the thiolate group of the substrate cysteine residue and activates it for the nucleophilic attack on the C<sub>1</sub> atom of GGPP.<sup>[108]</sup> In contrast, serine can be expected to coordinate much weaker to zinc, since hydroxyl groups are poor ligands for this metal ion.

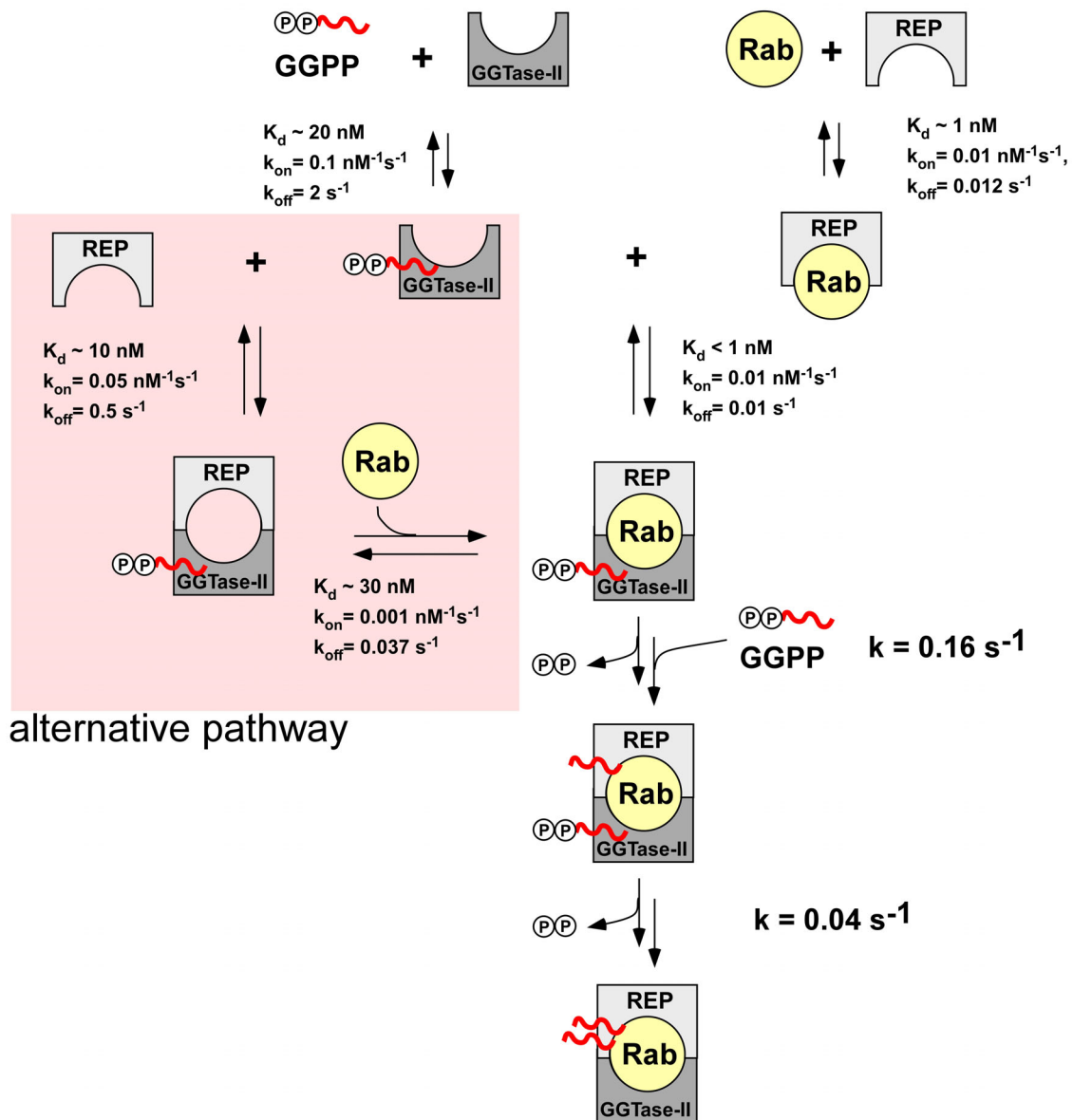


Figure 3-16: Mechanism of Rab protein digeranylgeranylation. Modified from Thomä et al.<sup>[106]</sup> The specified rate constants ( $k_{on}$ ,  $k_{off}$ ) and dissociation constants ( $K_d$ ) refer to interactions involving the mammalian Rab7 and REP-1 isoforms.

The developed EPL strategy provides the means for elegantly circumventing these problems. As described in detail in chapter 3.1.1., a strategy was envisaged by which full length Rab7 can be generated from a C-terminally truncated N-terminal recombinant peptide corresponding to residues 1-201, and a synthetic C-terminal peptide corresponding to residues 202-207 (Figure 3-1). The Rab7 isoform was chosen because of its well characterized behaviour in the GGase-II catalyzed prenylation reaction.<sup>[113,114,116,118,199,300]</sup> Peptides carrying a single geranylgeranyl group attached to either biologically relevant residue (Cys<sup>205</sup>/Cys<sup>207</sup>) as well as the double modified structure were synthesised by Dr. Ines Heinemann, Department of

Chemical Biology, MPI-Dortmund. In order to characterize the interaction between the semi-synthetic Rab proteins and GGTase-II, fluorophores (dansyl, NBD) linked to the  $\epsilon$ -amino group of lysine were introduced by substituting the native Glu<sup>203</sup>, resulting in a modification that is known to be functionally tolerated (Figure 3-17).<sup>[199]</sup>

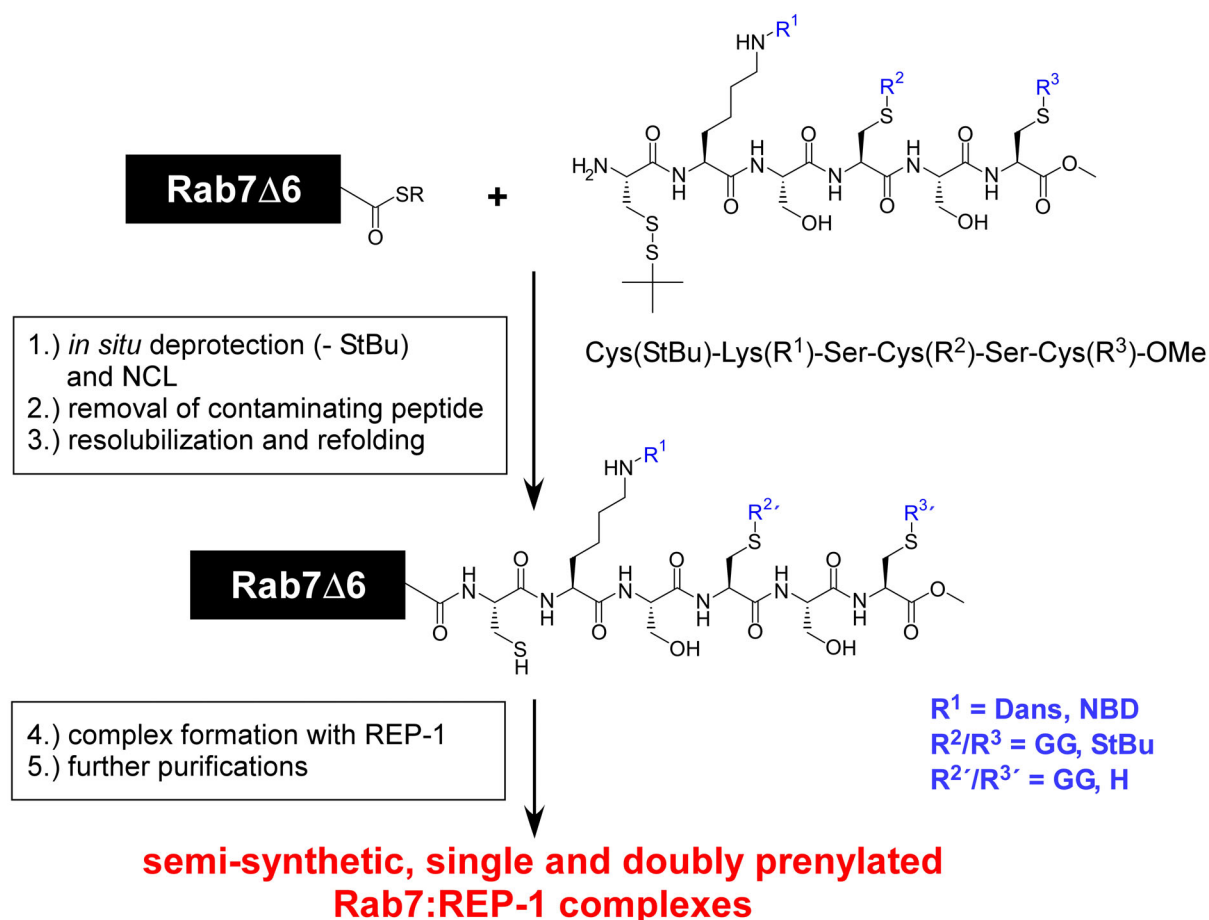


Figure 3-17: Semi-synthesis of Rab7 proteins representing the intermediates and the product of the GGTase-II mediated prenylation reaction by means of EPL.

Preparation of the Rab7 $\Delta$ 6-MESNA thioester protein, its ligation to the peptides and the purification of the semi-synthetic protein complexed to REP-1 were carried out as described in chapter 3.1. and the experimental section (5.3.2. and 5.3.3.). Co-elution of the fluorescently labeled Rab protein(s) and REP-1 upon analytical gel filtration confirmed the presence of a heteromeric complex (Figure 3-18). The elution volume of the complexes corresponded to an apparent molecular mass of about 150 kDa. Taking into account the familiar unusual behaviour of REP in gel filtration experiments and judged by the intensity of the individual protein bands from

Coomassie-Blue stained SDS-PAGE gels, a 1:1 stoichiometry of the heteromeric complex could be inferred.

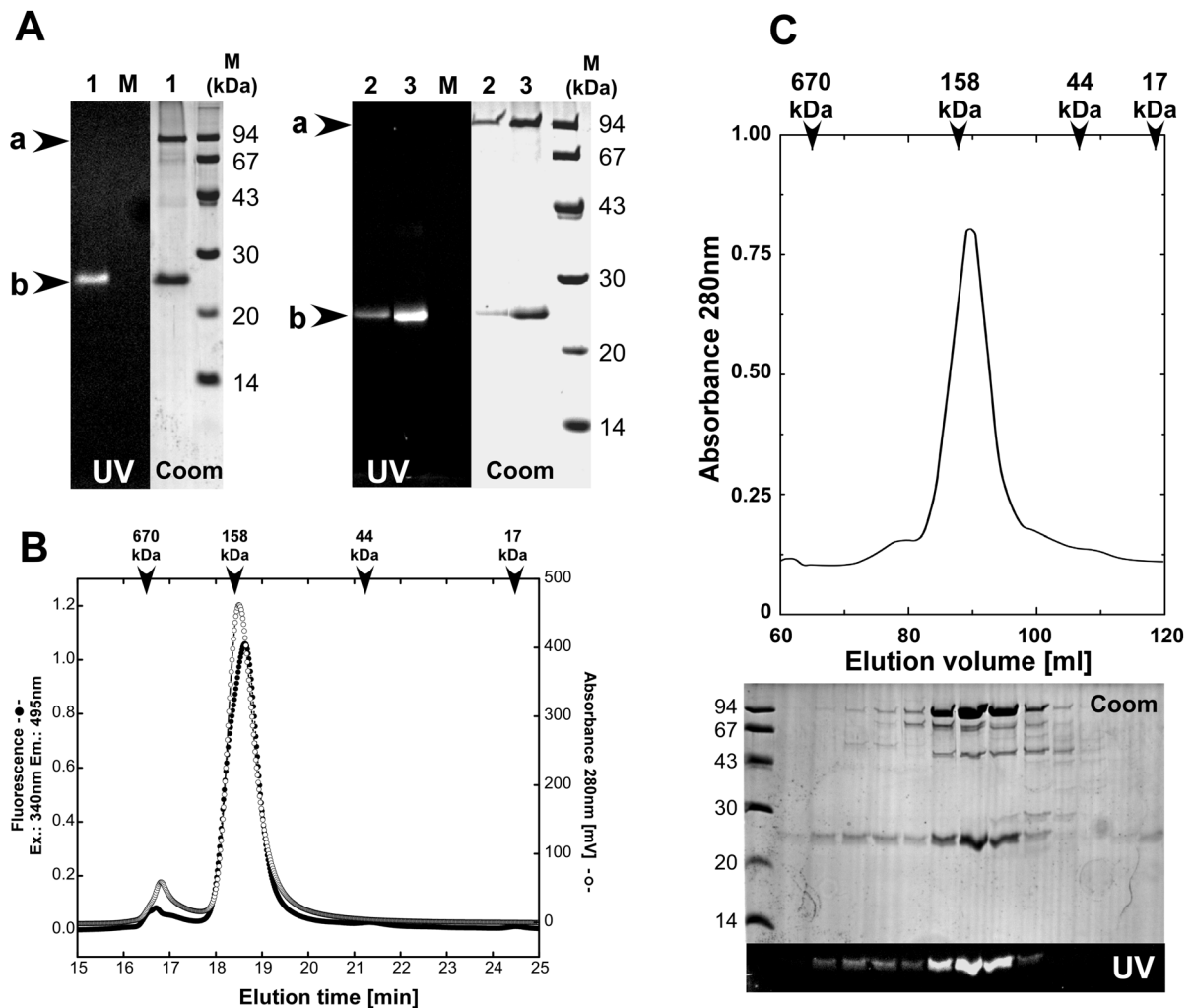


Figure 3-18: **A**) SDS-PAGE of the purified complexes (UV = fluorescence, Coom = Coomassie staining). Rab7 $\Delta$ 6-CK(Dans)SCSC(GG)-OMe:REP-1 (lane 1), Rab7 $\Delta$ 6-CK(Dans)SC(GG)SC(GG)-OMe:REP-1 (lane 2), and Rab7 $\Delta$ 6-CK(Dans)SC(GG)SC-OMe:REP-1 (lane 3). **B**) Analytical gel filtration of the Rab7 $\Delta$ 6-CK(Dans)SC(GG)SC-OMe:REP-1 complex. Column: Biosep-SEC-2000 column (60 x 0.78 cm). Detection was based on absorbance at 280 nm (-○-) or fluorescence at 495 nm observed upon excitation at 340 nm (-●-). **C**) Preparative gel filtration of Rab7 $\Delta$ 6-CK(Dans)SCSC(GG)-OMe:REP-1 complex using a Superdex-200 (26/60) column. The elution position of standard molecular weight markers is indicated by arrows. The analysis of the individual fractions by SDS-PAGE is shown below. The lower part (UV) represents the gel region corresponding to 20-30 kDa photographed in UV-light prior to Coomassie-blue staining (Coom).

The identities of the prenylated Rab proteins were confirmed by detailed mass spectroscopic analysis (Figure 3-19). In all cases the mass of the major signal was in accordance with the expected molecular masses of the ligated Rab proteins ( $\pm 15$  Da, which is within the error range of the MALDI spectrometer). Only little, if any, unligated Rab protein could be detected by MALDI-MS spectroscopy,

SDS-PAGE (see for example Figure 3-14) or RP-HPLC. These data suggest that the prepared Rab proteins are homogeneously prenylated and are able to form stoichiometric complexes with REP-1 indicating a native GTPase fold.

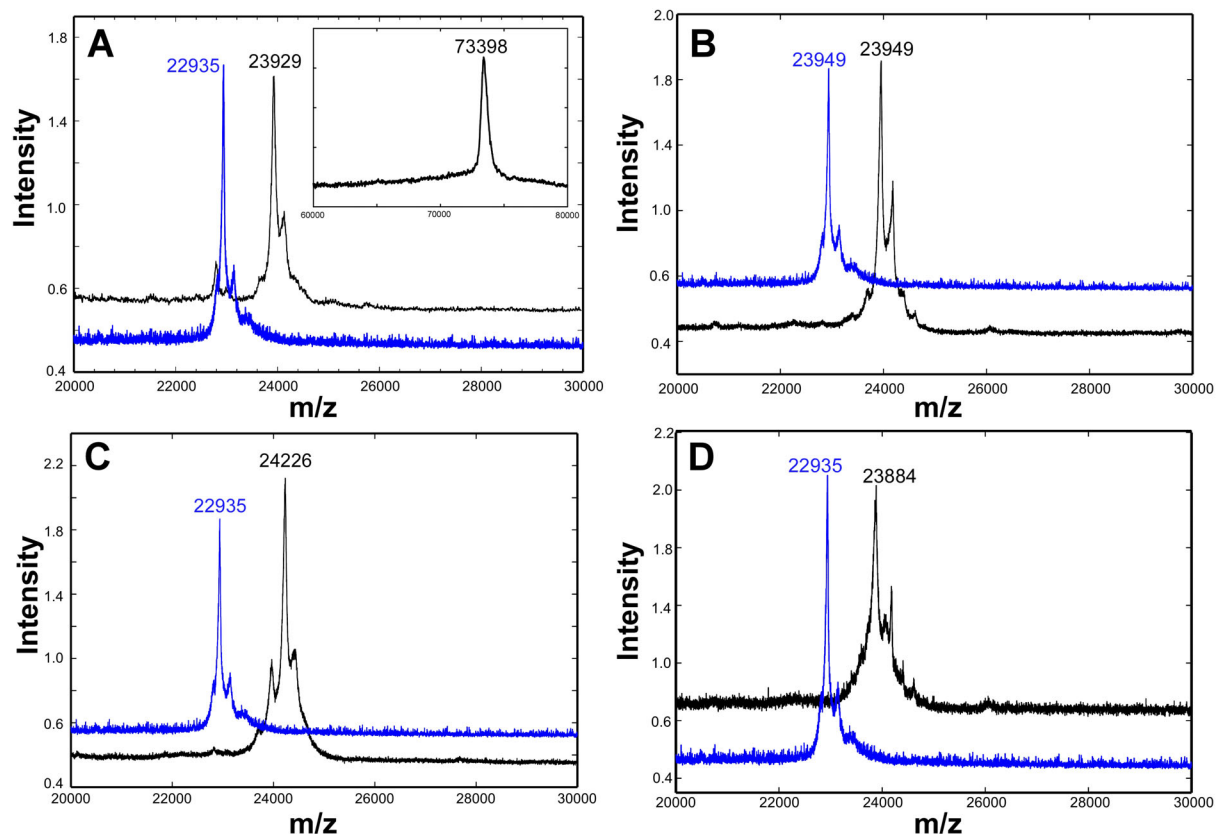


Figure 3-19: MALDI-MS analysis of semi-synthetic Rab:REP-1 protein complexes.  $^{2-201}$ Rab7 $\Delta$ 6-MESNA thioester (before ligation,  $M_{\text{calc}} = 22932$  Da) is shown in blue. **A)**  $^{2-201}$ Rab7 $\Delta$ 6-CK(Dans)SCSC(GG)-OMe ( $M_{\text{calc}} = 23939$  Da). The inset shows the range from 60-80 kDa and the signal corresponding to REP-1 ( $M_{\text{calc}} = 73475$  Da). **B)**  $^{2-201}$ Rab7 $\Delta$ 6-CK(Dans)SC(GG)SC-OMe ( $M_{\text{calc}} = 23939$  Da), **C)**  $^{2-201}$ Rab7 $\Delta$ 6-CK(Dans)SC(GG)SC(GG)-OMe ( $M_{\text{calc}} = 24212$  Da), and **D)**  $^{2-201}$ Rab7 $\Delta$ 6-CK(NBD)SCSC(GG)-OMe ( $M_{\text{calc}} = 23870$  Da). The deviation of the observed molecular masses from the calculated values is within the error range of the mass spectrometer. Matrix: sinapinic acid.

To further confirm the functionally active state of the complexes, their competence to act as a substrate in the prenylation reaction was investigated using an established assay.<sup>[301]</sup> The individual Rab:REP-1 complexes were incubated with GGTase-II and tritium labeled geranylgeranylpyrophosphate ( $[^3\text{H}]\text{-GGPP}$ ). After completion of the reaction (30 min), proteins were precipitated with ethanol/HCl and separated from excessive  $[^3\text{H}]\text{-GGPP}$  by filtration through glass-fiber filters. The amount of radioactivity incorporated into the proteinaceous material was determined by scintillation counting (Figure 3-20). Wild-type Rab7 protein incorporated twice as

much radioactivity than the single prenylated semi-synthetic Rab7 $\Delta$ 6-CK(Dans)SCSC(GG)-OMe protein and a Rab7 mutant lacking one of the prenylateable cysteines (Rab7C<sup>205</sup>S). These data suggest that the single prenylated protein could function as an acceptor for another geranylgeranyl group. Similar results were obtained for the other single prenylated proteins (Figure 3-20B). The unprenylated cysteine is therefore fully accessible indicating that the *in situ* deprotection of the StBu-protected cysteines during the ligation reaction was essentially quantitative. This is also in agreement with the mass spectroscopic data. The double prenylated semi-synthetic Rab7 $\Delta$ 6-CK(Dans)SC(GG)SC(GG)-OMe protein incorporated significantly lower amounts of radioactivity than the single prenylated proteins, still slightly more than the negative control without GGTase-II (Figure 3-20B, lane 3 and 5). Although the significance of this observation is not clear yet, one could speculate that GGTase-II could transfer an additional prenyl group to the third (ligation-) cysteine (Cys<sup>202</sup>), albeit with much lower efficiency. Triple prenylated Rabs have neither been identified *in vitro* nor *in vivo*, but this could simply be due to the fact, that Rabs possessing *three* prenylateable cysteines within their last six amino acids naturally do not exist.

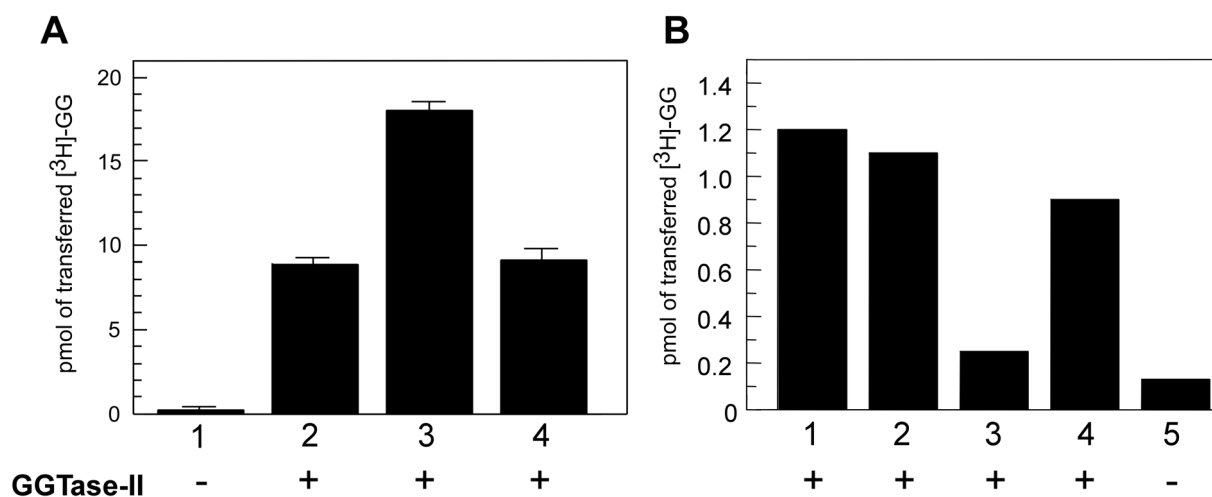


Figure 3-20: Incorporation of [<sup>3</sup>H]-geranylgeranyl into the semi-synthetic proteins catalyzed by GGTase-II. **A**) Prenylation of Rab7 $\Delta$ 6-CK(Dans)SCSC(GG)-OMe (lane 1, 2) in the absence (lane 1) and presence (lane 2) of GGTase-II. Rab7wt (lane 3) and the single cysteine mutant Rab7C<sup>205</sup>S (lane 4) are shown for comparison. **B**) Prenylation of Rab7 $\Delta$ 6-CK(Dans)SCSC(GG)-OMe (lane 1), Rab7 $\Delta$ 6-CK(Dans)SC(GG)SC-OMe (lane 2), Rab7 $\Delta$ 6-CK(Dans)SC(GG)SC(GG)-OMe (lane 3), and Rab7 $\Delta$ 6-CK(NBD)SCSC(GG)-OMe (lane 4). Lane 5 represents the negative control (Rab7wt in the absence of GGTase-II). All reactions contained 50 pmol [<sup>3</sup>H]-GGPP (15000 cpm/pmol), 11 pmol of the corresponding Rab7:REP-1 complex and 10 pmol of mammalian GGTase-II, unless otherwise indicated.

For quantitative analysis of the interaction of RabGGTase with the single prenylated reaction intermediates and the doubly prenylated product, a fluorescence assay was employed. Excitation and emission scans of the semi-synthetic Rab7:REP-1 protein complexes indicated that dansyl fluorescence could be excited either directly at 340 nm or via Fluorescence Resonance Energy Transfer (FRET) from tryptophan at 280 nm. Upon interaction with GGTase-II, an increase in the dansyl fluorescence was observed. When the dansyl fluorophore was excited via FRET at 280 nm the interaction resulted in an at least 300 % increase in fluorescence at around 500 nm (see Figure 3-22), whereas direct excitation of the dansyl fluorophore at 340 nm gave only a minor fluorescence increase of around 5% (not shown, but see for example <sup>[118]</sup>).

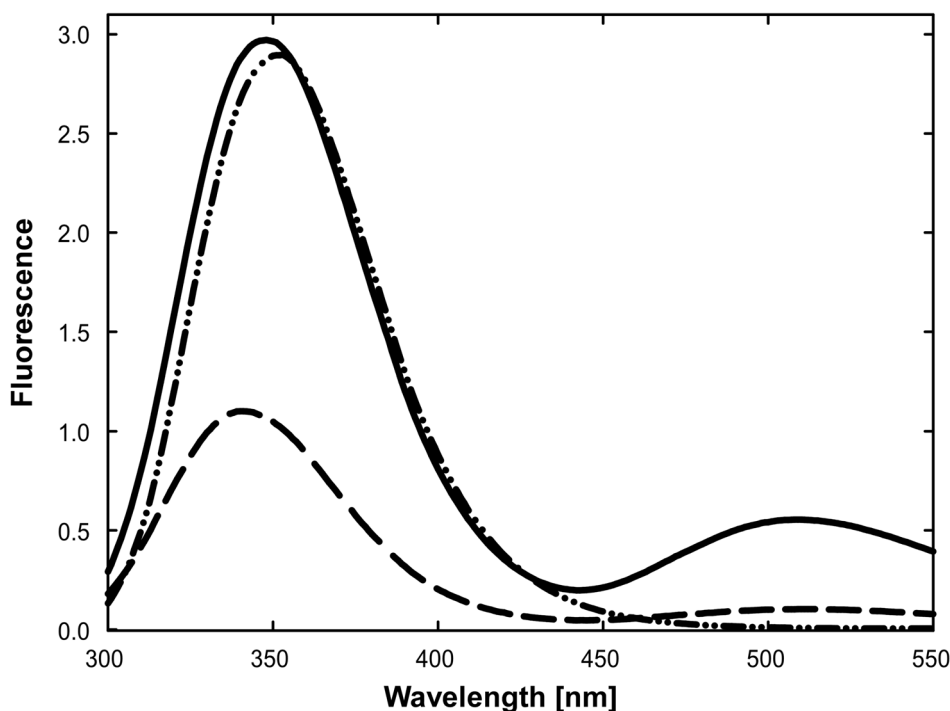


Figure 3-21: Emission scans of GGTase-II (---) and Rab7 $\Delta$ 6-CK(Dans)SC(GG)SC-OMe:REP-1 (--) alone and upon ternary complex formation (—). The concentration of each component was 200 nM and excitation was at 280 nm.

The change in fluorescence upon interaction is proportional to the amount of ternary Rab7:REP-1:GGTase-II complex formed, and can be utilized to determine the equilibrium constant of the interaction of Rab:REP with GGTase-II. Titrating small aliquots of GGTase-II to a solution of the individual Rab7:REP-1 complexes revealed that the change in fluorescence is saturable (Figure 3-22). However, addition of GGTase-II resulted also in an unspecific increase in fluorescence due to the increased concentration of tryptophan residues (mammalian GGTase-II contains a

total of 20 Trp-residues). This unspecific fluorescence increases linearly with increasing concentrations of GGTase-II, which usually becomes evident when the titration curve approaches saturation (Figure 3-22B). The contribution of the unspecific fluorescence can be determined by linear regression and allows for correction of the binding data (Figure 3-22C).

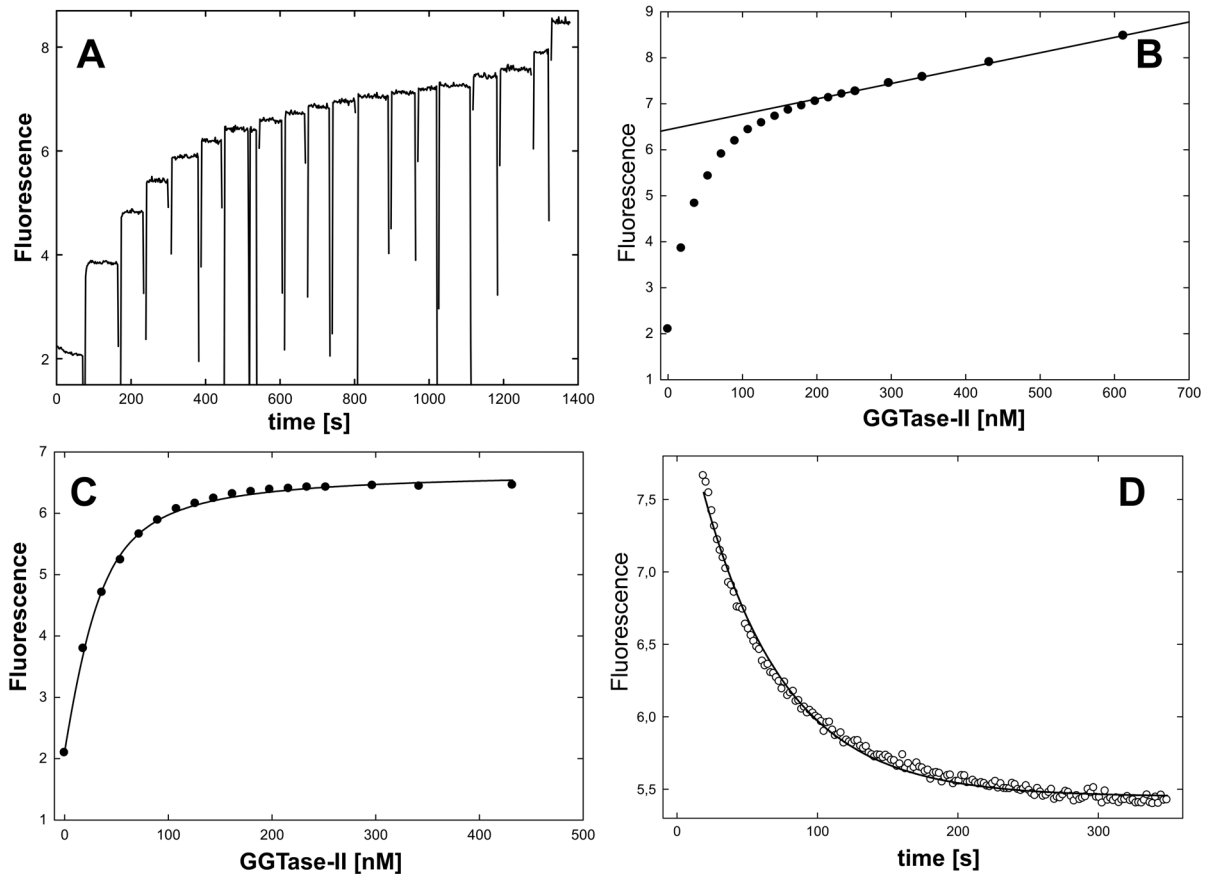


Figure 3-22: **A**) Fluorescence titration of ca. 100 nM Rab7 $\Delta$ 6-CK(Dans)SC(GG)SC(GG)-OMe:REP-1 complex with increasing concentrations of GGTase-II. At each breakdown of the fluorescence signal another portion of GGTase-II was added to the cuvette. **B**) The observed fluorescence was plotted as a function of the GGTase-II concentration. The straight line represents the increase in unspecific tryptophan fluorescence due to the addition of GGTase-II. The slope was used for data correction. **C**) Corrected titration data. The solid line represents a fit to the binding equation with a  $K_d$  of  $14 \pm 1$  nM. **D**) Displacement of the semi-synthetic fluorescently labeled Rab7:REP-1 complex from GGTase-II by addition of 1  $\mu$ M of doubly prenylated, wild type Rab7:REP-1 complex. The solid line represents a fit to a single exponential equation yielding a  $k_{off}$  of  $0.017 \pm 0.001$  s $^{-1}$ . The signal was based on FRET, exciting at 280 nm, while emission was observed at 495 nm.

The titration curves obtained from the equilibrium binding experiments were evaluated assuming a 1:1 stoichiometric binding mode for the interaction of GGTase-II with the Rab7:REP-1 complexes. The fluorescence ( $F$ ) observed after each step of GGTase-II addition is then described by the following equation:

$$F = F_{\min} + \left\{ K_d + [L]_0 + [P]_0 - \sqrt{(K_d + [L]_0 + [P]_0)^2 - 4[P]_0[L]_0} \right\} \frac{F_{\max} - F_{\min}}{2[P]_0}$$

where  $[L]_0$  and  $[P]_0$  refer to the total concentrations (free and bound) of ligand (L, corresponding to [GGTase-II]) and protein (P, [Rab7:REP-1 complex]), respectively.  $F_{\min}$  represents the fluorescence at  $[L]_0 = 0$ ,  $F_{\max}$  is the fluorescence at saturation (i.e.  $[L]_0 \rightarrow \infty$ ) and  $K_d$  is the dissociation constant that is to be determined. The derivation of this equation is described in more detail in the Appendix section 7.1.1. A least-squares fit of the obtained binding isotherms to this equation allowed estimation of  $K_d$  (Figure 3-22C). It is noteworthy, that under certain conditions (namely when  $[P]_0 \gg K_d$ ) the curves additionally provide reliable information concerning the stoichiometry of the interaction. In this case the curve resembles a rectangular hyperbola with a well defined turning point, which indicates the ligand concentration required for full occupation of the binding sites (see Figure 8-1). For example, inspection of the binding curve in Figure 3-22C reveals, that addition of approximately 100 nM GGTase-II is sufficient to saturate all binding sites on the Rab7:REP-1 complex. Since the concentration of the titrand was ca. 100 nM, it can be inferred that the stoichiometry of the interaction is 1:1.

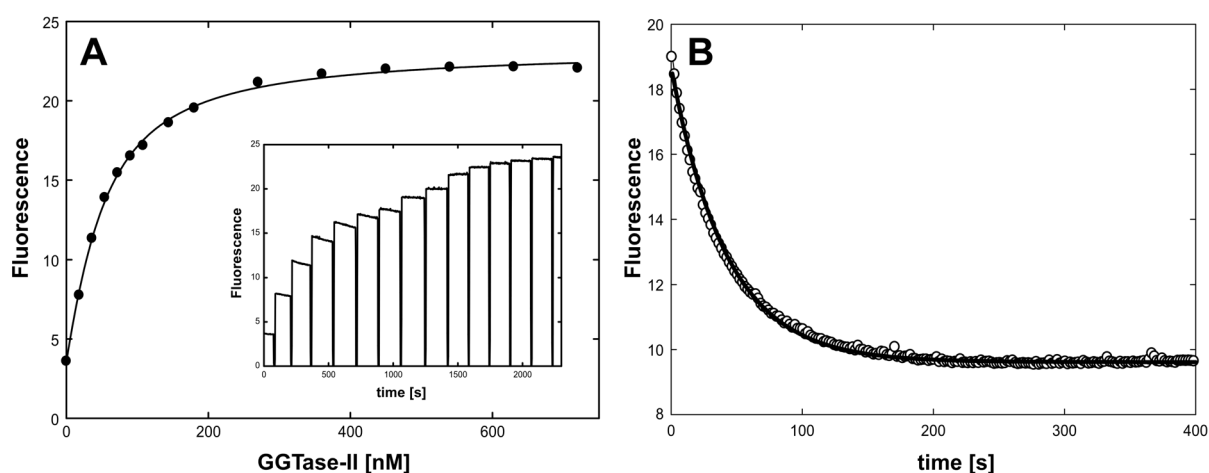


Figure 3-23: **A**) Fluorescence titration of 150 nM Rab7 $\Delta$ 6-CK(Dans)SC(GG)SC-OMe with GGTase-II. The solid line represents a fit to the binding equation yielding a  $K_d$  of  $35 \pm 4$  nM. The inset displays the original data (at each breakdown of the fluorescence signal another portion of GGTase-II was added into the cuvette). **B**) Displacement of the semi-synthetic complex from GGTase-II (each 150 nM) by addition of 1.4  $\mu$ M doubly prenylated, wild type Rab7:REP-1. The solid line represents a fit to a single exponential equation with a dissociation rate constant  $k_{\text{off}}$  of  $0.024 \pm 0.001$  s $^{-1}$ . The signal was based on FRET. Excitation was at 280 nm, while data were collected at 495 nm.

Reversal of the titration, i.e. titrating GGTase-II with increasing amounts of Rab7:REP-1 complex, produced comparable curves with essentially the same dissociation constants.<sup>[292]</sup>

The change in energy transfer observed upon interaction of the dansyl labeled Rab7:REP-1 complexes with GGTase-II can also be used to monitor the kinetics of

the reaction. The dissociation rate constants of the interaction were determined by displacement experiments. When the dansyl labeled Rab7:REP-1:GGTase-II complex is mixed with a large excess of fluorescently silent doubly prenylated Rab7:REP-1 complex, the observed time-trace describes the dissociation of the labeled complex (Figure 3-22D). The obtained curve can be fitted to a single exponential equation yielding a rate constant, which under the employed conditions corresponds to the rate constant of the dissociation reaction ( $k_{\text{off}}$ , see Appendix 7.1.2.).

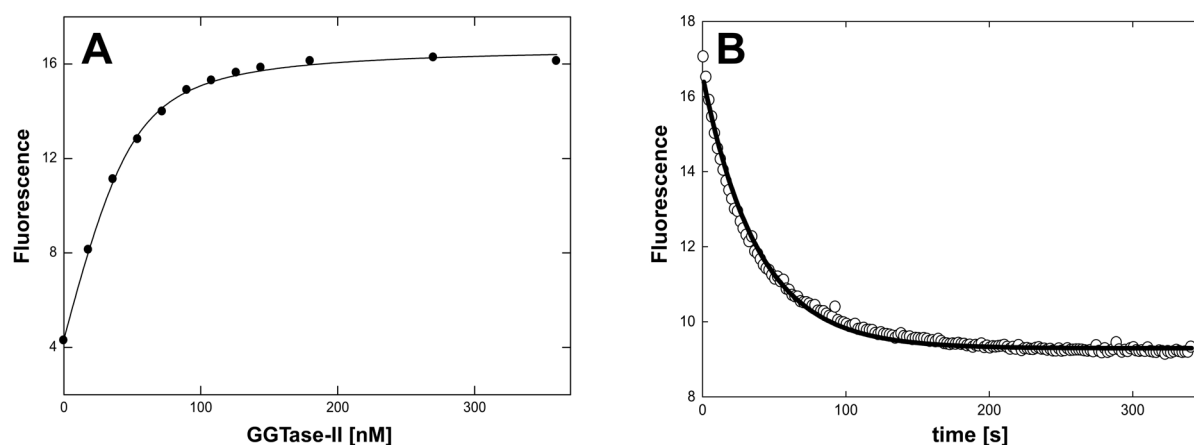


Figure 3-24: **A**) Fluorescence titration of 100 nM Rab7 $\Delta$ 6-CK(Dans)SCSC(GG)-OMe with GGTase-II. The solid line represents a fit to the binding equation yielding a  $K_d$  of  $7 \pm 2$  nM. **B**) Displacement of the semi-synthetic complex from GGTase-II by addition of 1.2  $\mu$ M doubly prenylated wild type Rab7:REP-1. The fit shown is to a single exponential with a rate constant  $k_{\text{off}}$  of  $0.027 \pm 0.001$  s $^{-1}$ . The signal was based on FRET. Excitation was at 280 nm, while data were collected at 495 nm.

The obtained dissociation constants and rate constants are summarized in Table 3-2 and are in good agreement with known literature values. Prenylation of Rab7:REP-1 results in a 3-15 fold higher affinity for GGTase-II when compared to the unprenylated protein. Both monoprenylated reaction intermediates are therefore tightly bound to GGTase-II. Interestingly, Rab7:REP-1 complex prenylated only on the internal cysteine residue (Cys<sup>205</sup>,  $K_d = 35$  nM) displayed a 3-5 fold decrease in affinity for GGTase-II as compared to the C-terminally monoprenylated (Cys<sup>207</sup>,  $K_d = 7$  nM) and doubly prenylated ( $K_d = 13$  nM) complexes.

The position of the Rab C-terminus in the ternary Rab:REP:GGTase-II complex is not known. Structure based modeling studies suggest that the unprenylated C-terminus is transferred to the GGTase-II upon interaction.<sup>[105]</sup> The C-terminus of single prenylated Rabs must be positioned near the active site of GGTase-II in order to be accessible for the second prenyl transfer reaction, since the large distance between the transferase active site and REP preclude a situation in which the conjugated

isoprenoid is bound to REP, while the adjacent cysteine protrudes into the active site.<sup>[105]</sup> Moreover, biochemical<sup>[116,118]</sup> and modeling<sup>[299]</sup> data indicate, that geranylgeranyl moieties attached to the Rab protein do not occupy the phosphoisoprenoid binding site at the active site of the transferase, but could be positioned in a nearby hydrophobic tunnel, patch or binding pocket.<sup>[299]</sup> It is conceivable that crucial functional groups mediating the interaction of the monoprenylated Rab C-terminus with GGTase-II involve the unprenylated cysteine residue (coordinated to the zinc ion) and the conjugated isoprenoid moiety.

Hence, the observed significant differences in affinities of the monoprenylated complexes for GGTase-II could be attributed to the different location of the unprenylated cysteine residue and the prenyl group attached to the other cysteine. In fact, these are the only structural features that distinguish these complexes. Following this line of argumentation, positioning of the prenyl group on the upstream cysteine (Cys<sup>205</sup>) could impose an unfavorable orientation of Cys<sup>207</sup>, which is reflected by the larger dissociation constant of the interaction. Conversely, accommodation of the isoprenoid attached to the C-terminal cysteine and coordination of Cys<sup>205</sup> to the zinc ion is preferred, which might explain the observed preference of GGTase-II for the terminal cysteine in the first round of prenylation.<sup>[116]</sup>

Complex	K <sub>d</sub> [nM]	k <sub>off</sub> [s <sup>-1</sup> ]
Rab7Δ6-CK(Dans)SCSC-OH:REP-1 <sup>[199,300]</sup>	111	-
Rab7Δ6-CK(Dans)SCSC( <b>GG</b> )-OMe:REP-1	7 ± 2	0.027 ± 0.001 0.017 ± 0.001 *
Rab7C205S;C207C( <b>GG</b> ):REP-1 <sup>[116]</sup>	~ 1	0.010
Rab7Δ6-CK(Dans)SC( <b>GG</b> )SC-OMe:REP-1	35 ± 4	0.023 ± 0.001
Rab7Δ6-CK(Dans)SC( <b>GG</b> )SC( <b>GG</b> )-OMe:REP-1	13 ± 1	0.019 ± 0.001
Rab7Δ6-CK(Dans)SC( <b>GG</b> )SC( <b>GG</b> )-OH:REP-1 <sup>[118]</sup>	2	0.017

Table 3-2: Interaction of GGTase-II with unprenylated Rab7:REP-1, single prenylated reaction intermediates and doubly prenylated product as described by the dissociation constants (K<sub>d</sub>) and the rate constants of the dissociation step (k<sub>off</sub>). The values are the mean and the standard error of at least three independent measurements. For the sake of comparison, values from the literature were incorporated into the table and are marked by the corresponding references. The values were determined at T = 25° C (\* 20° C).

The dissociation rate constants (k<sub>off</sub>) are essentially identical in case of the monoprenylated complexes, indicating that the differences in affinity must be due to a difference in the association rate constants. Moreover, the dissociation rate constants of the single prenylated reaction intermediates were found to be lower than the

second prenylation step ( $k = 0.04 \text{ s}^{-1}$  [116]), suggesting that dissociation is not obligatory for double prenylation of Rab proteins.

The known impact of GGPP on the affinities of GGTase-II for its unprenylated substrate and doubly prenylated product (see above)<sup>[118]</sup> raises the question whether the interaction with the single prenylated reaction intermediates is influenced by GGPP or not. Studies employing single prenylated cysteine mutant proteins indicate that the dissociation rate constant is essentially unaffected by the presence of GGPP.<sup>[116]</sup> Unfortunately, comparable studies using the obtained semi-synthetic Rab:REP complexes could not further address this question, since as expected, addition of GGPP to the single prenylated ternary complexes is sufficient to initiate the second prenyl transfer reaction (Figure 3-20). In this context, GGPP analogs in which the ester moiety is replaced by an enzymatically inert functionality could prove useful in the future (Figure 3-25). Such compounds cannot be catalytically transferred onto Rab proteins, while it is likely that their binding to GGTase-II is more or less unimpaired.

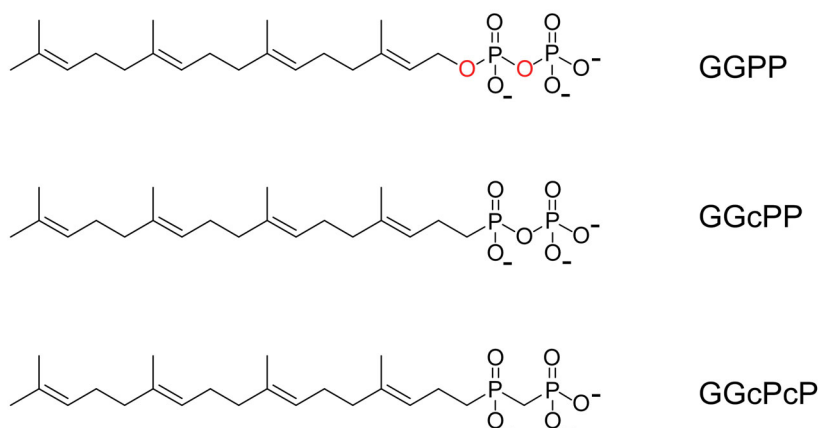


Figure 3-25: GGPP and derivatives thereof, which cannot be transferred by GGTase-II. GGPP = geranylgeranylpyrophosphate, GGcPP = geranylgeranylmethylphosphonylphosphate, GGcPcP = geranylgeranylmethylphosphinylmethylphosphonate.

### 3.3. A sensitive, real-time fluorescence based prenylation assay

The competence of the single prenylated semi-synthetic Rab proteins to accept another isoprenoid group by GGTase-II catalysis inspired us to check whether the transfer of the prenyl group can be observed by fluorescence changes of the dansyl reporter group. The proximity of the fluorophore to the prenylation site as well as the known sensitivity of dansyl toward environmental changes can be assumed to provide a sensitive measure for the prenylation state of the Rab C-terminus and should allow to follow the prenylation reaction in real-time.

When the single prenylated Rab7:REP-1 complexes (ca. 75 nM) were mixed with equal amounts of transferase, formation of the ternary complex could be inferred from the strong fluorescence increase observed at 510 nm upon excitation at 280 nm. The concentrations of the individual components were chosen based on the obtained  $K_d$  values (section 3.2.). Under such conditions the Rab:REP:GGTase-II complex can be expected to be the predominant species, since the concentrations of all proteins are far above the respective  $K_d$  value. The enzyme is only capable of performing a single turnover, since neither REP-1 nor GGTase-II are limiting factors. Addition of GGPP (10  $\mu$ M) instantly resulted in a decline of the fluorescence signal. The observed reaction was essentially completed within 10 min and the obtained time traces could be fitted to a double exponential equation (Figure 3-26A). Under the same conditions, the observed changes of the fluorescence amplitude were in case of the single prenylated Rab substrates significantly larger than for the doubly prenylated Rab protein (Figure 3-26A). The low fluorescence change observed in case of the latter possibly represents low efficiency transfer of a third prenyl group onto the ligation cysteine, which is also in agreement with results presented earlier (Section 3.2. and Figure 3-20).

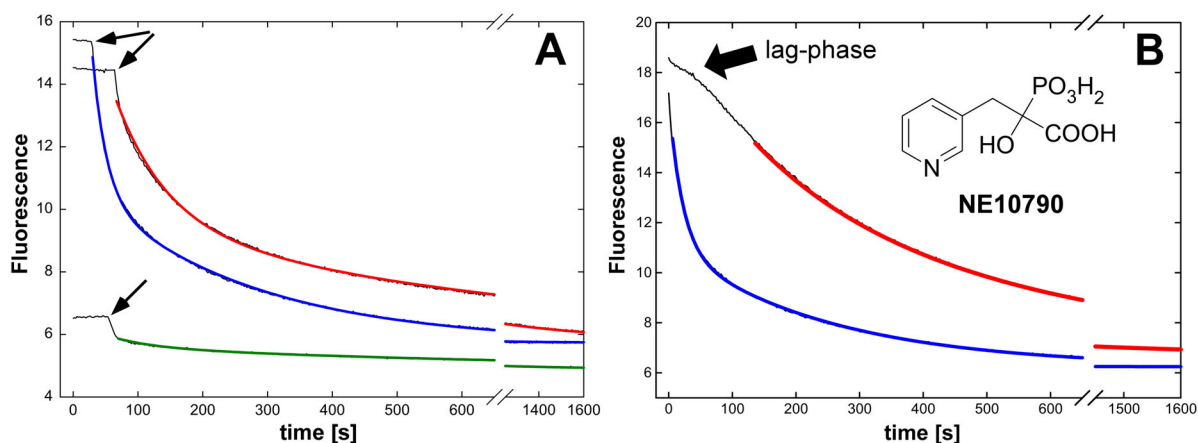


Figure 3-26: **A)** 75 nM of either Rab7 $\Delta$ 6-CK(Dans)SCSC(GG)-OMe (blue), Rab7 $\Delta$ 6-CK(Dans)SC(GG)SC-OMe (red) or Rab7 $\Delta$ 6-CK(Dans)SC(GG)SC(GG)-OMe (green) in complex with REP-1 were incubated with 75 nM GGTase-II. At the moment indicated by arrows 10  $\mu$ M GGPP was added. **B)** Fluorescence changes seen upon mixing 75 nM Rab7 $\Delta$ 6-CK(Dans)SCSC(GG)-OMe:REP-1:GGTase-II with 10  $\mu$ M GGPP in the absence (blue) and presence (red) of 500  $\mu$ M inhibitor NE10790. Excitation and emission monochromators were set to 280 nm and 510 nm, respectively. The colored curves represent fits to a double exponential equation. The individual rate constants are summarized in Table 3-3.

In order to further confirm that the observed reaction reflects the second prenyl transfer reaction, the experiment was repeated in the presence of a known GGTase-II inhibitor. NE10790 is a phosphonocarboxylate-based inhibitor specific for

GGTase-II and prevents Rab prenylation when present in high micromolar concentrations ( $IC_{50} \sim 600 \mu\text{M}$ ).<sup>[302]</sup> Addition of this compound (500  $\mu\text{M}$ ) to the *in vitro* prenylation reaction significantly slowed down the rate of fluorescence decrease, suggesting that the observed reaction indeed represents the catalytic prenylation step (Figure 3-26B). Interestingly, upon pre-incubation of GGTase-II with the inhibitor and initiation of the reaction by addition of GGPP, the initial progression of the reaction was significantly delayed. This lag-phase (Figure 3-26B) might be attributed to a (slow) displacement of the inhibitor by GGPP, suggesting that both compounds, at least partially, have a common binding site on the enzyme. The structural similarity between the phosphonocarboxylate functionality and the pyrophosphate structure of GGPP seems to support this notion. A possible candidate site could be the basic cluster previously identified in the GGTase-II structure, which has been proposed to bind the GGPP head-group.<sup>[108]</sup>

The observation that the obtained time traces can only be described by double exponential equations indicates that the process on the molecular level is composed of at least two steps, which give rise to fluorescence changes. This seems sensible, because the reaction is not only composed of the phosphoisoprenoid binding and catalytic transfer step, but presumably also comprises rearrangement and isomerization steps in the active site as well as pyrophosphate release and transfer of the Rab C-terminus onto REP. The obtained rate constants are summarized in Table 3-3.

Substrate	$k_1$ [ $\text{s}^{-1}$ ]	$k_2$ [ $\text{s}^{-1}$ ]	$K_d$ [ $\text{nM}$ ]*
Rab7 $\Delta$ 6-CK(Dans)SCSC( <b>GG</b> )-OMe	0.047	0.004	$7 \pm 2$
Rab7 $\Delta$ 6-CK(Dans)SCSC( <b>GG</b> )-OMe + 500 $\mu\text{M}$ <b>NE10790</b>	0.005	0.002	-
Rab $\Delta$ 6-CK(Dans)SC( <b>GG</b> )SC-OMe	0.012	0.002	$35 \pm 4$
Rab7 $\Delta$ 6-CK(Dans)SC( <b>GG</b> )SC( <b>GG</b> )-OMe	0.015	0.001	$13 \pm 1$

Table 3-3: Rate constants obtained from *in vitro* prenylation reactions under single turn-over conditions. The concentrations of GGTase-II, REP-1 and Rab substrate were approximately 75 nM. GGPP concentration was 10  $\mu\text{M}$  ( $T = 25^\circ \text{C}$ ).  $k_1$  and  $k_2$  represent the obtained rate constants of the fast and slow phases, respectively. \* Refers to the observed dissociation constant of the interaction of the corresponding Rab7:REP-1 complexes with GGTase-II (from Table 3-2).

The rate constants of the fast phase ( $k_1$ ) are in excellent agreement with values previously reported in the literature for the second prenyl transfer reaction: On the basis of a HPLC assay, Thomä et al. estimated the rate constant of the second

prenyl transfer reaction as  $0.04 \text{ s}^{-1}$  using Rab7 $\Delta$ 6-CK(Dans)SCSC-OH as a substrate.<sup>[116]</sup> Studies employing the traditional *in vitro* prenylation assay that measures the incorporation of [<sup>3</sup>H]-geranylgeranyl into proteins, allowed the determination of steady-state parameters of the double prenylation reaction, yielding a  $k_{\text{cat}}$  of ca.  $0.03 \text{ s}^{-1}$  for various Rab substrates.<sup>[115]</sup>

These data strongly support the presumption, that the observed fluorescence changes are directly or indirectly linked to the second isoprenoid transfer reaction, which can be described by the rate constant of the fast phase ( $k_1$ ). The data from Table 3-3 indicate, that the second prenylation of the upstream cysteine (Cys<sup>205</sup>) is approximately 4 times faster compared to the prenylation of the terminal Cys<sup>207</sup>. Apparently, the tighter bound single prenylated reaction intermediate is also faster converted to the doubly prenylated product. This could be rationalized in view of the discussion regarding the observed differences in affinities of the single prenylated Rab7:REP-1 complexes for GGTase-II presented in section 3.2. One could argue, that binding of the first geranylgeranyl group to GGTase-II influences the fixation of the unprenylated cysteine in the active site and that this different orientation accounts for the observed differences in affinities. Interaction of the cysteine with the active site of GGTase-II probably involves the essential zinc ion, which activates the thiol group for the nucleophilic attack on the C1 of GGPP (stabilization of the thiolate form decreases the cysteine's sulfhydryl  $\text{p}K_{\text{a}}$  and increases its nucleophilicity). It is conceivable that stronger stabilization (stronger binding, lower  $K_{\text{d}}$  value) results in stronger activation of the cysteine (higher reactivity, faster prenyl transfer). This could explain, that in the examined cases the affinities of the reaction intermediates for GGTase-II are directly related to their ability to accept the second prenyl group. However, it is important to keep in mind, that the precise rate-determining step of the molecular reaction is not necessarily the enzymatic transfer step. Other steps, either preceding or following the nucleophilic substitution reaction could as well be influenced by the different prenyl pattern or by a different orientation of the conjugated isoprenoids in the active site.

The known rate constants for the first and the second prenylation reaction are summarized in Figure 3-27. From these, one could conclude, that the majority of Rab7 proteins proceeds to double prenylation by first acquiring prenylation on the C-terminal cysteine, followed by modification of the upstream cysteine.<sup>[116]</sup> However,

taking into account the heterogeneous nature of Rab prenylation motifs, the preference of GGTase-II could be different for other Rabs.<sup>[117,217]</sup>

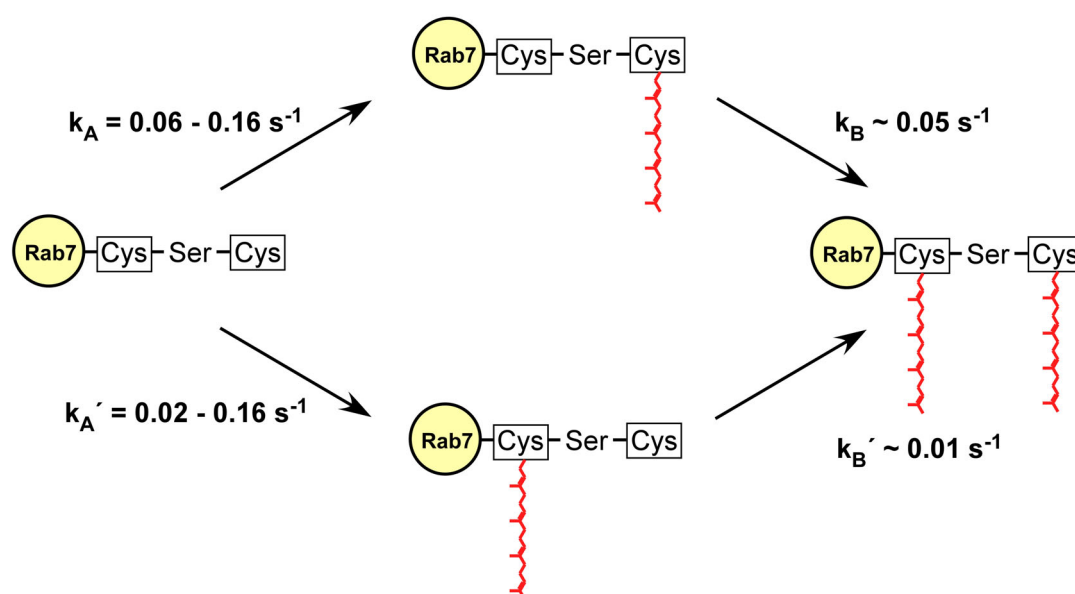


Figure 3-27: Rate constants describing the Rab7 double prenylation reaction under saturating concentrations of REP-1, GGTase-II, Rab7, and GGPP. The rate constants of the first prenyl transfer ( $k_A$  and  $k_{A'}$ ) were determined by employing single cysteine mutant proteins (lower limit). The upper limit refers to the value determined by analyzing the prenylation of Rab7wt protein (dansyl labeled), which leads transiently to the accumulation of single prenylated proteins (since  $k_A > k_B$ ).<sup>[116]</sup> The  $k_B$  values were determined in this study and represent the  $k_1$  values of Table 3-3.

### 3.4. The molecular basis of Rab:RabGDI interaction

REP and GGTase mediate the crucial posttranslational modification of all known Rabs, and thus are essential general regulators of Rab protein functioning. Another well known regulatory protein factor that seems to act on all Rab GTPases<sup>[303,304]</sup> is Rab GDP dissociation inhibitor (RabGDI), which exhibits numerous biochemically well defined functions.<sup>[305]</sup> RabGDI binds exclusively to the geranylgeranylated and GDP bound form of Rab proteins,<sup>[126,306]</sup> and slows the dissociation of GDP from the GTPase.<sup>[56]</sup> RabGDI also facilitates the extraction of inactive (i.e. GDP bound) Rab proteins from membranes by forming stoichiometric complexes<sup>[57]</sup> and subsequently delivers them to defined compartments,<sup>[60,61]</sup> thus ensuring specific Rab recycling (Rab cycle, see Figure 1-2). As discussed in the introductory chapter, efficient Rab shuttling between membranes requires additional membrane bound factors, termed RRF and GDF.

The molecular basis of some of the aspects of RabGDI functioning has previously been addressed by structural and mutational studies (reviewed by<sup>[307]</sup>). RabGDI is

composed of two domains, a large (ca. 340 AA) domain I, and a smaller (100 AA), entirely  $\alpha$ -helical domain II (Figure 3-28).<sup>[308]</sup> Mutational analysis identified a highly conserved region at the apex of domain I, that plays a critical role in the binding of Rab proteins (Rab binding platform).<sup>[58,125]</sup> A second region located between domain I and II has been implicated in the extraction of membrane-bound Rab proteins and probably mediates the interaction of RabGDI with the putative membrane bound receptors (termed mobile effector loop, MEL).<sup>[59,309]</sup>

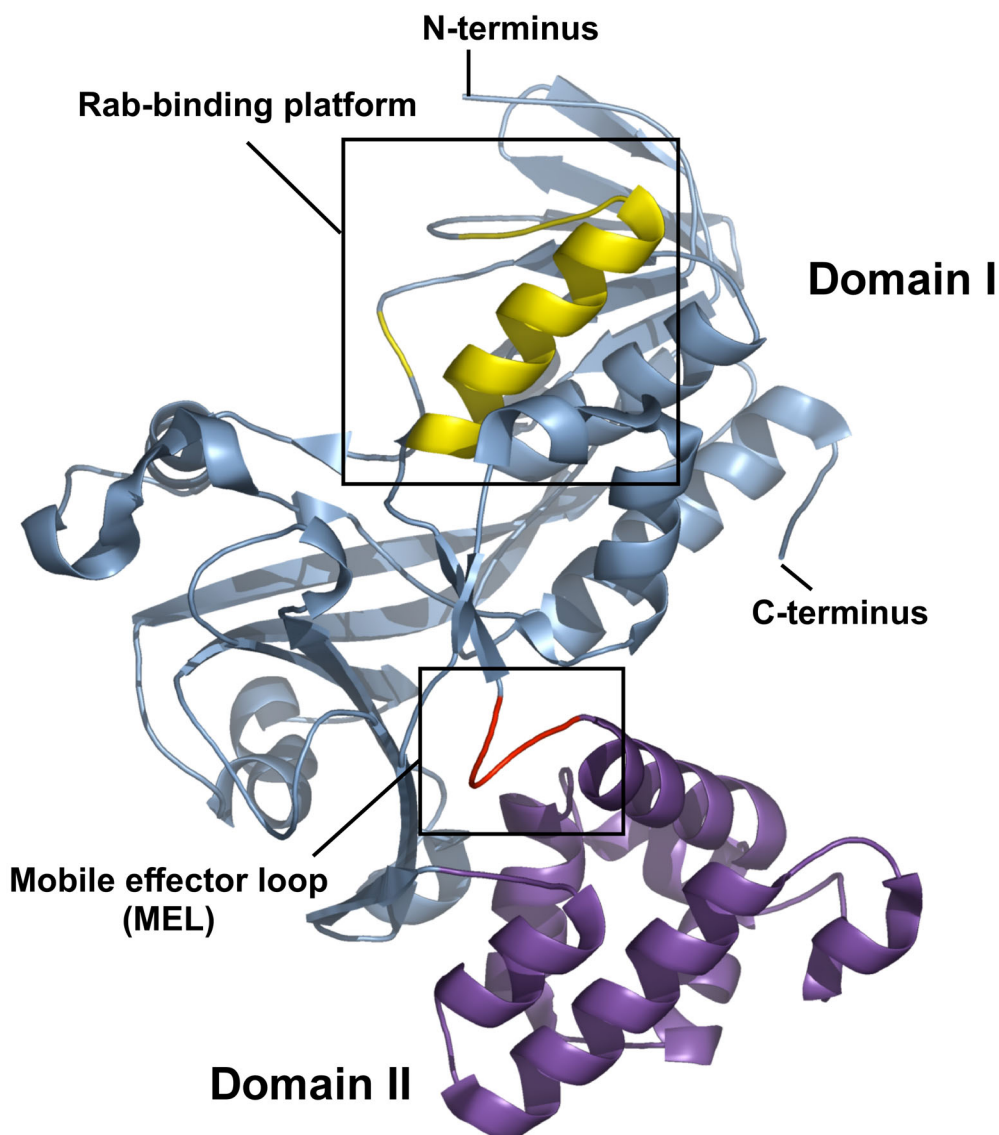


Figure 3-28: Ribbon representation of the structure of bovine  $\alpha$ -RabGDI at 1.04 Å resolution (PDB entry code: 1D5T).<sup>[309]</sup> The protein is composed of two domains. Domain I is colored light-blue, domain II is colored violet. The Rab-binding platform (yellow) and the mobile effector loop (red) are highlighted.

However, the available structures of apo-RabGDI<sup>[58,308]</sup> cannot provide a structural explanation for the observed RabGDI activities mentioned above. A more detailed structural analysis is required in order to achieve a molecular understanding of RabGDI functioning. Ideally, this should include the elucidation of the binary Rab:RabGDI complex structure, to further characterize the specific interactions between the prenylated Rab and RabGDI. Although this structure has been eagerly awaited (e.g. <sup>[310]</sup>), little progress was made in this direction probably due to problems associated with the expression and purification of prenylated Rabs. Classical procedures, such as expression in eucaryotic cells,<sup>[270,271]</sup> purification from animal tissues<sup>[272,311]</sup> or *in vitro* prenylation,<sup>[312,313]</sup> typically suffer from low yields, a difficult purification procedure and high costs, precluding the production of homogenously prenylated Rabs in large amounts. The developed EPL strategy could alternatively be employed to circumvent these problems. As was demonstrated in the previous sections, the reaction is capable of generating homogenously prenylated Rab proteins. The reaction and subsequent purification steps can be anticipated to be adjustable to multi-milligram amounts of protein, typically required for extensive crystallization trials, provided that the Rab-thioester and the prenylated peptide are readily accessible. As shown in Table 3-1, a number of prenylated Rab:RabGDI complexes were envisaged for EPL semi-synthesis utilizing the described protocols (complexes No. 2, 9, 11, 12, 15, and 16 from Table 3-1). These complexes are composed of different Rab family members (e.g. Rab7, Ypt7, Ypt1), which comprised C-terminal deletions of various length ( $\Delta 2$  to  $\Delta 7$ ) and were ligated to various peptides. Since mono-geranylgeranylated Rabs can also complex to RabGDI,<sup>[303,314,315]</sup> the peptide part could be designed to carry either a single or both geranylgeranyl moieties.

RabGDI also does not strictly require C-terminal carboxyl-methylation for efficient interaction with Rab proteins,<sup>[306,315]</sup> suggesting that C-terminally modified as well as unmodified peptides could be used for ligation and subsequent complex formation. Some of the peptides contained fluorophores, which easily allowed tracking of the ligated protein during purification experiments; a tool that proved especially useful in the early stages of the project. The peptides were synthesised by members of the Waldmann lab, Department of Chemical Biology, MPI-Dortmund (see Table 5-1 for details). Ligation of the various Rab proteins to the different peptides was efficient, typically giving ligation yields of at least 70 % (often > 95 %) with respect to the

utilized Rab-thioester under the described conditions (Chapter 3.1.). Unfortunately, semi-synthetic and *in vitro* refolded Rab proteins containing the dansyl fluorophore linked to the C-terminus (No. 11 and 15 from Table 3-1), failed in forming any detectable complex with RabGDI, as could be inferred from gel filtration experiments, SDS-PAGE and mass spectroscopic analysis. These Rabs also failed to interact with the REP-1 protein (chapter 3.1.5.). At the simplest level of interpretation, this could be explained with the considerably increased bulkiness of the dansyl fluorophore as compared to the tolerated methylester, which could sterically interfere with the accommodation of the Rab C-terminus on REP and RabGDI. Given the conserved structure and function within the RabGDI/CHM family,<sup>[105,307,308,310]</sup> it seems plausible that both REP and RabGDI utilize a similar mode of interaction with the Rab C-terminus, that is in both cases affected by the aforementioned modification.

The successfully obtained complexes (No. 2, 9, 12, and 16, Table 3-1) were further utilized for crystallization trials, which were carried out by Dr. Alexey Rak, Department of Physical Biochemistry, MPI-Dortmund. Eventually, two of these complexes, namely the single and doubly prenylated Ypt1:RabGDI complex, could be crystallized. The diffraction data were collected to 1.5 and 1.4 Å resolution, respectively.

#### **3.4.1. The structure of monoprenylated Ypt1 in complex with RabGDI**

Single prenylated Ypt1 $\Delta$ 2-CC(GG) in complex with yeast RabGDI was prepared in a total amount of ca. 20 mg in a single ligation and purification setup, as described before, which corresponds to 7-8 mg of semi-synthetic Ypt1 GTPase. The final recovery yield of Ypt1 protein was ca. 50 %. The identities of the individual proteins were verified by MALDI-MS and LC-ESI-MS analysis (Figure 3-29A, B, D) and only very little, if any, unligated Ypt1 protein could be detected. The produced complex appeared to be of excellent purity as could be inferred from SDS-PAGE experiments (Figure 3-29C).

Furthermore, gel filtration experiments confirmed the critical importance of the geranylgeranyl moiety for the interaction of Ypt1 with RabGDI (Figure 3-30B). When a mixture of Ypt1 $\Delta$ 2-MESNA thioester and RabGDI was applied to a gel filtration column, separate elution of both components was observed, whereas the semi-synthetic complex eluted as a single symmetric peak.

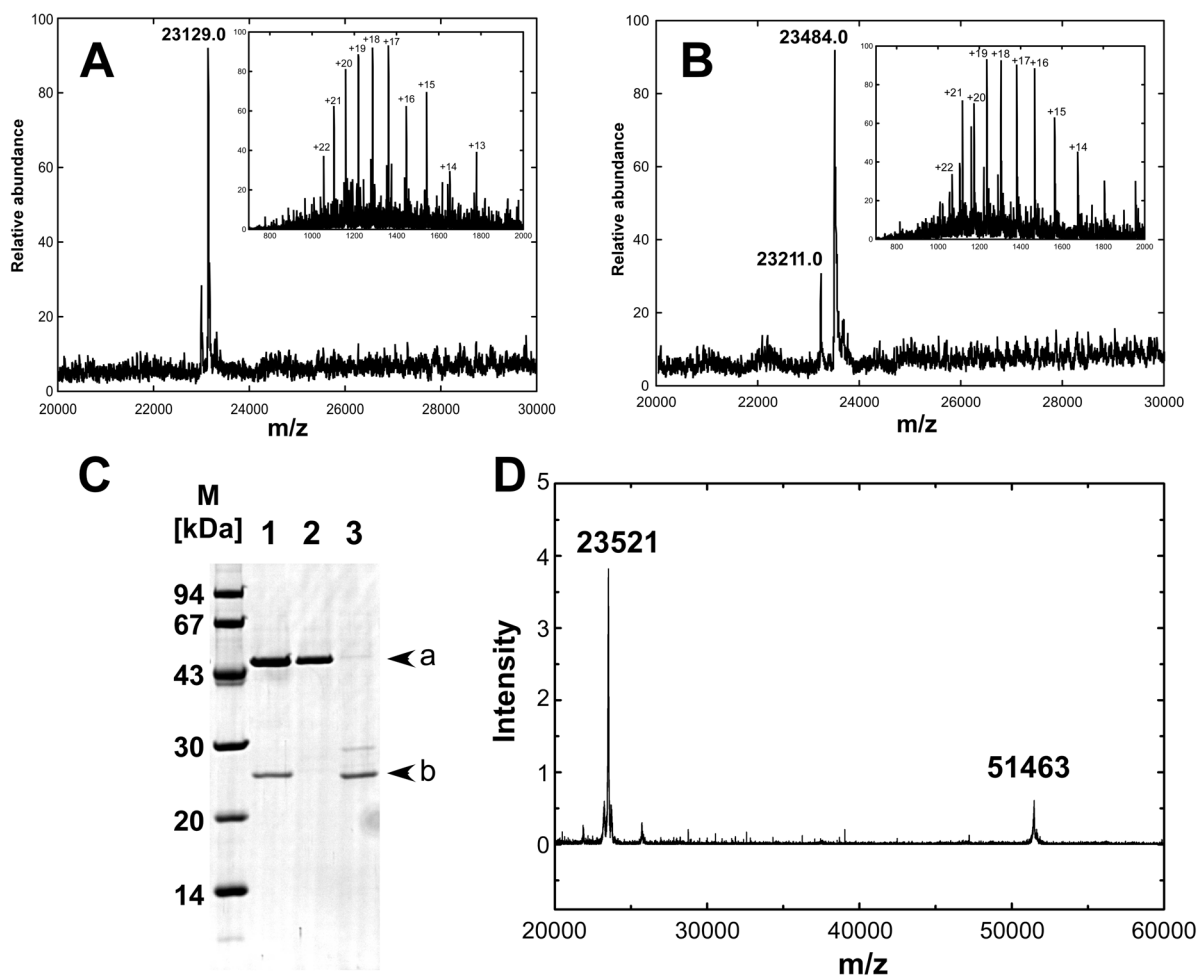


Figure 3-29: Preparation of the Ypt1 $\Delta$ 2-CC(GG):yRabGDI complex. **A**) LC-ESI-MS spectrum of  $^{1-204}$ Ypt1 $\Delta$ 2-MESNA thioester ( $M_{\text{calc}} = 23131$  Da) and of **B**)  $^{1-204}$ Ypt1 $\Delta$ 2-CC(GG) ( $M_{\text{calc}} = 23486$  Da). **C**) SDS-PAGE gel of the obtained semi-synthetic Ypt1 $\Delta$ 2-CC(GG):yRabGDI complex after gel filtration (lane 1). Yeast RabGDI (lane 2) and Ypt1 $\Delta$ 2-MESNA thioester (lane 3) are shown for comparison. Arrows indicate the migration of yRabGDI (a) and Ypt1 (b). **D**) MALDI-TOF-MS of the semi-synthetic complex. The theoretical molecular mass of yRabGDI is 51401 Da. The discrepancy of the determined values for the Ypt1 $\Delta$ 2-CC(GG) protein measured by ESI-MS (B, 23484 Da) and MALDI-MS (D, 23521 Da), is due to the inaccuracy of the MALDI spectrometer.

In case of the latter, the observed elution time corresponded approximately to a molecular weight of 80 kDa indicating the presence of a 1:1 Ypt1:RabGDI complex. Thus, a single prenyl group is sufficient to confer binding of Ypt1 to RabGDI, which is in agreement with previous observations.<sup>[303,314,315]</sup> From these experiments one could also conclude, that the obtained complex is indeed *homogenously* prenylated, since no residual unligated Ypt1 thioester could be detected. Crystallization, determination of the initial phases by molecular replacement, model building and refinement, and the final analysis of the structure were carried out by Dr. Alexey Rak, Dr. Olena Pylypenko and Dr. Kirill Alexandrov, Department of Physical Biochemistry, MPI-Dortmund (for details see <sup>[295]</sup>). The obtained 1.5 Å resolution model is presented in Figure 3-31.

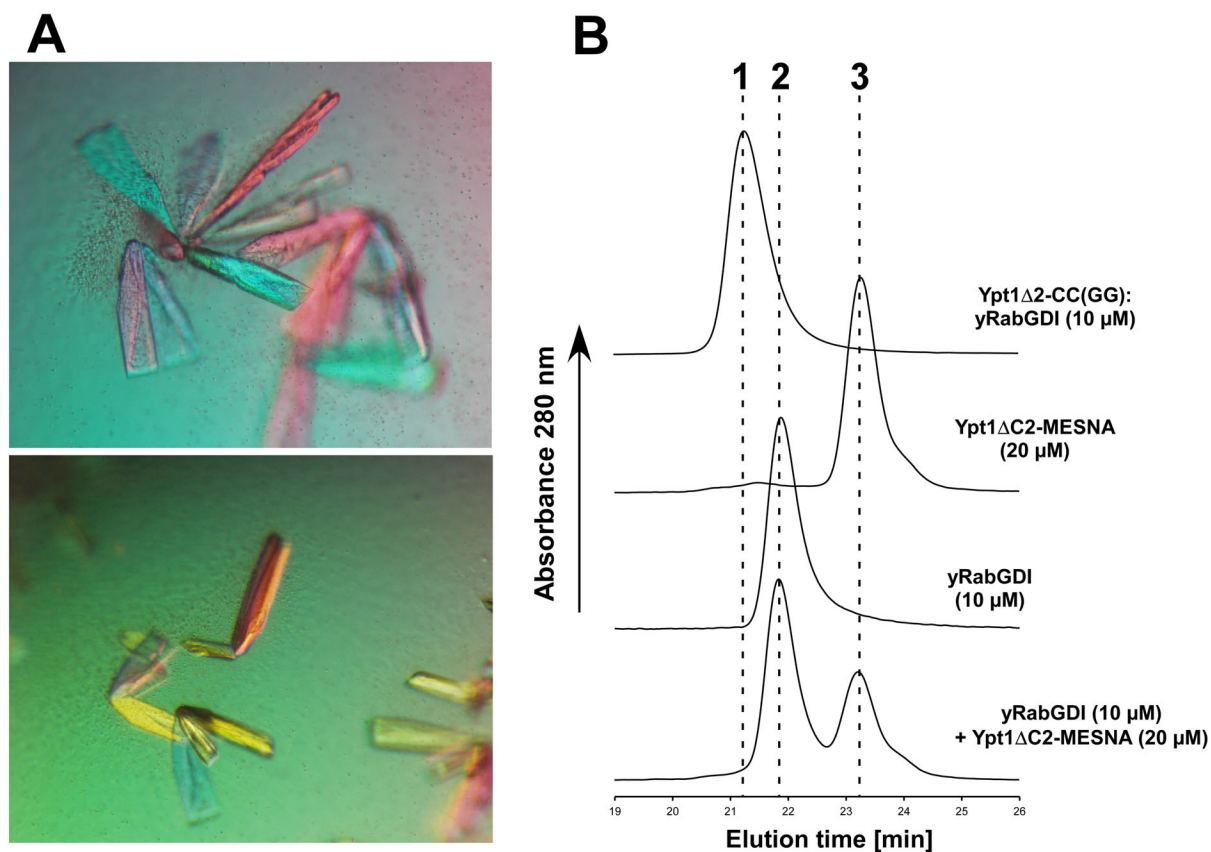


Figure 3-30: **A)** Crystals of Ypt1 $\Delta$ 2-CC(GG):yRabGDI obtained by Dr. Alexey Rak (Department of Physical Biochemistry, MPI-Dortmund). For details of the crystallization conditions see <sup>[295]</sup>. **B)** GF-HPLC analysis of the Ypt1 $\Delta$ 2-CC(GG):yRabGDI complex. The elution time of the binary complex (1), of monomeric yRabGDI (2) and Ypt1 $\Delta$ 2-MESNA thioester (3) are indicated.

The GTPase domain of Ypt1 binds primarily to RabGDI by forming contacts with the previously identified Rab-binding platform of RabGDI.<sup>[58,308]</sup> On the part of Ypt1 this interaction involves the switch I and II regions, that function as conformational sensors for the GDP and GTP nucleotide bound state of GTPases.<sup>[75-77]</sup> Contacts between the switch regions and the Rab-binding platform are therefore expected to be responsible for the observed preference of RabGDI for the GDP bound conformation of Rab proteins (see below). The Rab binding platform as well as the switch regions are highly conserved within their respective protein families and among different species, which allow a relatively low number of RabGDI isoforms<sup>\*\*\*</sup> to interact with all of the more than 60 Rab proteins.

\*\*\* At least three RabGDI isoforms were identified in mammalian organisms (for nomenclature see <sup>[307]</sup>), which exhibit largely the same biochemical activities mentioned above. Still, the specific localization of certain RabGDI isoforms to distinct tissues or subcellular compartments as well as their functional specificity for a certain subset of Rabs seem to suggest a specialized functional role for each isoform.<sup>[316-318]</sup>

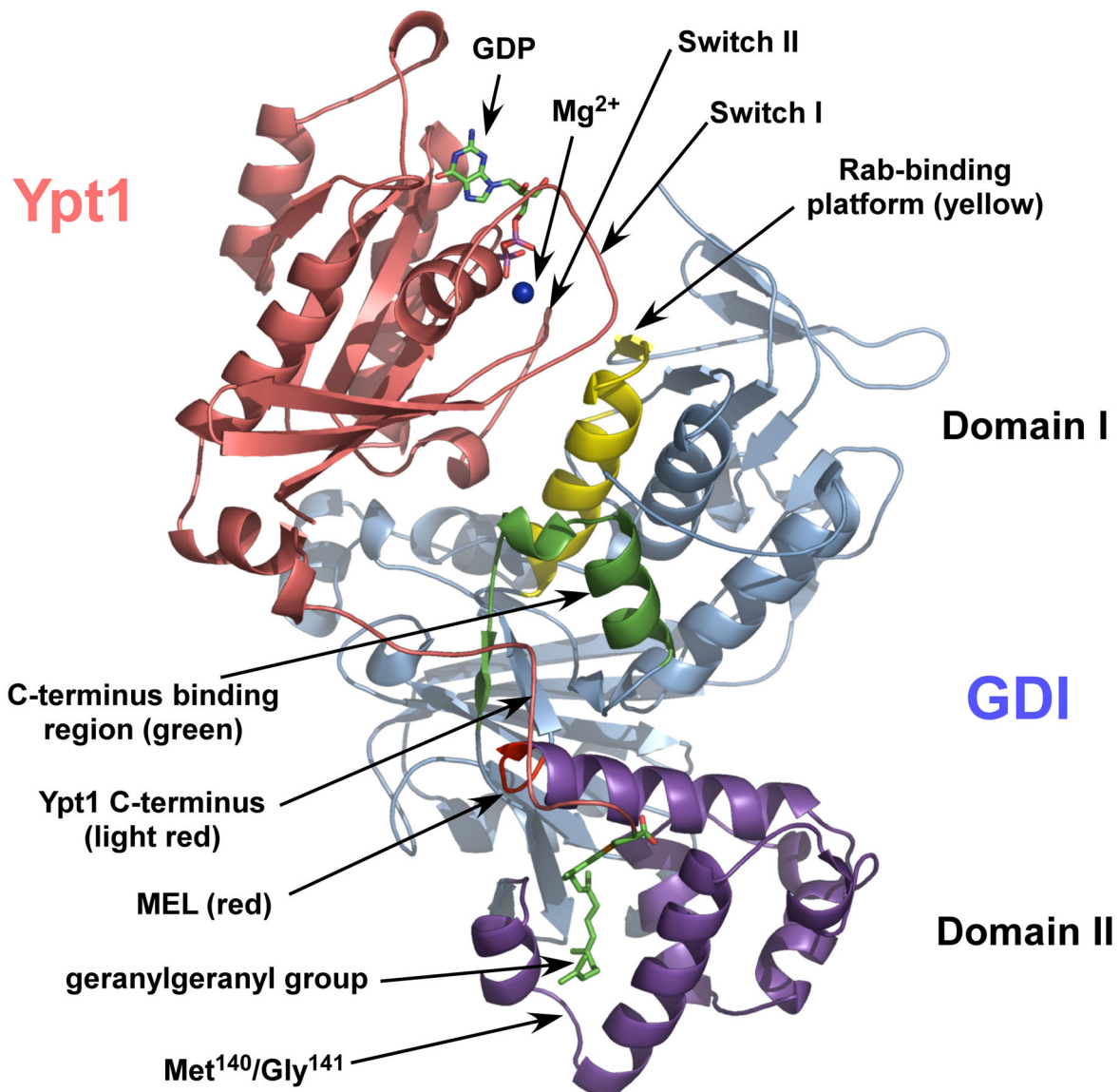


Figure 3-31: Ribbon representation of the structure of the semi-synthetic, single prenylated Ypt1:RabGDI complex at 1.5 Å resolution. Ypt1 (light red), the RabGDI domains I (light blue) and II (violet), the Rab-binding platform (yellow), the C-terminus binding region (CBR, green), the mobile effector loop (MEL, red), and the  $Mg^{2+}$ -ion (blue sphere) are indicated. The geranylgeranylated C-terminal cysteine residue 206 of Ypt1 and the bound nucleotide are shown in stick representation in atomic colors. The residues 199 to 205 of Ypt1, which are located directly upstream of Cys(GG)<sup>206</sup>, are disordered and were modeled into the structure. Reproduced from Rak et al.<sup>[295]</sup>

Additional important contacts between both molecules are established by interactions involving the last 20 C-terminal amino acid residues of Ypt1 including the hydrophobic isoprenoid. This region passes from the apex of RabGDI domain I down to the domain II in an extended conformation and terminates at a hydrophobic pocket harboring the geranylgeranyl moiety. The Ypt C-terminus is held in place by forming a number of interactions with surface exposed residues of RabGDI, including the mobile effector loop (Figure 3-32). A second region, termed C-terminus binding region (CBR) is located above the MEL, and appears to induce a 90° turn in the

C-terminus directing it toward the lipid-binding site of domain II. The importance of this patch for efficient coordination of the Rab C-terminus to RabGDI is supported by the finding, that a number of mutations impairing Rab membrane extraction or delivery localize to this region. For example, mutation of Thr<sup>105</sup> of yeast RabGDI to alanine is associated with defective Rab membrane delivery leading to accumulation of Rab:RabGDI in the cytosol.<sup>[319]</sup> In contrast, substitution of Ile<sup>92</sup> by proline in mammalian  $\alpha$ -RabGDI (corresponding to Ile<sup>100</sup>Pro in yeast RabGDI) reduces the ability of RabGDI to extract Rabs from membranes increasing the membrane-bound pool of the protein.<sup>[320]</sup> The latter RabGDI mutation in humans has been linked to one form of X-linked non-specific mental retardation (MRX), a disorder that severely impairs the intellectual and learning abilities of affected males.<sup>[320]</sup> The Ile<sup>92</sup>Pro mutation could potentially lead to significant structural changes in RabGDI, since Ile<sup>92</sup> is part of helix C and proline is a notorious helix-breaker.

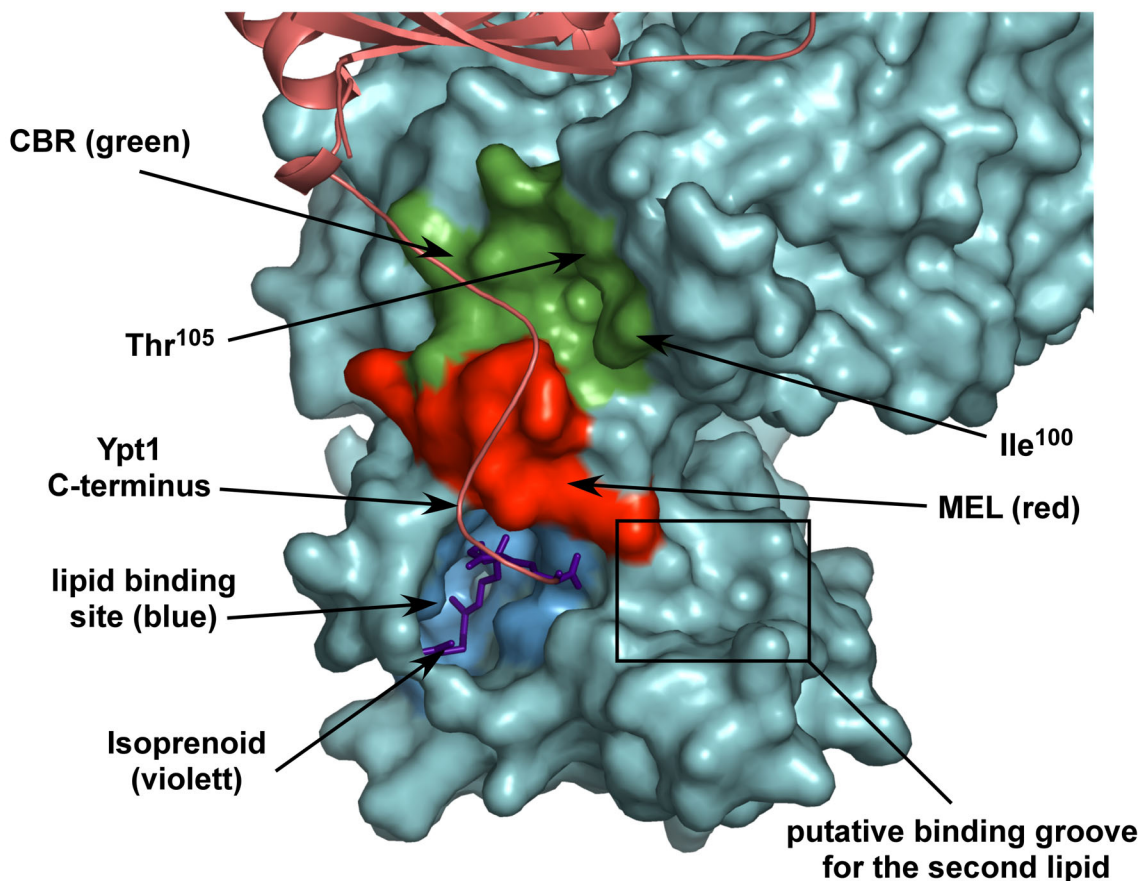


Figure 3-32: Interaction of the Ypt1 C-terminus with RabGDI. Ypt1 is displayed in ribbon representation (light red) whereas RabGDI is shown in surface representation (turquoise). CBR (green), MEL (red) and the lipid-binding pocket (blue) interact with the last 20 amino acid residues of Ypt1. The second isoprenoid is possibly bound to a hydrophobic groove in proximity to the identified isoprenoid binding pocket (indicated by a box). The locations of isoleucine<sup>100</sup> and threonine<sup>105</sup> on RabGDI are shown by an arrow. Modified from Rak et al.<sup>[295]</sup>

Because the role of the CBR in the presented structure appears to be in directing the Ypt C-terminus to the isoprenoid binding site on domain II via the MEL, mutations in this region can alternatively be expected to directly affect the accommodation of the isoprenoid on domain II. The C-termini of Rab proteins are highly heterogeneous with respect to sequence and in length (hypervariable region), and largely determine the targeting of Rab proteins to distinct subcellular compartments, as was mentioned before (Chapter 1-2).<sup>[89,90]</sup> It is therefore conceivable that these regions must be recognized by putative membrane bound receptors, which are involved in the extraction and removal process. On the part of RabGDI, biochemical experiments have led to the suggestion that the mobile effector is involved in this interaction.<sup>[59,309]</sup> Indeed, in the obtained structure both components are well exposed and are positioned in close proximity to each other, demonstrating in a figurative manner their mutual presentation to the (putative) receptor by RabGDI. This could additionally explain the effect of the above-mentioned CBR mutations on the ability of RabGDI to extract and deliver Rabs from and to membranes. In these cases, the C-terminus could be forced to adopt a conformation, that is only poorly recognizable by the receptors mediating Rab membrane insertion or removal, which could lead to the observed redistribution of the Rab proteins.

In principle, the extended surface of RabGDI between the Rab-binding platform and the lipid binding site seems to be suitable for acceptance of Rab C-termini of varying length. However, these tails typically range from 20 to more than 40 amino acid residues (beside the low degree of sequence conservation) and one could therefore assume, that the precise mode of the interaction is different. Moreover, these interactions could account for the observed differences in affinities of RabGDI toward various Rab family members.<sup>[308,321]</sup>

The geranylgeranyl group is anchored in a crooked conformation in a deep cavity, which shields the lipid from the bulk water molecules and is formed by hydrophobic residues of RabGDI domain II (Figure 3-32). This observation was largely surprising, since the cavity is apparently neither present in the structures of apo- $\alpha$ RabGDI<sup>[308,309]</sup> nor in the structure of the related REP-1 complexed to GGTase-II.<sup>[105]</sup> Superimposition of these structures with the obtained Ypt1:RabGDI complex structure indicated, that the pocket appears as a result of conformational shifts in domain II upon binding of Ypt1.<sup>[295]</sup> Still, the molecular details (as well as the driving force) leading to the formation of the lipid-binding cavity are presently unclear.

Furthermore, the identified isoprenoid binding site on domain II is in contradiction to a previous structural study of bovine  $\alpha$ -RabGDI co-crystallized with a Cys(GG)-OMe ligand, which proposed a hydrophobic patch on domain I below the Rab-binding platform as the coordination site of the geranylgeranyl group.<sup>[322]</sup> Nevertheless, independent mutational studies seem to support the genuineness and functional importance of the lipid binding site identified in the Ypt1:RabGDI complex structure. For example, the Met<sup>140</sup>Ile/Gly<sup>141</sup>Ser yeast RabGDI mutant protein has been shown to be defective in Rab membrane loading and Rab membrane delivery.<sup>[319]</sup> Both residues are located at the bottom of the identified hydrophobic cavity (Figure 3-31), and a substitution of both residues can therefore be expected to influence the conformation of the lipid binding pocket and coordination of the Ypt1 isoprenoid. Moreover, inspection of the obtained structure revealed the critical importance of Lys<sup>145</sup> in the formation of the lipid-binding site by keeping two helices of domain II separated from each other. Mutation of this residue to alanine dramatically decreased the ability of RabGDI to extract Ypt1 from membranes.<sup>[295]</sup> Very recently, the structure of the monoprenylated Rab7:REP-1 complex was solved to 2.2 Å resolution and could confirm the location of the isoprenoid harbouring cavity on domain II<sup>†††</sup>.<sup>[324]</sup> The available space in the lipid-binding cavity is limited, precluding the simultaneous binding of two isoprenoids to this site (Figure 3-32). The search for an alternative site capable of accommodating the second geranylgeranyl group revealed a hydrophobic surface groove in close vicinity to the identified cavity on domain II as the most likely candidate site (Figure 3-32). The 1.4 Å resolution structure of doubly prenylated Ypt1 complexed to RabGDI can be expected to resolve this issue. This complex was prepared in a similar manner by means of EPL, and the obtained structure is currently under investigation (see Figure 3-35A).

In the structure of the mono-prenylated Ypt1:yRabGDI complex, the C-terminal  $\alpha$ -carboxyl group of Ypt1 appears to point toward the domain II of RabGDI. One could hypothesize that binding of the isoprenoid group in the hydrophobic cavity effectively restricts the conformational freedom of the C-terminal cysteine residue, which is supported by the presence of interpretable electron density for this residue. In such a case, bulky C-terminal substituents (e.g. -NH-(CH<sub>2</sub>)<sub>2</sub>-NH-Dans) would clash

---

<sup>†††</sup> This complex was generated by preparative *in vitro* prenylation of the Rab7 protein containing a single cysteine mutant.<sup>[313,323]</sup> A similar approach could not be applied to the preparative production of Rab:RabGDI complexes due to experimental difficulties associated with the exchange of REP-1 for RabGDI following the prenylation reaction.

with residues of RabGDI domain II, which could explain the observed inability of RabGDI to interact with Rab proteins modified in such a way. On the other hand, the available space seems to be sufficient for accommodation of a sterically much less demanding methylester. Modeling studies of short prenylated peptides bound to the RabGDI domain II seem to support this notion (see Figure 3-33).

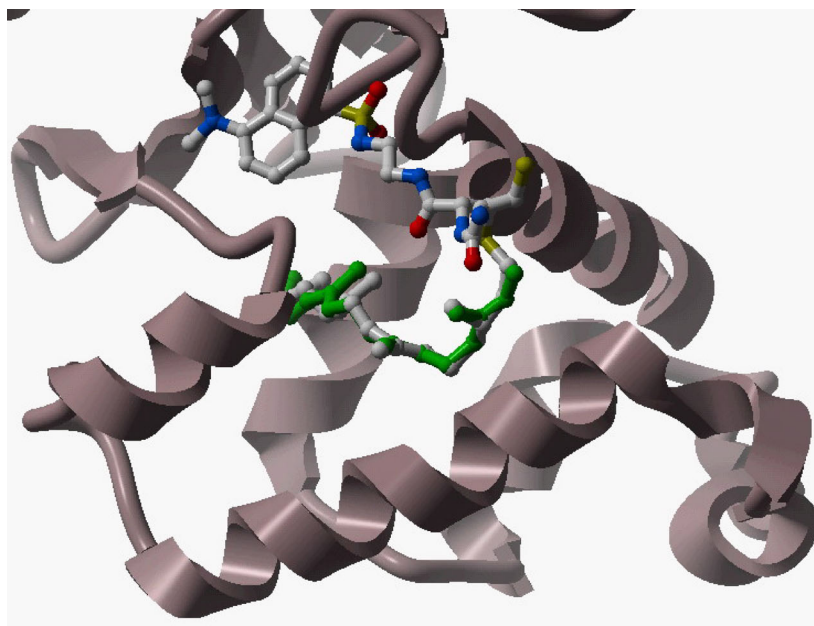


Figure 3-33: Model showing the interaction of the peptide Cys-Cys(GG)-NH-(CH<sub>2</sub>)<sub>2</sub>-NH-Dans with RabGDI domain II (grey ribbon representation). The peptide (atomic colors) is superimposed with the geranylgeranyl lipid (green) identified in the crystal structure. Binding of the isoprenoid group in the hydrophobic cavity brings the C-terminal  $\alpha$ -carboxyl group in close contact with residues of RabGDI. This results in sterical conflicts between bulky substituents linked to the C-terminus of Rab proteins and RabGDI domain II.

The structure also provides a plausible explanation for the GDP-dissociation inhibitory effect of RabGDI exerted on Rab proteins. This seems due to a stabilization of the switch I and II regions in a closed conformation upon interaction with the Rab-binding platform of RabGDI.<sup>[295]</sup> The stiffness of this conformation compared to the flexibility of switch I and II regions in the structures of uncomplexed Rab proteins (e.g. <sup>[78]</sup>) can be expected to effectively hinder the nucleotide release from Rabs. This is illustrated by numerous mostly polar interactions formed between conserved residues present in the Rab-binding platform (and partially in the CBR) and the switch I and II regions (Figure 3-34). Especially the interaction between the side chain guanidino group of RabGDI Arg<sup>248</sup> and the backbone carbonyl oxygen of the highly conserved Ypt Asp<sup>63</sup> seems to indirectly enhance the binding of GDP via a

network of interactions. For example, the Asp<sup>63</sup> sidechain carboxyl group is in hydrogen bond distance to one of four water molecules, which are ligands of the Mg<sup>2+</sup> ion. On the other side the Mg<sup>2+</sup> ion is coordinating to the  $\beta$ -phosphate group of GDP. Thus it seems likely that the Arg<sup>248</sup>/Ypt<sup>63</sup> interaction stabilizes the coordination of the Mg<sup>2+</sup> ion and consequentially decreases the extent of GDP release.

Comparison of the present Ypt1:RabGDI structure with the GppNHp (a enzymatically non-hydrolyzable analog of GTP) bound Ypt7 structure revealed, that the switch regions in both structures adopt different conformations.<sup>[295]</sup> The GTP-bound conformation possibly gives rise to clashes between the switch regions and the Rab-binding platform, which explains the observed preference of RabGDI for GDP bound Rabs.

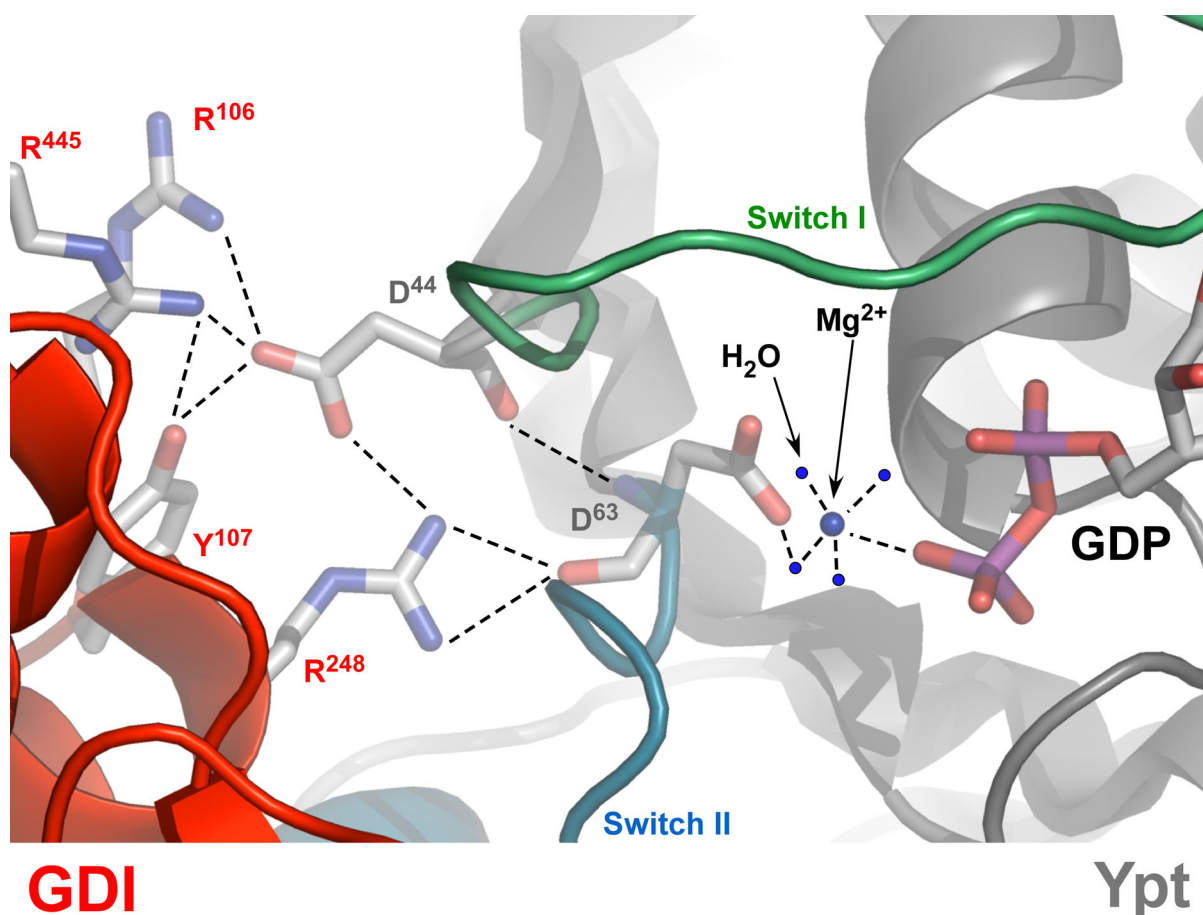


Figure 3-34: Interactions between the switch I and II regions of Ypt (grey, right side) and the Rab-binding platform of RabGDI (red, left side). Residues involved in this interaction are shown in stick representation in atomic colors. Hydrogen bonds are indicated by dashed lines. See text for description. Reproduced from Rak et al.<sup>[295]</sup>

In conclusion, the developed semi-synthetic strategy was shown to be suitable for the generation of homogeneously prenylated Rabs in preparative amounts (i.e. several milligram). The quality of the prepared complexes and of the obtained structural data substantiate the potency and versatility of the EPL strategy as an important alternative to established classical techniques. Needless to say, that the utility of such a strategy for structural studies is not restricted to prenylated Rabs. For example, in a recent report a very similar strategy was envisaged, in order to study the effects of C-terminal phosphorylation on the structure (1.8 Å resolution) and oligomerization behaviour of the SMAD-2 transcription factor.<sup>[325]</sup>

### **3.5. Other semi-synthetic complexes intended for crystallographic analysis**

The general applicability of the EPL strategy for the semi-synthesis of prenylated Rab proteins could be further demonstrated by the generation of a variety of other complexes. For example double prenylated Ypt1 $\Delta$ 3-CC(GG)C(GG) in complex with yeast RabGDI was prepared in a total amount of 16 mg. The obtained complex was of excellent purity and was crystallized by Dr. Alexey Rak, Department of Physical Biochemistry, MPI-Dortmund (Figure 3-35A). X-Ray diffraction data of these crystals were collected to 1.4 Å resolution. The preliminary structural analysis of the obtained data thus far did not reveal a well-defined electron density for the second conjugated isoprenoid group indicating that it is rather flexible and does not have a clearly specified position on the RabGDI surface. This appears logical, since two very strongly bound isoprenoids could possibly not be transferred into the lipid bilayer during Rab membrane delivery. Further structural analysis will be needed in order to clarify the localization of the second geranylgeranyl residue.

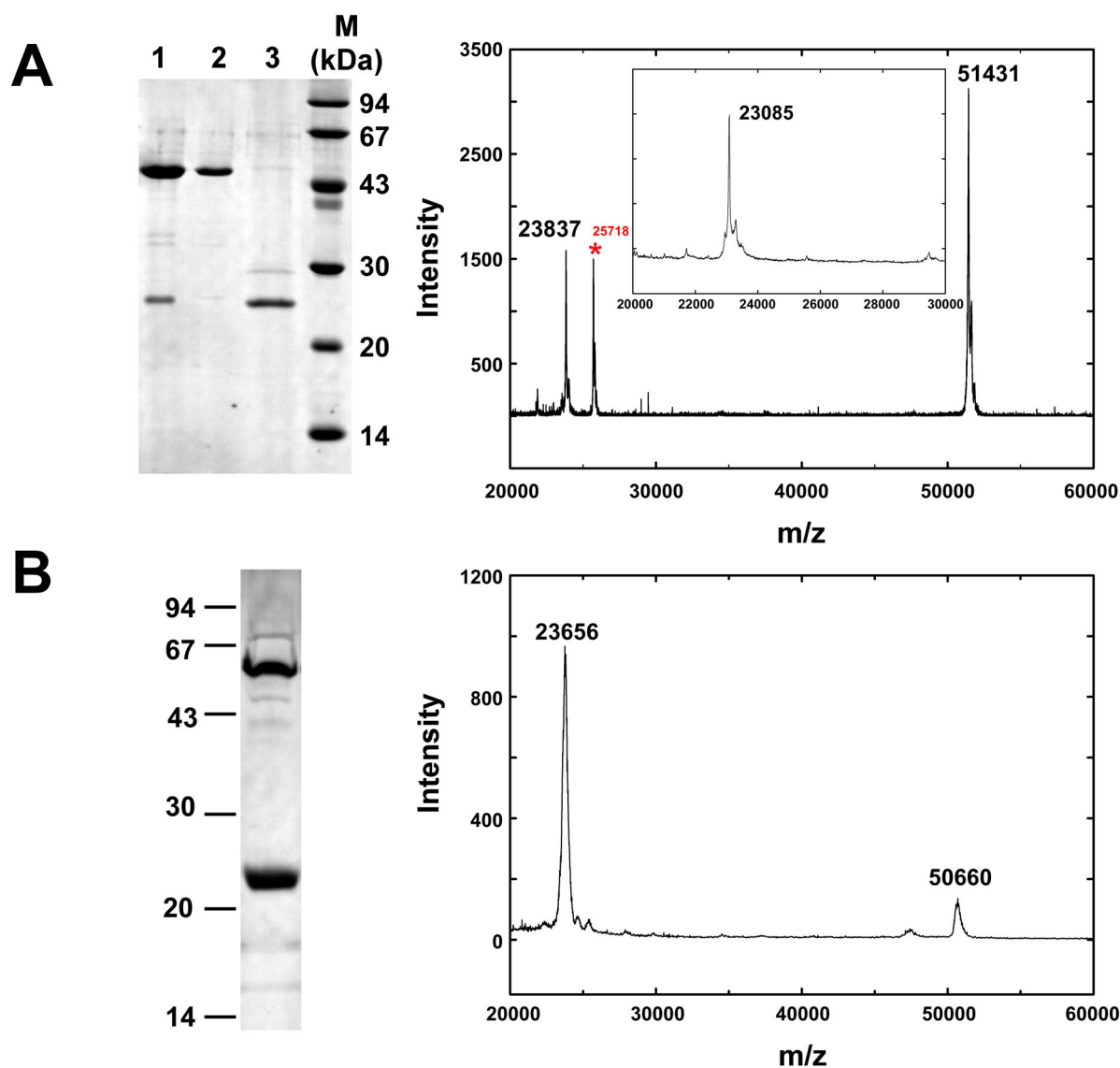


Figure 3-35: **A**) SDS-PAGE gel and MALDI-MS analysis of Ypt1 $\Delta$ 3-CC(GG)C(GG):yRabGDI complex. In the SDS-PAGE experiment the complex was loaded on lane 1. yRabGDI (lane 2) and  $^{1-203}$ Ypt1 $\Delta$ 3-MESNA thioester (lane 3) are shown for comparison. The calculated molecular weights of  $^{1-203}$ Ypt1 $\Delta$ 3-CC(GG)C(GG) and yRabGDI are 23861 Da and 51401 Da, respectively. The red star marks the signal corresponding to the doubly charged yRabGDI ion (RabGDI+2H) $^{2+}$ . The inset shows the MALDI-MS spectrum of  $^{1-203}$ Ypt1 $\Delta$ 3-MESNA thioester ( $M_{\text{calc}} = 23076$  Da). **B**) SDS-PAGE gel and MALDI-MS analysis of the complex between Rab7 $\Delta$ 2-CC(GG)C $^{205}$ S and bovine RabGDI-1. The calculated molecular weights of  $^{2-205}$ Rab7 $\Delta$ 2-CC(GG)C $^{205}$ S and RabGDI-1 are 23660 Da and 50595 Da, respectively.

Other examples of protein complexes prepared by the outlined EPL strategy include the mammalian single prenylated Rab7:RabGDI-1 complex (Figure 3-35B), the yeast single prenylated Ypt1:MRS6p complex (Figure 3-36A), and the yeast single prenylated Ypt1:MRS6p:GGTase-II complex (Figure 3-36B). Although these complexes could not be crystallized so far, their preparation was straightforward using the elaborated protocols. In all cases the desired product was formed as could be inferred from mass spectroscopic experiments and the complexes appeared to be

of high purity. Thus taken together, the EPL semi-synthesis approach is generally applicable to a variety of Rab proteins and different peptides.

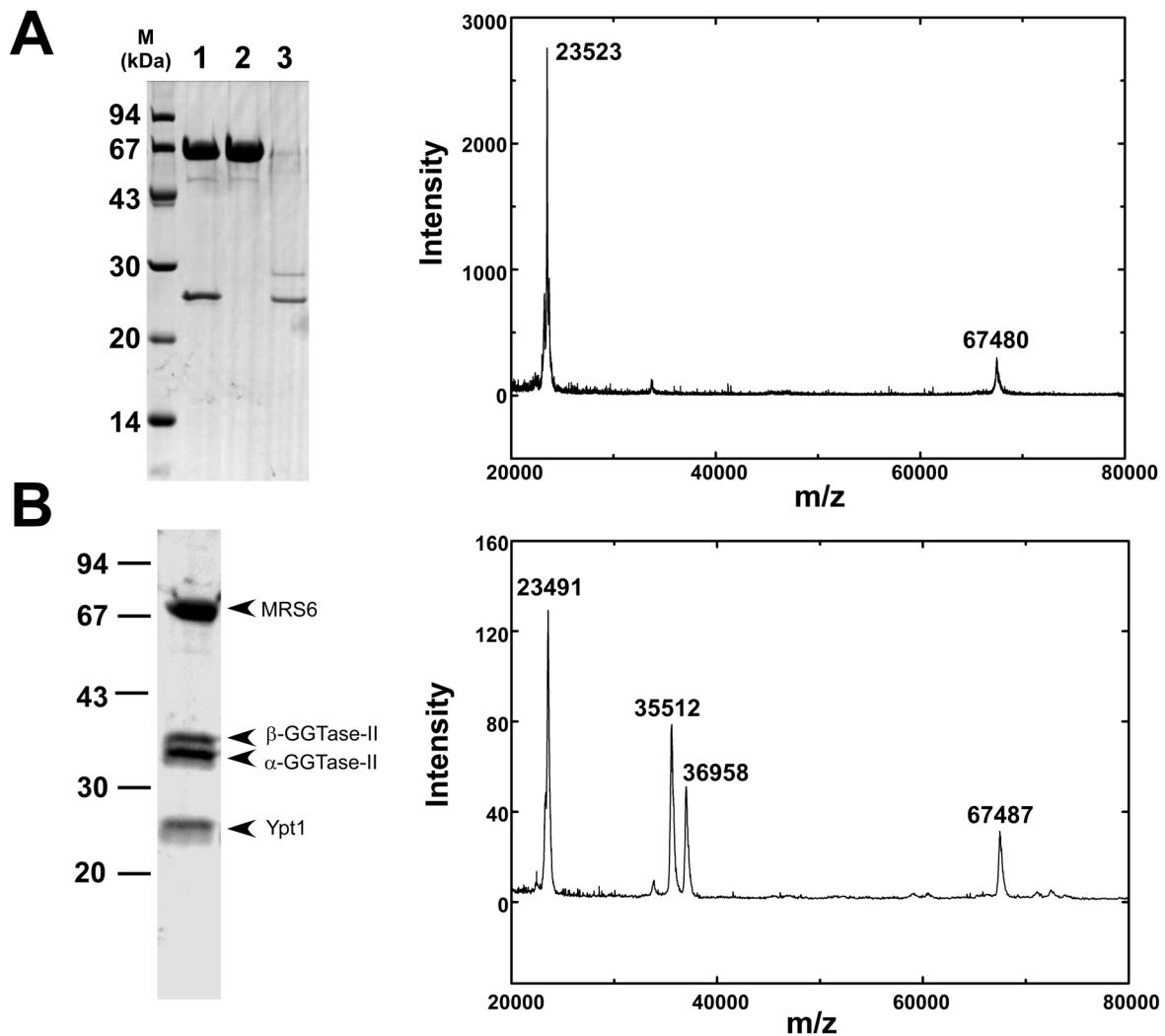


Figure 3-36: **A**) SDS-PAGE gel and MALDI-MS analysis of Ypt1Δ2-CC(GG):MRS6p complex. In the SDS-PAGE experiment the complex was loaded on lane 1. MRS6p (lane 2) and Ypt1Δ2-MESNA thioester (lane 3) are shown for comparison. The calculated molecular weights of  $^{1-204}$ Ypt1Δ2-CC(GG) and MRS6p are 23486 Da and 67545 Da, respectively. **B**) SDS-PAGE gel and MALDI-MS analysis of Ypt1Δ2-CC(GG):MRS6p:yGGTase-II.  $^{1-204}$ Ypt1Δ2-CC(GG) ( $M_{\text{calc}} = 23486$  Da), GGTase-II  $\alpha$ -subunit ( $M_{\text{calc}} = 35440$  Da), GGTase-II  $\beta$ -subunit ( $M_{\text{calc}} = 36860$  Da), MRS6p ( $M_{\text{calc}} = 67545$  Da).

# 4. Summary and Conclusions

*“An expert is a man who has made all the mistakes which can be made,  
in a narrow field.”*

*Niels Bohr*

## 4. Summary and Conclusions

Native chemical ligation (NCL) and the related technique, expressed protein ligation (EPL), have been extremely useful for the synthesis of various proteins in the past. In particular the concept of EPL elegantly demonstrates the usefulness of combining the fields of chemistry and biology in order to address complex physiological and biochemical questions.

The present study aimed at adapting the EPL methodology to the semi-synthesis of prenylated Rab proteins, which exert many important functions during vesicular transport in eukaryotic cells. To this end, short prenylated peptides, which were chemically synthesized by our collaborators from Prof. Waldmann's lab at the MPI-Dortmund, were coupled site-specifically to the C-terminus of truncated Rab proteins. During this work some interesting and thus far unknown aspects of this reaction were observed. First, the EPL reaction with prenylated peptides was found to be strictly dependent on the presence of certain detergents. Although the role of these detergents in the ligation reaction remains elusive, one could hypothesize that they function as micellar catalysts. The micellar reaction media could prove useful in the future for the synthesis and solubilization of very hydrophobic polypeptide segments such as integral membrane protein domains. Secondly, Rab thioesters terminating in glutamine or asparagine seem to be prone for side reactions, which probably involves the formation of cyclic imides. These side products were found to be capable of reacting with prenylated peptides under the typical reaction conditions. These studies also clearly point out the restrictions of applying chemical methods to the solution of biological problems, namely the necessity to work in an aqueous environment in order to preserve the solubility and the functional state of biological macromolecules. Although the remarkable solvent incompatibility of the Rab proteins and the examined prenylated peptides could be overcome, the employed conditions gave rise to protein denaturation. Eventually, the prenylated Rab proteins could be 'revived' by an *in vitro* refolding approach. The obtained semi-synthetic proteins were complexed to specific interacting proteins, such as RabGDI, REP-1 and GGTase-II, indicating, that the Rab proteins indeed adopted the correctly folded state. This was further confirmed by GGTase-II activity assays.

Using this approach, for the first time both single prenylated Rab proteins, representing the genuine intermediates of the GGTase-II catalyzed prenylation

reaction, were obtained. The interaction of these single prenylated Rabs with GGTase-II was further explored by taking advantage of fluorophores incorporated into the synthetic prenylated peptides. Different fluorophore attachment sites were tested in order to study the consequences of the fluorophore incorporation on the function of the GTPase. The obtained results could show, that the single prenylated proteins are tightly bound to GGTase-II with dissociation constants ( $K_d$ ) in the lower nanomolar range. Furthermore, the determined dissociation rate constants ( $k_{off}$ ) of this interaction revealed, that dissociation of the single prenylated intermediate is not required for Rab double prenylation.

The introduced fluorophore could also be utilized for the time-resolved monitoring of the prenylation reaction. Under conditions permitting only a single enzymatic turnover, the rates of the second prenyltransfer reaction were determined, which are in excellent agreement with values recently reported in the literature. The obtained data indicate, that the tighter bound single prenylated reaction intermediate is also faster converted to the double prenylated product. This suggests, that GGTase-II has evolved an active site that clearly prefers one of the two possible reaction intermediates for the second round of prenylation (namely that intermediate, which is prenylated on the C-terminal cysteine residue). Together with the results of previous studies these observations imply, that at least in the case of Rab7 the majority of proteins proceed to double prenylation by acquiring the first isoprenoid on the C-terminal cysteine residue followed by geranylgeranylation of the upstream cysteine residue.

Another major aim of the present study was to provide multi-milligram amounts of semi-synthetic and prenylated Rab proteins in complex with various interacting proteins for crystallographic studies. Out of six complexes tested in crystallization trials, two were crystallized and the structures were determined to very high resolutions (1.5 Å and 1.4 Å). The obtained structures of the single and doubly prenylated Ypt1:RabGDI complexes permit important insights into the mechanisms of RabGDI mediated Rab membrane extraction and delivery and a plausible explanation for the GDP dissociation inhibitory effect.

In conclusion, the developed EPL approach seems to be perfectly suited for the generation of homogeneously prenylated Rab proteins in large quantities (i.e. several milligram). The outlined protocols are easy to perform and should permit the production of functionalized Rab proteins on a routine basis.

The proteins generated in such a manner were demonstrated to be valuable tools for biochemical and biophysical studies.

## 4. Summary and Conclusions (german)

*Native chemical ligation (NCL)* und die verwandte Technik *Expressed Protein Ligation (EPL)* haben sich in der Vergangenheit als äußerst nützlich für die Synthese von verschiedenen Proteinen erwiesen. Insbesondere das Konzept der *EPL* demonstriert auf elegante Weise die Nützlichkeit einer Kombination von Chemie und Biologie, um komplexe biochemische und physiologische Fragestellungen zu beantworten.

Das Ziel der vorliegende Arbeit war es, die *EPL* Methode für die Semisynthese von prenylierten Rab Proteinen zu entwickeln. Rab GTPasen haben eine Schlüsselfunktion bei der Kontrolle des intrazellulären vesikulären Transportes in eukaryotischen Zellen. Die posttranslationale Modifikation von zwei Cysteinen mit je einem hydrophoben Lipid (Prenylierung) im C-terminalen Bereich der Rab Proteine wird von der Geranylgeranyltransferase II (GGTase-II) katalysiert und ist essentiell, um den Rab Proteinen die Ausübung ihrer Funktionen zu ermöglichen.

Im Rahmen dieser Arbeit wurden kurze, geranylgeranylierte (C<sub>20</sub> isoprenoide Verbindung) Peptide mit Hilfe der *EPL* spezifisch C-terminal an verkürzte Rab Protein  $\alpha$ -Thioester gekuppelt. Bei diesen Studien wurden einige interessante (und bis dato nicht beschriebene) Aspekte dieser Reaktion beobachtet. Es konnte festgestellt werden, dass die erfolgreiche Synthese der lipidierten Peptid-Protein-Konjugate die Verwendung bestimmter Additive, insbesondere von Detergenzien, voraussetzte. Obwohl die Wirkungsweise der Detergenzien bei der Reaktion nicht eindeutig bestimmt werden konnte, lässt sich dennoch vermuten, dass sie als mizellare Katalysatoren fungieren. Diese Erkenntnisse könnten sich in Zukunft bei der Synthese von anderen (integralen) Membranproteinen als nützlich erweisen. Desweiteren konnte beobachtet werden, dass Rab Protein  $\alpha$ -Thioester zu Nebenreaktionen neigen, wenn es sich bei der C-terminal aktivierten Aminosäure um Asparagin oder Glutamin handelt. Diese Nebenreaktionen führen zur Zyklisierung der C-terminalen Aminosäure. Die entstandenen Imide konnten interessanterweise unter den typischen *EPL* Bedingungen mit prenylierten Peptiden umgesetzt werden.

Die durchgeführten Untersuchungen zeigen auch die Einschränkungen einer Anwendung chemischer Methoden auf die Beantwortung biologischer Fragestellungen auf, insbesondere die Notwendigkeit in wässrigen Lösungsmittel zu arbeiten, um die Löslichkeit und den funktionalen Zustand biologischer

Makromoleküle zu erhalten. Obwohl die bemerkenswerte Lösungsmittelinkompatibilität der Rab Protein  $\alpha$ -Thioester und der untersuchten prenylierten Peptide gelöst werden konnte, so führten die angewandten Bedingungen dennoch zur Denaturierung der Proteine. Die Rückfaltung der lipidierten Rab Proteine konnte in dieser Studie zum ersten Mal erfolgreich durchgeführt werden. Die erhaltenen semisynthetischen Rab Proteine sind biologisch aktiv und konnten mit bekannten Interaktionspartnern komplexiert werden (z.B. mit RabGDI, REP-1, GGTase-II).

Das ausgearbeitete Verfahren erlaubte zum ersten Mal die Generierung von einfach prenylierten Rab Proteinen, die als Intermediate bei der GGTase-II katalysierten Prenylierungsreaktion kurzzeitig auftreten. Mit Hilfe der Fluoreszenzspektroskopie und Fluoreszenzmarkern, die in die synthetischen Peptide eingebaut wurden, konnte die Wechselwirkung dieser Intermediate mit der GGTase-II detailliert studiert werden. Die erhaltenen Dissoziationskonstanten (die diese Interaktion beschreiben) konnten zeigen, dass die Intermediate sehr fest an die GGTase-II gebunden sind. Mit Hilfe der ebenfalls bestimmten Geschwindigkeitskonstanten der Dissoziation konnte darüberhinaus ein Modell entwickelt werden, nach dem eine Dissoziation der einfach prenylierten Intermediate im Verlauf der Rab Doppelprenylierungsreaktion nicht zwangsläufig stattfinden muss.

Die eingeführten Fluoreszenzmarker ermöglichten ferner die Zeit aufgelöste Beobachtung des enzymatischen Umsatzes der einfach prenylierten Intermediate zum doppelprenylierten Produkt. Die Daten lassen darauf schließen, dass die GGTase-II eine klare Präferenz für eines der zwei möglichen Reaktionsintermediate aufweist. Zumindest im Falle von Rab7 scheint demnach die Mehrheit der Proteine zuerst C-terminal prenyliert zu werden, gefolgt von der Modifizierung des intern lokalisierten Cysteins.

Ein weiteres Ziel der vorliegenden Arbeit war die Generierung von prenylierten Rab Proteinen im Multimilligramm Maßstab für kristallografische Studien. Auch in diesem Fall wurden die semisynthetischen Rab Proteine an Interaktionspartner komplexiert. Sechs Komplexe konnten im präparativen Maßstab gewonnen werden, von denen zwei erfolgreich kristallisiert werden konnten. Die Strukturen der einfach und doppelt prenylierten Rab:RabGDI Komplexe wurden mit hoher Auflösung bestimmt und ermöglichten erstmals einen strukturellen Einblick in die Funktion von RabGDI.

Zusammenfassend kann gesagt werden, dass das entwickelte EPL Verfahren ideal erscheint, um homogen prenylierte Rab Proteine in preparativer Menge zu erhalten.

Die ausgearbeiteten Protokolle sind leicht durchführbar und sollten die routinemäßige Produktion von unterschiedlich funktionalisierten Rab Proteinen ermöglichen. Die Nützlichkeit solcher Proteine konnte in dieser Arbeit mit Hilfe von biochemischen und biophysikalischen Studien demonstriert werden.

# 5. Materials and Methods

*“Science is a collection of successful recipes.”*

*Paul Valery*

## 5. Materials and Methods

### 5.1. Materials

#### 5.1.1. Chemicals

All chemicals were purchased from the following companies with the highest purity available.

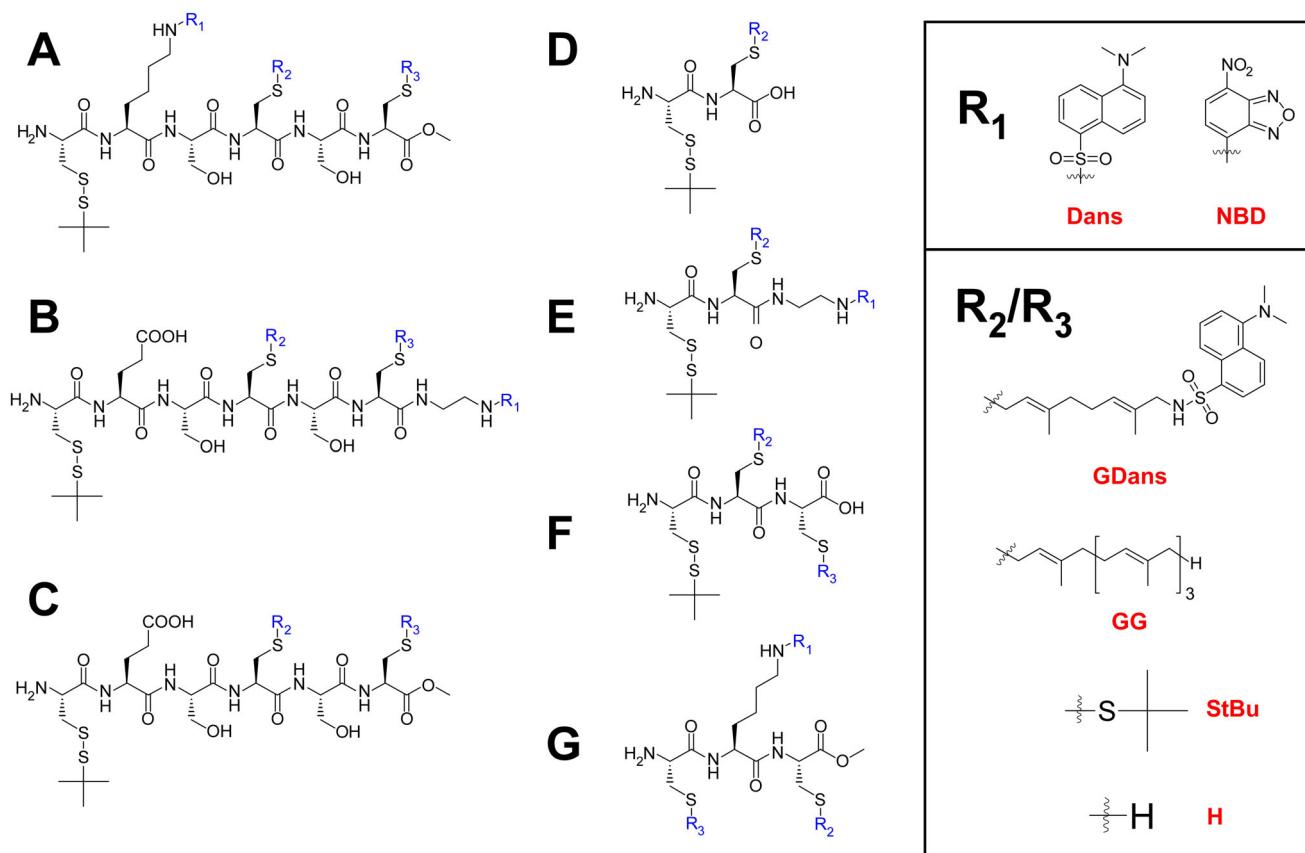
Supplier	Compound
Applichem Darmstadt, Germany	Acrylamid/Bisacrylamide (37.5:1, 30 %), methanol, GdmHCl, ammoniumsulfate
Gerbu Gaiberg, Germany	DTT, DTE, SDS, HEPES, EDTA, glycerol, isopropyl- $\beta$ -D-thiogalactopyranoside (IPTG)
Hampton Research, Laguna Niguel, CA, USA	Detergent Screen Kit I-III
JT Baker Deventer, NL	Acetonitrile, ethanol, 2-propanol, acetone, urea, chloroform, dichloromethane, dipotassium hydrogenphosphate, potassium dihydrogenphosphate, potassium hydroxide, hydrochloric acid, sodium chloride, potassium chloride
Merck Darmstadt, Germany	Ammonium persulfate (APS), sodium hydroxide
Pharma Waldhof Düsseldorf, Germany	GDP
Roth Karlsruhe, Germany	CHAPS, CTAB, TRIS
Serva Heidelberg, Germany	TEMED, bromphenol blue, Coomassie Brilliant Blue R250, Triton X-100, ampicillin (Amp), DMSO, $\beta$ -mercaptoethanol
Sigma Taufkirchen, Germany	GGPP, sinapinic acid, ethidium bromide, BSA, trifluoroacetic acid, LDAO, agarose, phenylmethylsulfonylfluoride (PMSF),

Table 5-1: Chemicals

#### 5.1.2. Peptides

All peptides used in this study were synthesised by members of Prof. Waldmann's group at the Max-Planck-Institute of Molecular Physiology, Dortmund and the University of Dortmund. Table 5-2 and the accompanying figure summarize a selection of peptides, which were coupled to truncated Rab/Ypt proteins by means of EPL. Synthetic procedures and analytical data can be found in the indicated references. The peptides were typically provided as a pale yellowish oil. Stock

solutions of 20-40 mM were usually prepared in dichloromethane/methanol (1:10) solvent systems and were stored at  $-80^{\circ}\text{C}$  under an atmosphere of argon.<sup>[221]</sup>



No.	Name	Core structure	R1	R2	R3	Source and References
1	H-Cys(StBu)-Lys(Dans)-Ser-Cys(GG)-Ser-Cys(GG)-OMe	A	Dans	GG	GG	Dr. Ines Heinemann [219,293]
2	H-Cys(StBu)-Lys(Dans)-Ser-Cys(StBu)-Ser-Cys(GG)-OMe	A	Dans	StBu	GG	Dr. Ines Heinemann [219,292]
3	H-Cys(StBu)-Lys(Dans)-Ser-Cys(GG)-Ser-Cys(StBu)-OMe	A	Dans	GG	StBu	Dr. Ines Heinemann [219,293]
4	H-Cys(StBu)-Lys(NBD)-Ser-Cys(StBu)-Ser-Cys(GG)-OMe	A	NBD	StBu	GG	Dr. Ines Heinemann [219]
5	H-Cys(StBu)-Glu-Ser-Cys(GG)-Ser-Cys(GG)-NH(CH <sub>2</sub> ) <sub>2</sub> NH-Dans	B	Dans	GG	GG	Anja Watzke [220,294]
6	H-Cys(StBu)-Glu-Ser-Cys(GG)-Ser-Cys(GDans)-OMe	C	-	GG	GDans	Dr. Lucas Brunsveld [294]
7	H-Cys(StBu)-Cys(GG)-OH	D	-	GG	-	Anja Watzke [295,220]
8	H-Cys(StBu)-Cys(GG)-NH(CH <sub>2</sub> ) <sub>2</sub> NH-Dans	E	Dans	GG	-	Anja Watzke [220]
9	H-Cys(StBu)-Cys(GG)-Cys(GG)-OH	F	-	GG	GG	Anja Watzke [220]
10	H-Cys(StBu)-Lys(Dans)-Cys(GG)-OMe	G	Dans	GG	StBu	Dr. Ines Heinemann [219]
11	H-Cys-Lys(Dans)-Cys(GG)-OMe	G	Dans	GG	H	Dr. Ines Heinemann [219]

Table 5-2: Peptides used in this study

The peptide H-Cys-Lys-Lys-Arg-Arg-Leu-Lys-Cys(GG)-NH-(CH<sub>2</sub>)<sub>2</sub>-NH-Dans was synthesised by Daniel Gottlieb, Department of Chemical Biology, MPI-Dortmund.

### 5.1.3. General instrumentation

Protein purification was usually carried out on a Pharmacia Biotech GradiFrac system (Uppsala, Sweden). Centrifugation was performed using Eppendorf 5415C/D bench-top centrifuges (Eppendorf, Cologne, Germany) or a Avanti J20-XP Centrifuge from Beckman Coulter (Palo Alto, CA, USA). For preparative ultracentrifugation a Beckmann Optima L-70K centrifuge was used. SDS-PAGE was performed using the Biorad Mini-Protean II system. Measurements of the pH were performed using a pH-meter 761 from Calimatic Knick (Berlin, Germany). Deionized water (ddH<sub>2</sub>O) was produced by an apparatus from Millipore (Eschborn, Germany). Dialysis tubes (MWCO: 14 kDa) were from Schleicher and Schuell (Dassel, Germany). For concentration of proteins various devices from Millipore (Eschborn, Germany) were used. Representations of crystal structures were created with the program Pymol ([www.pymol.org](http://www.pymol.org)). Modeling studies were carried out by Dr. Kirill Alexandrov, MPI-Dortmund using the ICM 3.0.25j software package (Molsoft, USA).

### 5.1.4. Frequently used buffers and growth media

#### *LB medium*

0.5 % (w/v) yeast extract  
1 % (w/v) tryptone  
1 % (w/v) NaCl

#### *SDS-PAGE running buffer (10x)*

0.25 M Tris-HCl  
2 M glycine  
1 % (w/v) SDS

#### *SDS-PAGE stacking gel buffer*

0.5 M Tris-HCl, pH 6.8  
0.4 % (w/v) SDS

#### *SDS-PAGE resolving gel buffer*

1.5 M Tris-HCl, pH 8.8  
0.4 % (w/v) SDS

#### *SDS-PAGE loading buffer (2x)*

100 mM Tris-HCl, pH 6.8  
4 % (w/v) SDS  
20 % (v/v) glycerol  
200 mM DTT  
0.05 % (w/v) bromophenol blue

#### *Coomassie stain solution*

10 % (v/v) acetic acid  
40 % (v/v) methanol  
0.1 % (w/v) Coomassie Brilliant Blue R250

<i>Coomassie destain solution</i>		<i>TAE buffer (1x)</i>	
10 % (v/v)	acetic acid	40 mM	Tris acetate
50 % (v/v)	methanol	2 mM	EDTA
<i>PBS (10x)</i>		<i>DNA loading buffer (5x)</i>	
80 g	NaCl	10 %	Ficoll 400
2 g	KCl	50 mM	Na <sub>2</sub> EDTA, pH 8.0
14.4 g	Na <sub>2</sub> HPO <sub>4</sub> · 2 H <sub>2</sub> O	0.05 % (w/v)	SDS
2.4 g	KH <sub>2</sub> PO <sub>4</sub>	0.15 % (w/v)	bromphenol blue
ddH <sub>2</sub> O to 1 l		0.15 % (w/v)	xylene cyanol (optional)

## 5.2. Analytical methods

### 5.2.1. MALDI-TOF-mass spectrometry

MALDI spectra were recorded on a Voyager-DE Pro Biospectrometry workstation from Applied Biosystems (Weiterstadt, Germany). Protein samples were desalted using small GF spin columns (Quiagen, Hilden, Germany) and mixed with an equal volume of sample matrix (10 mg/ml sinapinic acid and 0.1 % (v/v) TFA in water/acetonitril (1:1)). The mixture was quickly spotted on a MALDI sample plate, air-dried and spectra were measured with the following device settings: acceleration voltage = 25 kV, grid voltage = 93 %, extraction delay time = 750 ns and guide wire = 0.3 %. The laser intensity was manually adjusted during the measurements in order to obtain optimal signal to noise ratios. Calibrations were carried out using a protein mixture of defined molecular mass (Sigma). Spectra recording and data evaluation was performed using the supplied Voyager software package. The accuracy of the method for proteins within the molecular weight range of 20-30 kDa is ca.  $\pm$  20 Da (Dr. Heino Prinz, MPI-Dortmund, personal communication).

### 5.2.2. LC-MS measurements

LC-MS analysis was performed on an Agilent 1100 series chromatography system (Hewlett Packard) equipped with an LCQ electrospray mass spectrometer (Finnigan, San Jose, USA) using Jupiter C4 columns (5  $\mu$ m, 15 x 0.46 cm, 300 Å pore-size) from Phenomenex (Aschaffenburg, Germany). For LC-separations a gradient of buffer B (0.1 % formic acid in acetonitrile) in buffer A (0.1 % formic acid in water) with a constant flow-rate of 1 ml/min was employed. Upon sample injection, a ratio of

20 % buffer B was kept constant for 2 min. Elution was achieved using a linear gradient of 20-50 % buffer B in buffer A over 13 min followed by a steep gradient (50-90 % buffer B) over 3 min. The column was extensively flushed for at least 10 min with 95 % buffer B. Data evaluation and deconvolution was carried out using the Xcalibur software package. The accuracy of the method for proteins within the molecular weight range of 20 kDa is ca.  $\pm$  1-2 Da (Dr. Heino Prinz, MPI-Dortmund, personal communication).

### 5.2.3. Analytical reversed-phase (RP) and gel filtration (GF) HPLC

Analytical reversed-phase (RP) and gel filtration (GF) chromatography were performed on a Waters 600 chromatography instrument equipped with a Waters 2475 fluorescence detector and a Waters 2487 absorbance detector (Waters, Milford, MA, USA). Jupiter C4 columns (5  $\mu$ m, 15 x 0.46 cm, 300 Å pore-size) from Phenomenex (Aschaffenburg, Germany) were used for RP separations, whereas Biosep-SEC-2000 columns (60 x 0.78 cm, separation range 1-300 kDa, Phenomenex) were used for gel filtration. Chromatographic GF separations were performed using 50 mM sodium phosphate, pH 7.0, 50 mM NaCl, 2 mM DTE, 10  $\mu$ M GDP, 1 mM MgCl<sub>2</sub> as a running buffer at a flow rate of 0.7 ml/min. Separation was usually complete within 30 min.

For RP separations the following gradient of buffer B (0.1 % TFA in acetonitrile) in buffer A (0.1 % TFA in water) at a flow rate of 1 ml/min was used: The column was equilibrated with 5 % buffer B in buffer A. Upon sample injection this ratio was kept isocratic for 2 min followed by a linear gradient (5-30 % buffer B) over another 2 min. Individual components eluted upon a linear gradient (30-70 % buffer B) over 10 min and another isocratic phase (70 % buffer B) of 4 min. Afterwards the column was flushed for at least 10 min with 100 % buffer B in order to elute hydrophobic compounds (e.g. geranylgeranylated peptides). Data analysis was carried out using the Millennium software package provided by Waters.

### 5.2.4. Denaturing SDS-PAGE

Typically 15 % SDS-PAGE gels were used for the analysis of Rab proteins (MW of ca. 24 kDa). The corresponding volumes of the individual components as indicated by Table 5-2 were mixed and the resolving gel was cast using a Biorad Multi-casting apparatus (10 gels). After the resolving gel was polymerized, a stacking gel mix was

prepared and cast atop the resolving gel. Protein samples were prepared by adding an equal amount of SDS-PAGE sample buffer (2x) and heated for 5 min at 95° C. Gels were run at ca. 10 V/cm until the bromphenol blue front had entered the buffer solution. Fluorescently labeled proteins were visualized by exposing the unstained SDS-PAGE gel to UV light. The proteins were subsequently stained using a solution of Coomassie brilliant blue.

Type of gel (%)	Acrylamide/ bisacrylamide (29:1, 30 %)	ddH <sub>2</sub> O	Resolving gel buffer	Stacking gel buffer	TEMED	10 % APS
<b>Resolving gel, 70 ml</b>						
<b>10 %</b>	23.5 ml	27.6 ml	17.1 ml	---	29 µl	700 µl
<b>15 %</b>	34.2 ml	15.7 ml	17.1 ml	---	29 µl	700 µl
<b>Stacking gel, 30 ml</b>						
<b>5 %</b>	4.9 ml	20 ml	---	3.7 ml	300 µl	29 µl

Table 5-3: Pipeting scheme for SDS-PAGE gels. TEMED = *N,N,N',N'*-tetramethylethylenediamine; APS = ammoniumpersulfate.

### 5.2.5. Western-Blot

The unstained SDS-PAGE gel was equilibrated together with 6 sheets of Gel-blotting paper and a nitrocellulose membrane (both from Schleicher & Schuell, Dassel, Germany) of approximately the same size for 10 min in transfer buffer (250 mM Tris-HCl, pH 8.3, 192 mM glycine, 1.3 mM SDS, 10 % methanol (v/v)). A blot sandwich was constructed in the following order: cathode - 3 sheets of Whatmann filter paper - gel - nitrocellulose membrane - 3 sheets of Whatmann filter paper - anode. The transfer was carried out for 1-2 h at a current of 1.5 mA/cm<sup>2</sup> in a Semi-Phor semi-dry blot apparatus from Hoefer Scientific Instruments (San Francisco, CA, USA). The efficiency of transfer can be judged by staining the gel with Coomassie Blue or by staining of the membrane with Ponceau S solution (5 g/l Ponceau S in acetic acid/ddH<sub>2</sub>O (1:100)). The membrane was briefly washed 3 times with PBS and subsequently blocked for at least 1 h with hot blocking solution (5 % non-fat dry milk, 0.1 % Tween-20 in PBS). The membrane was briefly washed 3 times with wash solution (0.06 % non-fat dry milk, 0.01 % Tween-20 in PBS) and incubated with the primary antibody solution for at least 1 h. Polyclonal primary and

secondary antibody sera were typically diluted 1:1000 to 1:10000 with 0.6 % non-fat dry milk, 0.01 % Tween-20 in PBS prior to use. The membrane was briefly washed 3 times with wash solution and incubated with the horseradish peroxidase coupled secondary antibody for 1 h. The membrane was rinsed 3 times with wash solution and 3 times with PBS. Horseradish peroxidase conjugates were detected using the ECL kit (Amersham, UK).

### 5.3. Biochemical methods

#### 5.3.1. Expression and purification of GGTase-II, REP-1, RabGDI, MRS6p and Rab7wt

All proteins were kindly prepared and provided by Anca Niculae (Department of Physical Biochemistry, MPI-Dortmund). Mammalian RabGGTase was purified from *E. coli* BL21(DE3) codon plus cells expressing a hexahistidine-GST tagged  $\alpha$ -subunit and an untagged  $\beta$ -subunit.<sup>[313]</sup> Briefly, following cell growth, induction and lysis of the cells, GGTase-II was purified from crude homogenate using Ni-NTA Sepharose columns (Pharmacia). The affinity tag was removed by digestion with TEV protease. A second Ni-NTA chromatography was performed in order to remove the cleaved-off hexahistidine tag, uncleaved GGTase-II and TEV protease. For production of GST tagged GGTase-II (see chapter 4.3.3.), the eluate of the first Ni-NTA column was further purified by anion-exchange chromatography (Poros 50 HQ columns, Perseptive Biosystems, Framingham, MA, USA) and dialysis. REP-1 was purified from insect cells infected with recombinant baculovirus<sup>[326]</sup> or from recombinant yeast *S. cerevisiae*.<sup>[327]</sup> The protein was purified by a combination of Ni-NTA affinity and gel filtration chromatography. Rab7 and RabGDI wild-type proteins were expressed and purified in a similar manner.<sup>[114,328]</sup> Expression and Purification of MRS6p is described elsewhere.<sup>[205]</sup>

#### 5.3.2. Expression and purification of Rab/Ypt-thioester proteins

All semi-synthetic Rab and Ypt proteins either in complex with REP-1, MRS6p, RabGDI or uncomplexed were prepared according to the devised protocols shown below (4.3.2. and 4.3.3.). Although the method is generally applicable, certain critical points are discussed in more detail in chapter 3.

The plasmid coding for the desired Rab/Ypt-Intein-CBD construct was transformed into *E. coli* BL21(DE3) cells using electroporation and transformants were selected on

ampicillin (50 mg/l) agar plates. A single colony was inoculated into 5 ml of LB medium containing 125 mg/l Ampicillin and the culture was grown overnight at 37° C. This pre-culture was used to seed 2 l of fresh LB medium (containing 125 mg/l ampicillin) and the culture was incubated at 37° C until the absorbance at 600 nm ( $OD_{600}$ ) reached 0.5 - 0.7. The cells were cooled down on ice, IPTG was added to a final concentration of 0.5 mM and overnight (or 10 - 12 h) induction was performed at 20° C. The cells were cooled down to 4° C and all subsequent steps were performed at this temperature. Cells were harvested by centrifugation (5000 g, 20 min, 4° C) and washed once in PBS. Cells could be stored frozen at -80° C at this point. Levels of protein expression before and after induction were determined by SDS-PAGE. The bacterial pellet was resuspended in lysis buffer (25 mM sodium phosphate, pH 7.5, 0.5 M NaCl, 1 mM PMSF, 2 mM  $MgCl_2$ , 10  $\mu$ M GDP) and the cells were lysed by passing them twice through a Microfluidizer. A fresh portion of 0.5 mM PMSF and Triton X-100 (1 % final concentration) were added. The lysate was cleared by ultracentrifugation (30000 g, 40 min, 4° C) and the supernatant was transferred to Falcon tubes. An appropriate amount of chitin beads, equilibrated with lysis buffer containing 1 % Triton X-100 was added and the mixture was incubated for 2 h on a rotating wheel at 4° C (1 ml of beads can bind about 2 mg of fusion-protein. The total amount of expressed fusion protein can be estimated by SDS-PAGE and Coomassie Blue staining). The suspension was centrifuged (2500 g, 5 min, 4° C) and the supernatant removed. To remove unspecifically bound material beads were washed 4 times with lysis buffer containing 1 % Triton X-100 followed by 4 times washing with buffer without the detergent. Cleavage of the fusion protein was induced by adding powdered MESNA to the beads suspension to a concentration of 0.5 M and overnight incubation at room temperature. The supernatant was collected by centrifugation and was passed over a gel filtration column equilibrated with ligation buffer (20 mM sodium phosphate, pH 7.5, 100  $\mu$ M  $MgCl_2$ , 100  $\mu$ M GDP). The pooled fractions were concentrated to at least 10 mg/ml and shock frozen using liquid nitrogen. The proteins could be stored at -80° C for at least 2 years without loss of ligation efficiency. Yields typically ranged from 20 - 40 mg of Rab/Ypt protein thioester per liter of bacterial culture.

### 5.3.3. Ligation of geranylgeranylated peptides to Rab/Ypt-thioester

500  $\mu$ l of Rab/Ypt-thioester protein (typically 20 mg/ml, ca. 500 nmol) in ligation buffer was supplemented with 50 mM CTAB and 125 mM MESNA (final concentrations). The reaction is initiated by adding 3.5 - 5  $\mu$ mol of the peptide in a suitable solvent (peptide stock solutions of 30 mM were often prepared in methanol/dichloromethane solvent systems). The reaction mixture was incubated overnight at 37° C with vigorous agitation. Under these reaction conditions ligated and unligated proteins usually precipitated together with excessive peptide. The reaction mixture was centrifuged and the supernatant removed. The pellet was washed once with 1 ml methanol, 4 times with 1 ml methylenchloride, 4 times with 1 ml methanol and 4 times with 1 ml Milli-Q (ddH<sub>2</sub>O) water at room temperature in order to resolubilize contaminating peptide and unligated protein. The progress of the purification was monitored by SDS-PAGE. The precipitate was dissolved in denaturation buffer (100 mM Tris-HCl, pH 8.0, 6 M GdmHCl, 100 mM DTE, 1 % CHAPS, 1 mM EDTA) to a final protein concentration of 0.5 - 1.0 mg/ml and incubated overnight at 4° C with slight agitation. The solution can be stored (indefinitely) at this point at -80° C. The solution was cleared from any insoluble material by centrifugation or by filtration through 0.2  $\mu$ m celluloseacetate filter units (Schleicher & Schuell). The protein was then renatured by diluting it at least 25 fold drop-wise into refolding buffer (50 mM Hepes pH 7.5, 2.5 mM DTE, 2 mM MgCl<sub>2</sub>, 100  $\mu$ M GDP, 1 % CHAPS, 400 mM arginine-HCl, 400 mM trehalose, 1 mM PMSF, 1 mM EDTA) with gentle stirring at room temperature. Typically 10 portions of the denatured sample were stepwise added to the refolding vessel within 2 h (pulse renaturation). The mixture was incubated 30 min further at room temperature followed by a centrifugation step (30000 g, 30 min, 4° C) in order to remove aggregated material. An aliquot of the supernatant was TCA precipitated and analyzed by SDS-PAGE. The total amount of soluble protein was judged by the intensity of Coomassie blue stained protein bands.

#### *Variant A: Complex formation with RabGDI, MRS6p, REP-1 and GGTase-II*

An equimolar amount of the respective protein was added and the solution was incubated for 1 h on ice. The mixture was dialyzed against two 5 l changes of dialysis buffer (25 mM Hepes, pH 7.5, 2 mM MgCl<sub>2</sub>, 10  $\mu$ M GDP, 2.5 mM DTE,

100 mM  $(\text{NH}_4)_2\text{SO}_4$ , 10 % glycerol, 1 mM PMSF, 1 mM EDTA). The dialyzed material was concentrated to a protein concentration of 1 - 4 mg/ml using size-exclusion concentrators (MWCO: 30 kDa) and subsequently centrifuged (13000g, 5 min, 4° C) to remove insoluble material. The supernatant was loaded on a 26/60 Superdex-200 gel filtration column (Pharmacia) equilibrated with gel filtration buffer (25 mM Hepes, pH 7.5, 2 mM  $\text{MgCl}_2$ , 10  $\mu\text{M}$  GDP, 5 mM DTE, 100 mM  $\text{Na}_2\text{SO}_4$ , 1 mM EDTA, 10 % glycerol, for protein complexes intended for crystallization glycerol was omitted). The peak fractions containing the desired complex (SDS-PAGE) were pooled, concentrated to approximately 10 mg/ml and stored frozen at -80° C in multiple aliquots. The typical recovery yield ranged from 10 - 50 % with respect to starting Rab/Ypt-thioester.

#### *Variant B: Purification of uncomplexed, ligated protein*

The mixture was concentrated to ca. 10 - 20 ml using stirred size exclusion concentrators (MWCO: 10 kDa, Amicon). The retained protein solution was diluted with 100 ml of 25 mM Hepes, pH 7.5, 2 mM  $\text{MgCl}_2$ , 10  $\mu\text{M}$  GDP, 2.5 mM DTE, 100 mM  $(\text{NH}_4)_2\text{SO}_4$ , 0.6 % CHAPS and concentrated to a protein concentration of ca. 1 mg/ml. The mixture was loaded on a PD-10 desalting column (Amersham) equilibrated with the same buffer. The eluted protein was concentrated to 3 - 5 mg/ml using size-exclusion spin concentrators (MWCO: 10 kDa, Millipore) and shock-frozen in liquid nitrogen in multiple aliquots. The protein was stored at -80° C.

### **5.3.4. *In vitro* protein prenylation**

#### *Variant A : Preparative production of doubly prenylated Rab7:REP-1 complex*

Rab7wt (3.6 mg, 150nmol) was mixed with 11.1 mg REP-1 (150 nmol) in an Eppendorf tube. 22.5 mg of mammalian GST-GGTase-II (150 nmol) were mixed with 1  $\mu\text{mol}$  of geranylgeranylpyrophosphate (GGPP) in another tube. The buffer of both tubes was adjusted to 0.3 % CHAPS, 10  $\mu\text{M}$  GDP, and approximately 40 mM Hepes, pH 7.2, 5 mM DTE, 3 mM  $\text{MgCl}_2$  and 50 mM NaCl. Both tubes were incubated on ice for 2 min followed by mixing of the contents in order to initiate the prenylation reaction. Usually incubation at 37° C for 10 min was sufficient for > 90 % double prenylation of Rab7. The reaction mixture was diluted to 6 ml with *in vitro* prenylation

buffer (40 mM Hepes, pH 7.2, 50 mM NaCl, 5 mM DTE, 2.5 % CHAPS, 3 mM MgCl<sub>2</sub>, 10 μM GDP) and passed three times over a glutathion Sepharose 4B column (Pharmacia, 6 ml bed volume) equilibrated with the same buffer. The flow-through was loaded on a 26/60 Superdex 200 GF column (Pharmacia) equilibrated with *in vitro* prenylation buffer without CHAPS. Fractions containing binary Rab7:REP-1 complex were pooled, concentrated to approximately 20 mg/ml and stored at -80° C in multiple aliquots.

*Variant B: Incorporation [<sup>3</sup>H]-geranylgeranyl groups into Rab proteins.*

Standard reaction mixtures contained the following components in a final volume of 50 μl: 50 mM Hepes, pH 7.2, 5 mM MgCl<sub>2</sub>, 1 mM DTT, 3 mM Nonidet P-40, 5.5 μM [<sup>3</sup>H]-Geranylgeranylpyrophosphate (14000 cpm/pmol) and the indicated amounts of Rab:REP complex and GGTase-II. The reaction mixtures were incubated at room temperature for 20 min. The reaction was subsequently quenched by addition of 2 ml of 10% HCl in 90% ethanol. After 30 min, the reaction mixture was filtered through glass fiber filters (Whatman). The filters were rinsed twice with 96 % ethanol, immersed in scintillation liquid and counted for <sup>3</sup>H.

## 5.4. Biophysical methods

Fluorescence measurements were performed either with an Aminco SLM 8100 spectrofluorometer (Aminco, Silver Spring, MD, USA) or a Spex Fluoromax-3 spectrofluorometer (Jobin Yvon, Edison, NJ, USA). Measurements were carried out in 1 ml quartz cuvettes (Hellma) with continuous stirring and thermostated at 25° C unless otherwise indicated. Stopped-flow measurements were performed on a Applied Photophysics SX.18MV-R apparatus (Surrey, UK).

### 5.4.1. Fluorescence titrations – determination of K<sub>d</sub>

Steady-state fluorescence measurements for monitoring interactions between semi-synthetic Rab7:REP-1 complexes with GGTase-II were followed in 50 mM Hepes, pH 7.2, 50 mM NaCl and 5 mM DTE. Typically the dansyl labeled Rab7:REP-1 complex was placed in a cuvette in 1 ml of buffer to give a final concentration of ca. 100 - 200 nM and incubated for 5 min at 25° C. The excitation and emission monochromators were set to 280 nm and 495 nm, respectively. Small aliquots of

GGTase-II (typically 10-20 nM at each step) were then added to the cuvette, until the fluorescence signal was saturated or showed a continuous linear increase. The change in fluorescence was plotted as a function of the total GGTase-II concentration and corrected for unspecific fluorescence. The data was fitted to the following equation using GraFit 4.0 (Erithacus software):

$$Y = Y_{\min} + \left\{ K_d + [L]_0 + [P]_0 - \sqrt{(K_d + [L]_0 + [P]_0)^2 - 4[P]_0[L]_0} \right\} \frac{Y_{\max} - Y_{\min}}{2[P]_0}$$

where Y is the observed fluorescence after each step of titrator addition,  $Y_{\min}$  is the initial value at  $[L]_0 = 0$ ,  $Y_{\max}$  is the final value at saturation,  $[L]_0$  is the total (cumulative) concentration of GGTase-II,  $[P]_0$  is the Rab7:REP-1 complex concentration, and  $K_d$  is the equilibrium constant, which is to be determined (see appendix 7.1.1. for a derivation of this equation and further explanation).

#### 5.4.2. Transient kinetics – determination of $k_{\text{off}}$

For determination of  $k_{\text{off}}$ , the dansyl labeled semisynthetic Rab7:REP-1 complex (100 nM) was incubated with an equal amount of GGTase-II (100 nM) at 25° C in 1 ml of buffer (50 mM Hepes, pH 7.2, 50 mM NaCl and 5 mM DTE) for 5 min. The excitation wavelength was set to 280 nm, while data were collected at 495 nm. The fluorescently labeled complex was displaced from GGTase-II by addition of an at least 10 fold excess of double prenylated wtRab7:REP-1 complex (1 - 1.5  $\mu\text{M}$  final concentration, prepared as described in chapter 5.3.4.). Under certain conditions (which were applied in this case, see appendix), the obtained displacement curve could be fitted to a single exponential equation:

$$Y = Y_0 + Ae^{-k_{\text{off}}t}$$

where Y is the observed fluorescence,  $Y_0$  is the fluorescence at  $t = \infty$ , A is the signal amplitude, t is the time, and k is the rate constant, which equals  $k_{\text{off}}$  for dissociation of the semi-synthetic Rab7:REP-1 complex from GGTase-II. Data analysis was carried out using GraFit 4.0 (Erithacus software).

### 5.4.3. Monitoring the prenylation reaction

The prenylation of the semisynthetic Rab7 proteins was analysed using a Spex Fluoromax-3 spectrofluorometer (Jobin Yvon, Edison, NJ, USA) for long-term measurements, whereas a stopped-flow apparatus (Applied Photophysics, Surrey, UK) was used for examining the fast events occurring upon start of the reaction.

#### *Long-term measurements*

Typically, 50-100 nM of dansyl labeled semisynthetic Rab7:REP-1 complex was mixed with an equal amount of GGTase-II in a cuvette, containing 1 ml of buffer (50 mM Hepes, pH 7.2, 50 mM NaCl, 5 mM DTE, 2 mM MgCl<sub>2</sub>, 100 μM GDP). Following a 5 min incubation at 25° C permitting temperature equilibration, the reaction was started by adding geranylgeranyl-pyrophosphate to a final concentration of approximately 10 μM. Excitation and emission monochromators were adjusted to 280 nm and 510 nm, respectively. The data were fitted to a double exponential equation using GraFit 4.0 (Erithacus software):

$$Y = Y_0 + A_1 e^{-k_1 t} + A_2 e^{-k_2 t}$$

where Y is the observed fluorescence, Y<sub>0</sub> is the fluorescence at t = ∞, A<sub>1</sub> and A<sub>2</sub> are the signal amplitudes, t is the time, and k<sub>1</sub> and k<sub>2</sub> are the rate constants.

#### *Stopped-flow measurements*

Dansyl labeled Rab7:REP-1:GGTase-II ternary complex (ca. 200 nM) in 50 mM Hepes, pH 7.2; 50 mM NaCl, 5 mM DTE, 2 mM MgCl<sub>2</sub>, 100 μM GDP was rapidly mixed in the stopped-flow apparatus with an equal volume of geranylgeranylpyrophosphate in the same buffer (concentration ranged from 200 nM to 20 μM). Excitation was at 280 nm, while fluorescence was recorded through a 420 nm cut-off filter. Mixing and measuring chamber were thermostated at 25° C using a water bath. Typically, curves of 5 independent experiments were averaged using the software package provided by Applied Photophysics.

## 5.5. Molecular biology

### 5.5.1. Plasmids and bacterial strains

#### Plasmids

All plasmids were from the Department of Physical Biochemistry, MPI-Dortmund.

Plasmid Name	Insert	Resistance/ Selection marker	Application and References
pTYB1_Rab7 $\Delta$ 6	canine Rab7 $\Delta$ 6	Amp	Expression of insert-intein-CBD fusion proteins and generation of C-terminal $\alpha$ -thioesters. <sup>[199,292]</sup>
pTYB1_Ypt7 $\Delta$ 7	yeast Ypt7 $\Delta$ 7	Amp	
pTWIN1_Ypt1 $\Delta$ 2	yeast Ypt1 $\Delta$ 2	Amp	
pTWIN1_Rab7 $\Delta$ 2	canine Rab7 $\Delta$ 2	Amp	
pTWIN2_Ypt1 $\Delta$ 3	yeast Ypt1 $\Delta$ 3	Amp	
pTWIN1_Rab5a $\Delta$ 4	human Rab5a $\Delta$ 4	Amp	
pTWIN1_Rab5a $\Delta$ 5	human Rab5a $\Delta$ 5	Amp	
pGATEVmod_RabGGTase $\alpha$	rat RabGGTase $\alpha$	Amp	Coexpression of the RabGGTase subunits with a His <sub>6</sub> -GST tag on the N-terminus of the $\alpha$ -subunit. The tag can be cleaved off by TEV protease. <sup>[313]</sup>
pET30_RabGGTase $\beta$	rat RabGGTase $\beta$	Kan	
pET19mod_Rab7	canine Rab7wt	Amp	Expression of the corresponding protein N-terminally modified with a hexahistidine tag. The tag can be cleaved off by TEV protease. <sup>[114,295,328]</sup>
pET19mod_yGDI	yeast GDI	Amp	
* pFastBac_GDI-1	bovine GDI-1	Amp	
** pYES2_REP-1	rat REP-1	Amp URA3	Expression of REP-1 C-terminally modified with a hexahistidine tag in yeast. <sup>[327]</sup>
* pVL_REP-1	rat REP-1	Amp	Expression of REP-1 or MRS6p modified with a hexahistidine tag. <sup>[205,326]</sup>
pET30a_MRS6	yeast MRS6p	Kan	

Table 5-4: Plasmids used in this work. Empty pTWIN and pTYB vectors were obtained from New England Biolabs (Beverly, MA, USA). Typically expression was performed using one of the *E. coli* strains listed below. \* Expression in SF21 cells upon infection with recombinant baculovirus. \*\* Expression in yeast *S. cerevisiae* strain BJ5459. Amp = ampicillin, CBD = chitin-binding domain, Kan = kanamycin, URA3 = auxotrophic selection on minimal media without uracil.

*Bacterial strains*

XL1 Blue (Stratagene)	<i>recA1, endA1, gyrA96, thi-1, hsdR17, supE44, relA1, lac</i> [F', <i>proAB, lac<sup>q</sup>ZΔM15, Tn10 (Tet<sup>r</sup>)</i> ]
BL21(DE3) (Novagen)	F <sup>-</sup> , <i>ompT, lon, hsdS (r<sub>B</sub><sup>-</sup>, m<sub>B</sub><sup>-</sup>), dcm, gal, λ(DE3)</i>
BL21(DE3) Codon Plus RIL (Stratagene)	F <sup>-</sup> , <i>ompT, lon, hsdS (r<sub>B</sub><sup>-</sup>, m<sub>B</sub><sup>-</sup>), dcm, gal, λ(DE3), endA, Hte</i> [ <i>argU ileY leuW Cam<sup>r</sup></i> ]

**5.5.2. Preparation and transformation of competent cells**

1 l of LB medium was inoculated with 1 ml of an overnight-grown culture of the desired *E.coli* strain. Cells possessing antibiotic resistance genes (e.g. BL21(DE3) codon plus RIL) were grown in the presence of the corresponding antibiotic. The culture was incubated at 37° C on a shaker, until the OD<sub>600</sub> reached 0.5 (ca. 3 - 4 h). The culture was cooled on ice for 20 min, transferred to sterile centrifugation vessels and centrifuged for 10 min at 4° C and 2000 g. The supernatant was decanted.

*Variant A.: Transformation by Electroporation*<sup>[329]</sup>

The bacterial cell pellet was gently (!) resuspended in 5 ml of ice-cold sterile GYT (0.125 % (w/v) yeast extract, 0.25 % (w/v) tryptone, 10 % (v/v) glycerol) and recentrifuged as described above. Cells were resuspended in a final volume of 1 ml GYT, dispensed in 50 µl aliquots, shock frozen in liquid nitrogen and stored at -80° C. For transformation, approximately 1 ng of DNA was added to the thawed cell suspension in a chilled cuvette. Electrotransformation was carried out by applying a high voltage pulse using a *E.coli* Pulser from Biorad (conditions: 25 µF, 200 Ω, 2.5 kV). 1 ml of LB medium was added to the cell suspension and the culture was grown at 37° C for 1 h. Transformed Cells were selected on agar plates containing the corresponding antibiotics.

*Variant B.: Transformation using CaCl<sub>2</sub>*

The pellet was gently resuspended in 20 ml of ice-cold sterile 100 mM CaCl<sub>2</sub> solution and incubated on ice for 30 min. The cells were centrifuged at 2000 g for 5 min at 4° C and were resuspended in 1 - 5 ml of TFBII buffer (10 mM MOPS, pH 7.0, 75 mM CaCl<sub>2</sub>, 10 mM NaCl, 15 % glycerol). Aliquots of 50 - 100 µl were shock frozen in liquid nitrogen and stored frozen at -80° C.

For transformation, cells were thawed rapidly and approximately 1 ng of the desired plasmid DNA was added. The mixture was incubated on ice for 30 min without shaking. Cells were heat-shocked at 42° C for 60 sec and immediately cooled on ice for 2 min. 1 ml of LB medium was added to the tube and the culture was incubated at 37° C for 1 h, before recombinants were selected on agar plates supplemented with the corresponding antibiotics.

**5.5.3. Purification of DNA***DNA fragments*

DNA fragments produced by PCR amplification or restriction enzyme digestion were purified by preparative agarose gel electrophoresis. The band of interest was excised and extracted from the gel using a gel extraction kit from Quiagen or PQLab according to the instructions of the manufacturer.

*Agarose gel electrophoresis*

Depending on the size of the DNA fragment, the agarose concentration was between 0.8 and 1.2 % (w/v). The required amount of agarose was solubilized by heating in TAE buffer. Ethidium bromide was added to a final concentration of 0.01 % (w/v), the gel was poured into the gel casting equipment and allowed to polymerize. Samples were prepared in DNA loading buffer and the gels were run horizontally at 10 V/cm immersed in TAE-buffer until fragment separation was complete. A 1 kb DNA ladder (GibcoBRL) was used as a molecular weight standard.

### *Preparation of Plasmid DNA*

Plasmid DNA was prepared using the plasmid mini-prep kit (Quiagen or PQLab) as follows: A single bacterial colony was used to seed 2 ml of LB medium containing the appropriate antibiotic(s). The culture was grown overnight (10 - 12 h) at 37° C. Cells were harvested by centrifugation (3000 g, 5 min) and lysed by alkaline/SDS treatment. The precipitate (chromosomal DNA, lipids, proteins) was removed by centrifugation and the supernatant was loaded on a silica spin column. Following washing, the plasmid DNA was eluted using sterile TAE buffer or deionized water.

### *Ethanol precipitation*

The salt concentration of the DNA sample was adjusted to 250 - 300 mM sodium acetate, pH 5.5 and DNA was precipitated by adding ethanol (96 %) to a final concentration of ca. 70 % followed by a 30 min incubation at room temperature. After centrifugation (10000 g, 10 min, RT) and removal of the supernatant, the precipitate was washed once with 70 % ethanol and dried under vacuum.

## **5.5.4. PCR**

### *Preparative PCR*

Typically, a 50 µl reaction mixture comprised 1 - 5 ng of template (plasmid) DNA, 0.5 - 1.0 µM of upstream and downstream primers, 200 µM of each dNTP, 2-3 units of Expand High Fidelity Polymerase mix (Roche Diagnostics, Mannheim, Germany) and the corresponding reaction buffer and salts. A Biorad PE 9700 thermocycler from Applied Biosystems (Weiterstadt, Germany) was used for temperature control and cycling. Denaturation was for 1 min at 96° C, annealing for 1 min at 50 - 62° C depending on primer length and GC content, and extension was for 2 - 4 min (depending on the length of the amplicon). In general, 15 - 20 cycles were sufficient for efficient amplification.

### *Colony PCR screen*

Colonies were picked and resuspended in 20  $\mu$ l of sterile ddH<sub>2</sub>O in a PCR test tube using sterile eppendorf tips. 6  $\mu$ l of this suspension were mixed with 6  $\mu$ l of PCR mix (containing 400  $\mu$ M of each dNTP, 5 pmol of each primer, 1 unit of Taq polymerase (Sigma, Taufkirchen, Germany) in Taq buffer (2x)). The PCR reactions were carried out under the following conditions: Cells were disrupted by heating the PCR tubes for 3 min at 96° C followed by 25 cycles of denaturation for 30 sec at 96° C, annealing for 30 sec at 50 - 62° C, and primer extension for 40 sec at 72° C. The PCR products were analyzed by agarose gel electrophoresis.

An aliquot (1  $\mu$ l) of the initially obtained cell suspension was plated on agar plates containing the corresponding antibiotics.

### *DNA Sequencing*

For DNA sequencing of the cloned fragments the BigDyeDesoxy terminator cycle sequencing kit and a ABI Prism 373XL machine (Applied Biosystems, Weiterstadt, Germany) was used. The sequencing reactions contained 0.5 - 1  $\mu$ g plasmid DNA, 3 pmol of the corresponding primers, and 8  $\mu$ l BigDye termination mix in a final volume of 20  $\mu$ l. 25 cycles were performed with the following parameters: Denaturation for 30 sec at 96° C (for the first cycle 1 min), annealing for 1 min at 50° C, and primer extension for 4 min at 60° C. The DNA was ethanol precipitated (see above), washed twice with 70 % ethanol, dried, and analyzed by the in house sequencing facility.

#### **5.5.5. Restriction enzyme digestion**

Restriction enzyme digests of DNA fragments were performed as recommended by the manufacturer. The reaction was stopped by addition of DNA loading buffer. Fragments produced by restriction enzyme digestion were separated using agarose gel electrophoresis.

### 5.5.6. Ligation

For ligation 1-10 *f*mol of linear plasmid DNA was mixed with a 10 fold molar excess of fragment DNA. Ligation was performed in T4 DNA ligase buffer in a volume of 12.5  $\mu$ l, using 0.2 units of T4 DNA ligase (Roche Diagnostics, Mannheim, Germany) for 12 - 16 h at 16° C.

# 6. References

*“To invent, you need a good imagination and a pile of junk.”*

*Thomas Edison*

## 6. References

- [1] IUPAC-IUB Commission "IUPAC-IUB Commission on Biochemical Nomenclature. A One-Letter Notation for Amino Acid Sequences. Tentative Rules." *J. Biol. Chem.* (1968), **243**, 3557-3559.
- [2] Fasshauer, D., Sutton, R. B., Brunger, A. T., and Jahn, R. "Conserved structural features of the synaptic fusion complex: SNARE proteins reclassified as Q- and R-SNAREs." *Proc. Natl. Acad. Sci. U. S. A.* (1998), **95**, 15781-15786.
- [3] Sutton, R. B., Fasshauer, D., Jahn, R., and Brunger, A. T. "Crystal structure of a SNARE complex involved in synaptic exocytosis at 2.4 angstrom resolution." *Nature* (1998), **395**, 347-353.
- [4] Mayer, A., Wickner, W., and Haas, A. "Sec18p (NSF)-driven release of sec17p (alpha-SNAP) can precede docking and fusion of yeast vacuoles." *Cell* (1996), **85**, 83-94.
- [5] McNew, J. A., Weber, T., Parlati, F., Johnston, R. J., Melia, T. J., Sollner, T. H., and Rothman, J. E. "Close is not enough: SNARE-dependent membrane fusion requires an active mechanism that transduces force to membrane anchors." *J. Cell Biol.* (2000), **150**, 105-117.
- [6] Weber, T., Zemelman, B. V., McNew, J. A., Westermann, B., Gmachl, M., Parlati, F., Sollner, T. H., and Rothman, J. E. "SNAREpins: Minimal machinery for membrane fusion." *Cell* (1998), **92**, 759-772.
- [7] Peters, C., and Mayer, A. " $\text{Ca}^{2+}$ /calmodulin signals the completion of docking and triggers a late step of vacuole fusion." *Nature* (1998), **396**, 575-580.
- [8] Peters, C., Andrews, P. D., Stark, M. J. R., Cesaro-Tadic, S., Glatz, A., Podtelejnikov, A., Mann, M., and Mayer, A. "Control of the terminal step of intracellular membrane fusion by protein phosphatase 1." *Science* (1999), **285**, 1084-1087.
- [9] Peters, C., Bayer, M. J., Buhler, S., Andersen, J. S., Mann, M., and Mayer, A. "Trans-complex formation by proteolipid channels in the terminal phase of membrane fusion." *Nature* (2001), **409**, 581-588.
- [10] Mayer, A. "What drives membrane fusion in eukaryotes?" *Trends Biochem.Sci.* (2001), **26**, 717-723.
- [11] Blumenthal, R., Clague, M. J., Durell, S. R., and Epsand, R. M. "Membrane fusion." *Chem. Rev.* (2003), **103**, 53-69.
- [12] McNew, J. A., Parlati, F., Fukuda, R., Johnston, R. J., Paz, K., Paumet, F., Sollner, T. H., and Rothman, J. E. "Compartmental specificity of cellular membrane fusion encoded in SNARE proteins." *Nature* (2000), **407**, 153-159.
- [13] Sollner, T., Bennett, M. K., Whiteheart, S. W., Scheller, R. H., and Rothman, J. E. "A Protein Assembly-Disassembly Pathway in vitro That May Correspond to Sequential Steps of Synaptic Vesicle Docking, Activation, and Fusion." *Cell* (1993), **75**, 409-418.
- [14] Yang, B., Gonzalez, L., Prekeris, R., Steegmaier, M., Advani, R. J., and Scheller, R. H. "SNARE interactions are not selective - Implications for membrane fusion specificity." *J. Biol. Chem.* (1999), **274**, 5649-5653.
- [15] Grote, E., and Novick, P. J. "Promiscuity in Rab-SNARE interactions." *Mol. Biol. Cell* (1999), **10**, 4149-4161.
- [16] Tsui, M. M. K., and Banfield, D. K. "Yeast Golgi SNARE interactions are promiscuous." *J. Cell Sci.* (2000), **113**, 145-152.

- [17] Fasshauer, D., Antonin, W., Margittai, M., Pabst, S., and Jahn, R. "Mixed and non-cognate SNARE complexes - Characterization of assembly and biophysical properties." *J. Biol. Chem.* (1999), **274**, 15440-15446.
- [18] Pereira-Leal, J. B., and Seabra, M. C. "Evolution of the Rab family of small GTP-binding proteins." *J. Mol. Biol.* (2001), **313**, 889-901.
- [19] Bock, J. B., Matern, H. T., Peden, A. A., and Scheller, R. H. "A genomic perspective on membrane compartment organization." *Nature* (2001), **409**, 839-841.
- [20] Segev, N. "Ypt and Rab GTPases: insight into functions through novel interactions." *Curr. Opin. Cell Biol.* (2001), **13**, 500-511.
- [21] Christoforidis, S., McBride, H. M., Burgoyne, R. D., and Zerial, M. "The Rab5 effector EEA1 is a core component of endosome docking." *Nature* (1999), **397**, 621-625.
- [22] Smythe, E. "Direct interactions between rab GTPases and cargo." *Mol. Cell* (2002), **9**, 205-206.
- [23] Carroll, K. S., Hanna, J., Simon, I., Krise, J., Barbero, P., and Pfeffer, S. R. "Role of Rab9 GTPase in facilitating receptor recruitment by TIP47." *Science* (2001), **292**, 1373-1376.
- [24] McLauchlan, H., Newell, J., Morrice, N., Osborne, A., West, M., and Smythe, E. "A novel role for Rab5-GDI in ligand sequestration into calthrin-coated pits." *Curr. Biol.* (1998), **8**, 34-45.
- [25] Allan, B. B., Moyer, B. D., and Balch, W. E. "Rab1 recruitment of p115 into a cis-SNARE complex: Programming budding COPII vesicles for fusion." *Science* (2000), **289**, 444-448.
- [26] Hammer, J. A., and Wu, X. F. S. "Rabs grab motors: defining the connections between Rab GTPases and motor proteins." *Curr. Opin. Cell Biol.* (2002), **14**, 69-75.
- [27] Murray, J. W., and Wolkoff, A. W. "Roles of the cytoskeleton and motor proteins in endocytic sorting." *Adv. Drug Deliv. Rev.* (2003), **55**, 1385-1403.
- [28] Echard, A., Jollivet, F., Martinez, O., Lacapere, J. J., Rousselet, A., Janoueix-Lerosey, I., and Goud, B. "Interaction of a Golgi-associated kinesin-like protein with Rab6." *Science* (1998), **279**, 580-585.
- [29] Hill, E., Clarke, N., and Barr, F. A. "The Rab6-binding kinesin, Rab6-KIFL, is required for cytokinesis." *Embo J.* (2000), **19**, 5711-5719.
- [30] Fukuda, M., Kuroda, T. S., and Mikoshiba, K. "Slac2-a/melanophilin, the missing link between Rab27 and myosin Va - Implications of a tripartite protein complex for melanosome transport." *J. Biol. Chem.* (2002), **277**, 12432-12436.
- [31] Hume, A. N., Collinson, L. M., Rapak, A., Gomes, A. Q., Hopkins, C. R., and Seabra, M. C. "Rab27a regulates the peripheral distribution of melanosomes in melanocytes." *J. Cell Biol.* (2001), **152**, 795-808.
- [32] Bahadoran, P., Aberdam, E., Mantoux, F., Busca, R., Bille, K., Yalman, N., de Saint-Basile, G., Casaroli-Marano, R., Ortonne, J. P., and Ballotti, R. "Rab27a: A key to melanosome transport in human melanocytes." *J. Cell Biol.* (2001), **152**, 843-849.
- [33] Menasche, G., Pastural, E., Feldmann, J., Certain, S., Ersoy, F., Dupuis, S., Wulffraat, N., Bianchi, D., Fischer, A., Le Deist, F., and de Saint Basile, G. "Mutations in RAB27A cause Griscelli syndrome associated with haemophagocytic syndrome." *Nature Genet.* (2000), **25**, 173-176.

- [34] Pastural, E., Barrat, F. J., DufourcqLagelouse, R., Certain, S., Sanal, O., Jabado, N., Seger, R., Griscelli, C., Fischer, A., and DesaintBasile, G. "Griscelli disease maps to chromosome 15q21 and is associated with mutations in the myosin-Va gene." *Nature Genet.* (1997), **16**, 289-292.
- [35] Stein, M. P., Dong, J. B., and Wandinger-Ness, A. "Rab proteins and endocytic trafficking: potential targets for therapeutic intervention." *Adv. Drug Deliv. Rev.* (2003), **55**, 1421-1437.
- [36] Cao, X. C., Ballew, N., and Barlowe, C. "Initial docking of ER-derived vesicles requires Uso1p and Ypt1p but is independent of SNARE proteins." *Embo J.* (1998), **17**, 2156-2165.
- [37] Ungermann, C., Sato, K., and Wickner, W. "Defining the functions of trans-SNARE pairs." *Nature* (1998), **396**, 543-548.
- [38] Deneka, M., Neeft, M., and van der Sluijs, P. "Regulation of membrane transport by rab GTPases." *Crit. Rev. Biochem. Mol. Biol.* (2003), **38**, 121-142.
- [39] Whyte, J. R. C., and Munro, S. "Vesicle tethering complexes in membrane traffic." *J. Cell Sci.* (2002), **115**, 2627-2637.
- [40] Guo, W., Roth, D., Walch-Solimena, C., and Novick, P. "The exocyst is an effector for Sec4p, targeting secretory vesicles to sites of exocytosis." *Embo J.* (1999), **18**, 1071-1080.
- [41] Sacher, M., Jiang, Y., Barrowman, J., Scarpa, A., Burston, J., Zhang, L., Schieltz, D., Yates, J. R., Abeliovich, H., and Ferro-Novick, S. "TRAPP, a highly conserved novel complex on the cis-Golgi that mediates vesicle docking and fusion." *Embo J.* (1998), **17**, 2494-2503.
- [42] McBride, H. M., Rybin, V., Murphy, C., Giner, A., Teasdale, R., and Zerial, M. "Oligomeric complexes link Rab5 effectors with NSF and drive membrane fusion via interactions between EEA1 and syntaxin 13." *Cell* (1999), **98**, 377-386.
- [43] Seals, D. F., Eitzen, G., Margolis, N., Wickner, W. T., and Price, A. "A Ypt/Rab effector complex containing the Sec1 homolog Vps33p is required for homotypic vacuole fusion." *Proc. Natl. Acad. Sci. U. S. A.* (2000), **97**, 9402-9407.
- [44] Sato, T. K., Rehling, P., Peterson, M. R., and Emr, S. D. "Class C Vps protein complex regulates vacuolar SNARE pairing and is required for vesicle docking/fusion." *Mol. Cell* (2000), **6**, 661-671.
- [45] Siniosoglou, S., and Pelham, H. R. B. "An effector of Ypt6p binds the SNARE Tlg1p and mediates selective fusion of vesicles with late Golgi membranes." *Embo J.* (2001), **20**, 5991-5998.
- [46] Conibear, E., Cleck, J. N., and Stevens, T. H. "Vps51p mediates the association of the GARP (Vps52/53/54) complex with the late Golgi t-SNARE Tlg1p." *Mol. Biol. Cell* (2003), **14**, 1610-1623.
- [47] Zerial, M., and McBride, H. "Rab proteins as membrane organizers." *Nat. Rev. Mol. Cell Biol.* (2001), **2**, 107-117.
- [48] Stenmark, H., Parton, R. G., Steelemortimer, O., Lutcke, A., Gruenberg, J., and Zerial, M. "Inhibition of Rab5 GTPase Activity Stimulates Membrane-Fusion in Endocytosis." *Embo J.* (1994), **13**, 1287-1296.
- [49] Rybin, V., Ullrich, O., Rubino, M., Alexandrov, K., Simon, I., Seabra, M. C., Goody, R., and Zerial, M. "GTPase activity of Rab5 acts as a timer for endocytic membrane fusion." *Nature* (1996), **383**, 266-269.
- [50] Richardson, C. J., Jones, S., Litt, R. J., and Segev, N. "GTP hydrolysis is not important for Ypt1 GTPase function in vesicular transport." *Mol. Cell. Biol.* (1998), **18**, 827-838.

- [51] Horiuchi, H., Lippe, R., McBride, H. M., Rubino, M., Woodman, P., Stenmark, H., Rybin, V., Wilm, M., Ashman, K., Mann, M., and Zerial, M. "A novel Rab5 GDP/GTP exchange factor complexed to Rabaptin-5 links nucleotide exchange to effector recruitment and function." *Cell* (1997), **90**, 1149-1159.
- [52] Kishida, S., Shirataki, H., Sasaki, T., Kato, M., Kaibuchi, K., and Takai, Y. "Rab3a GTPase-Activating Protein-Inhibiting Activity of Rabphilin-3a, a Putative Rab3a Target Protein." *J. Biol. Chem.* (1993), **268**, 22259-22261.
- [53] Bernards, A. "GAPs galore! A survey of putative Ras superfamily GTPase activating proteins in man and Drosophila." *Biochim. Biophys. Acta-Rev. Cancer* (2003), **1603**, 47-82.
- [54] Burstein, E. S., and Macara, I. G. "Characterization of a Guanine Nucleotide-Releasing Factor and a GTPase-Activating Protein That Are Specific for the Ras-Related Protein P25rab3a." *Proc. Natl. Acad. Sci. U. S. A.* (1992), **89**, 1154-1158.
- [55] Strom, M., Vollmer, P., Tan, T. J., and Gallwitz, D. "A Yeast Gtpase-Activating Protein That Interacts Specifically with a Member of the Ypt/Rab Family." *Nature* (1993), **361**, 736-739.
- [56] Sasaki, T., Kikuchi, A., Araki, S., Hata, Y., Isomura, M., Kuroda, S., and Takai, Y. "Purification and Characterization from Bovine Brain Cytosol of a Protein That Inhibits the Dissociation of GDP from and the Subsequent Binding of GTP to Smg-P25a, a Ras P21-Like GTP-Binding Protein." *J. Biol. Chem.* (1990), **265**, 2333-2337.
- [57] Araki, S., Kikuchi, A., Hata, Y., Isomura, M., and Takai, Y. "Regulation of Reversible Binding of Smg P25a, a Ras P21-Like GTP-Binding Protein, to Synaptic Plasma-Membranes and Vesicles by Its Specific Regulatory Protein, GDP Dissociation Inhibitor." *J. Biol. Chem.* (1990), **265**, 13007-13015.
- [58] Luan, P., Balch, M. E., Emr, S. D., and Burd, C. G. "Molecular dissection of guanine nucleotide dissociation inhibitor function in vivo - Rab-independent binding to membranes and role of Rab recycling factors." *J. Biol. Chem.* (1999), **274**, 14806-14817.
- [59] Sakisaka, T., Meerlo, T., Matteson, J., Plutner, H., and Balch, W. E. "Rab-alpha GDI activity is regulated by a Hsp90 chaperone complex." *Embo J.* (2002), **21**, 6125-6135.
- [60] Soldati, T., Shapiro, A. D., Svejstrup, A. B. D., and Pfeffer, S. R. "Membrane Targeting of the Small GTPase Rab9 Is Accompanied by Nucleotide Exchange." *Nature* (1994), **369**, 76-78.
- [61] Ullrich, O., Horiuchi, H., Bucci, C., and Zerial, M. "Membrane Association of Rab5 Mediated by GDP-Dissociation Inhibitor and Accompanied by GDP/GTP Exchange." *Nature* (1994), **368**, 157-160.
- [62] DiracSvejstrup, A. B., Sumizawa, T., and Pfeffer, S. R. "Identification of a GDI displacement factor that releases endosomal Rab GTPases from Rab-GDI." *Embo J.* (1997), **16**, 465-472.
- [63] Sivars, U., Aivazian, D., and Pfeffer, S. R. "Yip3 catalyses the dissociation of endosomal Rab-GDI complexes." *Nature* (2003), **425**, 856-859.
- [64] Martincic, I., Peralta, M. E., and Ngsee, J. K. "Isolation and characterization of a dual prenylated Rab and VAMP2 receptor." *J. Biol. Chem.* (1997), **272**, 26991-26998.
- [65] Calero, M., and Collins, R. N. "Saccharomyces cerevisiae Pra1p/Yip3p interacts with yip1p and Rab proteins." *Biochem. Biophys. Res. Commun.* (2002), **290**, 676-681.
- [66] Matern, H., Yang, X. P., Andrulis, E., Sternglanz, R., Trepte, H. H., and Gallwitz, D. "A novel Golgi membrane protein is part of a GTPase-binding protein complex involved in vesicle targeting." *Embo J.* (2000), **19**, 4485-4492.
- [67] Yang, X. P., Matern, H. T., and Gallwitz, D. "Specific binding to a novel and essential Golgi membrane protein (Yip1p) functionally links the transport GTPases Ypt1p and Ypt31p." *Embo J.* (1998), **17**, 4954-4963.

- [68] Tang, B. L., Ong, Y. S., Huang, B., Wei, S., Wong, E. T., Qi, R., Horstmann, H., and Hong, W. "A membrane protein enriched in endoplasmic reticulum exit sites interacts with COPII." *J. Biol. Chem.* (2001), **276**, 40008-40017.
- [69] Barrowman, J., and Novick, P. "Three Yips for Rab recruitment." *Nat. Cell Biol.* (2003), **5**, 955-956.
- [70] Jones, S., Newman, C., Liu, F. L., and Segev, N. "The TRAPP complex is a nucleotide exchanger for Ypt1 and Ypt31/32." *Mol. Biol. Cell* (2000), **11**, 4403-4411.
- [71] Wurmser, A. E., Sato, T. K., and Emr, S. D. "New component of the vacuolar class C-Vps complex couples nucleotide exchange on the Ypt7 GTPase to SNARE-dependent docking and fusion." *J. Cell Biol.* (2000), **151**, 551-562.
- [72] Valencia, A., Chardin, P., Wittinghofer, A., and Sander, C. "The Ras Protein Family - Evolutionary Tree and Role of Conserved Amino-Acids." *Biochemistry* (1991), **30**, 4637-4648.
- [73] Dumas, J. J., Zhu, Z. Y., Connolly, J. L., and Lambright, D. G. "Structural basis of activation and GTP hydrolysis in Rab proteins." *Struct. Fold. Des.* (1999), **7**, 413-423.
- [74] Sprang, S. R. "G protein mechanisms: Insights from structural analysis." *Annu. Rev. Biochem.* (1997), **66**, 639-678.
- [75] Schlichting, I., Almo, S. C., Rapp, G., Wilson, K., Petratos, K., Lentfer, A., Wittinghofer, A., Kabsch, W., Pai, E. F., Petsko, G. A., and Goody, R. S. "Time-Resolved X-Ray Crystallographic Study of the Conformational Change in Ha-Ras P21 Protein on Gtp Hydrolysis." *Nature* (1990), **345**, 309-315.
- [76] Milburn, M. V., Tong, L., Devos, A. M., Brunger, A., Yamaizumi, Z., Nishimura, S., and Kim, S. H. "Molecular Switch for Signal Transduction - Structural Differences between Active and Inactive Forms of Protooncogenic Ras Proteins." *Science* (1990), **247**, 939-945.
- [77] Stroupe, C., and Brunger, A. T. "Crystal structures of a Rab protein in its inactive and active conformations." *J. Mol. Biol.* (2000), **304**, 585-598.
- [78] Constantinescu, A. T., Rak, A., Alexandrov, K., Esters, H., Goody, R. S., and Scheldig, A. J. "Rab-subfamily-specific regions of Ypt7p are structurally different from other RabGTPases." *Structure* (2002), **10**, 569-579.
- [79] Pasqualato, S., Senic-Matuglia, F., Renault, L., Goud, B., Salamero, J., and Cherfils, J. "The structural GDP/GTP cycle of Rab11 reveals a novel interface involved in the dynamics of recycling endosomes." *J. Biol. Chem.* (2004), **279**, 11480-11488.
- [80] Brennwald, P., and Novick, P. "Interactions of 3 Domains Distinguishing the Ras-Related GTP-Binding Proteins Ypt1 and Sec4." *Nature* (1993), **362**, 560-563.
- [81] Dunn, B., Stearns, T., and Botstein, D. "Specificity Domains Distinguish the Ras-Related GTPases Ypt1 and Sec4." *Nature* (1993), **362**, 563-565.
- [82] Pereira-Leal, J. B., and Seabra, M. C. "The mammalian Rab family of small GTPases: Definition of family and subfamily sequence motifs suggests a mechanism for functional specificity in the Ras superfamily." *J. Mol. Biol.* (2000), **301**, 1077-1087.
- [83] Pereira-Leal, J. B., Strom, M., Godfrey, R. F., and Seabra, M. C. "Structural determinants of Rab and Rab Escort Protein interaction: Rab family motifs define a conserved binding surface." *Biochem. Biophys. Res. Commun.* (2003), **301**, 92-97.
- [84] Ostermeier, C., and Brunger, A. T. "Structural basis of Rab effector specificity: Crystal structure of the small G protein Rab3A complexed with the effector domain of Rabphilin-3A." *Cell* (1999), **96**, 363-374.

- [85] Merithew, E., Hatherly, S., Dumas, J. J., Lawe, D. C., Heller-Harrison, R., and Lambright, D. G. "Structural plasticity of an invariant hydrophobic triad in the switch regions of Rab GTPases is a determinant of effector recognition." *J. Biol. Chem.* (2001), **276**, 13982-13988.
- [86] Chattopadhyay, D., Langsley, G., Carson, M., Recacha, R., DeLucas, L., and Smith, C. "Structure of the nucleotide-binding domain of Plasmodium falciparum Rab6 in the GDP-bound form." *Acta Crystallogr. Sect. D-Biol. Crystallogr.* (2000), **56**, 937-944.
- [87] Esters, H., Alexandrov, K., Constantinescu, A. T., Goody, R. S., and Scheidig, A. J. "High-resolution crystal structure of *S. cerevisiae* Ypt51(Delta C15)-GppNHp, a small GTP-binding protein involved in regulation of endocytosis." *J. Mol. Biol.* (2000), **298**, 111-121.
- [88] Terzyan, S., Zhu, G. Y., Li, G. P., and Zhang, X. J. C. "Refinement of the structure of human Rab5a GTPase domain at 1.05 angstrom resolution." *Acta Crystallogr. Sect. D-Biol. Crystallogr.* (2004), **60**, 54-60.
- [89] Chavrier, P., Gorvel, J. P., Stelzer, E., Simons, K., Gruenberg, J., and Zerial, M. "Hypervariable C-Terminal Domain of Rab Proteins Acts as a Targeting Signal." *Nature* (1991), **353**, 769-772.
- [90] Stenmark, H., Valencia, A., Martinez, O., Ullrich, O., Goud, B., and Zerial, M. "Distinct Structural Elements of Rab5 Define Its Functional Specificity." *Embo J.* (1994), **13**, 575-583.
- [91] Vandersluijs, P., Hull, M., Huber, L. A., Male, P., Goud, B., and Mellman, I. "Reversible Phosphorylation Dephosphorylation Determines the Localization of Rab4 During the Cell-Cycle." *Embo J.* (1992), **11**, 4379-4389.
- [92] Ayad, N., Hull, M., and Mellman, I. "Mitotic phosphorylation of rab4 prevents binding to a specific receptor on endosome membranes." *Embo J.* (1997), **16**, 4497-4507.
- [93] Kinsella, B. T., and Maltese, W. A. "Rab Gtp-Binding Proteins Implicated in Vesicular Transport Are Isoprenylated In vitro at Cysteines within a Novel Carboxyl-Terminal Motif." *J. Biol. Chem.* (1991), **266**, 8540-8544.
- [94] Newman, C. M. H., Giannakouros, T., Hancock, J. F., Fawell, E. H., Armstrong, J., and Magee, A. I. "Posttranslational Processing of Schizosaccharomyces-Pombe Ypt Proteins." *J. Biol. Chem.* (1992), **267**, 11329-11336.
- [95] Moores, S. L., Schaber, M. D., Mosser, S. D., Rands, E., Ohara, M. B., Garsky, V. M., Marshall, M. S., Pompliano, D. L., and Gibbs, J. B. "Sequence Dependence of Protein Isoprenylation." *J. Biol. Chem.* (1991), **266**, 14603-14610.
- [96] Casey, P. J., and Seabra, M. C. "Protein prenyltransferases." *J. Biol. Chem.* (1996), **271**, 5289-5292.
- [97] Caplin, B. E., Hettich, L. A., and Marshall, M. S. "Substrate Characterization of the Saccharomyces-Cerevisiae Protein Farnesyltransferase and Type-I Protein Geranylgeranyltransferase." *Biochim. Biophys. Acta-Protein Struct. Molec. Enzym.* (1994), **1205**, 39-48.
- [98] Roskoski, R., and Ritchie, P. "Role of the carboxyterminal residue in peptide binding to protein farnesyltransferase and protein geranylgeranyltransferase." *Arch. Biochem. Biophys.* (1998), **356**, 167-176.
- [99] Khosravifar, R., Lutz, R. J., Cox, A. D., Conroy, L., Bourne, J. R., Sinensky, M., Balch, W. E., Buss, J. E., and Der, C. J. "Isoprenoid Modification of Rab Proteins Terminating in CC or CXC Motifs." *Proc. Natl. Acad. Sci. U. S. A.* (1991), **88**, 6264-6268.
- [100] Kinsella, B. T., and Maltese, W. A. "Rab Gtp-Binding Proteins with 3 Different Carboxyl-Terminal Cysteine Motifs Are Modified In vivo by 20-Carbon Isoprenoids." *J. Biol. Chem.* (1992), **267**, 3940-3945.

- [101] Farnsworth, C. C., Seabra, M. C., Ericsson, L. H., Gelb, M. H., and Glomset, J. A. "Rab Geranylgeranyl Transferase Catalyzes the Geranylgeranylation of Adjacent Cysteines in the Small GTPases Rab1a, Rab3a, and Rab5a." *Proc. Natl. Acad. Sci. U. S. A.* (1994), **91**, 11963-11967.
- [102] Farnsworth, C. C., Kawata, M., Yoshida, Y., Takai, Y., Gelb, M. H., and Glomset, J. A. "C Terminus of the Small GTP-Binding Protein Smg P25a Contains 2 Geranylgeranylated Cysteine Residues and a Methyl-Ester." *Proc. Natl. Acad. Sci. U. S. A.* (1991), **88**, 6196-6200.
- [103] Smeland, T. E., Seabra, M. C., Goldstein, J. L., and Brown, M. S. "Geranylgeranylated Rab Proteins Terminating in Cys-Ala-Cys, but Not Cys-Cys, Are Carboxyl-Methylated by Bovine Brain Membranes in-Vitro." *Proc. Natl. Acad. Sci. U. S. A.* (1994), **91**, 10712-10716.
- [104] Giner, J. L., and Rando, R. R. "Novel Methyltransferase Activity Modifying the Carboxy-Terminal Bis(Geranylgeranyl)-Cys-Ala-Cys Structure of Small Gtp-Binding Proteins." *Biochemistry* (1994), **33**, 15116-15123.
- [105] Pylypenko, O., Rak, A., Reents, R., Niculae, A., Sidorovitch, V., Vioaca, M. D., Bessolitsyna, E., Thoma, N. H., Waldmann, H., Schlichting, I., Goody, R. S., and Alexandrov, K. "Structure of rab escort protein-1 in complex with Rab geranylgeranyltransferase." *Mol. Cell* (2003), **11**, 483-494.
- [106] Thoma, N. H., Iakovenko, A., Goody, R. S., and Alexandrov, K. "Phosphoisoprenoids modulate association of Rab geranylgeranyltransferase with REP-1." *J. Biol. Chem.* (2001), **276**, 48637-48643.
- [107] Seabra, M. C., Goldstein, J. L., Sudhof, T. C., and Brown, M. S. "Rab Geranylgeranyl Transferase - a Multisubunit Enzyme That Prenylates GTP-Binding Proteins Terminating in Cys-X-Cys or Cys-Cys." *J. Biol. Chem.* (1992), **267**, 14497-14503.
- [108] Zhang, H., Seabra, M. C., and Deisenhofer, J. "Crystal structure of Rab geranylgeranyltransferase at 2.0 angstrom resolution." *Struct. Fold. Des.* (2000), **8**, 241-251.
- [109] Seabra, M. C., Brown, M. S., Slaughter, C. A., Sudhof, T. C., and Goldstein, J. L. "Purification of Component-a of Rab Geranylgeranyl Transferase - Possible Identity with the Choroideremia Gene-Product." *Cell* (1992), **70**, 1049-1057.
- [110] Andres, D. A., Seabra, M. C., Brown, M. S., Armstrong, S. A., Smeland, T. E., Cremers, F. P. M., and Goldstein, J. L. "cDNA Cloning of Component-a of Rab Geranylgeranyl Transferase and Demonstration of Its Role as a Rab Escort Protein." *Cell* (1993), **73**, 1091-1099.
- [111] Sanford, J. C., Pan, Y., and Wessling-Resnick, M. "Prenylation of Rab5 Is Dependent on Guanine-Nucleotide-Binding." *J. Biol. Chem.* (1993), **268**, 23773-23776.
- [112] Seabra, M. C. "Nucleotide dependence of Rab geranylgeranylation - Rab escort protein interacts preferentially with GDP-bound Rab." *J. Biol. Chem.* (1996), **271**, 14398-14404.
- [113] Alexandrov, K., Simon, I., Iakovenko, A., Holz, B., Goody, R. S., and Scheidig, A. J. "Moderate discrimination of REP-1 between Rab7-GDP and Rab7-GTP arises from a difference of an order of magnitude in dissociation rates." *FEBS Lett.* (1998), **425**, 460-464.
- [114] Alexandrov, K., Simon, I., Yurchenko, V., Iakovenko, A., Rostkova, E., Scheidig, A. J., and Goody, R. S. "Characterization of the ternary complex between Rab7, REP-1 and Rab geranylgeranyl transferase." *Eur. J. Biochem.* (1999), **265**, 160-170.
- [115] Anant, J. S., Desnoyers, L., Machius, M., Demeler, B., Hansen, J. C., Westover, K. D., Deisenhofer, J., and Seabra, M. C. "Mechanism of Rab geranylgeranylation: Formation of the catalytic ternary complex." *Biochemistry* (1998), **37**, 12559-12568.
- [116] Thoma, N. H., Niculae, A., Goody, R. S., and Alexandrov, K. "Double prenylation by RabGGTase can proceed without dissociation of the mono-prenylated intermediate." *J. Biol. Chem.* (2001), **276**, 48631-48636.

- [117] Shen, F., and Seabra, M. C. "Mechanism of digeranylgeranylation of rab proteins - Formation of a complex between monogeranylgeranyl-rab and rab escort protein." *J. Biol. Chem.* (1996), **271**, 3692-3698.
- [118] Thoma, N. H., Iakovenko, A., Kalinin, A., Waldmann, H., Goody, R. S., and Alexandrov, K. "Allosteric regulation of substrate binding and product release in geranylgeranyltransferase type II." *Biochemistry* (2001), **40**, 268-274.
- [119] Alexandrov, K., Horiuchi, H., Steelemortimer, O., Seabra, M. C., and Zerial, M. "Rab Escort Protein-1 Is a Multifunctional Protein That Accompanies Newly Prenylated Rab Proteins to Their Target Membranes." *Embo J.* (1994), **13**, 5262-5273.
- [120] Cremers, F. P. M., Armstrong, S. A., Seabra, M. C., Brown, M. S., and Goldstein, J. L. "Rep-2, a Rab Escort Protein Encoded by the Choroideremia-Like Gene." *J. Biol. Chem.* (1994), **269**, 2111-2117.
- [121] Fujimura, K., Tanaka, K., Nakano, A., and Tohe, A. "The *Saccharomyces-Cerevisiae* Msi4 Gene Encodes the Yeast Counterpart of Component- $\alpha$  of Rab Geranylgeranyltransferase." *J. Biol. Chem.* (1994), **269**, 9205-9212.
- [122] Seabra, M. C., Brown, M. S., and Goldstein, J. L. "Retinal Degeneration in Choroideremia - Deficiency of Rab Geranylgeranyl Transferase." *Science* (1993), **259**, 377-381.
- [123] Seabra, M. C., Ho, Y. K., and Anant, J. S. "Deficient Geranylgeranylation of Ram/Rab27 in Choroideremia." *J. Biol. Chem.* (1995), **270**, 24420-24427.
- [124] Pereira-Leal, J. B., Hume, A. N., and Seabra, M. C. "Prenylation of Rab GTPases: molecular mechanisms and involvement in genetic disease." *FEBS Lett.* (2001), **498**, 197-200.
- [125] Wu, S. K., Zeng, K., Wilson, I. A., and Balch, W. E. "Structural insights into the function of the Rab GDI superfamily." *Trends Biochem.Sci.* (1996), **21**, 472-476.
- [126] Araki, S., Kaibuchi, K., Sasaki, T., Hata, Y., and Takai, Y. "Role of the C-Terminal Region of Smg P25a in Its Interaction with Membranes and the GDP/GTP Exchange Protein." *Mol. Cell. Biol.* (1991), **11**, 1438-1447.
- [127] Garrett, M. D., Zahner, J. E., Cheney, C. M., and Novick, P. J. "GDI1 Encodes a GDP Dissociation Inhibitor That Plays an Essential Role in the Yeast Secretory Pathway." *Embo J.* (1994), **13**, 1718-1728.
- [128] Calero, M., Winand, N. J., and Collins, R. N. "Identification of the novel proteins Yip4p and Yip5p as Rab GTPase interacting factors." *FEBS Lett.* (2002), **515**, 89-98.
- [129] Figueroa, C., Taylor, J., and Vojtek, A. B. "Prenylated Rab acceptor protein is a receptor for prenylated small GTPases." *J. Biol. Chem.* (2001), **276**, 28219-28225.
- [130] Fukui, K., Sasaki, T., Imazumi, K., Matsuura, Y., Nakanishi, H., and Takai, Y. "Isolation and characterization of a GTPase activating protein specific for the Rab3 subfamily of small G proteins." *J. Biol. Chem.* (1997), **272**, 4655-4658.
- [131] Wada, M., Nakanishi, H., Satoh, A., Hirano, H., Obaishi, H., Matsuura, Y., and Takai, Y. "Isolation and characterization of a GDP/GTP exchange protein specific for the Rab3 subfamily Small G proteins." *J. Biol. Chem.* (1997), **272**, 3875-3878.
- [132] Gomes, A. Q., Ali, B. R., Ramalho, J. S., Godfrey, R. F., Barral, D. C., Hume, A. N., and Seabra, M. C. "Membrane targeting of Rab GTPases is influenced by the prenylation motif." *Mol. Biol. Cell* (2003), **14**, 1882-1899.
- [133] Calero, M., Chen, C. Z., Zhu, W. Y., Winand, N., Havas, K. A., Gilbert, P. M., Burd, C. G., and Collins, R. N. "Dual prenylation is required for Rab protein localization and function." *Mol. Biol. Cell* (2003), **14**, 1852-1867.

- [134] Overmeyer, J. H., Wilson, A. L., and Maltese, W. A. "Membrane targeting of a Rab GTPase that fails to associate with Rab escort protein (REP) or guanine nucleotide dissociation inhibitor (GDI)." *J. Biol. Chem.* (2001), **276**, 20379-20386.
- [135] Ossig, R., Laufer, W., Schmitt, H. D., and Gallwitz, D. "Functionality and Specific Membrane Localization of Transport Gtpases Carrying C-Terminal Membrane Anchors of Synaptobrevin-Like Proteins." *Embo J.* (1995), **14**, 3645-3653.
- [136] Merrifield, R. B. "Solid Phase Peptide Synthesis. 1. Synthesis of a Tetrapeptide." *J. Am. Chem. Soc.* (1963), **85**, 2149-2154.
- [137] Gutte, B., and Merrifield, R. B. "Synthesis of Ribonuclease-A." *J. Biol. Chem.* (1971), **246**, 1922-1944.
- [138] Tam, J. P., Sheikh, M. A., Solomon, D. S., and Ossowski, L. "Efficient Synthesis of Human Type Alpha-Transforming Growth-Factor - Its Physical and Biological Characterization." *Proc. Natl. Acad. Sci. U. S. A.* (1986), **83**, 8082-8086.
- [139] Schneider, J., and Kent, S. B. H. "Enzymatic-Activity of a Synthetic-99 Residue Protein Corresponding to the Putative HIV-1 Protease." *Cell* (1988), **54**, 363-368.
- [140] Wlodawer, A., Miller, M., Jaskolski, M., Sathyanarayana, B. K., Baldwin, E., Weber, I. T., Selk, L. M., Clawson, L., Schneider, J., and Kent, S. B. H. "Conserved Folding in Retroviral Proteases - Crystal-Structure of a Synthetic HIV-1 Protease." *Science* (1989), **245**, 616-621.
- [141] Miller, M., Schneider, J., Sathyanarayana, B. K., Toth, M. V., Marshall, G. R., Clawson, L., Selk, L., Kent, S. B. H., and Wlodawer, A. "Structure of Complex of Synthetic HIV-1 Protease with a Substrate-Based Inhibitor at 2.3-Å Resolution." *Science* (1989), **246**, 1149-1152.
- [142] Schnolzer, M., and Kent, S. B. H. "Constructing Proteins by Dovetailing Unprotected Synthetic Peptides - Backbone-Engineered HIV Protease." *Science* (1992), **256**, 221-225.
- [143] Smith, R., Brereton, I. M., Chai, R. Y., and Kent, S. B. H. "Ionization states of the catalytic residues in HIV-1 protease." *Nat. Struct. Biol.* (1996), **3**, 946-950.
- [144] Nishiuchi, Y., Inui, T., Nishio, H., Bodi, J., Kimura, T., Tsuji, F. I., and Sakakibara, S. "Chemical synthesis of the precursor molecule of the Aequorea green fluorescent protein, subsequent folding, and development of fluorescence." *Proc. Natl. Acad. Sci. U. S. A.* (1998), **95**, 13549-13554.
- [145] Kemp, D. S., Leung, S. L., and Kerkman, D. J. "Models That Demonstrate Peptide-Bond Formation by Prior Thiol Capture. 1. Capture by Disulfide Formation." *Tetrahedron Lett.* (1981), **22**, 181-184.
- [146] Kemp, D. S., and Carey, R. I. "Synthesis of a 39-Peptide and a 25-Peptide by Thiol Capture Ligations - Observation of a 40-Fold Rate Acceleration of the Intramolecular O,N-Acyl-Transfer Reaction between Peptide-Fragments Bearing Only Cysteine Protective Groups." *J. Org. Chem.* (1993), **58**, 2216-2222.
- [147] Liu, C. F., and Tam, J. P. "Peptide Segment Ligation Strategy without Use of Protecting Groups." *Proc. Natl. Acad. Sci. U. S. A.* (1994), **91**, 6584-6588.
- [148] Tam, J. P., Lu, Y. A., Liu, C. F., and Shao, J. "Peptide synthesis using unprotected peptides through orthogonal coupling methods." *Proc. Natl. Acad. Sci. U. S. A.* (1995), **92**, 12485-12489.
- [149] Dawson, P. E., Muir, T. W., Clarklewis, I., and Kent, S. B. H. "Synthesis of Proteins by Native Chemical Ligation." *Science* (1994), **266**, 776-779.
- [150] Saxon, E., Armstrong, J. I., and Bertozzi, C. R. "A "traceless" Staudinger ligation for the chemoselective synthesis of amide bonds." *Org. Lett.* (2000), **2**, 2141-2143.

- [151] Nilsson, B. L., Kiessling, L. L., and Raines, R. T. "Staudinger ligation: A peptide from a thioester and azide." *Org. Lett.* (2000), **2**, 1939-1941.
- [152] Wieland, T., Bokelmann, E., Bauer, L., Lang, H. U., and Lau, H. "Über Peptidsynthesen. 8. Bildung Von S-Haltigen Peptiden Durch Intramolekulare Wanderung Von Aminoacylresten." *Annalen Der Chemie-Justus Liebig* (1953), **583**, 129-149.
- [153] Offer, J., Boddy, C. N. C., and Dawson, P. E. "Extending synthetic access to proteins with a removable acyl transfer auxiliary." *J. Am. Chem. Soc.* (2002), **124**, 4642-4646.
- [154] Offer, J., and Dawson, P. E. "N-alpha-2-mercaptobenzylamine-assisted chemical ligation." *Org. Lett.* (2000), **2**, 23-26.
- [155] Kawakami, T., and Aimoto, S. "A photoremovable ligation auxiliary for use in polypeptide synthesis." *Tetrahedron Lett.* (2003), **44**, 6059-6061.
- [156] Canne, L. E., Bark, S. J., and Kent, S. B. H. "Extending the applicability of native chemical ligation." *J. Am. Chem. Soc.* (1996), **118**, 5891-5896.
- [157] Dawson, P. E., and Kent, S. B. H. "Synthesis of native proteins by chemical ligation." *Annu. Rev. Biochem.* (2000), **69**, 923-960.
- [158] Kane, P. M., Yamashiro, C. T., Wolczyk, D. F., Neff, N., Goebel, M., and Stevens, T. H. "Protein Splicing Converts the Yeast Tfp1 Gene-Product to the 69-Kd Subunit of the Vacuolar H<sup>+</sup>-Adenosine Triphosphatase." *Science* (1990), **250**, 651-657.
- [159] Hirata, R., Nakano, A., Kawasaki, H., Suzuki, K., and Anraku, Y. "Molecular-Structure of a Gene, VMA1, Encoding the Catalytic Subunit of H<sup>+</sup>-Translocating Adenosine-Triphosphatase from Vacuolar Membranes of *Saccharomyces-Cerevisiae*." *J. Biol. Chem.* (1990), **265**, 6726-6733.
- [160] Perler, F. B. "InBase, the New England Biolabs Intein Database." *Nucleic Acids Res.* (1999), **27**, 346-347.
- [161] Evans, T. C., and Xu, M. Q. "Mechanistic and kinetic considerations of protein splicing." *Chem. Rev.* (2002), **102**, 4869-4883.
- [162] Gimble, F. S., and Thorner, J. "Homing of a DNA Endonuclease Gene by Meiotic Gene Conversion in *Saccharomyces-Cerevisiae*." *Nature* (1992), **357**, 301-306.
- [163] Telenti, A., Southworth, M., Alcaide, F., Daugelat, S., Jacobs, W. R., and Perler, F. B. "The *Mycobacterium xenopi* GyrA protein splicing element: Characterization of a minimal intein." *J. Bacteriol.* (1997), **179**, 6378-6382.
- [164] Southworth, M. W., Adam, E., Panne, D., Byer, R., Kautz, R., and Perler, F. B. "Control of protein splicing by intein fragment reassembly." *Embo J.* (1998), **17**, 918-926.
- [165] Lew, B. M., Mills, K. V., and Paulus, H. "Protein splicing in vitro with a semisynthetic two-component minimal intein." *J. Biol. Chem.* (1998), **273**, 15887-15890.
- [166] Mills, K. V., Lew, B. M., Jiang, S. Q., and Paulus, H. "Protein splicing in trans by purified N- and C-terminal fragments of the *Mycobacterium tuberculosis* RecA intein." *Proc. Natl. Acad. Sci. U. S. A.* (1998), **95**, 3543-3548.
- [167] Wu, H., Hu, Z. M., and Liu, X. Q. "Protein trans-splicing by a split intein encoded in a split DnaE gene of *Synechocystis* sp. PCC6803." *Proc. Natl. Acad. Sci. U. S. A.* (1998), **95**, 9226-9231.
- [168] Southworth, M. W., Benner, J., and Perler, F. B. "An alternative protein splicing mechanism for inteins lacking an N-terminal nucleophile." *Embo J.* (2000), **19**, 5019-5026.

- [169] Paulus, H. "Inteins as enzymes." *Bioorganic Chem.* (2001), **29**, 119-129.
- [170] Shao, Y., Xu, M. Q., and Paulus, H. "Protein splicing: Evidence for an N-O acyl rearrangement as the initial step in the splicing process." *Biochemistry* (1996), **35**, 3810-3815.
- [171] Xu, M. Q., Southworth, M. W., Mersha, F. B., Hornstra, L. J., and Perler, F. B. "In-Vitro Protein Splicing of Purified Precursor and the Identification of a Branched Intermediate." *Cell* (1993), **75**, 1371-1377.
- [172] Chong, S. R., Shao, Y., Paulus, H., Benner, J., Perler, F. B., and Xu, M. Q. "Protein splicing involving the *Saccharomyces cerevisiae* VMA intein - The steps in the splicing pathway, side reactions leading to protein cleavage, and establishment of an in vitro splicing system." *J. Biol. Chem.* (1996), **271**, 22159-22168.
- [173] Xu, M. Q., Comb, D. G., Paulus, H., Noren, C. J., Shao, Y., and Perler, F. B. "Protein Splicing - an Analysis of the Branched Intermediate and Its Resolution by Succinimide Formation." *Embo J.* (1994), **13**, 5517-5522.
- [174] Shao, Y., and Paulus, H. "Protein splicing: estimation of the rate of O-N and S-N acyl rearrangements, the last step of the splicing process." *J. Pept. Res.* (1997), **50**, 193-198.
- [175] Ding, Y., Xu, M. Q., Ghosh, I., Chen, X. H., Ferrandon, S., Lesage, G., and Rao, Z. H. "Crystal structure of a mini-intein reveals a conserved catalytic module involved in side chain cyclization of asparagine during protein splicing." *J. Biol. Chem.* (2003), **278**, 39133-39142.
- [176] Xu, M. Q., and Perler, F. B. "The mechanism of protein splicing and its modulation by mutation." *Embo J.* (1996), **15**, 5146-5153.
- [177] Hirata, R., and Anraku, Y. "Mutations at the Putative Junction Sites of the Yeast VMA1 Protein, the Catalytic Subunit of the Vacuolar Membrane H<sup>+</sup>-Atpase, Inhibit Its Processing by Protein Splicing." *Biochem. Biophys. Res. Commun.* (1992), **188**, 40-47.
- [178] Williams, N. K., Prosselkov, P., Liepinsh, E., Line, I., Sharipo, A., Littler, D. R., Curmi, P. M. G., Otting, G., and Dixon, N. E. "In vivo protein cyclization promoted by a circularly permuted *Synechocystis* sp PCC6803 DnaB mini-intein." *J. Biol. Chem.* (2002), **277**, 7790-7798.
- [179] Iwai, H., Lingel, A., and Pluckthun, A. "Cyclic green fluorescent protein produced in vivo using an artificially split PI-Pful intein from *Pyrococcus furiosus*." *J. Biol. Chem.* (2001), **276**, 16548-16554.
- [180] Otomo, T., Ito, N., Kyogoku, Y., and Yamazaki, T. "NMR observation of selected segments in a larger protein: Central-segment isotope labeling through intein-mediated ligation." *Biochemistry* (1999), **38**, 16040-16044.
- [181] Xu, R., Ayers, B., Cowburn, D., and Muir, T. W. "Chemical ligation of folded recombinant proteins: Segmental isotopic labeling of domains for NMR studies." *Proc. Natl. Acad. Sci. U. S. A.* (1999), **96**, 388-393.
- [182] Giriat, I., and Muir, T. W. "Protein semi-synthesis in living cells." *J. Am. Chem. Soc.* (2003), **125**, 7180-7181.
- [183] Ozawa, T., Nogami, S., Sato, M., Ohya, Y., and Umezawa, Y. "A fluorescent indicator for detecting protein-protein interactions in vivo based on protein splicing." *Anal. Chem.* (2000), **72**, 5151-5157.
- [184] Ozawa, T., Kaihara, A., Sato, M., Tachihara, K., and Umezawa, Y. "Split luciferase as an optical probe for detecting protein-protein interactions in mammalian cells based on protein splicing." *Anal. Chem.* (2001), **73**, 2516-2521.
- [185] Muir, T. W., Sondhi, D., and Cole, P. A. "Expressed protein ligation: A general method for protein engineering." *Proc. Natl. Acad. Sci. U. S. A.* (1998), **95**, 6705-6710.

- [186] Severinov, K., and Muir, T. W. "Expressed protein ligation, a novel method for studying protein-protein interactions in transcription." *J. Biol. Chem.* (1998), **273**, 16205-16209.
- [187] Evans, T. C., Benner, J., and Xu, M. Q. "Semisynthesis of cytotoxic proteins using a modified protein splicing element." *Protein Sci.* (1998), **7**, 2256-2264.
- [188] Chong, S. R., Mersha, F. B., Comb, D. G., Scott, M. E., Landry, D., Vence, L. M., Perler, F. B., Benner, J., Kucera, R. B., Hirvonen, C. A., Pelletier, J. J., Paulus, H., and Xu, M. Q. "Single-column purification of free recombinant proteins using a self-cleavable affinity tag derived from a protein splicing element." *Gene* (1997), **192**, 271-281.
- [189] Hofmann, R. M., and Muir, T. W. "Recent advances in the application of expressed protein ligation to protein engineering." *Curr Opin Biotechnol* (2002), **13**, 297-303.
- [190] Tolbert, T. J., and Wong, C. H. "New methods for proteomic research: Preparation of proteins with N-terminal cysteines for labeling and conjugation." *Angew. Chem.-Int. Edit.* (2002), **41**, 2171-2174.
- [191] Erlanson, D. A., Chytil, M., and Verdine, G. L. "The leucine zipper domain controls the orientation of AP-1 in the NFAT center dot AP-1 center dot DNA complex." *Chem. Biol.* (1996), **3**, 981-991.
- [192] Chytil, M., Peterson, B. R., Erlanson, D. A., and Verdine, G. L. "The orientation of the AP-1 heterodimer on DNA strongly affects transcriptional potency." *Proc. Natl. Acad. Sci. U. S. A.* (1998), **95**, 14076-14081.
- [193] Iwai, H., and Pluckthun, A. "Circular beta-lactamase: stability enhancement by cyclizing the backbone." *FEBS Lett.* (1999), **459**, 166-172.
- [194] Mathys, S., Evans, T. C., Chute, I. C., Wu, H., Chong, S. R., Benner, J., Liu, X. Q., and Xu, M. Q. "Characterization of a self-splicing mini-intein and its conversion into autocatalytic N- and C-terminal cleavage elements: facile production of protein building blocks for protein ligation." *Gene* (1999), **231**, 1-13.
- [195] Muir, T. W. "Semisynthesis of proteins by expressed protein ligation." *Annu. Rev. Biochem.* (2003), **72**, 249-289.
- [196] Cotton, G. J., Ayers, B., Xu, R., and Muir, T. W. "Insertion of a synthetic peptide into a recombinant protein framework: A protein biosensor." *J. Am. Chem. Soc.* (1999), **121**, 1100-1101.
- [197] Cotton, G. J., and Muir, T. W. "Generation of a dual-labeled fluorescence biosensor for Crk-II phosphorylation using solid-phase expressed protein ligation." *Chem. Biol.* (2000), **7**, 253-261.
- [198] Tolbert, T. J., and Wong, C. H. "Intein-mediated synthesis of proteins containing carbohydrates and other molecular probes." *J. Am. Chem. Soc.* (2000), **122**, 5421-5428.
- [199] Iakovenko, A., Rostkova, E., Merzlyak, E., Hillebrand, A. M., Thoma, N. H., Goody, R. S., and Alexandrov, K. "Semi-synthetic Rab proteins as tools for studying intermolecular interactions." *FEBS Lett.* (2000), **468**, 155-158.
- [200] Bader, B., Kuhn, K., Owen, D. J., Waldmann, H., Wittinghofer, A., and Kuhlmann, J. "Bioorganic synthesis of lipid-modified proteins for the study of signal transduction." *Nature* (2000), **403**, 223-226.
- [201] Blaschke, U. K., Silberstein, J., and Muir, T. W. "Protein engineering by expressed protein ligation" *Methods in Enzymology* (2000), **328**, 478-496.
- [202] Hackeng, T. M., Griffin, J. H., and Dawson, P. E. "Protein synthesis by native chemical ligation: Expanded scope by using straightforward methodology." *Proc. Natl. Acad. Sci. U. S. A.* (1999), **96**, 10068-10073.

- [203] Xu, M. Q., Paulus, H., and Chong, S. R. "Fusions to self-splicing inteins for protein purification" *Methods in Enzymology* (2000), **326**, 376-418.
- [204] Thoma, N. H., Iakovenko, A., Owen, D., Scheidig, A. S., Waldmann, H., Goody, R. S., and Alexandrov, K. "Phosphoisoprenoid binding specificity of geranylgeranyltransferase type II." *Biochemistry* (2000), **39**, 12043-12052.
- [205] Dursina, B., Thoma, N. H., Sidorovitch, V., Niculae, A., Iakovenko, A., Rak, A., Albert, S., Ceacareanu, A. C., Kolling, R., Herrmann, C., Goody, R. S., and Alexandrov, K. "Interaction of yeast Rab geranylgeranyl transferase with its protein and lipid substrates." *Biochemistry* (2002), **41**, 6805-6816.
- [206] Owen, D. J., Alexandrov, K., Rostkova, E., Scheidig, A. J., Goody, R. S., and Waldmann, H. "Chemo-enzymatic synthesis of fluorescent Rab 7 proteins: Tools to study vesicular trafficking in cells." *Angew. Chem.-Int. Edit.* (1999), **38**, 509-512.
- [207] Liu, X. H., and Prestwich, G. D. "Didehydrogeranylgeranyl (Delta Delta GG): A fluorescent probe for protein prenylation." *J. Am. Chem. Soc.* (2002), **124**, 20-21.
- [208] Kale, T. A., Raab, C., Yu, N., Dean, D. C., and Distefano, M. D. "A photoactivatable prenylated cysteine designed to study isoprenoid recognition." *J. Am. Chem. Soc.* (2001), **123**, 4373-4381.
- [209] Kuhlmann, J., Tebbe, A., Volkert, M., Wagner, M., Uwai, K., and Waldmann, H. "Photoactivatable synthetic Ras proteins: "Baits" for the identification of plasma-membrane-bound binding partners of Ras." *Angew. Chem.-Int. Edit.* (2002), **41**, 2546-2550.
- [210] Volkert, M., Uwai, K., Tebbe, A., Popkirova, B., Wagner, M., Kuhlmann, J., and Waldmann, H. "Synthesis and biological activity of photoactivatable N-Ras peptides and proteins." *J. Am. Chem. Soc.* (2003), **125**, 12749-12758.
- [211] Quellhorst, G. J., Allen, C. M., and Wessling-Resnick, M. "Modification of Rab5 with a photoactivatable analog of geranylgeranyl diphosphate." *J. Biol. Chem.* (2001), **276**, 40727-40733.
- [212] Bukhtiyarov, Y. E., Omer, C. A., and Allen, C. M. "Photoreactive Analogs of Prenyl Diphosphates as Inhibitors and Probes of Human Protein Farnesyltransferase and Geranylgeranyltransferase Type-I." *J. Biol. Chem.* (1995), **270**, 19035-19040.
- [213] Black, S. D. "Development of Hydrophobicity Parameters for Prenylated Proteins." *Biochem. Biophys. Res. Commun.* (1992), **186**, 1437-1442.
- [214] Ghomashchi, F., Zhang, X. H., Liu, L., and Gelb, M. H. "Binding of Prenylated and Polybasic Peptides to Membranes - Affinities and Intervesicle Exchange." *Biochemistry* (1995), **34**, 11910-11918.
- [215] Silvius, J. R., and Lheureux, F. "Fluorometric Evaluation of the Affinities of Isoprenylated Peptides for Lipid Bilayers." *Biochemistry* (1994), **33**, 3014-3022.
- [216] Shahinian, S., and Silvius, J. R. "Doubly-Lipid-Modified Protein-Sequence Motifs Exhibit Long-Lived Anchorage to Lipid Bilayer-Membranes." *Biochemistry* (1995), **34**, 3813-3822.
- [217] Giannakouros, T., Newman, C. M. H., Craighead, M. W., Armstrong, J., and Magee, A. I. "Posttranslational Processing of Schizosaccharomyces-Pombe Ypt5-Protein - in-Vitro and in-Vivo Analysis of Processing Mutants." *J. Biol. Chem.* (1993), **268**, 24467-24474.
- [218] Valentijn, J. A., and Jamieson, J. D. "Carboxyl methylation of rab3D is developmentally regulated in the rat pancreas: correlation with exocrine function." *Eur. J. Cell Biol.* (1998), **76**, 204-211.
- [219] Heinemann, I. "Synthese und biologische Evaluierung semi-synthetischer Rab7-Proteine." Dissertation (2003), University of Dortmund.

- [220] Watzke, A. planned Dissertation, University of Dortmund.
- [221] Naider, F. R., and Becker, J. M. "Synthesis of prenylated peptides and peptide esters." *Biopolymers* (1997), **43**, 3-14.
- [222] Ludolph, B., Eisele, F., and Waldmann, H. "Solid-phase synthesis of lipidated peptides." *J. Am. Chem. Soc.* (2002), **124**, 5954-5955.
- [223] Schelhaas, M., Nagele, E., Kuder, N., Bader, B., Kuhlmann, J., Wittinghofer, A., and Waldmann, H. "Chemoenzymatic synthesis of biotinylated Ras peptides and their use in membrane binding studies of lipidated model proteins by surface plasmon resonance." *Chem.-Eur. J.* (1999), **5**, 1239-1252.
- [224] Xu, M. Q., and Evans, T. C. "Intein-mediated ligation and cyclization of expressed proteins." *Methods* (2001), **24**, 257-277.
- [225] Dubendorff, J. W., and Studier, F. W. "Controlling Basal Expression in an Inducible T7 Expression System by Blocking the Target T7 Promoter with Lac Repressor." *J. Mol. Biol.* (1991), **219**, 45-59.
- [226] Ikegami, T., Okada, T., Hashimoto, M., Seino, S., Watanabe, T., and Shirakawa, M. "Solution structure of the chitin-binding domain of *Bacillus circulans* WL-12 chitinase A1." *J. Biol. Chem.* (2000), **275**, 13654-13661.
- [227] Blaschke, U. K., Cotton, G. J., and Muir, T. W. "Synthesis of multi-domain proteins using expressed protein ligation: Strategies for segmental isotopic labeling of internal regions." *Tetrahedron* (2000), **56**, 9461-9470.
- [228] Valiyaveetil, F. I., MacKinnon, R., and Muir, T. W. "Semisynthesis and folding of the potassium channel KcsA." *J. Am. Chem. Soc.* (2002), **124**, 9113-9120.
- [229] Sydor, J. R., Mariano, M., Sideris, S., and Nock, S. "Establishment of intein-mediated protein ligation under denaturing conditions: C-terminal labeling of a single-chain antibody for biochip screening." *Bioconjugate Chem.* (2002), **13**, 707-712.
- [230] Ayers, B., Blaschke, U. K., Camarero, J. A., Cotton, G. J., Holford, M., and Muir, T. W. "Introduction of unnatural amino acids into proteins using expressed protein ligation." *Biopolymers* (1999), **51**, 343-354.
- [231] Kawasaki, M., Makino, S. I., Matsuzawa, H., Satow, Y., Ohya, Y., and Anraku, Y. "Folding-dependent in vitro protein splicing of the *Saccharomyces cerevisiae* VMA1 protozyme." *Biochem. Biophys. Res. Commun.* (1996), **222**, 827-832.
- [232] Schein, C. H., and Noteborn, M. H. M. "Formation of Soluble Recombinant Proteins in *Escherichia-Coli* Is Favored by Lower Growth Temperature." *Bio-Technology* (1988), **6**, 291-294.
- [233] Dawson, P. E., Churchill, M. J., Ghadiri, M. R., and Kent, S. B. H. "Modulation of reactivity in native chemical ligation through the use of thiol additives." *J. Am. Chem. Soc.* (1997), **119**, 4325-4329.
- [234] Lu, W. Y., Qasim, M. A., and Kent, S. B. H. "Comparative total syntheses of turkey ovomucoid third domain by both stepwise solid phase peptide synthesis and native chemical ligation." *J. Am. Chem. Soc.* (1996), **118**, 8518-8523.
- [235] Hirel, P. H., Schmitter, J. M., Dessen, P., Fayat, G., and Blanquet, S. "Extent of N-Terminal Methionine Excision from *Escherichia-Coli* Proteins Is Governed by the Side-Chain Length of the Penultimate Amino-Acid." *Proc. Natl. Acad. Sci. U. S. A.* (1989), **86**, 8247-8251.

- [236] Robinson, A. B., Scotchle, J. W., and McKerrow, J. H. "Rates of Nonenzymatic Deamidation of Glutaminyl and Asparaginyl Residues in Pentapeptides." *J. Am. Chem. Soc.* (1973), **95**, 8156-8160.
- [237] Stephenson, R. C., and Clarke, S. "Succinimide Formation from Aspartyl and Asparaginyl Peptides as a Model for the Spontaneous Degradation of Proteins." *J. Biol. Chem.* (1989), **264**, 6164-6170.
- [238] Chazin, W. J., Kordel, J., Thulin, E., Hofmann, T., Drakenberg, T., and Forsen, S. "Identification of an Isoaspartyl Linkage Formed Upon Deamidation of Bovine Calbindin-D9k and Structural Characterization by 2D H-1-NMR." *Biochemistry* (1989), **28**, 8646-8653.
- [239] Bornstein, P. "Structure of Alpha1-Cb8, a Large Cyanogen Bromide Produced Fragment from Alpha1 Chain of Rat Collagen - Nature of a Hydroxylamine-Sensitive Bond and Composition of Tryptic Peptides." *Biochemistry* (1970), **9**, 2408-2421.
- [240] Geiger, T., and Clarke, S. "Deamidation, Isomerization, and Racemization at Asparaginyl and Aspartyl Residues in Peptides - Succinimide-Linked Reactions That Contribute to Protein-Degradation." *J. Biol. Chem.* (1987), **262**, 785-794.
- [241] Clarke, S. "Propensity for Spontaneous Succinimide Formation from Aspartyl and Asparaginyl Residues in Cellular Proteins." *Int. J. Pept. Protein Res.* (1987), **30**, 808-821.
- [242] Smyth, D. G., Nagamatsu, A., and Fruton, J. S. "Some reactions of N-Ethylmaleimide." *J. Am. Chem. Soc.* (1960), **82**, 4600-4604.
- [243] Majima, E., Goto, S., Hori, H., Shinohara, Y., Hong, Y. M., and Terada, H. "Stabilities of the Fluorescent SH-Reagent Eosin-5-Maleimide and Its Adducts with Sulfhydryl Compounds." *Biochim. Biophys. Acta-Gen. Subj.* (1995), **1243**, 336-342.
- [244] Johansson, M., and Westerlund, D. "Determination of N-Acetylcysteine, Intact and Oxidized, in Plasma by Column Liquid-Chromatography and Postcolumn Derivatization." *Journal of Chromatography* (1987), **385**, 343-356.
- [245] Knight, P. "Hydrolysis of p-NN'-Phenylenebismaleimide and Its Adducts with Cysteine - Implications for Cross-Linking of Proteins." *Biochem. J.* (1979), **179**, 191-197.
- [246] Matsui, S., and Aida, H. "Hydrolysis of Some N-Alkylmaleimides." *J. Chem. Soc.-Perkin Trans. 2* (1978), 1277-1280.
- [247] Wu, C. W., Yarbrough, L. R., and Wu, F. Y. H. "N-(1-Pyrene)Maleimide - Fluorescent Cross-Linking Reagent." *Biochemistry* (1976), **15**, 2863-2868.
- [248] Wade, M., Laursen, R. A., and Miller, D. L. "Amino-Acid Sequence of Elongation-Factor Tu - Sequence of a Region Containing Thiol-Group Essential for Gtp Binding." *FEBS Lett.* (1975), **53**, 37-39.
- [249] Smyth, D. G., Konigsberg, W., and Blumenfeld, O. O. "Reactions of N-Ethylmaleimide with Peptides + Amino Acids." *Biochem. J.* (1964), **91**, 589-&.
- [250] Villain, M., Gaertner, H., and Botti, P. "Native chemical ligation with aspartic and glutamic acids as C-terminal residues: Scope and limitations." *Eur. J. Org. Chem.* (2003), 3267-3272.
- [251] Hjelmeland, L. M. "Removal of Detergents from Membrane-Proteins." *Methods in Enzymology* (1990), **182**, 277-282.
- [252] Feig, L. A., Urano, T., and Cantor, S. "Evidence for a Ras/Ral signaling cascade." *Trends Biochem.Sci.* (1996), **21**, 438-441.
- [253] Feig, L. A. "Ral-GTPases: approaching their 15 minutes of fame." *Trends Cell Biol.* (2003), **13**, 419-425.

- [254] Helenius, A., McCaslin, D. R., Fries, E., and Tanford, C. "Properties of Detergents." *Methods in Enzymology* (1979), **56**, 734-749.
- [255] Helenius, A., and Simons, K. "Solubilization of Membranes by Detergents." *Biochimica et Biophysica Acta* (1975), **415**, 29-79.
- [256] Tascioglu, S. "Micellar solutions as reaction media." *Tetrahedron* (1996), **52**, 11113-11152.
- [257] Rathman, J. F. "Micellar catalysis." *Curr. Opin. Colloid Interface Sci.* (1996), **1**, 514-518.
- [258] Cordes, E. H., and Dunlap, R. B. "Kinetics of Organic Reactions in Micellar Systems." *Accounts Chem. Res.* (1969), **2**, 329-337.
- [259] Duynstee, E. F. J., and Grunwald, E. "Organic Reactions Occurring in or on Micelles .1. Reaction Rate Studies of the Alkaline Fading of Triphenylmethane Dyes and Sulfonphthalein Indicators in the Presence of Detergent Salts." *J. Am. Chem. Soc.* (1959), **81**, 4540-4542.
- [260] Bunton, C. A., Cerichelli, G., Ihara, Y., and Sepulveda, L. "Micellar Catalysis and Reactant Incorporation in Dephosphorylation and Nucleophilic-Substitution." *J. Am. Chem. Soc.* (1979), **101**, 2429-2435.
- [261] Bunton, C. A., Romsted, L. S., and Thamavit, C. "The Pseudophase Model of Micellar Catalysis - Addition of Cyanide Ion to N-Alkylpyridinium Ions." *J. Am. Chem. Soc.* (1980), **102**, 3900-3903.
- [262] Gitler, C., Zarmi, B., and Kalef, E. "Use of Cationic Detergents to Enhance Reactivity of Protein Sulfhydryls" *Methods in Enzymology* (1995), **251**, 366-375.
- [263] Bunton, C. A., Romsted, L. S., and Sepulveda, L. "A Quantitative Treatment of Micellar Effects Upon Deprotonation Equilibria." *J. Phys. Chem.* (1980), **84**, 2611-2618.
- [264] Romsted, L. R., and Cordes, E. H. "Secondary Valence Force Catalysis .7. Catalysis of Hydrolysis of P-Nitrophenyl Hexanoate by Micelle-Forming Cationic Detergents." *J. Am. Chem. Soc.* (1968), **90**, 4404-&.
- [265] Kochendoerfer, G. G., Salom, D., Lear, J. D., Wilk-Orescan, R., Kent, S. B. H., and DeGrado, W. F. "Total chemical synthesis of the integral membrane protein influenza A virus M2: Role of its C-terminal domain in tetramer assembly." *Biochemistry* (1999), **38**, 11905-11913.
- [266] Kochendoerfer, G. G., Jones, D. H., Lee, S., Oblatt-Montal, M., Opella, S. J., and Montal, M. "Functional characterization and NMR Spectroscopy on full-length Vpu from HIV-1 prepared by total chemical synthesis." *J. Am. Chem. Soc.* (2004), **126**, 2439-2446.
- [267] Clayton, D., Shapovalov, G., Maurer, J. A., Dougherty, D. A., Lester, H. A., and Kochendoerfer, G. G. "Total chemical synthesis and electrophysiological characterization of mechanosensitive channels from Escherichia coli and Mycobacterium tuberculosis." *Proc. Natl. Acad. Sci. U. S. A.* (2004), **101**, 4764-4769.
- [268] Hunter, C. L., and Kochendoerfer, G. G. "Native Chemical Ligation of Hydrophobic Peptides in Lipid Bilayer Systems." *Bioconjugate Chem.* (2004), **15**, 437-440.
- [269] Neugebauer, J. M. "Detergents - an Overview." *Methods in Enzymology* (1990), **182**, 239-253.
- [270] Nuoffer, C., Peter, F., and Balch, W. E. "Purification of His(6)-Tagged Rab1 Proteins Using Bacterial and Insect-Cell Expression Systems." *Methods in Enzymology* (1995), **257**, 3-9.
- [271] Horiuchi, H., Ullrich, O., Bucci, C., and Zerial, M. "Purification of Posttranslationally Modified and Unmodified Rab5 Protein Expressed in Spodoptera-Frugiperda Cells." *Methods in Enzymology* (1995), **257**, 9-15.
- [272] Kikuchi, A., Nakanishi, H., and Takai, Y. "Purification and Properties of Rab3a." *Methods in Enzymology* (1995); Vol. **257**, 57-70.

- [273] Ren, M. D., Zeng, J. B., DeLemosChiarandini, C., Rosenfeld, M., Adesnik, M., and Sabatini, D. D. "In its active form, the GTP-binding protein rab8 interacts with a stress-activated protein kinase." *Proc. Natl. Acad. Sci. U. S. A.* (1996), **93**, 5151-5155.
- [274] Lilie, H., Schwarz, E., and Rudolph, R. "Advances in refolding of proteins produced in *E. coli*." *Curr. Opin. Biotechnol.* (1998), **9**, 497-501.
- [275] Jaenicke, R., and Rudolph, R. "Folding proteins" In: *Protein Structure, A Practical Approach*, IRL-Press, Oxford, New York, Tokyo (1989), 191-223.
- [276] Rudolph, R., and Lilie, H. "In vitro folding of inclusion body proteins." *Faseb J.* (1996), **10**, 49-56.
- [277] Becker, C. F. W., Hunter, C. L., Seidel, R., Kent, S. B. H., Goody, R. S., and Engelhard, M. "Total chemical synthesis of a functional interacting protein pair: The protooncogene H-Ras and the Ras-binding domain of its effector c-Raf1." *Proc. Natl. Acad. Sci. U. S. A.* (2003), **100**, 5075-5080.
- [278] Campbell-Burk, S. L., and Carpenter, J. W. "Refolding and Purification of Ras Proteins." *Methods in Enzymology* (1995), **255**, 3-13.
- [279] DeLoskey, R. J., Vandyk, D. E., Vanaken, T. E., and Campbell-Burk, S. "Isolation and Refolding of H-Ras from Inclusion-Bodies of *Escherichia-Coli* - Refold Procedure and Comparison of Refolded and Soluble H-Ras." *Arch. Biochem. Biophys.* (1994), **311**, 72-78.
- [280] Marston, F. A. O., and Hartley, D. L. "Solubilization of Protein Aggregates." *Methods in Enzymology* (1990), **182**, 264-276.
- [281] Wetlaufer, D. B., and Xie, Y. "Control of Aggregation in Protein Refolding - a Variety of Surfactants Promote Renaturation of Carbonic-Anhydrase." *Protein Sci.* (1995), **4**, 1535-1543.
- [282] Clark, E. D., Schwarz, E., and Rudolph, R. "Inhibition of aggregation side reactions during in vitro protein folding." *Methods in Enzymology* (1999), **309**, 217-236.
- [283] Rudolph, R., and Fischer, S. "Process for obtaining renatured protein." *US patent No. 4,933,434* (1989)
- [284] Rudolph, R. "Renaturation of Recombinant, Disulfide-Bonded Proteins From 'Inclusion Bodies'." In: *Modern Methods in Protein- and Nucleic Acid Research*, Walter de Gruyter, Berlin New York (1990), 149-171.
- [285] Middelberg, A. R. "Preparative protein refolding." *Trends Biotechnol.* (2002), **20**, 437-443.
- [286] Clark, E. D. "Protein refolding for industrial processes." *Curr. Opin. Biotechnol.* (2001), **12**, 202-207.
- [287] Hofmann, A., Tai, M., Wong, W., and Glabe, C. G. "A Sparse-Matrix Screen to Establish Initial Conditions for Protein Renaturation." *Anal. Biochem.* (1995), **230**, 8-15.
- [288] Timasheff, S. N., and Arakawa, T. "Stabilization of protein structure by solvents." In: *Protein Structure & Function: A Practical Approach*, IRL Press, Oxford (1988), 331-345.
- [289] Khosravifar, R., Clark, G. J., Abe, K., Cox, A. D., McLain, T., Lutz, R. J., Sinensky, M., and Der, C. J. "Ras (CXXX) and Rab (CC/CXC) Prenylation Signal Sequences Are Unique and Functionally Distinct." *J. Biol. Chem.* (1992), **267**, 24363-24368.
- [290] Sasaki, T., Kaibuchi, K., Kabcenell, A. K., Novick, P. J., and Takai, Y. "A Mammalian Inhibitory GDP/GTP Exchange Protein (GDP Dissociation Inhibitor) for Smg P25a Is Active on the Yeast Sec4 Protein." *Mol. Cell. Biol.* (1991), **11**, 2909-2912.

- [291] Reents, R. "Synthese und biologische Evaluierung von neo-Ras-Proteinen." Dissertation (2002), University of Dortmund.
- [292] Alexandrov, K., Heinemann, I., Durek, T., Sidorovitch, V., Goody, R. S., and Waldmann, H. "Intein-mediated synthesis of geranylgeranylated Rab7 protein in vitro." *J. Am. Chem. Soc.* (2002), **124**, 5648-5649.
- [293] Durek, T., Alexandrov, K., Goody, R. S., Hildebrand, A., Heinemann, I., and Waldmann, H. "Synthesis of Fluorescently Labeled Mono- and Doubly Prenylated Rab7 GTPase." in preparation for *J. Am. Chem. Soc.*
- [294] Brunsveld, L., Watzke, A., Durek, T., Alexandrov, K., Goody, R. S., and Waldmann, H. "Synthesis of Functionalized RabGTPases by Combination of Solution and Solid Phase Lipopeptide Synthesis with Expressed Protein Ligation." in preparation for *J. Am. Chem. Soc.*
- [295] Rak, A., Pylypenko, O., Durek, T., Watzke, A., Kushnir, S., Brunsveld, L., Waldmann, H., Goody, R. S., and Alexandrov, K. "Structure of Rab GDP-Dissociation Inhibitor in Complex with Prenylated YPT1 GTPase." *Science* (2003), **302**, 646-650.
- [296] Rak, A., Reents, R., Pylypenko, O., Niculae, A., Sidorovitch, V., Thoma, N. H., Waldmann, H., Schlichting, I., Goody, R. S., and Alexandrov, K. "Crystallization and preliminary X-ray diffraction analysis of the Rab escort protein-1 in complex with Rab geranylgeranyltransferase." *J. Struct. Biol.* (2001), **136**, 158-161.
- [297] Desnoyers, L., and Seabra, M. C. "Single prenyl-binding site on protein prenyl transferases." *Proc. Natl. Acad. Sci. U. S. A.* (1998), **95**, 12266-12270.
- [298] Witter, D. J., and Poulter, C. D. "Yeast geranylgeranyltransferase type-II: Steady state kinetic studies of the recombinant enzyme." *Biochemistry* (1996), **35**, 10454-10463.
- [299] Long, S. B., Casey, P. J., and Beese, L. S. "Reaction path of protein farnesyltransferase at atomic resolution." *Nature* (2002), **419**, 645-650.
- [300] Alexandrov, K., Scheidig, A. J., and Goody, R. S. "Fluorescence methods for monitoring interactions of Rab proteins with nucleotides, Rab escort protein, and geranylgeranyltransferase" *Methods in Enzymology* (2001), **329**, 14-31.
- [301] Seabra, M. C., and James, G. L. "Prenylation Assays for Small GTPases" In: *Methods in Molecular Biology*, Humana Press, Totowa, NJ (1998), **84**, 251-260.
- [302] Coxon, F. P., Helfrich, M. H., Larijani, B., Muzylak, M., Dunford, J. E., Marshall, D., McKinnon, A. D., Nesbitt, S. A., Horton, M. A., Seabra, M. C., Ebetino, F. H., and Rogers, M. J. "Identification of a novel phosphonocarboxylate inhibitor of Rab geranylgeranyl transferase that specifically prevents Rab prenylation in osteoclasts and macrophages." *J. Biol. Chem.* (2001), **276**, 48213-48222.
- [303] Ullrich, O., Stenmark, H., Alexandrov, K., Huber, L. A., Kaibuchi, K., Sasaki, T., Takai, Y., and Zerial, M. "Rab GDP Dissociation Inhibitor as a General Regulator for the Membrane Association of Rab Proteins." *J. Biol. Chem.* (1993), **268**, 18143-18150.
- [304] Regazzi, R., Kikuchi, A., Takai, Y., and Wollheim, C. B. "The Small GTP-Binding Proteins in the Cytosol of Insulin-Secreting Cells Are Complexed to GDP Dissociation Inhibitor Proteins." *J. Biol. Chem.* (1992), **267**, 17512-17519.
- [305] Pfeffer, S. R., Diracsvejstrup, A. B., and Soldati, T. "Rab-GDP Dissociation Inhibitor - Putting Rab-GTPases in the Right Place." *J. Biol. Chem.* (1995), **270**, 17057-17059.
- [306] Musha, T., Kawata, M., and Takai, Y. "The Geranylgeranyl Moiety but Not the Methyl Moiety of the Smg-25a Rab3a Protein Is Essential for the Interactions with Membrane and Its Inhibitory GDP GTP Exchange Protein." *J. Biol. Chem.* (1992), **267**, 9821-9825.

- [307] Alory, C., and Balch, W. E. "Organization of the Rab-GDI/CHM superfamily: The functional basis for choroideremia disease." *Traffic* (2001), **2**, 532-543.
- [308] Schalk, I., Zeng, K., Wu, S. K., Stura, E. A., Matteson, J., Huang, M. D., Tandon, A., Wilson, I. A., and Balch, W. E. "Structure and mutational analysis of Rab GDP-dissociation inhibitor." *Nature* (1996), **381**, 42-48.
- [309] Luan, P., Heine, A., Zeng, K., Moyer, B., Greasely, S. E., Kuhn, P., Balch, W. E., and Wilson, I. A. "A new functional domain of guanine nucleotide dissociation inhibitor (alpha-GDI) involved in Rab recycling." *Traffic* (2000), **1**, 270-281.
- [310] Zhang, H. "Binding platforms for rab prenylation and recycling: Rab escort protein, RabGGT, and RabGDI." *Structure* (2003), **11**, 237-239.
- [311] Kikuchi, A., Yamashita, T., Kawata, M., Yamamoto, K., Ikeda, K., Tanimoto, T., and Takai, Y. "Purification and Characterization of a Novel GTP-Binding Protein with a Molecular-Weight of 24,000 from Bovine Brain Membranes." *J. Biol. Chem.* (1988), **263**, 2897-2904.
- [312] Overmeyer, J. H., and Maltese, W. A. "Prenylation of Rab proteins in vitro by geranylgeranyltransferases" *Methods in Enzymology* (2001), **329**, 31-39.
- [313] Kalinin, A., Thoma, N. H., Iakovenko, A., Heinemann, I., Rostkova, E., Constantinescu, A. T., and Alexandrov, K. "Expression of mammalian geranylgeranyltransferase type-II in Escherichia coli and its application for in vitro prenylation of Rab proteins." *Protein Expr. Purif.* (2001), **22**, 84-91.
- [314] Soldati, T., Riederer, M. A., and Pfeffer, S. R. "Rab GDI - a Solubilizing and Recycling Factor for Rab9-Protein." *Mol. Biol. Cell* (1993), **4**, 425-434.
- [315] Beranger, F., Cadwallader, K., Porfiri, E., Powers, S., Evans, T., Degunzburg, J., and Hancock, J. F. "Determination of Structural Requirements for the Interaction of Rab6 with RabGDI and Rab Geranylgeranyltransferase." *J. Biol. Chem.* (1994), **269**, 13637-13643.
- [316] Yang, C. Z., Slepnev, V. I., and Goud, B. "Rab Proteins Form in-Vivo Complexes with 2 Isoforms of the GDP-Dissociation Inhibitor Protein (GDI)." *J. Biol. Chem.* (1994), **269**, 31891-31899.
- [317] Nishimura, N., Nakamura, H., Takai, Y., and Sano, K. "Molecular-Cloning and Characterization of 2 Rab GDI Species from Rat-Brain - Brain-Specific and Ubiquitous Types." *J. Biol. Chem.* (1994), **269**, 14191-14198.
- [318] Shisheva, A., and Czech, M. P. "Association of cytosolic Rab4 with GDI isoforms in insulin-sensitive 3T3-L1 adipocytes." *Biochemistry* (1997), **36**, 6564-6570.
- [319] Gilbert, P. M., and Burd, C. G. "GDP dissociation inhibitor domain II required for Rab GTPase recycling." *J. Biol. Chem.* (2001), **276**, 8014-8020.
- [320] D'Adamo, P., Menegon, A., Lo Nigro, C., Grasso, M., Gulisano, M., Tamanini, F., Bienvenu, T., Gedeon, A. K., Oostra, B., Wu, S. K., Tandon, A., Valtorta, F., Balch, W. E., Chelly, J., and Toniolo, D. "Mutations in GDI1 are responsible for X-linked non-specific mental retardation." *Nature Genet.* (1998), **19**, 134-139.
- [321] Shapiro, A. D., and Pfeffer, S. R. "Quantitative-Analysis of the Interactions between Prenyl Rab9, GDP Dissociation Inhibitor-Alpha, and Guanine-Nucleotides." *J. Biol. Chem.* (1995), **270**, 11085-11090.
- [322] An, Y., Shao, Y., Alory, C., Matteson, J., Sakisaka, T., Chen, W., Gibbs, R. A., Wilson, I. A., and Balch, W. E. "Geranylgeranyl switching regulates GDI-Rab GTPase recycling." *Structure* (2003), **11**, 347-357.

- [323] Rak, A., Pylypenko, O., Niculae, A., Goody, R. S., and Alexandrov, K. "Crystallization and preliminary X-ray diffraction analysis of monoprenylated Rab7 GTPase in complex with Rab escort protein 1." *J. Struct. Biol.* (2003), **141**, 93-95.
- [324] Rak, A., Pylypenko, O., Niculae, A., Pyatkov, K., Goody, R. S., and Alexandrov, K. "Structure of the Rab7:REP-1 complex: Insights into the mechanism of Rab prenylation and choroideremia disease." *Cell* (2004), in press.
- [325] Wu, J. W., Hu, M., Chai, J., Seoane, J., Huse, M., Li, C., Rigotti, D. J., Kyin, S., Muir, T. W., Fairman, R., Massague, J., and Shi, Y. "Crystal structure of a phosphorylated Smad2. Recognition of phosphoserine by the MH2 domain and insights on Smad function in TGF-beta signaling." *Mol Cell* (2001), **8**, 1277-1289.
- [326] Armstrong, S. A., Brown, M. S., Goldstein, J. L., and Seabra, M. C. "Preparation of Recombinant Rab Geranylgeranyltransferase and Rab Escort Proteins" *Methods in Enzymology* (1995), **257**, 30-41.
- [327] Sidorovitch, V., Niculae, A., Kan, N., Ceacareanu, A. C., and Alexandrov, K. "Expression of mammalian Rab Escort Protein-1 and -2 in yeast *Saccharomyces cerevisiae*." *Protein Expr. Purif.* (2002), **26**, 50-58.
- [328] Simon, I., Zerial, M., and Goody, R. S. "Kinetics of interaction of Rab5 and Rab7 with nucleotides and magnesium ions." *J. Biol. Chem.* (1996), **271**, 20470-20478.
- [329] Tung, W. L., and Chow, K. C. "A Modified Medium for Efficient Electrotransformation of *Escherichia-Coli*." *Trends Genet.* (1995), **11**, 128-129.
- [330] Wang, Z. X., Kumar, N. R., and Srivastava, D. K. "A Novel Spectroscopic Titration Method for Determining the Dissociation-Constant and Stoichiometry of Protein Ligand Complex." *Anal. Biochem.* (1992), **206**, 376-381.
- [331] Fatania, H. R., Matthews, B., and Dalziel, K. "On the Mechanism of NADP<sup>+</sup>-Linked Isocitrate Dehydrogenase from Heart-Mitochondria. 1. The Kinetics of Dissociation of NADPH from Its Enzyme Complex." *Proc. R. Soc. Lond. Ser. B-Biol. Sci.* (1982), **214**, 369-387.

# 7. Appendices

*“The reasonable man adapts himself to the world.  
The unreasonable man persists in trying to adapt the world to himself.  
Therefore all progress depends on the unreasonable man.”*

George Bernard Shaw

## 7. Appendices

### 7.1. Derivation of equations

#### 7.1.1. Reversible second-order reactions - equilibrium titrations<sup>[330]</sup>

This mode of binding can be described by the following equations, where  $[P]^G$ ,  $[L]^G$  and  $[PL]^G$  are the equilibrium concentrations of protein (P), ligand (L) and protein:ligand complex (PL) and  $K_d$  is the corresponding equilibrium constant, which is to be determined.



With  $[P]^G = [P]_0 - [PL]^G$        $[L]^G = [L]_0 - [PL]^G$

this will result in 
$$K_d = \frac{([P]_0 - [PL]^G) \cdot ([L]_0 - [PL]^G)}{[PL]^G}$$

where  $[P]_0$  and  $[L]_0$  are the total concentrations (free and bound) of protein and ligand, respectively.

This can be rearranged to 
$$0 = ([PL]^G)^2 - [PL]^G(K_d + [L]_0 + [P]_0) + [P]_0[L]_0$$

The solutions of this quadratic equation are :

$$(eq. 1) \quad [PL]^G = \frac{1}{2} \left\{ (K_d + [L]_0 + [P]_0) \pm \sqrt{(K_d + [L]_0 + [P]_0)^2 - 4[P]_0[L]_0} \right\}$$

Simple calculations can demonstrate, that only the subtraction will produce meaningful results (because  $[PL]^G$  can only be  $\leq [P]_0$ ). The fractional completion of the binding reaction ( $r$ ) can be observed using spectroscopic techniques and corresponds to :

$$r = \frac{[PL]^G}{[P]_0} = \frac{Y - Y_{\min}}{Y_{\max} - Y_{\min}}$$

Where  $Y$  is some experimental observable, such as fluorescence intensity, anisotropy or absorbance. This equation is only valid if the quantity  $Y$  is (a) a linear function of the fractional completion of the reaction and (b) does not depend on other reactions. This equation can be rearranged to:

$$(eq. 2) \quad Y = Y_{\min} + [PL]^G \frac{Y_{\max} - Y_{\min}}{[P]_0}$$

Replacing  $[PL]^G$  in eq. 2 with eq. 1 will result in :

$$(eq. 3) \quad Y([L]_0) = Y_{\min} + \left\{ K_d + [L]_0 + [P]_0 - \sqrt{(K_d + [L]_0 + [P]_0)^2 - 4[P]_0[L]_0} \right\} \frac{Y_{\max} - Y_{\min}}{2[P]_0}$$

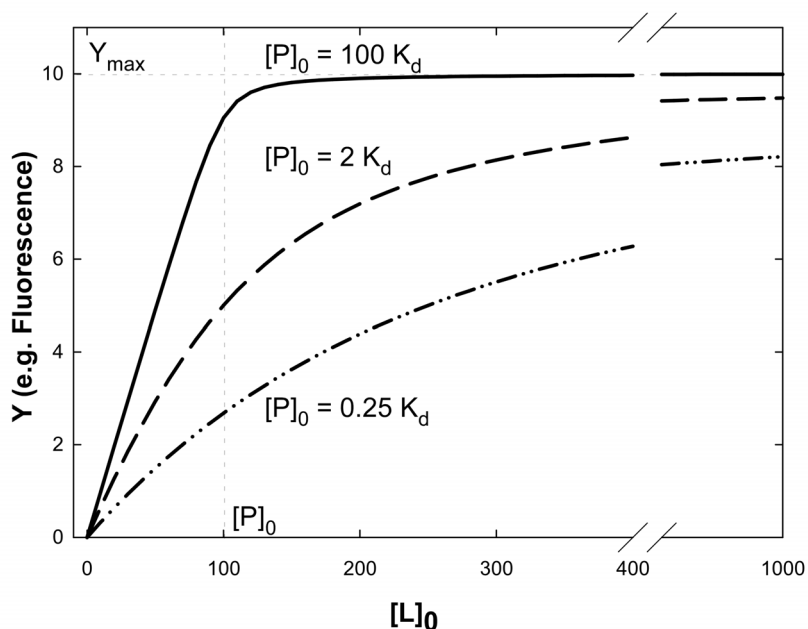


Figure 7-1: Simulation of titration curves. In all cases 100 nM of protein ( $= [P]_0$ ) was titrated with increasing concentrations of Ligand.  $Y_{\max}$  and  $Y_{\min}$  were set to 10 and zero, respectively. The behaviour of the curves depends on the ratio of  $K_d$  to  $[P]_0$ .  $K_d = 1$  nM (—),  $K_d = 50$  nM (- - -) and  $K_d = 400$  nM (-·-·-·-).

### 7.1.2. Kinetics of ligand dissociation (e.g. <sup>[331]</sup>)

The dissociation rate constant ( $k_1$ ) of a labeled ligand ( $L^*$ ) from its complex ( $PL^*$ ) can be determined by displacing it with an unlabeled ligand ( $L$ ). The simplest model that describes both reactions is:



The disappearance of  $PL^*$  can then be described by

$$(eq. 4) \quad \frac{d[PL^*]}{dt} = k_{-1}[L^*][P] - k_1[PL^*].$$

It can be assumed, that in the present case both the labeled and the unlabeled ligand interact with the protein in a similar manner and that the rate constants describing the association and dissociation reaction are in the same order of magnitude (i.e.  $k_1 \sim k_2$  and  $k_{-1} \sim k_{-2}$ ). If one chooses the concentrations of the components such that  $[L^*] \sim [P] \ll [L]$ , then the association rate of the competitor  $L$  with the free protein is significantly faster than the reassociation of the labeled ligand  $L^*$  (i.e.  $k_2[L] \gg k_{-1}[L^*][P]$ ), which would make the dissociation of  $PL^*$  quasi irreversible. Under such conditions the concentration of free (unbound) protein  $P$  is very low ( $[P] \rightarrow 0$ ) and the term  $k_{-1}[L^*][P]$  is negligible. This will give

$$(eq. 5, 6) \quad \frac{d[PL^*]}{dt} = -k_1[PL^*] \quad \text{and upon integration} \quad [PL^*] = [PL^*]_0 e^{-k_1 t}.$$

## Acknowledgements

*“If I have seen further, it is by standing on the shoulders of giants.”*

*Isaac Newton*

I am taking this opportunity to thank all those who have assisted me in one way or the other with my Ph.D. project. First, I would like to express my gratitude to my supervisors Prof. Dr. Roger Goody and Dr. Kirill Alexandrov. They have always been extremely generous with their time, knowledge and ideas and allowed me great freedom in my research. Equally important, I am grateful for their persistent motivation and their concerns for my well being.

I would like to thank my third supervisor and reviewer of my thesis, Prof. Dr. Herbert Waldmann for his suggestions and comments on my thesis and for providing the peptides that were used in this study. I would also like to thank the many people from the Waldmann lab who have collaborated with me and contributed to various parts of this research, in particular Dr. Ines (Dörte) Heinemann, Anja Watzke, Dr. Lucas (Luc) Brunsveld and Torben Lessman. Without their skilfull synthesised peptides this work would not have been possible.

I am also grateful to all who have been a part of the Alexandrov research team. I have enjoyed working with skilful colleagues and friends, in a very inspiring and helpful atmosphere. I am particularly grateful to Anca Niculae for preparing the many proteins I consumed throughout my studies and to Dr. Alex Rak and Dr. Lena Pylypenko for their great contribution to the structural part of this thesis.

Thanks are also due to Dr. Heino Prinz and Dr. Petra Janning for fruitful discussions on the mass spectroscopic analysis.

Thanks also go to all colleagues of the MPI Dortmund who have contributed to an extraordinarily friendly and helpful working environment and made working on this thesis a fun and pleasurable experience.

I would also like to thank Dr. Ines Heinemann, Anja Watzke and Aymelt Itzen for their constructive comments on the manuscript.

Last but not least, I am greatly indebted to my family and friends for their understanding, patience and support during the entire period of my study.